Preclinical Assessment of Experimental Therapeutics

for CLN6 Batten Disease

A thesis submitted for the requirements of a

Master of Science in Neuroscience

at the University of Otago

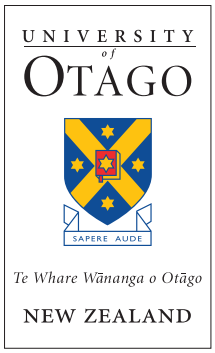

MADELINE GRACE MCINTYRE WILSON

2020

Dedicated to Eugene Harris, PhD.

Abstract

Neuronal ceroid lipofuscinoses (NCLs; Batten disease) are a group of thirteen genetically heterogenous lysosomal storage diseases that, collectively, are the most common cause of fatal neurodegeneration in children. CLN6 Batten disease (CLN6 BD), also known as Lake-Cavanagh disease, is a late infantile onset variant of the NCLs caused by loss-of-function mutations in the *CLN6* gene. Mutations in both alleles of the gene result in classic NCL symptoms – blindness, epilepsy and progressive cognitive and motor decline – as well as characteristic pathophysiological features such as premature and accelerated neuronal cell death, chronic neuroinflammation and the intracellular accumulation of autofluorescent storage material in lysosomes. As a monogenic, inherited and fatal disorder, CLN6 BD is an excellent candidate for experimental gene therapy.

Several preclinical and clinical trials of gene therapy have been conducted for a range of genetic disorders, including several NCL variants, and these have shown promising results. Subsequently, a clinical phase I/II CLN6 BD trial was initiated by the Gray Foundation and Amicus Therapeutics in 2016. This trial, which is ongoing at the time of writing, has produced optimistic safety and tolerance interim data. But, past experience with clinical gene therapy trials for several other genetic and metabolic disorders suggests that any improvements will not be curative. For this reason, the Gray Foundation began to investigate complementary treatments that might augment the therapeutic efficacy of gene therapy in CLN6 BD.

This project used a naturally occurring murine model of CLN6 BD (the $Cln6^{nclf}$ mouse) to investigate the efficacy of two small molecule (drug) therapies – gemfibrozil and cannabidiol (CBD) – alone and in combination with adenovirus associated virus (AAV2/9)-mediated gene therapy, as protection against the CLN6 behavioural phenotype. Specifically, $Cln6^{nclf}$ and C57Bl/6 (control) mice received a unilateral intracerebroventricular (i.c.v) injection

of gene therapy (an AAV2/9 vector expressing *hCLN6* under the control of a chicken β-actin gene promoter) or saline (1x PBS) on post-natal days 0-2. Post-weaning, mice were dosed orally (every second day) with either gemfibrozil, CBD, a combination of the two drug therapies or a vehicle solution. Behavioural testing (ataxia phenotyping and rotarod performance) was conducted at 6, 9 and 12 months of age.

Testing of over 500 animals determined that the oral administration of gemfibrozil, CBD, or a combination of the two drugs did not make any consistently significant improvements to untreated or gene-therapy treated $Cln6^{nclf}$ mouse behaviour. The study was successful, however, in reaffirming the apparent efficacy of i.c.v gene therapy in protecting against CLN6 BD behaviour in $Cln6^{nclf}$ mice (of both sexes), with no significant reduction in behavioural scores, when compared to healthy controls.

This study represents the first long-term, large-scale preclinical study of this particular combination of therapies for CLN6 BD. It provides a solid foundation for further work searching for a comprehensive and curative treatment regimen for CLN6 BD.

Acknowledgements

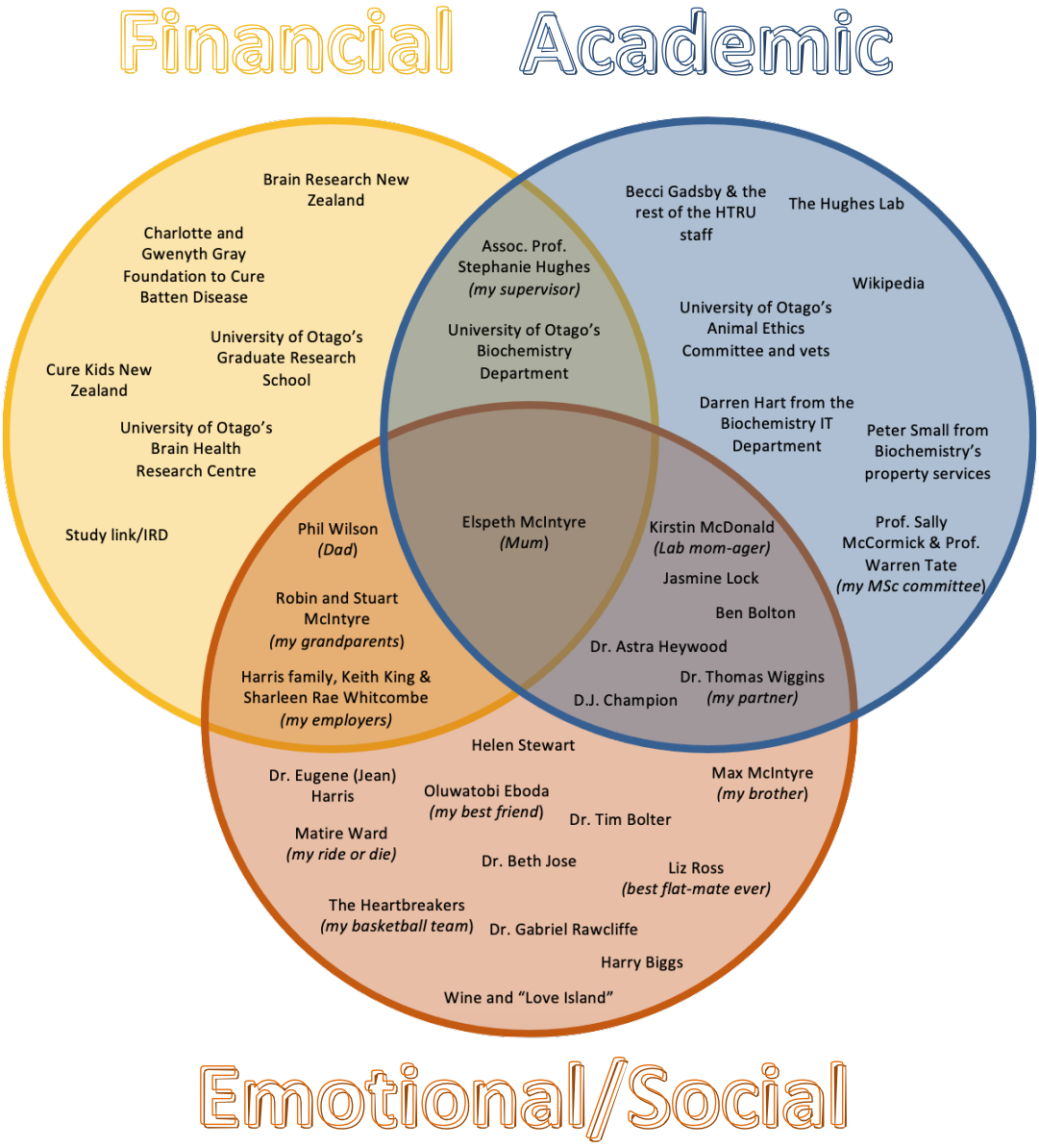

Table of Contents

List of Tables

List of Figures

List of Abbreviations

AAV	Adeno-associated virus
AAV9	Adeno-associated virus, serotype 9
AEC	University of Otago's Animal Ethics Committee
AD	Alzheimer's disease
ADBE	Activity-dependent bulk endocytosis
ALS	Amyotrophic lateral sclerosis
AFI	Amaurotic familial idiocy
ATPase	Mitochondrial ATP synthase
AV(s)	Autophagic vacuole(s)
BBB	Blood brain barrier
BD	Batten disease
BPU	University of Otago's Behavioural Phenotyping Unit
BTN1	Battenin
CAG	Promoter with cytomegalovirus enhancer, chicken beta-actin gene and splice acceptor of rabbit beta-globin gene.
CB1/2	Cannabinoid receptor 1/2
CB	Another abbreviation used to describe the CAG promoter (see CAG)
CBC	Cannabichromene
CBD	Cannabidiol
CBDA	Cannabidiolic acid
CBGA	Cannabigerol
CBN	Cannabinol
CD68	Cluster of differentiation 68
CEO	Chief executive officer
CLEAR	Co-ordination lysosomal expression and regulation
CLN	Ceroid lipofuscinoses, neuronal
$Cln6^{nclf}$	Naturally occurring *Cln6*$^{-/-}$ mutant murine model; sometimes referred to as the nclf mouse.
CNCL	Congenital neuronal ceroid lipofuscinosis
CNS	Central nervous system
CMV	Cytomegalovirus
CSF	Cerebrospinal fluid
CTSD	Cathepsin D
CTSF	Cathepsin F
C57Bl/6	C57 black, subtype-6 mouse model (healthy control)
Da	Dalton
DAPI	4', 6-diamindino-2phenylindole
DNA	Deoxyribonucleic acid
DNAJC5	DnaJ heat shock protein family (Hsp40) member C5
ds	Double stranded

EPA	New Zealand's Environmental Protection Agency
EPMR	Progressive epilepsy with mental retardation
ER	Endoplasmic reticulum
ERT	Enzyme replacement therapy
FDA	Food and Drug Administration Agency
fLINCL	Finnish variant late infantile neuronal ceroid lipofuscinosis
GABA	Gamma-aminobutyric acid
Gem	Gemfibrozil (fibrate drug; Lopid)
GFAP	Glial fibrillary accessory protein
GFP	Green fluorescent protein
GM2	Ganglioside monosialic 2
GPCR(s)	G-protein coupled receptor(s)
GPP	Geranylpyrophosphate
GRN	Progranulin
GROD(s)	Granular osmophilic deposit(s)
h	Human
HD	Huntington's disease
HSC	Haematopoietic stem cells
HTRU	University of Otago's Hercus Taieri Resource Unit
HTS	High throughput screening
ICC	Immunocytochemistry
i.c.v	Intracerebroventricular (injection)
IHC	Immunohistochemistry
INCL	Infantile neuronal ceroid lipofuscinosis
IP	Intraperitoneal (injection)
JNCL	Juvenile neuronal ceroid lipofuscinosis
KDa	Kilodalton
LAMP1	Lysosomal-associated membrane protein 1
LAMP2	Lysosomal-associated membrane protein 2
LEP	Left ear punch
LINCL	Late infantile neuronal ceroid lipofuscinosis
LSD(s)	Lysosomal storage disease(s)
LV	Lentivirus
M6P	Mannose-6-phosphate
M6PR	Mannose-6-phosphate-receptor
mRNA	Messenger ribonucleic acid
M/F	Male/Female
NCL(s)	Neuronal ceroid lipofuscinosis/es
NEP	No ear punch
NWOCH	Nationwide Ohio Children's Hospital
OA	Olivetolic acid
P0/1/2	Post-natal day 0/1/2

PB	Phosphate buffer
PBS	Phosphate buffer saline
PC2	Physical containment level 2
PD	Parkinson's disease
PFA	Paraformaldehyde
PPAR	Peroxisome proliferator-activator receptors (family)
PPARα	Peroxisome proliferator-activator receptor alpha
PPARβ	Peroxisome proliferator-activator receptor beta
PPARɣ	Peroxisome proliferator-activator receptor gamma
PPE	Personal protection equipment
PPRE	Peroxisome proliferator response element
PPT1	Palmitoyl protein thioesterase 1
REP	Right ear punch
RLEP	Right and left ear punch
RREP	Double right ear punch
ROS	Reactive oxygen species
RNA	Ribonucleic acid
RSV	Resveratrol
RT	Reverse transcriptase
Saposin(s)	Sphingolipid activator protein(s)
SEM	Standard error of the mean
sc	Self-complementary
ss	Single-stranded
SV	Synaptic vesicle
THC	TransΔ9-tetrahydrocannabinol
THCA	Tetrahydrocannabinolic acid
TFEB	Transcription factor EB
TM	Transmembrane
TPP1	Tripeptidyl peptidase 1
UPR	Unfolded protein response
UTR	Untranslated region
vLINCL	Variant late infantile neuronal ceroid lipofuscinosis
VPL	Ventroposterior lateral thalamic nuclei
VPM	Ventroposterior medial thalamic nuclei
WT	Wildtype
♂	Male
♀	Female

Note on Gene and Protein Nomenclature

Human (or sheep) DNA or mRNA	e.g. *CLN6*
Mouse DNA or mRNA	e.g. *Cln6*
Human or Mouse (or sheep) protein	e.g. CLN6

Chapter 1: Introduction

1.1 Overview

The neuronal ceroid lipofuscinoses (NCLs) are a heterogeneous group of fatal neurodegenerative lysosomal storage disorders, with fourteen genetic variants identified to date. While each variant on its own is rare, collectively the NCLs represent the most common paediatric neurodegenerative disorders in the world (Williams, 2011). Almost all NCLs are inherited in an autosomal recessive Mendelian manner and are caused by one or more mutations in several different genes of known and unknown function, sometimes referred to as the ceroid lipofuscinosis genes (*CLN1* through *14*, with *CLN9* predicted but not yet identified) (Mole & Cotman, 2015; Schulz et al., 2004). Although the NCLs are primarily regarded as a family of childhood disorders, age of onset ranges from congenital ('at-birth') through to early adulthood (known as 'Kuf's disease')(Kufs, 1925).

Clinical symptoms can differ between types of NCL but usually include progressive psychomotor degeneration, loss of vision ('amaurosis'), myoclonic seizures, personality changes and dementia. Prognosis can vary from months to years, but all of the NCLs are currently considered incurable, chronic in nature and nearly always result in the premature death of the patient (Nita et al., 2016; Rider et al., 1988).

While they vary in many aspects of pathophysiology, including genetic basis, age of onset, symptoms and rate of disease progression, all NCLs are characterised by three classical features: (1) the progressive loss of post-mitotic cells in the central nervous system (CNS), which leads to atrophy in the cerebral and cerebellar cortices, (2) neuroinflammation, and (3) the lysosomal accumulation of autofluorescent storage material within neurons (Cooper et al., 2015 Nelvagal et al., 2019; Palmer et al., 2013). The relationship between these features,

particularly as to whether one causes or is the result of the others, remains an area of ongoing enquiry.

Mutations in the *CLN6* gene result in a variant late infantile NCL (vLINCL) phenotype, sometimes referred to as Lake-Cavanagh or CLN6 Batten disease (BD). Until recently, the function of the CLN6 protein was essentially uncharacterised, though it was known to localise in the endoplasmic reticulum (ER) and to have a multi-pass transmembrane structure (Alroy et al., 2011; Gao et al., 2002; Wheeler et al., 2002). It is now believed to play a role in a multi-protein complex responsible for the transportation of several lysosomal enzymes from their place of synthesis, within the ER, to their place of function, within the lysosome (Bajaj et al., 2019). Children with mutations in both *CLN6* alleles start presenting with vLINCL symptoms in early childhood, around 4 to 5 years of age, and disease progression is relatively swift, with death invariably occurring in early to late teens (Alroy et al., 2011).

Monogenic, inherited, fatal disorders like CLN6 BD present as the perfect subject for an experimental treatment known as viral vector-mediated gene therapy (gene therapy). This practical compatibility, combined with the support of a parent-based charity called the Gray Foundation, motivated a 2016 phase 1/2 clinical trial in Nationwide Ohio's Children's Hospital (Trial No. NCT02725580, *Clinicaltrials.gov* 2016). The trial included 13 children, all diagnosed with CLN6 BD, and involved the intrathecal ('spinal canal') injection of a viral vector carrying a healthy copy of the human *CLN6* gene into the lumbar ('lower back') spinal cord region. This trial, which remains ongoing, was the first of its kind and has already yielded promising interim data, with Amicus Therapeutics chief executive officer (CEO) John Crawley stating:

> *"These interim clinical data suggest that our gene therapy in CLN6 Batten disease has the potential to halt the progression of this devastating fatal disease that, untreated, destroys brain function and kills children….It is remarkable that most children in this study appear to show stabilisation, particularly the younger children who were able to maintain high baseline motor and language scores for up to two years."*
>
> *- John Crawley from Amicus Therapeutics, 2019*

Despite this optimistic press-release, and the evidence that this experimental therapy was generally well tolerated by patients, the 2016 trial is unlikely to produce a cure. Participants who were treated post-symptom onset still appear to be declining, though whether this decline is slower than it would be without the treatment has yet to be determined. With this in mind, the Gray Foundation enlisted the Hughes lab in early 2018 to carry out a large-scale, pre-clinical trial in a naturally occurring mouse model of CLN6 BD to mirror the gene therapy used in the children in 2016 and to assess whether the use of two different small molecule therapies, alone and in combination with gene therapy and each other, had any synergistic effect on the CLN6 BD phenotype. This trial, involving over 540 mice and almost two years of work, forms the basis of this thesis.

1.2 History of the Neuronal Ceroid Lipofuscinoses (NCLs; Batten disease)

The early history of paediatric neurodegenerative diseases, including the NCLs, is that there is very little early history of paediatric neurodegenerative disease. Unlike other well-known diseases, such as cancer or tuberculosis, which have references in medical literature dating back to the invention of written language, the concept of neurodegeneration as a nosological classification, especially in children, is relatively new to medicine (Breasted, 1930; Cave & Demonstrator, 1939; Morse et al., 1964). Prior to the 19th century, western literature tended

to categorise many of the behavioural symptoms of neurodegeneration, such as dementia, chorea and epilepsy, as signs of broad medico-social conditions like ‘madness’, ‘simpleness’ and ‘feeble-mindedness’. It is also likely that the premature death of children affected by neurodegenerative diseases like the NCLs would have gone predominantly unnoticed due to generalised high infant mortality rates prior to the industrial revolution and modern medicine (Jennekens, 2014; Kanner, 1962; Kauffman, 1976).

Over the past two centuries our medical, social and cultural interpretations of the NCLs have evolved rapidly, primarily dictated by our increasing understanding of the biological basis of heredity and a variety of neurodegenerative and metabolic illnesses. The narrative of the NCLs has been closely intertwined with other inherited neurodegenerative disorders, such as Tay-Sachs’ and Niemann-Pick’s disease (Sachs, 1896; Wyburn-Mason, 1943a, 1943b). This section briefly touches upon this evolution through three main eras, each determined by the technological resources available to NCL researchers at the time.

1.2.1 The Amaurotic Familial Idiocies (AFIs): an era of clinical description and categorisation

The earliest tools used to study the NCLs, as is the case with most diseases, were detailed descriptions of clinical symptoms and gross pathology at autopsy. While they are often referred to as ‘Batten disease’, after the British neurologist Frederick Batten who described one form of the disease in 1906, the first clinical description of the NCLs is actually believed to have been written by a rural Norwegian physician, Dr. Otto Christian Stengel, in 1826 (Batten, 1902; Stengel, 1826). Stengel’s report describes the development of a mysterious disease in four siblings, born to two apparently healthy parents. In all four cases, this disease began with vision impairment around the age of six and quickly progressed into loss of mental and physical faculties, epileptic fits and “mania” (Stengel, 1826).

His report, written originally in Norwegian, went largely unnoticed by the International medical community until over a century later, when it was translated into English by A. J. Nissen, and the 'singular disease' Stengel described was recognised to be compatible with what is now known as CLN3 Batten disease, or classical juvenile neuronal ceroid lipofuscinosis (Nissen, 1954).

Despite Stengel's work being overlooked, the NCLs started to gain academic attention through other observations, namely those of British ophthalmologist Warren Tay and American neurologist Bernard Sachs. During his presidential address to the New York Neurological Society in 1896, Sachs presented the concept of 'amaurotic familial idiocy' (AFI) – a fatal disorder comprising of progressive vision loss and 'regression' of mental and physical development that he had observed in two infant siblings, four years apart. Their almost identical disease progressions led him to recognise the "family character" of the disease and during his assessments of the children he discovered both siblings to possess a rare ocular manifestation, a 'brownish-red, fairly circular spot' within a larger white disc on the retina of both eyes (**Figure 1.1**), identical to the one that had been characterised in 1881 by Tay (Sachs, 1896; Tay, 1884).

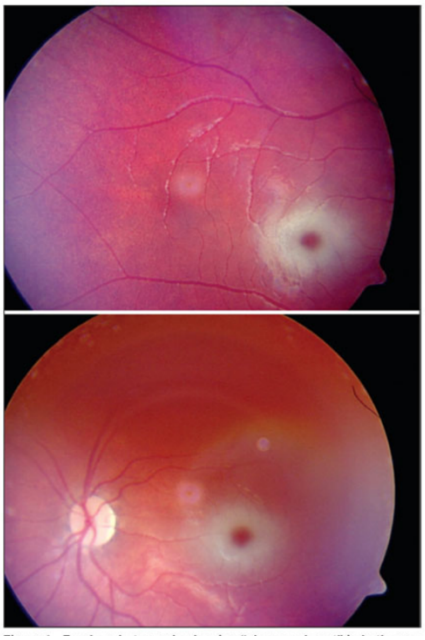

Figure 1.1 | Tay-Sachs 'cherry red' spot. Fundus photographs showing the characteristic 'cherry-red spot' of Tay-Sachs disease. Originally described by ophthalmologist Warren Tay in 1881 and used as inclusion criteria for the amaurotic familial idiocies (AFIs) by Bernard Sachs. Image taken from a case report by *Aragão et al., 2009*.

Sach's proposed AFI category expanded during the turn of the 20th century, thanks to a number of clinical descriptions of other familial cases of progressive childhood dementia and vision loss by British, German and Czech authors (Batten, 1902; Batten & Mayou, 1915; Bielschowsky, 1914; Jansky, 1909; Spielmeyer, 1905; Vogt, 1905). Similarities in post-mortem pathology also began to be recorded, with granular, 'lipid-like' material being found in neurons of deceased patients. The biochemical basis of these deposits wouldn't be determined until much later in the century, but it was frequently referred to as 'lipofuscin' (meaning 'dark fat') or 'ceroid' (Hueck, 1912).

Unlike the original Tay-Sachs descriptions, many of these new cases demonstrated later onset (post-infancy), varying symptomology and showed little consistency in terms of patient ethnicity (the original cases described by Sachs were from Ashkenazi Jewish families)(Sachs, 1896).

1.2.2 The Neuronal Ceroid Lipofuscinoses (NCLs): an era of biochemistry and ultrastructure

By the 1950s a precarious and conflicted classification system had been developed for the AFIs, based primarily on clinical accounts of age of onset, and consisted, depending on who you asked, of five categories or variants of AFI: congenital, infantile, late infantile, juvenile and adult (Sandifier, 1959; Zeman & Hoffman, 1962). There was a lot of debate between researchers as to whether these diseases were all variants of a single genetic disease, differing only in intensity and age of onset, or if they were separate, albeit similar, metabolic disorders (Sandifier, 1959; Wyburn-Mason, 1943a, 1943b; Wolfgang, Zeman & Hoffman, 1962).

In order to bring clarity to a field weighed down by inconsistencies and uncertainty, the researchers Wolfgang Zeman and Paul Dyken proposed a new classification system in 1969, based on recent biochemical and ultrastructural observations that divided the AFIs into two distinct groups: Tay-Sachs disease and the NCLs (Zeman & Dyken, 1969).

The NCLs, however, remained difficult to define – even with the help of new techniques and technologies - and were referred to by Zeman and Dyken as a "collection of heterogeneous entities" that could be "characterised by autosomal recessive inheritance, progressive failure of vision, intellectual faculties and motor function, and recurrent seizures," as well as "more variable age of onset and the presence of retinal abnormalities other than the 'cherry red spot'" (Zeman & Dyken, 1969).

This overarching category encompassed the late infantile, juvenile and adult forms of the AFIs, all of which could be histologically and ultrastructurally differentiated from Tay-Sachs (and other gangliosidoses) due to a normal sphingolipid (aka ganglioside) profile and the presence of intraneural autofluorescent storage material. The biochemical character of the storage material still remained elusive, though it resembled the build-up of the 'lipopigment'

aka ‘lipofuscin’ aka ‘ceroid’ (coloured fat) associated with natural ageing processes, from which the NCLs got their name (Endicott & Lillie, 1944; Lillie et al., 1941; Seehafer & Pearce, 2006). Late infantile NCL (LINCL) cases showed characteristic ‘curvilinear’ (curved line) patterns of this storage material (**Figure 1.2.B**), when examined by electron microscope, while the juvenile form could be distinguished by its predominantly ‘fingerprint-like’ patterns (**Figure 1.2.C**) (Mole & Haltia, 2014). Almost five years after the establishment of the NCL category, a new, infantile, type of NCL was described by Haltia (1973a; 1973b) and Santavuori (1973), histologically characterised by the presence of storage material with a finely granular structure (‘granular osmophilic deposits’ or GRODs; **Figure 1.2.A**).

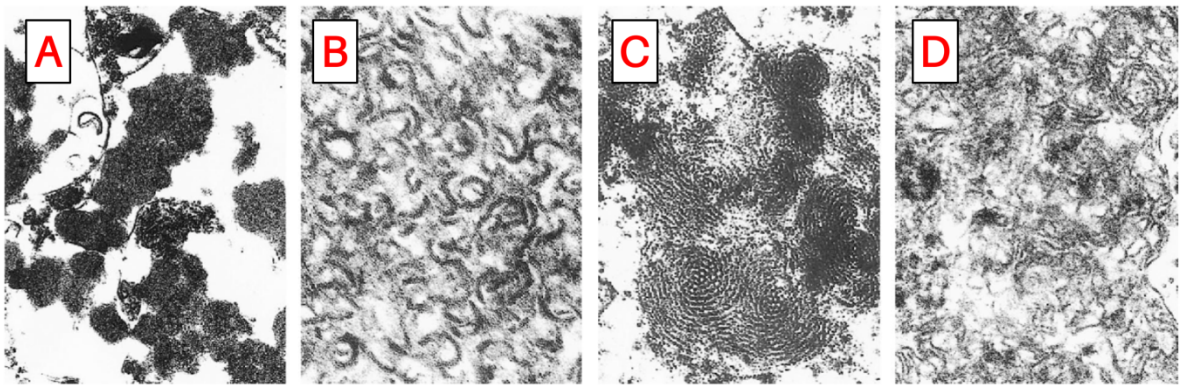

Figure 1.2| The four forms of NCL intraneural storage deposits. Electron microscopy helped researchers elicit the ultrastructures of abnormal intraneural deposits that had been observed in nervous tissue at autopsy of NCL patients. Four types were identified: (A) granular osmiophilic deposits (GRODS), now associated with CLN1 BD, 310,000x; (B) curvilinear profiles typical of classic late infantile neuronal ceroid-lipofuscinosis or CLN2, 320,000x; (C) ‘fingerprint bodies’ are the primary form of intraneuronal inclusions in the juvenile form of NCL or CLN3, 330,000x; and (D) many inclusions in the variant forms of late infantile neuronal ceroid-lipofuscinosis correspond to the rectilinear complex, such as CLN5 and CLN6, 315,000x. Image modified from *Haltia, 2003.*

By the end of the 70s, there were, according to Zeman, four ‘official’ NCL variants: infantile (aka INCL or ‘Haltia-Santavuori disease’), late infantile (LINCL or ‘Jansky-Bielschowsky disease’), juvenile (JNCL or ‘Spielmeyer-Sjogren disease’) and adult (‘Kuf’s disease’)(Bielschowsky, 1914; Haltia, Rapola, & Santavuori, 1973; Jansky, 1909; Kufs, 1925; Santavuori et al., 1973; Spielmeyer, 1905; Zeman, 1976). A canine form had also been reported in English Setter dogs (Koppang, 1992; Koppang, 1969). Despite Zeman’s best efforts,

however, the NCL's continued to defy neat categorisation, and a spectrum of 'atypical' cases began to be reported in the 80s and 90s. Some of these were named after the geological areas in which they were found, e.g. the 'Finnish', 'Indian' or 'Turkish' NCLs (Elleder et al., 1997; Lake & Cavanagh, 1978; Santavuori et al., 1991, 1982; Tyynelä et al., 1997; Williams et al., 1999), while others appeared to display an autosomal dominant inheritance pattern at odds with the traditionally 'autosomal recessive' inheritance that many had come to associate with the NCLs (Boehme et al., 1971; Nijssen et al., 2006; Nosková et al., 2011; Sjögren, 1931). Additionally, a multitude of naturally-occurring NCL animal models had been discovered, including cats (Green & Little, 1974), sheep (Jolly & West, 1976), cattle (Read & Bridges, 1969) and goats (Fiske & Storts, 1988).

It was, ultimately, the use of a series of elegant biochemical assays that restored a little order to the chaotic field of NCL research when, in the late 1980s, Palmer et al., (1988) finally characterised the storage material found within the neurons of a South Hampshire sheep NCL model. Due to their 'fatty' appearance, previous studies had focused, unsuccessfully, on identifying a lipid or lipid-like substance. Palmer et al., however, found that the major component (two-thirds) of storage material isolated from the ovine tissue to be a low-molecular-weight *protein* and, only three years later, determined this protein to be subunit C of mitochondrial ATP synthase (subunit C) (Fearnley et al., 1990; Palmer et al., 1989; **Figure 1.3**).

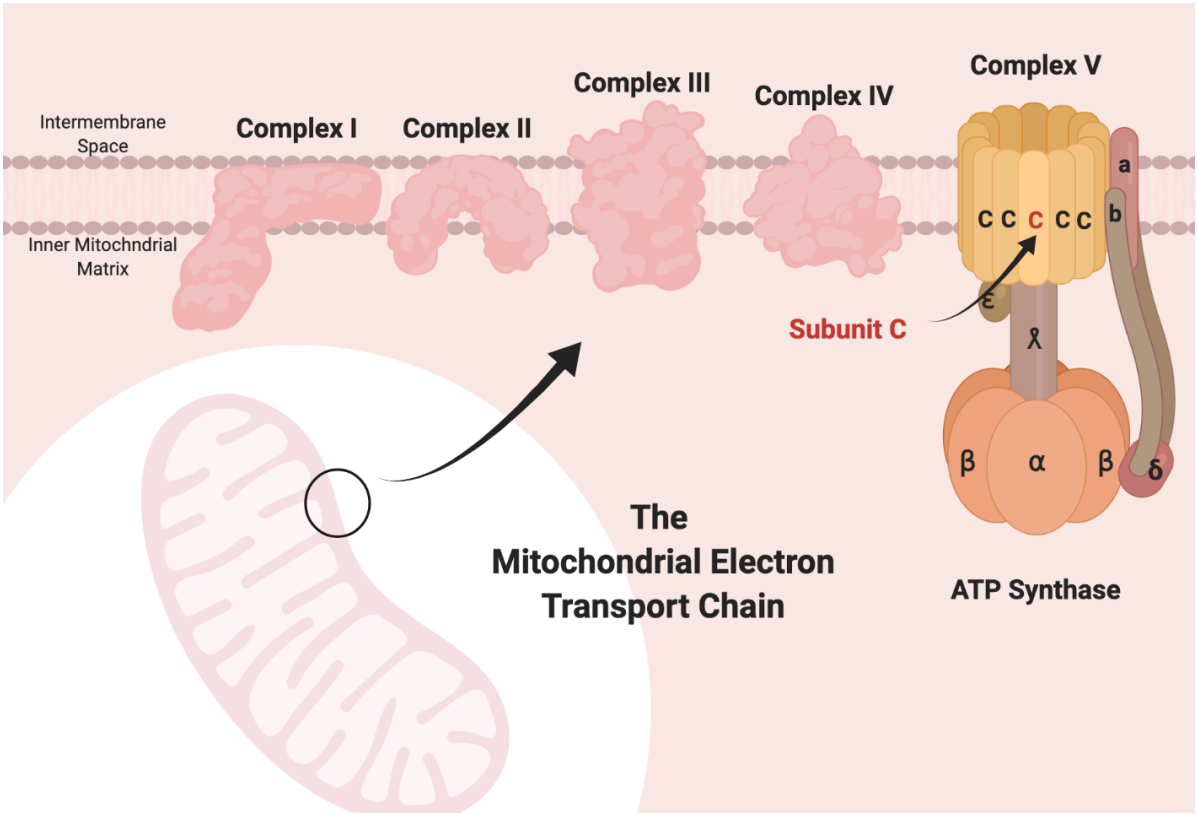

Figure 1.3 | Subunit C of the mitochondrial ATP synthase. The major protein component of most forms of storage material found in the NCLs is subunit c of the mitochondrial ATP synthase. ATP synthases are large, transmembrane protein complexs responsible for the creation of the energy storage molecule adenosine triphosphate (ATP). While they can be located all over the cell, the majority are found embedded in the inner membranes of the cell's mitochondria, where they act as the fifth and final component of the electron transport chain. Image made by author using *BioRender.com*.

This mitochondrial protein turned out to be the primary component of storage material in most forms of human and animal NCLs, with the key exception of infantile human NCL (INCL) (Tyynelä et al., 1993). The storage material in this particular variant was determined to be a combination of sphingolipid activator proteins (saposins) A and D, and was later found to also be present in a few rare animal models (congenital ovine and the miniature schnauzer model), as well as an adult human NCL variant known as Parry disease (Nijssen et al., 2006; Palmer et al., 1997). Saposin storage material produced the GROD ultrastructure originally observed by Haltia and Santavuori in the 70s (**Figure 1.2.A**), while subunit C appeared to produce a wide variety of ultrastructures including the curvilinear and fingerprint patterns associated with the late infantile and juvenile forms of NCL (Mole et al., 2011).

1.2.3 *Lysosomal genes, lysosomal storage diseases (LSDs): an era of genetics*

Around the same time that Zeman and Dyken first differentiated the NCLs from gangliosidoses like Tay-Sachs disease, another category of disease was beginning to appear in the medical lexicon: lysosomal storage diseases (LSDs). The lysosome, from which the LSDs get their name, had only been discovered by Belgian cytologist Christian de Duve ten years earlier, in the mid-to-late 1950s. Through a series of cell fractionation studies and biochemical techniques, de Duve and his collaborators had come to recognise that every cell in the human body possessed a group of membrane-bound organelles that contained highly acidic enzymes (Appelmans & De Duve, 1955; Appelmans et al., 1955; Berthet & De Duve, 1951; De Duve et al., 1955; Gianetto & De Duve, 1955). These organelles, named 'lysosomes', were characterised as the waste management and recycling centres of the cell and it was their dysfunction, or that of the hydrolysing enzymes they contained, that came to be seen as the uniting feature of LSDs (Hers, 1965). The relationship between this newly-established group of metabolic disorders and the NCLs wouldn't become clear, however, until the mid to late 90s, driven by the genetic revolution and the consequent genetic and functional identification of the first NCL proteins.

The era of NCL genetics really began when, in 1989, Eiberg et al. released a study linking the mutated protein responsible for JNCL to the haptoglobin locus on the long arm of chromosome 16. This was followed, in relatively quick succession, by Vesa et al. (1995) using a combination of positional cloning and fluorescent *in-situ* hybridisation genetic techniques to confirm the identity of the first NCL-causing gene. They found that INCL, as described by Haltia and Santavuori, was caused by a mutation in the palmitoyl-protein thioesterase (*PPT1*) gene, which encodes a lysosomal hydrolase enzyme (Vesa et al., 1995). This discovery, while an exciting use of new genetic technologies and techniques in itself, contributed further layers of complexity to the study of an already exceedingly complicated group of diseases and raised

the question of whether these disorders needed to be recategorized, again, as LSDs. The argument for recategorization was compounded by the further discovery, using a biochemical approach, of another lysosomal enzyme, tripeptidyl peptidase 1, as being responsible for the LINCL variant (Sleat et al., 1997).

The following five years saw the genes underlying five different NCL variants cloned, with some determined to be soluble enzymes and others transmembrane in structure. The location and function of these newly discovered proteins wasn't necessarily evident at the time, with some still remaining unidentified today, but their identification lead to the introduction of a new genetic classification for the NCLs – one that has remained in use for the past decade. At the time of this publication, human NCLs are currently classified into fourteen genetic forms from *CLN1* through to *CLN14* (with *CLN9* predicted but not yet identified)(see **Table 1.1**).

While not all of the currently identified *CLN* genes encode lysosomal enzymes, many (if not all), are associated with the larger endosomal-autophagic-lysosomal network (Bennett & Hofmann, 1999). The role of the lysosome and its associated pathways has proven to be more complex than initially realised (Walkley, 2007). Due to our ever-growing knowledge about the function and roles of the lysosome, the lysosomal storage disorder category has had its qualifying parameters expanded since its introduction in the 1960s to encompass proteins involved further afield than just the intraluminal lysosomal compartment itself (Hers, 1965). This has allowed the NCLs to be comfortably classified as LSDs and join the ranks of a heterogeneous group of over 50 genetically-distinct metabolic diseases (Bennet & Hofmann, 1999).

Table 1.1 | Summary table of human NCL variants, based on a genetic classification system. Clinical phenotype: * indicates the disease phenotype experienced by complete loss of function of the related gene, while bolded phenotypes are non-NCL disorders that can be caused by mutations in the same gene. Most of the information for this table was taken from *Mole & Cotman., 2015*.

NCL variant	Eponym(s)	Former name(s)	Gene	Cytogenetic location	Number of unique NCL-causing mutations	Protein product	Protein topology	Protein localisation	Clinical phenotype
CLN1	Santavuori-Haltia disease or Kufs disease	Infantile NCL (INCL)	*PPT1/CLN1*	1p34.2	71 (as of 2017)	Palmitoyl protein thioesterase 1 (PPT1)	Soluble	Lysosomal	Infantile*, late infantile, juvenile and adult
CLN2	Jansky-Bielschowsky disease	Late infantile NCL (LINCL)	*TPP1/CLN2*	11p15.4	129 (as of 2018)	Tripeptidyl peptidase I (TPP1)	Soluble	Lysosomal	Late infantile*, juvenile, **protracted, SCAR7**
CLN3	Spielmeyer-Sjögren disease	Juvenile NCL (JNCL)	*CLN3*	16p12.1	78 (as of 2017)	'Battenin' (CLN3)	Transmembrane	Lysosomal	Juvenile* protracted, **retinitis pigmentosa**
CLN4	Parry disease	Adult-onset NCL (ANCL)	*DNAJC5/CLN4*	20q13.33	3 (as of 2019)	DnaJ homolog subfamily C member 5 aka cysteine string protein α (CSPα)	Vesicle-associated membrane protein (VAMP)	Cytoplasm and membranes of vesicles in the presynaptic terminal	Autosomal dominant adult onset
CLN5	Kufs disease	Finnish late infantile NCL (fLINCL)	*CLN5*	13q21.3-32	37 (as of 2017)	Ceroid-lipofuscinosis neuronal protein 5 (CLN5)	Soluble	Lysosomal	Late infantile*, Juvenile, protracted, adult
CLN6	Lake-Cavanagh disease or Kufs disease (type A)	Variant late infantile NCL (vLINCL)	*CLN6*	15q23	70 (as of 2017)	Ceroid-lipofuscinosis neuronal protein 6 (CLN6)	Transmembrane	ER	Late infantile*, Protracted, adult (Kufs, type A), **teenage progressive myoclonic epilepsy**
CLN7	na	Turkish late infantile	*MFSD8/CLN7*	4q28.2	39 (as of 2017)	Major facilitator superfamily domain	Transmembrane	Lysosomal	Late infantile*, juvenile protracted

		NCL (tLINCL)				containing 8 (MFSD8)			
CLN8	Northern Epilepsy/EPMR	Variant late infantile NCL (vLINCL)	*CLN8*	8p23	35 (as of 2017)	Ceroid-lipofuscinosis neuronal protein 8	Transmembrane	ER and/or ER-Golgi	Late infantile*, **Northern epilepsy aka progressive epilepsy with mental retardation (EPMR)**
CLN9	Variant Juvenile NCL (VJNCL)	NA	*CLN9* (proposed locus)	Unidentified	Any JNCL that isn't CLN3-associated	Ceroid-lipofuscinosis neuronal protein 9 (proposed)	Unidentified	Unidentified	Non-CLN3 juvenile
CLN10	Congenital NCL or Kufs disease	Congenital NCL	*CTSD/CLN10*	11p15.5	10 (as of 2017)	Cathepsin D	Soluble	Lysosomal	Congenital*, late infantile, juvenile, adult
CLN11	Kufs disease	Adult NCL	*GRN/CLN11*	17q21.32	3 (as of 2017)	Progranulin	Soluble/Secreted	Secreted/the lumen of secreted vesicles	Adult*, **frontotemporal lobar dementia**
CLN12	NA	Parkinson disease 9	*CLN12/ATP13A2*	1p36.13	1 (as of 2017)	Cation-transporting ATPase 13A2	Transmembrane		Variant juvenile, **Kufor-Rakeb syndrome**
CLN13	NA	-	*CLN13/CTSF*	11q13.2	11 (as of 2017)	Ceroid-lipofuscinosis neuronal protein 13	Soluble	Lysosomal	Adult (Kufs, type B)
CLN14	NA	-	*CLN14/KCTD7*	7q11.21	1 (as of 2017)	Potassium channel tetramerisation domain containing 7	Associated with cellular membranes	Cytosomal	Infantile, p**rogressive myoclonic epilepsy-3, opsoclonus-myoclonus ataxia-like syndrome**
CLCN6	NA	-	*CLCN6*	1p36.22	2 (as of 2017)	Chloride transport protein 6	Associated with endosomal membranes	Endosomal	Adult
SGSH	NA	-	-	-	2 (as of 2017)	N-sulphoglucosamine sulphohydrolase	Soluble	Lysosomal	Adult, **late infantile MPSIIIA**

Table 1.1 | Summary table of human NCL variants, based on a genetic classification system. Clinical phenotype: * indicates the disease phenotype experienced by complete loss of function of the related gene, while bolded phenotypes are non-NCL disorders that can be caused by mutations in the same gene. Most of the information for this table was taken from *Mole & Cotman., 2015*.

1.3 NCL genes and proteins

Despite having similar, sometimes clinically indistinguishable, phenotypes, the era of genetics taught researchers and clinicians that the NCLs were a group of genetically distinct disorders, demonstrating a high degree of locus heterogeneity between variants, with 14 genes implicated in their pathology at time of publication. There are also currently families with NCL-like syndromes which remain genetically undetermined (Mole & Cotman, 2015).

All known NCL genes, often referred to as the 'ceroid lipofuscinosis neuronal' (*CLN*) genes, are located on autosomal chromosomes and, with two notable exceptions, are inherited in a Mendelian recessive manner. In 2011, Noskova et al. identified an autosomal dominant mutation in the *DNAJ5* gene as the underlying cause of adult onset CLN4 Batten disease (Nosková et al., 2011). The only other example of non-recessive inheritance in the NCLs was an extremely rare instance of non-Mendelian uniparental disomy, in which the proband received only one copy of chromosome 8 from their mother, instead of a copy from each parent, and this chromosome replicated itself ('complete isodisomy') to form a homologous pair and, as a result, a homozygous mutation in the *CLN8* gene (Vantaggiato et al., 2009).

As previously mentioned, the majority of *CLN* genes have been found to encode proteins involved in the endosomal-autophagic-lysosomal compartment and secretory vesicle pathways – with the majority being either lysosomal enzymes involved in the intraluminal degradation of cellular waste (CLN1/PPT1, CLN2/TPP1, CLN5, CLN10/CTSD and CLN13/CTSF) or lysosomal transmembrane proteins (CLN3, CLN7, and CLN13). CLN6 and CLN8, however, localise to the endoplasmic reticulum (ER), while progranulin (CLN11/GRN) is found in the lumen of secretory vesicles. CLN4 and CLN14 are cytoplasmic proteins and are peripherally

associated with cellular/vesicular membranes. CLN9 has been hypothesised but not yet identified (Mole & Cotman, 2015; Schulz et al., 2004).

Our understanding of the gene-protein relationship that underpins each variant of NCL is critically important when it comes to potential treatment strategies, as is our understanding of the functions and structures of NCL proteins under both physiological and pathological conditions. The NCL forms caused by enzyme dysfunction or deficiency, for example, are excellent candidates for enzyme replacement therapies (see **section 1.6.1**), whereas the variants caused by mutations in transmembrane or uncharacterised proteins prove to be less compatible with such approaches and thus provide unique therapeutic challenges.

To further complicate the development of effective treatment strategies, each variant of the NCL appears to demonstrate some degree of allelic heterogeneity. This can result in varying ages of onset, in disease severity, and disease progression between patients with different mutations in the same gene. There are also known cases of mutations in different *CLN* genes causing clinically similar phenotypes (mutations in *CLN5*, *CLN6*, *CLN7* and *CLN8* have all been known to cause late infantile onset)(Mole & Cotman, 2015). Finally, there are also several instances of mutations within the *CLN* genes giving rise to non-NCL diseases (**Table 1.1**). This non-linear and, at times, unpredictable genotype-phenotype relationship can make differential diagnosis difficult and may complicate potential future therapies by delaying the start of treatment, which may have serious consequences – as preclinical data have shown that early intervention is critical in neurodegeneration (Cabrera-Salazar et al., 2007).

1.4 Animal models

The study of disease mechanisms and potential therapeutics for diseases as complex as the NCLs wouldn't be possible without readily available animal models. Fortunately, the NCLs lend themselves to model systems, with the *CLN* genes being highly conserved across mammalian species, and translational studies using both naturally occurring and genetically engineered forms of NCLs in animals have been at the core of NCL research for many decades (Cooper, 2003). The use of animal models has allowed researchers to move beyond the post-mortem snapshot of human autopsy and given them access to any tissue, at any time-point, from early stages of development until death. Beyond this, behavioural assays of well-characterised animal models allow for efficacy studies of potential therapeutics in a controlled, closed system that wouldn't be possible with human patients.

In order to be established as a tool to study a human NCL variant, each animal model needs to, at a minimum, exhibit the three key pathological NCL phenotypes: (1) progressive neurodegeneration, (2) neuroinflammation, and (3) the presence of intraneural, autofluorescent storage material. Today, there are a variety of different model organisms that have been designed to or naturally meet these criteria for each form of NCL – including several non-vertebrates – and each has its own advantages and disadvantages (Phillips et al., 2006). This section will only cover vertebrates used for NCL research, as only these models can be used for the type of preclinical research that makes up the practical component of this thesis.

1.4.1 Small animal models

Rodents, specifically mice (*Mus musculus*) and rats (*Rattus norvegicus domestica*), have been the preferred animal model in many of the life sciences for over a century. Murine (mouse) models in particular have played a key role in translational NCL research. They have proven to

be excellent research tools due to their availability, relatively low cost, ease of use and manipulation, and rapid reproductive cycle. Inbred strains of rodents are particularly useful when studying genetic disorders such as the NCLs, as they are bred to be genetically identical and this reduces variability in genotype and phenotype (Cooper, 2003; Fox et al., 2006). The most successful murine models used in NCL research today are those that demonstrate these qualities along with analogous symptoms, age of disease onset and rate of disease progression as their human counterparts – scaled, of course, due to the fact that healthy mice have considerably shorter lifespans than humans (see **section 1.7.4**).

Today, there are eighteen murine strains available to researchers, summarised in **Table 1.2**, which model the CLN1 (x2), CLN2 (x2), CLN3 (x4), CLN5 (x1), CLN6 (x1), CLN8 (x1), and CLN10 (x1) variants, along with a series of 'NCL-like' syndromes (x7)(Eliason et al., 2007; Gao et al., 2002; Glascock et al., 2011b; Gupta et al., 2001; Jalanko et al., 2005; Katz et al., 1999; Mitchison et al., 1999; Mole, 2018; Morgan et al., 2013; Sleat et al., 2004; Wheeler et al., 2002). Murine models can either be genetically engineered (as is the case with the CLN1, CLN2, CLN3, CLN10 and NCL-like syndrome models) or be 'naturally occurring' (as the CLN6 and CLN8 models are) (Bronson et al., 1999; Messer & Flaherty, 1986; Ranta et al., 1999; Wheeler et al., 2002). Genetically engineered NCL mice have been made using a selectable marker (Gupta et al., 2001; Katz et al., 1999; Kopra et al., 2004) or *cre-lox* technology (Cotman et al., 2002). The majority of the NCL murine models used today have been bred or engineered from a small subset of mouse strains, including the Jackson Laboratory's C57 Black 6 (C57Bl/6) mouse, which allows for meaningful comparisons to be made between the different disease forms.

Table 1.2 | Summary table of currently available NCL mouse models.

Form of NCL	Mouse Model	Creation method	Reference
CLN1	$Ppt1^{\Delta ex4}$	Targetted deletion via *cre/lox* technology	*Jalanko et al., 2005*
	$Ppt1^{-/-}$	Knockout cassette	*Gupta et al., 2001*
CLN2	$Tpp1^{-/-}$	Targeted Arg447His point mutation via *cre/lox* technology	*Sleat et al., 2004*
	$Cln2^{R207X/R207X}$	Combination of targeted nonsense mutation via *cre/lox* and flipase-mediated excision of a neo cassette	*Geraets et al., 2017*
CLN3	$Cln3^{\Delta ex1-6}$	Mutation knock-in	*Mitchison et al., 1999*
	$Cln3^{\Delta ex7/8}$	Mutation knock-in	*Cotman et al., 2002*
	$Cln3^{\Delta ex7/8neo}$	Neo cassette deletion	*Katz et al., 1999*
	$Cln3^{lacZ/lacZ}$	*lacZ* knock-in	*Eliason et al., 2007*
CLN5	$Cln5^{-/-}$	Neo cassette deletion	*Kopra et al., 2004*
CLN6	$Cln6^{nclf}$ aka 'nclf'	Naturally occurring	*Bronson et al., 1998*
CLN7	$Msfd8^{(tma1)}$	l*acZ* knock-in	*Damme et al., 2014*
CLN8	$Cln8^{mnd}$ aka 'mnd'	Naturally occuring	*Bronson et al., 1993 and Chang et al., 1994*
CLN10	$Ctsd^{-/-}$	Neo cassette deletion	*Partanen et al., 2003*
NCL-like syndromes	$Clcn3^{-/-}$	*Cln3* replacement vector	*Dickerson et al., 2002*
	Clcn6	Knockout cassette	*Poët et al., 2006*
	$Clcn7^{-/-}$	Knockout cassette	*Kornak et al., 2001*
	Grey lethal (gl)	Naturally occuring	*Chalhoub et al., 2003*
	ctsf	Neo cassette deletion	*Tang et al., 2006.*
	Ctsb/l	Neo cassette deletion	*Roth et al., 2000.*

While less common in NCL research, the tropical zebrafish (*Danio rerio*) has also been known to lend itself to the study of human health and disease. Zebrafish have been utilised by several research groups looking into fundamental biology of the NCLs, as well as the potential of experimental therapeutics such as gene therapy and/or CRISPR-Cas technology (Russell & Mahmood, 2011; Wlodawer et al., 2003). Genetically, several zebrafish genes have been discovered to be homologous with all currently identified human *CLN* genes, though the fact that the zebrafish genome underwent duplication during teleost evolution (reviewed in Blomme et al., 2006) means that some *CLN* genes have more than one potential orthologue, such as CLN4/DNAJC5, CLN6 and CLN7/MFSD8. Whether all these candidate zebrafish genes

are ‘true’ orthologues, or now have an unrelated subspecialisation, is an area of ongoing investigation (Bond et al., 2013).

The major advantages of zebrafish models pertain mostly to their well-characterised CNS and their ability to produce large numbers of offspring via external fertilization, allowing for manipulation to occur at any point from fertilization onwards (Bond et al., 2013; Schmid & Haass, 2013; Wang et al., 2007). Their young also develop in clear, external embryonic sacs – allowing for observation of key phases of prenatal development. These are some of the factors that make zebrafish excellent tools for fast, high-throughput experiments, such as drug discovery or toxicity assays (Kalueff et al., 2014) and an interesting candidate model organism for NCL work relating to prenatal pathologies.

1.4.2 Large animal models

While not as common in NCL studies, the use of large animals, defined as any non-rodent mammal used in research, offers distinct advantages over smaller animal models – primarily due to their closer mimicry of human NCL pathology and anatomical similarities (Casal & Haskins, 2006). Rodents, for example, have lissencephalic brains – that is, they lack the folds (gyri and sulci) present in the human cortex – and this, along with the obvious disparity in brain size and brain-to-body ratio, may account for many of the behavioural and histopathological differences observed between the mouse and human forms of NCL . Larger animals offer researchers a bridge between NCL studies conducted in rodents and fish and clinical trials in humans, due to their larger gyrencephalic brains, more complex body systems and ability to recapitulate a larger spectrum of the NCL symptoms experienced by human patients.

The use of large animals in NCL research has also provided access to a wide range of naturally occurring, directly orthologous NCL variant models. This makes them a precious

resource considering there are only two naturally occurring murine models – Cln6^{nclf} (CLN6 BD) and mnd (CLN8 BD) mice – and that zebrafish models are somewhat complicated by a series of unique evolutionary diversification events. The use of naturally occurring NCL models is arguably preferable to bioengineered ones, in that they are less expensive and time-consuming to produce, circumvent ethical issues related to the creation of transgenic organisms and are often less likely to display symptoms or side-effects unrelated to the human NCL pathology they are modelling. A variety of naturally-occurring NCL models have been discovered in sheep (CLN5, CLN6, and CLN10), dogs (CLN1, CLN2, CLN6, CLN8, and CLN10), cattle (CLN5), and non-human primates (CLN7), and several NCL-like syndromes have been described in cats and goats, though the genetic basis of these have yet to be identified (Awano et al., 2006; Cook et al., 2002; Houweling et al., 2006; Jolly & West, 1976; Katz et al., 2005; Koppang, 1992; Melville et al., 2005; Chalkley et al., 2014). Alongside these, a transgenic CLN3 porcine (pig) model was characterised for the first time in mid-2019 (Johnson & Sturdevant, et al., 2019).

1.5 Proposed mechanism(s) of disease for the NCLs

In order to determine the where, when and how of potential new NCL therapies, it is critical for researchers to better define disease onset and progression. The work that has done so far points to the fact that, despite these diseases having similar key features and phenotypes to each other and other LSDs, the mechanisms by which these are reached are probably quite different between variants (Palmer et al., 2013).

This section contains an overview of the work that has been done across the NCLs to characterise their similarities and elicit their pathophysiological differences and its purpose is to better contextualise the therapies under investigation in this thesis' practical component. It should be noted that this is by no means a comprehensive discussion of the minutiae of NCL pathophysiology and, due to the many outstanding questions that remain areas of ongoing enquiry, the features discussed below are not presented in the clean, chronological order of events that one would desire when discussing the natural history of a disease. It is not possible, at this stage, to move from mutated gene to mutated protein to affected cell pathway to the multitude of characteristic phenotypes associated with the NCLs, so instead aspects of pathophysiology will be presented as isolated vignettes, and discussion will focus on what we know so far, and how we know it. This approach is intended to provide a solid biological background for later sections on potential therapeutics for the NCLs in general and, more specifically, the therapies chosen for investigation in this thesis.

1.5.1 The pronounced vulnerability of the CNS to NCL pathology

The NCLs are, indisputably, neurological disorders. Despite the CLN proteins being ubiquitously expressed in of the cells in the human body, it is, invariably, the progressive, accelerated loss of neurons that results in the spectrum of debilitating symptoms and

premature deaths of NCL patients (Autti et al., 1992; Jadav et al., 2014; Mitchison et al., 2004). Researchers remain uncertain why this particular population of cells demonstrates such vulnerability to the effects of mutated *CLN* genes compared to somatic cells, but some suggest it may be due to the post-mitotic nature of neurons and their limited capacity for renewal or replacement (Mitchison et al., 2004). Others suggest that the protein products of *CLN* genes may possess neuron-specific roles critical for the survival of these cells (Lehtovirta, 2001; Luiro, 2001). The PPT1 protein, for example, which was characterised as a lysosomal hydrolase in the 90s, was found to be targeted to the axons in neurons and to differ in size and modification from PPT1 extracted from fibroblasts (Ahtiainen et al., 2003; Heinonen et al., 2000; Lyly et al., 2007).

It is also possible that the endosomal-lysosomal pathway protein expression profile of neurons leaves them more vulnerable to errors in this pathway. For instance, neurons do not express cathepsin C, a lysosomal protease with compensatory activity related to that of CLN protein TPP1. This mean that, in the absence of TPP1 (CLN2), any substrates that TPP1 would normally cleave for lysosomal degradation in neural cells remain intact, building up in the brain's lysosomes and potentially contributing to the progression of CLN2 BD. Non-neural tissue, in comparison, is spared due to the somatic expression of cathepsin C which has extensive activity on TPP1's substrates and can compensate (Bernardini & Warburton, 2002).

These theories are challenged, however, by the paradoxical relative expression levels of CLN proteins in neural tissue compared to the rest of the body. There appears to be no direct relationship between the expression levels of the NCL proteins and the extent of degradation experienced by cells in their absence, since many tissues and organs in the body express far higher levels of CLN proteins than neurons and appear to experience little, if any negative consequences from their absence (Palmer et al., 2013). That being said, it should not

be assumed that these non-neural tissues are completely unaffected. Many demonstrate a build-up of storage material similar to that seen in nervous tissue, in fact NCL diagnoses traditionally rely on skin and rectal biopsies, and some animal NCL models have displayed extra-neural pathology such as splenomegaly (Brett & Lake, 1975; Cotman et al., 2002). It is possible that, given enough time, these tissues would also begin to experience deleterious effects from *CLN* mutations – perhaps the slowing or cure of neurodegeneration will result in the uncovering of further disease complications in other organs and cell groups (Rietdorf et al., 2019).

1.5.2 Selective regional and neuronal loss within the CNS

While neurodegeneration is a common feature across all variants of human NCL, the regional and temporal distribution of neural atrophy is highly heterogenous. Histopathological analysis of patients' brains at autopsy have demonstrated that while cerebellar, cortical and hippocampal regions of the brain appear to be affected across the spectrum of NCL variants, there are markedly graded effects on neuronal survival in different regions of the brain. Animal models have been critical in studying these differences, though they are complicated by inter-species differences and the influence of strain background and mutation type on comparative studies.

While initial studies focused on the cerebral cortex as the principal pathological target for the NCLs, investigations in several mouse NCL models (including CLN1, CLN8 and CLN10) have indicated that the loss of thalamic nuclei and relay neurons proceeds any cortical degeneration, identifying the thalamus as having a key, if still uncharacterised, role in the pathology of most types of NCL (Kielar et al., 2007; Kuronen, 2012; Partanen et al., 2008). These studies also confirmed previous observations of the apparently targeted degeneration of somatosensory regions with the brain. A recent study in ctsd mice, for example, found early

thalamic neurodegeneration to occur only in the ventroposterior medial and ventroposterior lateral (VPM/VPL) nuclei and not in neighbouring thalamic structures. The VPM/VPL nuclei are key components of the somatosensory system, responsible for receiving somatosensory information from lower brain centres and relaying it to higher cortical somatosensory regions. The fact that these particular nuclei were found to be singularly affected early in disease pathogenesis complements older studies in cadaver tissue and other animal models that indicated neuron loss occurs earlier and is far more pronounced in somatosensory regions of the cortical mantle than motor areas, as it is these regions that are directly connected to the VPM/VPL.

However, these findings, like most aspects of NCL pathology, are not universal – with a study in the CLN5 BD mouse model indicating a cortical origin for neuron loss, which only subsequently occurs in the thalamus (von Schantz et al., 2009). This study echoes similar work done in the CLN6 South Hampshire sheep model (OCLN6), where characteristic NCL changes, like loss of GABAergic interneurons in the thalamus, were not seen until after changes in the neocortex and cerebral hemispheres had occurred (Oswald et al., 2001, 2005, 2008).

1.5.3 Glial cell activation and neuroinflammation

Neuroinflammation refers to the complex cellular and biochemical responses of the nervous system to trauma, infection or neurodegeneration. This innate immune response has been linked to many lysosomal storage and neurodegenerative diseases including Alzheimer's disease (AD), Parkinson's disease (PD) and the NCLs, though whether this response is protective or a contributing factor to disease progression has yet to be determined (W. W. Chen et al., 2016; Heneka et al., 2015; Hirsch et al., 2012).

Glial cells within the CNS, particularly microglia, are responsible for maintaining tissue homeostasis and responding to pathological stimuli. As the resident immune cells, it is the

microglias role to survey the microenvironment in the brain and spinal cord and produce chemicals that influence the activity of neighbouring astrocytes (another type of glial cell) and neurons.

Under normal, healthy circumstances, microglia and astrocytes demonstrate deactivated phenotypes that promote cellular function through neurotropic and anti-inflammatory factors. Under pathological conditions, however, glial cells become 'activated' and prompt an inflammatory response to help engage the immune system and/or begin repairs to tissue damage. This response is supposed to be transient and self-limiting, with the tissue eventually transitioning back to a deactivated state once the infection has been cleared or tissue damage has been resolved.

Chronic inflammation of the nervous system can occur, and usually indicates the either some component of the immune response has failed to self-regulate or that the underlying inflammatory stimulus still persists. While a normal neuroinflammatory response can be neuroprotective, persistent, uncontrolled inflammation of the CNS can result in the build-up of neurotoxic materials and/or amplify neurodegenerative processes.

Glial cell activation is a key pathophysiological feature shared by all the NCL variants, though the regions of the CNS in which this activation occurs, along with it's timing during disease progression, varies from form to form (Cooper et al., 2015). Originally, it was assumed that chronic inflammation seen in the NCLs was a protective response to the pathological accumulation of autofluorescent storage material in cells. This hypothesis has been challenged in recent years by several studies in animal models that show glial activation and the inflammatory response are present far earlier in disease progression than first assumed, before storage material has even begun to accumulate, and is a far better predictor of future neurodegeneration than the presence of storage bodies.

Neuroinflammation can be identified, post-mortem, using a variety of markers including the upregulated expression of inflammation-associated genes, increased extra-cellular levels of pro-inflammatory factors like chemokines or cytokines, staining for activation markers on microglia and astrocytes, the presence of lymphocytes in CNS tissue and/or increased production of auto-antibodies. Some, if not all, of these markers have been used to identify the presence of neuroinflammation in animal and human NCL tissue samples, firmly establishing it as a ubiquitous feature in all known NCL variants.

1.5.4 Malfunction of the endosomal-lysosomal-secretory compartment and imparied autophagy

It should be evident, by now, that the NCLs are the result of the dysfunction or absence of one or more proteins within the endosomal-lysosomal-secretory compartment. Every *CLN* gene identified to date encodes a protein or enzyme that has been associated with the lysosome, ER or secretory vesicles in some way – a fact that played a key role in the NCLs' reclassification as LSDs. To the unitiated, it can seem strange to refer to distinct organelles such as lysosomes, the ER and vesicles as a pathway or 'compartment', but several decades of research has determined that these unique cellular components are closely associated due to their roles in a wide variety of complex , important and interlinked cellular processes. While many, if not all, of these processes are critical to cellular homeostasis and therefore relevant to the study of neurodegeneration, one pathway in particular, autophagy, has distinguished itself as potentially critical to the natural history of neurodegenerative storage disorders like the NCLs.

Autophagy, meaning 'self-eating' (from the Greek *auto-* for 'self' and *phagy* for 'eating'), is a term used to describe several complex and strictly regulated pathways by which the cell degrades, recycles and removes damaged or unnecessary materials (Klionksy, 2008; de Duve, 1962). To date, three forms of autophagy have been described: *micro*autophagy, where degradative bodies like the lysosome directly engulf cytoplasmic material via

membrane invagination; *chaperone-mediated* autophagy, where materials are tagged and targeted to the lysosome for degradation via intermediary chaperone-proteins, and; *macro*autophagy, the process where expendable components of the cell are isolated and targetted to various degradative bodies within a double-membraned vesicle called the autophagolysosome (Wattiaux, 1966; de Duve, 1963; Kaushik et al., 2012). Macroautophagy, which will hereafter be referred to simply as 'autophagy', is of particular relevance to the NCLs and other neurodegenerative disorders, as it is this process that is responsible for the majority of cellular waste turnover and because neurons seem to demonstrate a singular vulnerability to autophagic dysfunction compared to other cell populations. Why this is the case remains unclear, though it has been hypothesised that because of their size, extreme polarization and post-mitotic nature, neurons are more dependent on autophagy for survival (Tooze et al., 2008). Whatever the reason may be, the relationship between autophagic function and neurodegeneration is clear, with patients with neurodegenerative diseases, such as AD or spinal-bulbar muscular dystrophy, having been found to possess an inordinantly high frequency of mutations in autophagy-related genes (*ATG* genes)(Nixon, 2013).

Autophagy can be described as a series of vesicle fusion events that target, encapsulate and eventually degrade cytosolic materials in a repetitive process often referred to as autophagic flux. It can be broken down into five primary stages: (1) induction, (2) nucleation, (3) elongation and maturation, (4) lysosomal fusion and, (5) content degradation (**Figure 1.4**). The process is initated by a cytoplasmic protein-structure known as the 'pre-autophagosomal structure' or 'phagophore assembly site' (PAS). From this, a double-membraned compartment known as the phagophore is formed, which elongates to surround and isolate cytoplasmic materials targeted for degradation. Once the membrane of the phagophore fuses, creating a complete compartment, it forms the mature autophagosome. This structure then fuses with

a lysosome, forming an autolysosome, and releases its contents into the lysosome's highly acidic lumen. The autophagosome and its contents are consequently broken down into their constitutent parts by the lysosome's hydrolases, and these parts are then either released back into the cytoplasm, chaperoned to other parts of the cell for recycling, or removed from the cell entirely by secretory pathways (Wang, 2003).

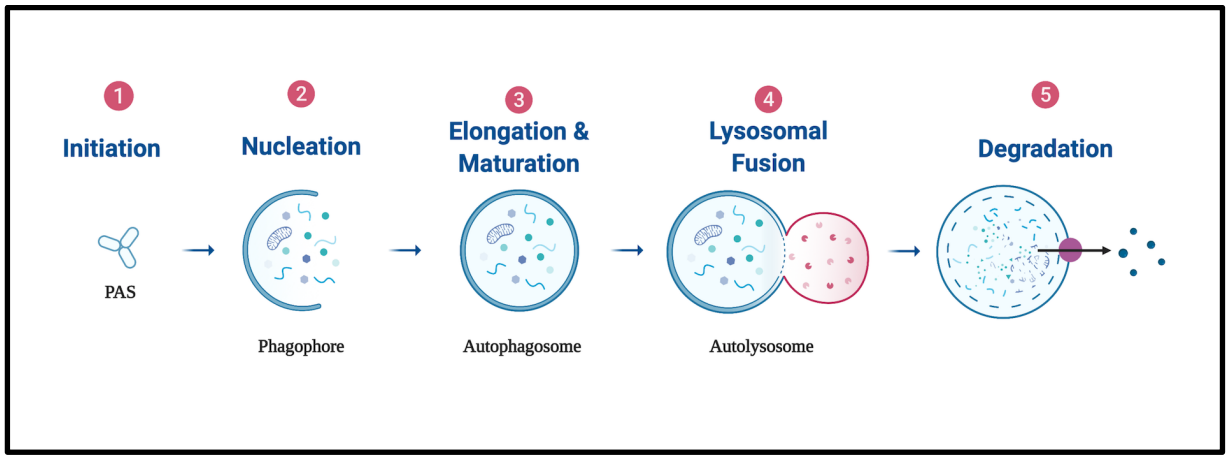

Figure 1.4 | Overview of the macroautophagic pathway. Autophagy is comprised of five main stages or phases: (1) Initiation, where the cytosolic pre-autophagosomal structure (PAS) begins to construct a lipid-based membrane, usually in response to some environmental stressor/cellular signalling; (2) Nucleation, a double-membraned structure is formed – the phagophore - and begins to encircle cytoplasmic constituents tagged for degradation; (3) Elongation and maturation, Once the phagophore has completely sequestered the cytoplasmic constituents and both ends of the membrane have sealed, the structure is now known as the autophagosome; (4) Lysosomal fusion, the autophagosome fuses with a lysosome and releases its contents in the lysosome's acidic lumen; (5) The cytosolic material, along with the autophagosome structure itself, are degraded by lysosomal hydrolases. Image made by author using *Biorender.com*.

Autophagy alterations have been reported in several NCL *in vitro* and *in vivo* models, implicating its dysfunction as a shared feature of these disorders. In fact, one of the key hallmarks of the NCLs – the accumulation of lysosomal storage material – is itself an indication of some form of autophagy-related inhibition and lysosomal clearance. Further evidence of autophagic dysfunction in the NCLs includes the abnormally high levels of a protein closely associated with the formation of autophagosomal membranes, known as LC3-II, that has been detected in the nervous tissue of Cln3$^{\Delta ex7/8}$, Cln6^{nclf} and Cln10/ctsd mice, which indicates hyperactive autophagic function (Thelen et al., 2012). More recently, a study using CLN7-deficient mice found a build-up of autophagosomes and other autophagy-related substrates,

suggesting the absence or dysfunction of the CLN7 protein might be causing a block in autophagic flux. Similar accumulations of autophagic components have been seen in fibroblasts derived from CLN6 BD patients (Brandenstein, 2015; Cannelli et al., 2009). A pathological increase in autophagic and lysosomal compartments, associated with defective autosome maturation, has also been identified in CLN2 and CLN3 patient-specific induced pluritpotent stem cell (iPSC)-derived neuronal cells (Vidal-Donet et al., 2013), though the mechanism by which these changes occur in CLN3 patients is still unknown – due primarily to the fact that the function of CLN3 has yet to be elicited.

Many questions remain as to autophagy's role in the pathophysiology of neurodegenerative storage diseases like the NCLs. In fact, there is still debate regarding whether the autophagic changes seen in neurodegeneration are the consequence of pathology or cellular attempts to rescue the cell from environmental stressors (Colacurcio et al., 2018; Tooze & Schiavo, 2008). Either way, autophagy presents as a key area of research for the NCLs, especially because the pathway offers several opportunities for therapeutic intervention. Many compounds, both naturally occuring and synthetic, have been found to act on different parts of the autophagic pathway, from the upregulation or inhibition of key autophagic genes, to the augmentation or circumvention of specific events within the pathway that may be affected by dysfunctional NCL proteins. While still in its infancy, autophagic modulation therapy is an exciting new field of research for researchers and clinicians and will be discussed in more detail in the following section.

1.6 NCL disease management and treatment strategies

Due to their unique pathophysiology, neurodegenerative diseases such as the NCLs present researchers and clinicians with a wide range of therapeutic challenges and considerations. These include: (a) developing an effective, comprehensive and non-toxic treatment that addresses both the underlying pathology and symptoms of a specific NCL variant in humans, (b) circumnavigating any potential host immune response that might be elicited from the introduction of foreign or novel protein-based therapies; (c) determining the optimum therapeutic window for treatment, (d) establishing either long-term and/or non-invasive means of therapy administration and outcome measurements and, (e) overcoming the unique practical obstacles presented by a systemic disease that primarily targets, but is not limited to, the nervous system.

There is currently no cure for any variant of NCL, and the majority of therapies available to date tend to focus on symptom amelioration and palliative care. Several experimental treatments have become available in recent years that seem to hold promise, if not as a complete cure then at least in terms of slowing disease progression. The clinical data regarding the long term efficacy of these treatments, however, is scarce – with many funded after only a single, short-term clinical trial – and the future of patients who take them is by no means secured. In light of this, it remains critical that NCL research remains focused on improving the therapies that are already available, investigating the potential of combination or complementary treatments and on generating new therapeutic technologies.

Aside from the treatments themselves, another critical area of concern for those hoping to develop a cure is the timing of therapeutic intervention. With the exception of CLN10, where diagnosis usually occurs at birth, most NCL patients are usually only diagnosed

after they start presenting with symptoms, which means that a lot of neurological damage may have already been done before they start receiving treatment. Preclinical studies have shown that even the most promising of experimental therapeutics have limited efficacy when administered at later stages of disease progression (Cabrera-Salazar et al., 2007; Sondhi et al., 2008). This means an optimal therapeutic window for every NCL variant needs to be identified and taken advantage of. Whether this is done by neonatal screening programmes or through the use of novel biomarker tests at specific ages will depend on the unique biology of each variant, as well as practical and economic factors.

NCL variants caused by the dysfunction or absence of an integral transmembrane protein, such as CLN6, CLN7, CLN8 and CLN12 (**Table 1.1**), have been said to offer an even greater therapeutic challenge due to their apparent resistance to some of the more successful NCL therapies being developed, such as enzyme replacement therapy (ERT; **section 1.6.1**). Why this is the case is still unknown, but possibly due to the inability of exogenous proteins to embed themselves in the appropriate membrane without the correct post-translational modifications an endogenous protein would normally receive when generated within the cell. Additionally, these proteins are unable to be secreted and transferred in therapeutic concentrations to neighbouring cells, a process that is observed in soluble protein variants of NCL treated with ERT and is known as 'cross-correction'. The absence of cross-correction in transmembrane variants of NCL means that each cell within the CNS, or at least the large majority, needs to be individually targetted by a potential therapy in order to achieve an effective amelioration of the disease phenotype (Cooper, 2008).

1.6.1 Enzyme replacement therapy (ERT)

As its name suggest, enzyme replacement therapy (ERT), is a therapeutic strategy that replaces absent or deficient enzymes in the cell, traditionally via intravenous (IV) infusion. The

technique was first proposed in the mid-1960s by Christian de Duve – the same researcher who identified and characterised the lysosome in the mid-50s – and his collaborator Roscoe Brady (de Duve, 1964). In terms of treating metabolic disorders, such as LSDs, ERT has proved to be the most successful therapy to date. The first commercially available ERT product, Algucerase, received orphan drug approval from the FDA in 1991 as a treatment for Gaucher's disease (Weinreb et al., 2002). It has since been successfully trialled as a therapy for Fabry disease (Schaefer et al., 2009) and Pompe disease (Angelini & Semplicini, 2012).

Four NCL variants are known to be the result of lysosomal enzyme deficiencies, CLN1 (PPT1), CLN2 (TPP1), CLN10 (CTSD) and CLN13 (CTSF), making them prime candidates for ERT. Preclinical ERT studies for the NCLs, to date, have focused primarily on CLN1/PPT1 and CLN2/TPP1. Intraveous and intrathecal delivery systems of ERT have been tested and proven to be well tolerated in Ppt1 knockout ($Ppt1^{-/-}$) mice, with purified recombinant PPT1 causing significant clearance of storage material from peripheral tissues and a reduction in astrocytosis and glial activation (Hu et al., 2012; Lu et al., 2010, 2015). Notably, storage material in the brain tissue of these mice was found to be less effectively cleared by the therapy than in their somatic tissue – highlighting the challenge the blood brain barrier (BBB) presents to the development of effective therapeutic strategies for neurological disorders such as the NCLs. Permeabilisation of the BBB is possible, in fact several proof-of-concept studies have been conducted in rodent models, but it appears that currently available techniques risk further exacerbating neuronal damage (da Fonseca et al., 2014; Neuwelt et al., 1981; Rite et al., 2007; Saraiva et al., 2016; Young et al., 2004).

Since the risks of BBB permeabilization still appear too great, researchers and clinicians have sought out other methods of circumventing the BBB. It is for this reason that ICV and intrathecal modes of delivery have become more popular than the more traditional

intravenous route for ERT treatment of neurological disorders. Initial safety tests of recombinant TPP1 (for LINCL/CLN2 BD), delivered via catheters implanted into the lateral ventricle (i.c.v) or subarachnoid space (intrathecal), have been conducted in mouse and dog models of CLN2 BD. These delivery methods appeared to be efficacious, resulting in reduced storage material, region-specific neuron loss and neuroinflammation (Chalkley et al., 2014; Chang et al., 2008; Young et al., 2004).

Based on these promising results, the first FDA-approved recombinant enzyme therapeutic for Batten disease, cerliponase alfa (also known as Brinerua or BMN190) was developed by BioMarin Pharmaceutical and evaluated for safety in a clinical phase I/II CLN2 BD study (Trial No. NCT01907087; *Clinicaltrial.gov* 2013), the results of which were published in 2018. The study enlisted 24 CLN2 BD patients, all between the ages of 3 and 16 years of age, all of whom had an intracerebroventricular reservoir and cannula surgically inserted into the lateral ventricle of their right hemisphere. Patients then received either 30, 100 or 300 mg of cerliponase alfa via a 4-hour infusion procedure every second week. Patients on lower doses were slowly escalated up until all participants in the study were receiving 300 mg of the drug each fortnight. The ERT proved a great success, with the dosage being well tolerated and substantially delaying motor, language and cognitive decline in participants compared to historical age-matched controls (Schulz et al., 2018, 2017). The success of the trial has since launched three more, multicentre, multi-national trials (Trial No's. NCT02485899, NCT02678689, NCT02963350, *Clinicaltrials.gov* 2015, 2016).

While ERT has a lot of potential as an effective therapeutic for enzyme based NCLs, it has a lot of obstacles to overcome before it can be considered curative. These include, as previously mentioned, an effective and safe means of crossing the BBB, as well as the need to avoid triggering undesired immunologic reactions in patients with a foreign enzyme. Finally,

there remains a need for a sustained delivery method that doesn't leave patients dependant on fortnightly infusions – an inconvenient and expensive means of treating a chronic disorder. ERT's efficacy as a treatment for the other, non-enzyme-dependent variants of NCL is also limited due to the fact that it can only replace soluble, free-moving enzymes such as PPT1 and TPP1. Many forms of the NCLs, and other LSDs, are caused by the dysfunction integral membrane proteins, often receptors and ligands, and these require localisation to a specific cellular membrane in order to carry out their function. ERT appears to have limited capacity to assist in treating these specific forms of protein-deficiency and so alternative therapeutic strategies are required.

1.6.2 Stem cell therapy (SCT)

Stem cell therapy (SCT), sometimes referred to as 'regenerative medicine', has been explored as a potential therapy in both humans and in several animal models of NCL. Originally, NCL researchers hoped that SCT would allow for the regeneration of cells lost in advanced disease, but it has since been determined that this isn't currently possible in mice, which have smaller brains with 'easier-to-reach' therapeutic targets. In light of this, stem cell research has refocused on preserving what function remains in patients by transplanting cells that secrete a healthy version of the *CLN* gene whose absence or dysfunction underlies a NCL variant's pathology (Mole et al., 2019; Tamaki et al., 2009).

In order for SCT to be successful, cells need to be transplanted in locations where the enzyme they produce can reach the most affected tissues – in the case of the NCLs, this would be the CNS. Transplantation of enzyme-expressing haematopoietic stem cells (HSCs) has been trialled in several peripheral tissues, such as bone marrow and intravenously, but the success of those trials was limited – mostly likely due to the expressed enzyme being unable to cross the BBB (Lake et al., 1997; Lonnqvist et al., 2001).

More recently, SCT research has begun to focus on the use of a specific type of stem cell, known as 'neural progenitor cells' (NPCs; sometimes also called neural stem cells or NSCs). NPCs are particularly useful for the treatment of neurological disorders because they readily differentiate into neurons and are able to integreate with the host's nervous system. Preclincial studies in the $Ppt1^{-/-}$ mouse model demonstrated proof of concept with successful integration and migration of human graft cells after transplantation into the anterior cortex of neonate mice. Not only did the cells integrate, grafted mice also demonstrated reduced autofluoroscent storage material and delayed onset of motor deficits (Tamaki et al., 2009).

Whether such an approach would be successful in the treatment of an NCL variant caused by mutations in a transmembrane protein, as is the case in CLN6 BD, has yet to be seen, though an alternative NPC-based approach, where the cells express neuroprotective factors rather than the deficient enzyme itself, has been trialed in the $Cln6^{nclf}$ mouse model (Jankowiak et al., 2015). In this study, researchers transduced NPCs with a lentivirus expressing ciliary neurotrophic factor (CNTF), which is a cytokine that been proven to rescue retinal degeneration in some animal models (Wen et al., 2012). The CNTF-expressing cells were transplanted via intravitreal injection to one eye of $Cln6^{nclf}$ mice, while cells expressing green fluorescent protein (GFP) were injected into the other as a control. Six weeks post-injection it was found that the NPCs had attached and formed a layer on the retina, where they subsequently differentiated into CNTF-expressing astrocytes. The local presence of this neuroprotective cytokine resulted in increased retinal thickness and upregulated photoreceptors in comparison to the GFP-expressing control (Jankowiak et al., 2015), proving that NPCs have the potential to be at least powerful treatments for some aspects of NCL pathology, such as retinal degeneration, if not curative.

Studies such as these formed the basis of a phase I SCT clinical trial for CLN1 and CLN2 BD (Trial No. NCT00337636, *Clinicaltrials.gov,* 2015). In this trial, human CNS-derived stem cells (HuCNS-SCs) that expressed healthy PPT1 and/or TPP1 protein were transplanted into CLN1 or CLN2 BD via a total of six subcortical injections in both hemispheres. While the treatment was well tolerated and proven safe, and post-mortem PCR analysis of some particpants' brains indicated successful grafting of the HuCNS-SCs, little to no clinical efficacy was observed in terms of slowing or halting disease progression (Selden et al., 2013).

1.6.3 Gene therapy

Viral-mediated gene therapy, despite having a history complicated by dramatic (and even fatal) side-effects in several ill-fated human trials, is emerging once more as one of the most exciting potential therapies for neurodegenerative diseases. Researchers are able to package healthy copies of a gene into a replication-deficient, recombinant virus and exploit the virus's natural tendency to infect cells in order to transfer that gene into a cell or group of cells. This is useful when the target cell or tissues possess a single mutated gene that requires correction, as is the case with the neurons of NCL patients. The healthy gene in the virus can be used by the cell's transcription and translational machinery to create functional, wild-type proteins which, in turn, can compensate for a dysfunctional or absent protein produced by the cell's original, mutated gene (**Figure 1.5**).

Several parameters need to be considered when designing or choosing a viral vector to carry a healthy gene into the CNS, these include (a) the transductive parameters of the virus itself, including the maximum amount of genetic material it can carry, its ability to transduce dividing and/or non-dividing cells, and any cell-specific tropism it might demonstrate; (b) the route of administration; and (c) the expression threshold required for therapeutic efficacy.

The most common viruses used for gene therapy are retroviruses, lentiviruses (LVs), adenoviruses and adeno-associated viruses (AAVs). Each species of virus has its own advantages and limitations, making it more or less suitable as a vector for neurodegenerative diseases such as the NCLs. The use of AAVs for NCL gene therapy has become popular over the past couple of decades due to the diverse number of AAV serotypes or pseudoserotypes available, with 12 serotypes identified so far, and the different properties these serotypes can confer, especially when experimentally recombined.

AAVs are nonenveloped, single-stranded (ss) viruses from the *Parvoviridae* family. Unlike many viruses, AAVs are innately non-pathogenic, elicit poor responses from the host's immune system and have broad cell tropism – meaning they can target and transduce a variety of different tissues efficiently (Naso et al., 2017). The methods by which AAV serotypes actually initiate transduction and penetrate the cell barrier are not well understood, though it is evident that it involves a series of complex interactions between glycan moieties for attachment to the cell surface (Pillay et al., 2017). Once inside the cell, AAVs move their genetic material to the nucleus and there it persists as an episome – a circular plasmid of extra-genomic material. This feature of the AAV life cycle means that there is low risk of insertional mutagenesis occuring within the host genome, but also results in viral genome depletion after a certain number of cell divisions – making AAVs better suited for gene therapy in post-mitotic cell groups, such as neurons (Naso et al., 2017).

Other limitations of AAVs include their delayed expression in transduced cells, as it can take up to 2 weeks for a cell to reach its expression peak post-transduction, and their small size – with ss AAV vectors only able to package up to 4.7 kb of DNA at a time (Ferrari et al., 1996;. McCarty et al., 2003; McCarty, 2008). The use of self-complementary (sc) AAV vectors has helped address the transduction delay experienced when using ss AAVs, as it bypasses the

requirement for DNA synthesis to convert the ss viral DNA into an active, usable double-stranded (ds) piece of DNA. This solution, however, exacerbates the second limitation of AAVs, their small size – as researchers have to package both complementary DNA strands into one viral particle as a single strand that can fold-in on itself once within the cell compartment. This halves the amount of 'space' available for a gene, with a maximum size of 2.3 kb (Naso et al., 2017).

Immunogenecity is also an important consideration when choosing an AAV serotype for use in gene therapy. Wildtype AAVs 'infect' humans regularly, meaning that most people have developed an arsenal of AAV antibodies which can negatively impact the success of gene therapy. The potential for a host immune reaction against the viral vector creates the need for immune screening prior to the administration of gene therapy, and in cases where the patient is found to have developed immunity agains the vector, alternative vectors or even therapies need to be considered (Johnson et al., 2019).

There have been several preclinical trials using a specific AAV serotype derived from rhesus monkeys, AAVrh.10, which has potential as an alternative to the more common serotype used in gene therapy – AAV2 – since most people have not been in direct contact with rhesus monkeys and so may not have had the opportunity to develop immunity against AAVrh.10 (Sondhi et al., 2007, 2012).

The majority of preclinical and clinical NCL gene therapy trials to date have focused on the CLN1/INCL and CLN2/LINCL variants. CLN1 BD was successfully treated via multiple intracranial injections of AAV2 carrying the human gene for PPT1 (*hPPT1*) in $Ppt1^{-/-}$ mice. The virus-mediated therapy increased *PPT1* expression levels and improved some CLN1 phenotypes – including behavioural deficits and accumulation of storage material within the CNS. These improvements, however, were limited – with histopathological changes only

observed near the injection sites, possibly due to the limited distribution of the viral vector (Griffey et al., 2006, 2004, 2005). Intracranial delivery of AAV2 encoding human *CLN2* into $Tpp1^{-/-}$ mice yielded similar, promising yet limited, results (Sondhi et al., 2005; Passini et al., 2006).

Intraventricular administration of AAV2 encoding canine *TPP1* (*caTPP1*) in a canine model of CLN2 BD also saw a reduction in NCL pathology, with reduced glial activation, improved behaviour and increased lifespan. In this study, the vector was administered into the circulating cerebroventricular spinal fluid (CSF), rather than directly into cortical tissue as it was with the $Ppt1^{-/-}$ and $Tpp1^{-/-}$ mice, which appeared to faciliate more widespread transduction of the virus throughout the brain. The majority, however, ended up transducing the ependymal lining of the third and fourth ventricles, meaning large parts of the CNS remained unaffected by the therapy (Vuillemenot et al., 2015).

It became evident from studies such as these that the major limitation of the AAV2 viral vector, a favourite for NCL gene therapy because of its neural tropism and strong levels of transgene expression in local tissue, was its reduced ability to transduce cells throughout the entire CNS from a single administration site. While injection into the CSF appeared to increase the range of transduction to some extent, further measures to promote adequate distribution of the vector throughout the host's CNS were needed. Once such measure included the use of the AAV2 gene expression cassette with capsids (external shells) from other AAV serotypes that were known to have wider transduction distributions. To date, a variety of different combinations have been used experimentally in NCL animal models including AAV2/1, AAV2/5 and AAV2/9 (Cabrera-Salazar et al., 2007; Macauley et al., 2014; Shyng et al., 2017) .

One of these studies, by Cabrera-Salazar et al (2007), looked at the administration of AAV1-*hTPP1* into several different brain regions of presymptomatic 4-week-old and post-symptomatic 11-week old Tpp1$^{-/-}$ mice. Treatment at both ages resulted in pathological and behavioural improvements, though the mice that were treated presymptomatically performed significantly better in every parameter measured versus their post-symptomatic counterparts. This study, and several that have been conducted since, indicates that gene therapy has the potential to be a powerful therapy when applied early in disease progression, but will only be able to delay or prevent the NCL pathology, not reverse it (Cabrera-Salazar et al., 2007; Johnson et al., 2019).

Despite the mixed results of preclinical animal studies, several NCL clinical trials in human patients have been completed or are currently underway. The first of these looked at the safety and efficacy of AAV2/9 for the treatment of CLN2 BD, and involved 10 participants all in the moderate-to-severe stages of CLN2 BD - according to the Steinfeld et al (2002) CLN2 BD phenotype staging system (Trial No. NCT00151216, *Clinicaltrials.gov;* Steinfeld et al., 2002; Worgall et al., 2008). The treatment was found to be well tolerated, with no adverse events, and neurological decline appeared to be delayed or slowed compared to historical non-treated controls (Worgall et al., 2008). This trial has since formed the basis for two more, which are currently ongoing (Trial No. NCT01161576, *Clinicaltrials.gov*; Trial No. NCT01514985, *Clinicaltrials.gov*). There is also a phase I/II clinical trial currently underway that is looking at the safety and efficacy of AAV2/9-*hCLN6* in 12 CLN6 BD patients. This trial is known as the 'Gray Foundation trial' and is one of the primary motivations for the practical component of this thesis (Trial No. NCT02725580, *Clinicaltrials.gov*, see **section 1.7.4** for more detail).

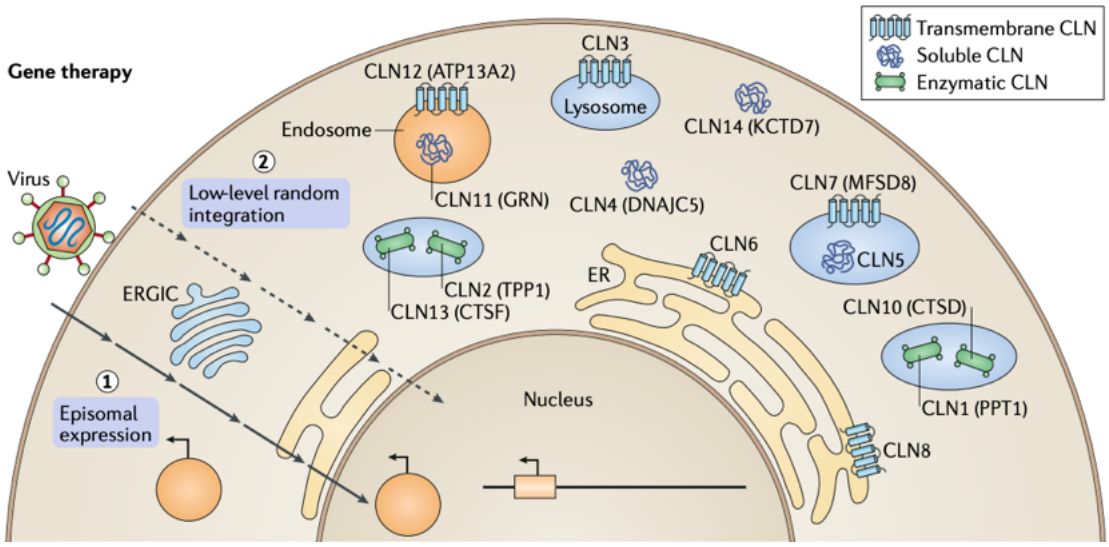

Figure 1.5 | Schematic overview of the principles of viral-mediated gene therapy. Image taken from *Johnson et al., 2019.*

1.6.4 Small molecule therapies

Many different pharmaceutical and biological agents, referred to here as small molecule therapies, have been investigated as potential treatments for the NCL variants over the past few decades. Most of these have been compounds known to target specific aspects of NCL pathophysiology, such as anti-inflammatories, neuroprotective agents, autophagy and/or lysosome function modulators or small molecules that are known to upregulate *CLN*-gene expression (Johnson et al., 2019).

1.6.4.a Anti-inflammatories and neuroprotective agents

Chronic neuroinflammation has been characterised as a key component in all NCL variants and its reduction has shown varying levels of symptom alleviation in several *in vivo* models. Mycophenolate mofetil, an immunosuppressant commonly used to prevent organ rejection, was tested in $Cln3^{-/-}$ mice and found to significantly reduce neuroinflammation and improve motor performance (Seehafer et al., 2011). This work formed the basis of a clinical phase II safety trial in CLN3 BD patients which found that the compound, while safe and well tolerated, was ineffective in reducing, delaying or preventing clinical outcomes in patients

(NCT01399047; *Clinicaltrials.gov*; Augustine et al., 2019). Whether this was due to the drug itself having no effect, or the short time frame of the trial is an area for further investigation.

Other anti-inflammatory compounds that have been investigated in models of NCL include the FDA-approved drug teriflunomide, which inhibits the proliferation of activated immune cells, in $Cln3^{-/-}$ mice, and fingolimod, which stops lymphocytes from emigrating into the CNS, in $Ppt1^{-/-}$ mice. Both were found to reduce cortical and retinal thinning, as well as reduce neuronal death overall (Groh et al., 2017). Steroids have also been trialled clinically as potential treatments, with prednisolone being found to reduce autoantibody levels and improve motor performance in older CLN3 BD patients (~17-18 years) but having no apparent effect on disease symptoms or progression in younger patients (Åberg et al., 2008). The drug's benefits were significantly outweighed, however, by the adverse psychiatric effects and infections experienced by many of the patients in the trial. Other steroids are being explored in ongoing trials for other neurodegenerative disorders, such as Duchenne muscular dystrophy and Niemann-Pick disease, and the results of these trials may have clinical relevance for NCL patients.

Finally, several neuroprotective compounds have been hypothesised as having clinical relevance to NCL patients due to their positive effects in a range of other neurological and neurodegenerative disorders. These include, but are not limited to, anti-oxidants, cytoskeletal stabilizers, anti-apoptic compounds, AMPA receptor agonists (which reduce excitotoxicity) and, most importantly for this thesis, cannabinoids.

1.6.4.b Cannabinoids and CBD

Cannabinoids, in particular the non-psychotropic cannabidiol (CBD), present an interesting area of research as potential NCL therapies due to their polymorphic neuroprotective qualities. To date, very little research has been conducted, either in humans or animal models,

with regard to the effects of cannabinoids on any variant of NCL. Despite this, many NCL patients are being supplemented with CBD oil by parents with and without prescription due to its purported analgesic (pain-relief), anxiolytic (anti-anxiety), antiepileptic (anti-seizure) and neuroprotective effects (Wibbeler et al., 2019; Stephanie Hughes, personal communication). Since patients are already receiving CBD as a supplementary treatment, it is critical we gain a better understanding of its potential pharmacological effects in order to better contextualise the data generated from the practical component of this thesis.

Cannabinoids, also referred to as phytocannabinoids, are a group of C21 terpenophenolic compounds generated by the decarboxylation of secondary metabolites produced, primarily, by plants in the *Cannabis* genus. It should be noted that cannabinoids and cannabinoid-like compounds are now beginning to be discovered in a wide range of other plant genii, including *Echinacea* and *Radula*, but our understanding of these is still in its infancy (see Kumar et al., 2019, for a comprehensive review of cannabimimetic plants)(Chicca et al., 2009; Kumar et al., 2019; Raduner et al., 2006; Toyota et al., 1994). *Cannabis indica* (*C. indica*; sometimes misnamed '*sativa*'), infamous for its widespread recreational use as 'marijuana' or 'weed', and its close, hemp-producing relative *Cannabis sativa* (*C. sativa*), produce varying ratios of eight acidic metabolites in their glandular trichomes which, when exposed to heat, oxidation or light, undergo non-enzymatic transformations into at least 144 naturally occurring cannabinoids. The most well-known and abundant of these are trans-9-tetrahydrocannabinol (THC), CBD, cannabigerol (CBG), cannabinol (CBN) and cannabichromene (CBC)(**Figure 1.6**) (Hanuš et al., 2016).

To date, the majority of research into phytocannabinoids and their potential medical applications has focused primarily on THC and CBD. This is due, in part, to their relative abundance compared to other cannabinoids, their use in the chemotaxonomic classification

of different species within the *Cannabis* genus (*C. sativa*, for instance, has a low THC/CBD ratio, making it useful for hemp production but less-favoured as a recreational drug, whereas the opposite is true of *C. indica*) and the fact that THC has been identified as the active compound responsible for cannabis' psychoactive effects (Gaoni & Mechoulam, 1964; Mechoulam & Gaoni, 1965). Their acidic precursors, THCA and CBDA, can be found in the oil or sebum-like substance produced by *C. indica* or *C.sativa's* glandular trichomes, particularly the capitate-stalked trichomes located in and around the calyxes of female plants' budding flowers. These acids are derived from a common precursor molecule, cannabigerolic acid (CBGA), which – in turn – is a product of the condensation of a monoterpenoid precursor, predominantly geranylpyrophosphate (GPP), with a phenolic precursor, olivetolic acid (OA; see **Figure 1.6** for outline of cannabinoid biosynthesis). All these compounds are part of the plant's secondary metabolism pathway and are believed to be produced to deter predators, attract pollinators and/or act as a 'sunscreen' for the plant against harmful UV rays.

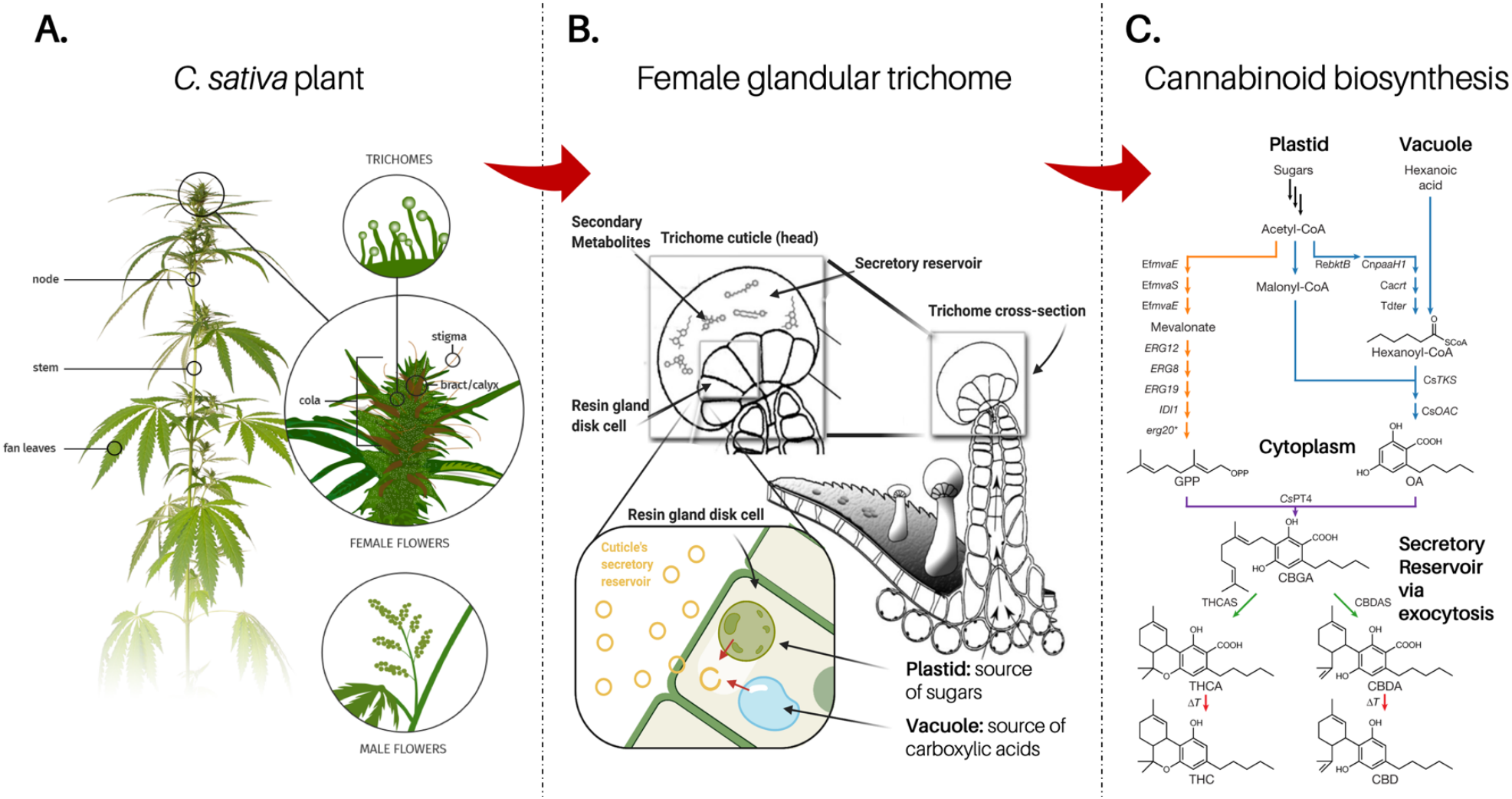
A.
C. sativa plant
TRICHOMES
node
stem
fan leaves
stigma
bract/calyx
cola
FEMALE FLOWERS
MALE FLOWERS
B.
Female glandular trichome
Secondary Metabolites
Trichome cuticle (head)
Secretory reservoir
Trichome cross-section
Resin gland disk cell
Resin gland disk cell
Cuticle's secretory reservoir
Plastid: source of sugars
Vacuole: source of carboxylic acids
C.
Cannabinoid biosynthesis
Plastid
Vacuole
Sugars
Hexanoic acid
Acetyl-CoA
EfmvaE
EfmvaS
EfmvaE
Mevalonate
ERG12
ERG8
ERG19
IDI1
erg20*
Malonyl-CoA
RebktB
CnpaaH1
Cacrt
Tdter
Hexanoyl-CoA
CsTKS
CsOAC
Cytoplasm
GPP
OA
CsPT4
CBGA
Secretory Reservoir via exocytosis
THCAS
CBDAS
THCA
CBDA
ΔT
ΔT
THC
CBD

⇐ **Figure 1.6 | Biosynthesis of cannabinoids within the glandular trichomes of female *C. sativa* flowers (opposite page).** A. Cannabinoid biosynthesis can take place within the trichomes of both male and female *C. sativa* (or *C.indica*) plants, but the highest concentrations are found within glandular capitate-stalked trichomes that cover the female flowers. B. Each capitate-stalked trichome has a stalk and cuticle (or head). The raw components used to make cannabinoids (sugars and hexanoic acid) are transported through the cells within the stalk via systems of intra- and intercellular transport, before reaching the resin gland disk cells (RGDC) located at the base of the trichome cuticle. A series of chemical reactions are carried out within the RGDC cytoplasm (detailed in C) and cannabinoid acids are released as sebum droplets into the cuticle's secretory reservoir. Here cannabinoid acids can come into contact with sunlight, which transforms the acids into their associated cannabinoid end-products. C. A basic outline of the chemical reactions that are involved in the biosynthesis of cannabinoids from sugar and hexanoic acid. Blue arrows indicate reactions that occur within the RGDC vacuole, orange arrows indicate reactions that occur within the RGDC plastid. Purple and green arrows indicate reactions that occur within the RGDC cytoplasm, and red arrows indicate reactions that occur within the trichome cuticle's secretory reservoir. Image made by author.

While modern use of cannabis and cannabinoids like THC and CBD continues to be rooted in recreation and the realm of 'alternative' medicines, increasing clinical and public interest in these compounds for disease and symptom management has made way for research into their pharmacodynamics and pharmacokinetics (Lucas et al., 2018). However, there is still limited information in these areas – particularly for the less common cannabinoids – and further research is needed to address major gaps in the knowledge required for optimal production and prescription of these medicines.

The most common route of administration for recreational cannabis (and cannabinoids) is via inhalation of smoke (Newmeyer et al., 2016), though cannabinoids have also been known to be administered orally, via oromucosal preparations, intravenously and transdermally in clinical and research settings (Lucas et al., 2018). The pharmacokinetics of cannabinoids administered via inhalation have been found to be similar to those administered intravenously, with both THC and CBD reaching peak plasma concentrations after 3 to 10 minutes. THC bioavailability after inhalation has been reported to range between 10 and 35%, whereas inhaled CBD was found to have an average bioavailability of 31% (Grotenhermen, 2003; Ohlsson et al., 1986).

Oromucosal preparations of cannabinoids (e.g. via nasal sprays) were found to produce lower plasma concentrations of THC and CBD than inhalation via smoking or vaporisation, but higher concentrations than oral administration (Therapeutic Goods Administration, 2013). THC and CBD have poor oral bioavailibility due to their lipophilic qualities, with some studies estimating it to be as low as 6% for both compounds (Agurell et al., 1981; Dinis-Oliveira, 2016; Eichler et al., 2012; Gaston & Friedman, 2017). Additionally, cannabinoids absorbed through the gastrointestinal tract have to undergo hepatic 'first-pass' metabolism, resulting in lower peak plasma levels and a longer delay before reaching that peak. While little is known about the metabolism of THC and CBD, it is likely that both compounds would produce interactions with other drugs that are also metabolised in the liver – due to their shared used of cytochrome P450 isozymes (Eichler, 2012; Dinis-Oliveira, 2016). For instance, both cannabis and tobacco smoking induce CYP1A2 activity. When the compounds are smoked together, this induction becomes additive. This suggests a significant drug interaction would be likely to occur if a patient took cannabis and a drug that is also metabolised by CYP1A2 (Anderson & Chan, 2016). There have also been one-off case reports of mental health episodes, such as mania and/or delirium, being induced by the coadministration of cannabis and certain medications like fluoxetine and disulfiram (Lacoursiere & Swatek, 1983; Mackie & Clark, 1994). None of these incidents, however, have involved the use of medical-grade, purified cannabinoids.

While their lipophilic structure makes oral administration less-than-ideal, that same structure allows cannabinoids like THC and CBD to distribute easily throughout the body and, importantly for neurodegenerative diseases like the NCLs, cross the BBB (Calapai et al., 2020). There is some evidence to say distribution is affected by an individual's body size and composition, and chronic cannabis use can result in the deposition of cannabinoids in adipose

tissue, resulting in the persistence of cannabinoid activity for weeks post-administration (Lucas et al., 2018). Many studies have shown that the elimination half-life of cannabinoids such as THC and CBD depend on the frequency and quantity of cannabis use which, combined with individual factors such as fat composition and diet, makes it difficult to estimate an exact half-life or rate of elimination for either compound. For instance, Smith-Kielland et al. (1999) found the half-life of THC in prison inmates who identified as 'infrequent' users of cannabis to be approximately 1.3 days, whereas a population model created by Heuberger et al. (2015) describes a 'fast' initial half-life of approximately 6 minutes, followed by a 'long' terminal half-life of 22 hours for the same compound. An even longer elimination half-life fo THC has been observed in 'heavy' users, which has been attributed to slow-release from bodily compartments such as fat stores (Toennes et al., 2008). Similarly, CBD has been reported to have a varying half-life depending on route of administration: the average half-life following intravenous dosing was observed to be approximately 24 hours, while the half-life of inhaled CBD was found to be 31 hours (Ohlsson et al., 1986). Consroe et al. (1991) found that 'chronic' users (aka individuals who self-administered cannabis daily for a minimum of four weeks) elicited a CBD half-life ranging between 2 to 5 days.

Like all phytocannabinoids, the structure of THC and CBD give them varying affinities for specialised G-protein coupled receptors (GPCRs) within the human body, known as cannabinoid receptors (CB_1 and CB_2 receptors). These receptors are present on the surface membranes of cells throughout all the major organ systems and have roles in a series of physiological processes that assist with maintaining homeostasis including appetite, pain perception, mood and memory. Devane et al. identified the first of these endogenous receptors, cannabinoid receptor 1 (CB_1), in rat brains in 1988 while researching the psychoactive effects of the cannabinoid THC, choosing to name their discovery after the class

of compounds that had helped them identify it (Devane et al., 1988). Cannabinoid receptor 2, (CB_2) was discovered five years later (Munro et al., 1993). While both receptors are GPCRs and can be activated to varying degrees by different cannabinoids, they are distinguishable by a 48% amino acid sequence difference in structure, varying tissue distribution, signalling mechanisms and sensitivity to different cannabinoids (Howlett et al., 2002). CB_1 receptors, for example, are located primarily throughout the central and peripheral nervous systems, with one of their main functions being to inhibit neurotransmitter release at neural synapses. CB_2 receptors, in comparison, are found primarily in peripheral tissues and organs and are highly associated with the immune system (Howlett et al., 2002). THC demonstrates a high affinity for both CB_1 and CB_2 *in vitro* and *in vivo*, and it is the strong activation of these receptors and their associated signalling pathways that is believed to be responsible for THC's powerful psychotropic qualities (Costa, 2007).

It was originally assumed that CBD would have a similar affinity for the CB receptors, and that this agonism would be responsible for the plethora of neurological effects attributed to its use. This, however, turned out not to be the case. While CBD can bind to CB_1 and CB_2, it appears to have low to negligible agonist activity at these receptors *in vivo* and may even act in an antagonistic manner at low doses (M.-H. Rhee et al., 1997). Recent studies even suggest that CBD negatively modulates CB_1 receptors via an allosteric mechanism (Laprairie et al., 2015).

CBD's pharmacological effects are now believed to be due to activation of alternative receptors and pathways, as well as the cannabinoid's innate chemical properties. It's antiepileptic qualities, for instance, have been attributed to its modulation of transient receptor potential (TRP; vanilloid1) channels and, more recently, its role in the reduction of neuronal excitability through interaction with the GPR55 receptor (Kaplan et al., 2017). No

work has been specifically done with CBD and the myoclonic seizures experienced by NCL patients, but there have been several small 'generalised seizure' studies conducted with various cannabinoids, mostly THC, that have included NCL patients (Lorenz, 2002).

Besides its antiepilpetic action, CBD has been reported to possess several other pharmacological attributes that would be valuable in the treatment of NCLs. For instance, CBD's ability to stimulate vanilloid 1 is also associated with an analgesic effect, as stimulation of this receptor results in the desensitisation of sensory nociceptors (Baamonde et al., 2005; Iannotti et al., 2014; McCarberg & Barkin, 2007). Pain has been reported in many cases of NCL (Barney et al., 2015; Breau et al., 2010), though its diagnosis and management is often complicated by NCL patients' compromised language and cognitive abilities (Mannerkoski et al., 2001). NCL patients also often experience mood disorders and anxiety, making CBD's reported anxiolytic (anti-anxiety) and antidepressant qualities pertinent to treatment. These effects are believed to be the result of CBD's allostoric modulation of $GABA_A$ receptors and/or activity at $5HT_{1A}$ receptors (Bakas et al., 2017; Zanelati et al., 2010).

Aside from addressing symptoms like seizures, pain and mood disorders, CBD also has the potential to address the pathology underlying NCLs. Neuroinflammation, discussed previously, is a key feature of all NCL variants and believed to be closely associated with – or even causative of – neurodegeneration. CBD has been known to reduce inflammation via the inhibition of [3H] adenosine uptake in murine microglia and macrophages and it has been found to suppress human B cell chemokine production in vitro (Carrier et al., 2006; Formukong et al., 1988; Watzl et al., 1991). Several studies in rodent models of AD demonstrated that CBD is also able to reduce neuroinflammation caused by protein toxicitiy by impairing the expression of nitric oxide synthase (iNOS) and interleukin 1β (IL-1β), though the signalling pathways by which it exerts these effects remained uncharacterised until recently (G Esposito

et al., 2009). There is now mounting evidence that many of the neuroprotective and anti-inflammatory effects exerted by CBD may be the result of nuclear binding to a family of receptors known as the peroxisome proliferator-activated receptors (PPARs)(O'Sullivan, 2007).

The PPARs are a class of ligand-activated transcription factors that belong to the steroid/thyroid hormone superfamily of nuclear receptors (Berger & Moller, 2002). Traditionally regulated by lipid and steroid metabolites, they are believed to control the expression of a wide range of genes, many related to autophagy, lysosomal clearance, lipid and glucose metabolism and inflammation, among other cellular processes. They regulate gene expression by heterodimerizing with the retinoid X receptor (RXR) and binding to specific DNA sequences in the nucleus known as peroxisome proliferator response elements (PPREs), which are located in the enhancer regions of genes. In order to be 'activated', and exert its downstream effects on gene expression, the PPAR-RXR heterodimer must be bound by a ligand, such as a steroid, hormone or drug. In the absence of ligand-binding, the PPAR-RXR complex is bound by one of several possible co-repressor proteins, leaving it in an inactive state. Upon ligand binding, however, the complex undergoes a conformational change that allows for the release of the co-repressor protein and allows for the formation of a transcriptional apparatus that includes the ligand, the PPAR-RXR complex and a variety of co-activator proteins, including p300. This apparatus allows for nucleosome remodelling and the assembly of a transcriptional pre-initiation complex on target gene promoters within the nucleus (Berger & Moller, 2002)(**Figure 1.7**). To date, there are currently three isoforms of PPAR identified: PPARα, PPARβ (sometimes called PPARδ) and PPARɣ. Each is encoded by a separate gene and has a unique tissue distribution pattern, though all appear to be potentially relevant to the treatment of NCLs as therapeutic targets due to their polymorphic properties

and close relationship to several of the underlying pathological processes common across all NCL variants (Bookout et al., 2006; Kersten, 2008). Activation of the PPARs, either by endogenous or exogenous ligands, has been proven to result in a wide range of anti-inflammatory and neuroprotective qualities both in vivo and in vitro (see more on PPAR signalling and PPARα activation as a potential therapeutic target for the NCLs in **section 1.6.4.c**) (Aoun et al., 2003; Drew et al., 2006; Duvanel et al., 2003; Niino, 2007; Rhee et al., 2003; Uryu et al., 2002; Xu et al., 2005; Zander et al., 2002).

CBD's neuroprotective and anti-inflammatory properties have recently been directly linked to PPARɣ signalling in a rat model of AD, with the antagonism of the PPARɣ pathway resulting in a significantly reduced effect of CBD on reactive gliosis and, subsequently, neuronal damage (Esposito et al., 2011). Less extensive work has been done examining CBD's ability to bind to and activate the other two PPAR receptors, α and β, but there have been several studies linking other cannabinoid compounds to their activation and using this binding-affinity therapeutically for neurodegenerative disorders such as AD and multiple sclerosis (Loría et al., 2010; Scuderi et al., 2011, 2012).

1.6.4.c Substrate reduction therapy and autophagy modulators

Several pharmaceutical compounds have been investigated as potential therapies for BD due to their ability to modulate autophagic and lysosomal biogenesis pathways within the cell (Gavin et al., 2013; Levin et al., 2014; Trial No. NCT00028262, *Clinicaltrials.gov*). Autophagic and lysosomal dysfunction has been linked to most of the variants of NCL to date, highlighting their shared importance in the pathophysiologies of this group of diseases.

Substrate reduction therapy (SRT) is a therapeutic strategy based on the partial inhibition of an enzyme (or enzymes) involved in the synthesis of a pathologically accumulating substrate, such as the saposins or mitochondrial subunit C that are histologically

characteristic of the NCLs. One of the many drugs that have been evaluated for this purpose is cysteamine bitartrate, a lysomotropic aminothiol salt traditionally used to manage kidney function. In 2001, cysteamine bitartrate was found to successfully enhance lysosomal storage clearance in CLN 1-deficient cell cultures, and so was used in a phase IV (interventional) clinical trial (Gavin et al., 2013; Trial No. NCT00028262, *Clinicaltrials.gov)*. Ten participants, all diagnosed with CLN 1 BD, took a daily oral dose of 60 mg/kg of cysteamine bitartrate until they were determined to have declined to a vegetative state or withdrew from the trial. All patients were found to have a complete absence of storage material in circulating lymphocytes by 8 months, but unfortunately this did not translate into any significant clinical improvement in disease progression (Levin et al., 2014).

While SRT drugs such as cysteamine bitartrate target the enzymes and precursor proteins involved in the production of intracellular storage material, another similar therapeutic strategy approaches the problem from the opposite direction. Instead of preventing or reducing the production of storage material in the first place, autophagic modulation involves the upregulation of key enzymes involved in the autophagy pathway – allowing increased clearance of the unwanted storage material from the cell (Coutinho et al., 2016).

A group of drugs that has proven particularly promising as autophagic modulators for the NCLs are fibrates, which have demonstrated varying abilities to modulate lysosomal biogenesis and autophagic pathways both *in vitro* and *in vivo* for several neurodegenerative disorders (Agarwal et al., 2017; Bordet et al., 2006; Esmaeili et al., 2016).

Fibrates are a class of known PPARα agonists, commonly used as lipid-lowering agents in patients with hypercholesterolaemia. PPARα is one of the three known peroxisomal proliferator-activated receptors (described in **section 1.6.4.b**) and, once activated, has been

shown to possess a wide range of neuroprotective properties via its downstream activation of anti-inflammatory, autophagic and lipid metabolising pathways (Esmaeili et al., 2016; Agarwel et al., 2017).

Researchers and clinicians became particularly interested in fibrates as potential therapies for neurodegenerative diseases due to their binding and activation of the neuroprotective PPARα receptor, along with the discovery and characterisation of a protein known as transcription factor EB (TFEB)(Napolitano & Ballabio, 2016; Settembre & Ballabio, 2011; Settembre et al., 2011). TFEB, encoded by the *TFEB* gene, is sometimes referred to as the 'master regulator' of the expression of *other* genes involved in autophagy and lysosomal biogenesis, amongst many other cellular processes, and its expression is upregulated by the binding of the PPARα-RXRα- transcriptional complex to *TFEB* PPREs (Napoliano & Ballabio, 2016; Chen et al., 2021).

Increased TFEB activity, which is closely associated with upregulated PPARα activation and subsequent *TFEB* transcription, has been shown to produce a variety of anti-inflammatory and neuroprotective effects in several neurodegenerative (and lysosomal storage) disorder models. For instance, upregulation of TFEB has been seen to result in increased htt turnover and the elimination of protein aggregates in a mouse model of Huntington's disease (La Spada, 2012; Tsunemi et al., 2012). Similarly, TFEB activation has been shown to improve the folding, trafficking, and activity of a destabilised glucocerebrosidase in a Gaucher disease cell culture and has been shown to rescue activity of a β-hexosaminidase mutant in fibroblasts taken from Tay-Sachs disease patients (Awad et al., 2015; Song et al., 2013).

The fact that fibrates activate the PPARs, especially PPARα, as part of their lipid-lowering mechanism of action (**Figure 1.7**), along with the fact that the PPARα-RXRα has been identified as a key regulator of TFEB expression, establishes fibrates as a potential therapeutic

for the NCLs via their downstream autophagy modulation activity (Esmaeili et al., 2016; Agarwel et al., 2017).

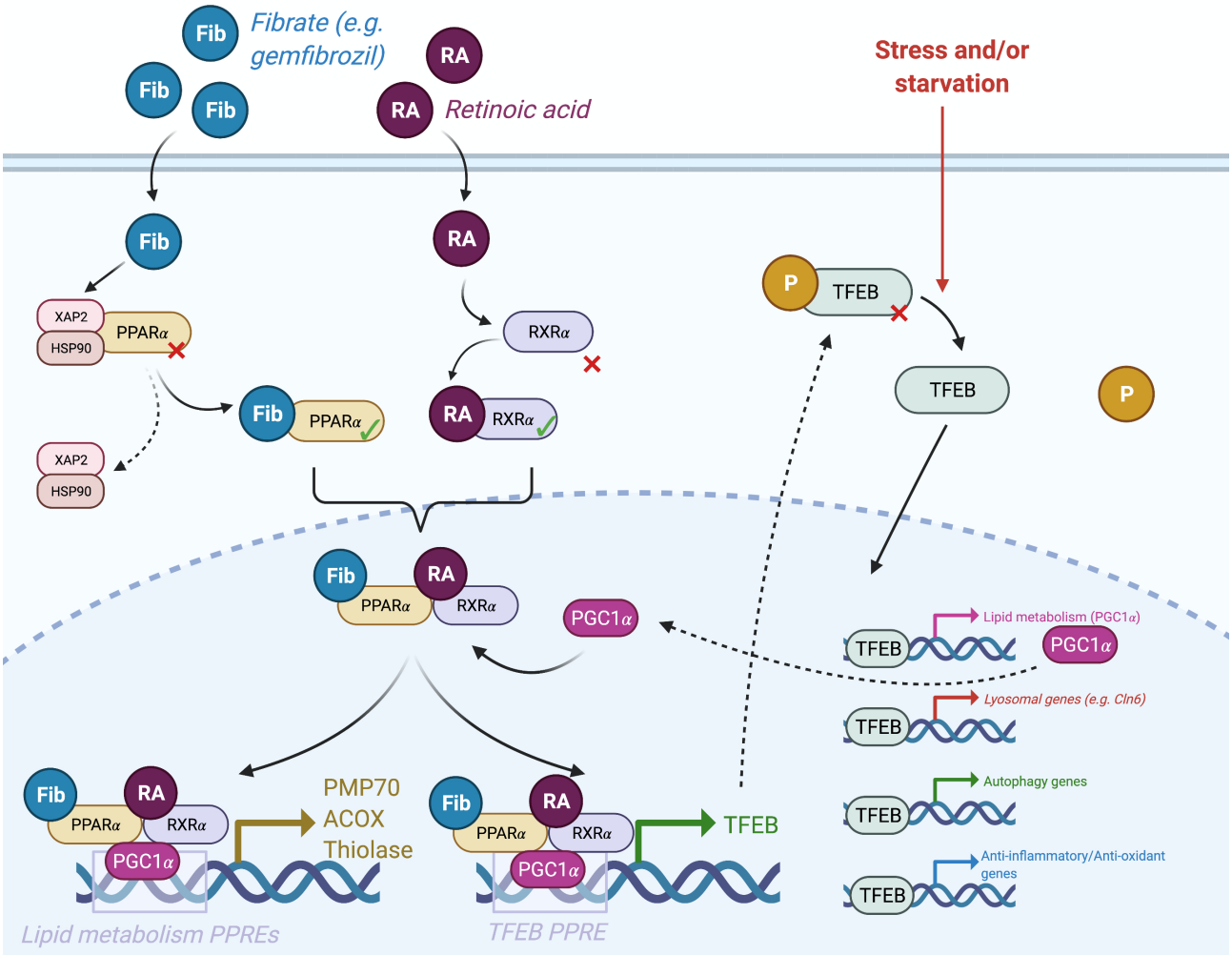

Figure 1.7 | Schematic overview of PPARα agonism within the cell. Many classes of small molecule therapy, such as fibrates, influence lysosomal biogenesis and autophagic processes via the activation of PPARα nuclear receptors, which consequently causes the upregulation of the 'master regulator' of autophagic genes – transcription factor EB (TFEB). Image created by author using *BioRender.com*.

The most commonly prescribed fibrates are fenofibrate (also known as Tricor) and gemfibrozil (also known as Lopid). Both were introduced as lipid-lowering agents in the mid-1970s and are indicated for the treatment of primary hypercholesterolaemia; mixed dyslipidaemia; and/or hypertriglyceridaemia in adults. The lipid-modifying activity of these drugs has been seen in clinical practice and characterised both *in vivo* and *in vitro*, with both acting as PPARα ligands and exerting their effects via PPARα-mediated upregulation of the

transcription of a variety of lipid-lowering proteins, including lipoprotein lipase, and via the downregulation of apoprotein C-III, an inhibitor of lipoprotein lipase activity (Fazio & Linton, 2004; Staels et al., 1998).

Both fenofibrate and gemfibrozil, along with several other fibrates such as bezafibrate and clofibrate, have been investigated as potential therapies for several neurodegenerative diseases, including several forms of the NCLs. For example, fenofibrate, bezafibrate and gemfibrozil were all found to have beneficial effects on the health of lymphoblast lines derived from CLN3 BD patients, while fenofibrate, gemfibrozil and clofibrate were found to restore several lysosomal and autophagic deficits in $Cln6^{-/-}$ cells (Best, 2017; Hong et al., 2016). Furthermore, gemfibrozil has also been successfully tested *in vivo* in $Cln2^{-/-}$ and $Cln6^{nclf}$ mouse models, with drug-treated mice exhibiting improved motor performance, longevity and decreased intracellular storage material accumulation when compared to untreated counterparts (Best et al., 2017; Ghosh et al., 2012).

As lipid-lowering agents, fenofibrate is often preferred over gemfibrozil due to its longer half-life (20 versus 2 hours) and higher efficacy, with fenofibrate being found to produce significantly greater reductions in total cholesterol, LDL and triglycerides and significantly increased levels of HDL (Packard et al., 2002). Additionally, gemfibrozil is a strong inhibitor of the metabolic enzyme CYP2C8, whose activity is key for the safe metabolism of a wide range of medications such as dabrafenib, loperamide, montelukast and rosiglitazone, amongst others, and therefore must be taken with caution in combination with other drugs. In contrast, fenofibrate is only a weak inhibitor of CYP2C8 and far fewer drug-drug interactions have been reported (Prueksaritanont et al., 2005; Schelleman et al., 2014; Tornio et al., 2017).

Despite fenofibrate being preferred clinically as a lipid-lowering agent, the literature currently suggests that gemfibrozil offers more potential as an NCL therapy, particularly in the

treatment of CLN2 and CLN6 BD – though, to date, there have been no clinical trials run to investigate the effects of any fibrate in patients with any form of NCL, so it is difficult to ascertain whether gemfibrozil will prove to be more efficacious clinically (Best et al., 2017; Ghosh et al., 2012).

Gemfibrozil, when prescribed clinically to treat lipid disorders in adults, is usually given as a twice-daily 600 mg oral dose, to be taken approximately 30 minutes before morning and evening meals. Alternatively, a single dose of 900 mg can be prescribed, to be taken 30 minutes before evening meals (FDA.gov, 2021; “Lopid (Gemfibrozil)" *Rxlist.com*, 2021). In clinical trials, individual oral doses have ranged between 600-1600 mg without producing significant increases in side effects – demonstrating that the drug has a relatively wide therapeutic index (FDA.gov, 2021; Fereshetian et al., 1998).

Gemfibrozil is rapidly and completely absorbed from the gastrointestinal (GI) tract and into enterohepatic circulation. Bioavailability of the drug is close to 100% and is highest when gemfibrozil is taken 30 minutes before food (Miller & Spence, 1998; Spence, 1998). Animal studies have shown peak plasma concentrations to occur an hour after oral administration, though studies in humans have demonstrated variability in this timing depending on whether the patient is taking one or two daily doses. A single 900 mg dose in healthy adults, for example, was shown to reach peak plasma concentrations of 33 ug/mL approximately 1-2 hours after ingestion. Another study, where participants took two daily doses of 600 mg each, showed peak plasma concentrations of 16-23 ug/mL approximately 1-2 hours after dosing (Busse et al., 2009). Approximately 95% of gemfibrozil is protein (albumin) bound and its volume of distribution is estimated to be 0.8 L/kg. Plasma concentrations of gemfibrozil vary widely between individuals, but tend to increase proportionally with increasing dose, though

there is no established relationship between plasma concentration and therapeutic response (Lilja et al., 2005).

Gemfibrozil is metabolised by liver and excreted primarily in the urine as metabolites (fecal elimination is about 6% in adults). Gemfibrozil's elimination half-life has been calculated to be approximately 1.5 hours ("AHFS Drug Information," Bethesda, 2009). As mentioned previously, gemfibrozil is a strong inhibitor of the liver metabolism enzyme CYP2C8, but also affects CYP2C9, OATP1B1 and OATP2B1 – meaning it can increase the elimination time, increase the toxicity and decrease the efficacy of a wide range of other drugs (Schelleman et al., 2014; Tornio et al., 2017). One source lists gemfibrozil as having interactions with 131 different medications, including common ones such as aspirin, metformin and several different antibiotics, so it is evident that caution must be taken when prescribing this drug (Lopid, *RXlist.com* 2021; Lopid®, *FDA.gov* 2021).

A randomised, double-blind, five-year trial of gemfibrozil in adult men at risk of coronary heart disease, dubbed the 'Helsinki Heart Study', demonstrated that common side effects of gemfibrozil include gastrointestinal symptoms such as dyspepsia, abdominal pain and acute appendicitis (Frick et al., 1987; Pfizer, 2021). During the first year of the study, 11.3% of the subjects (n = 2051) reported "moderate to severe upper gastrointestinal symptoms", in comparison to only 7% of the placebo group, though these rates decreased to 2.4% and 1.2% respectively over the four final years of the trial (Frick et al., 1987). Gastrointestinal side effects relating to the use of oral gemfibrozil in mice, particularly in disease models derived from the C57Bl/6 strain (such as the $Cln6^{nclf}$ and APP/PS1 transgenic Alzheimer's models), is also suspected due to observational data collected from several of the Hughes Lab's preliminary studies involving the regular oral dosing of large mouse cohorts. APP/PS1 mice, for example, were observed as experiencing higher rates of neophobia and, at a later stage of

experimentation, food rejection when given jelly pellets dosed with gemfibrozil than those given control pellets only containing a vehicle (50:50 DMSO and Tween® 20 solution) control (Stephanie Hughes and Stephanie Mercer, personal communication 2019). Such observations, however, have not been confirmed to be linked to GI side effects and would require further investigation to confirm a link. Aside from gastrointestinal disturbances, other human studies have indicated gemfibrozil, when taken with an HMG-CoA reductase inhibitor, to be associated with an increased risk of rhabdomyolysis. Rhabdomyolysis is a musculoskeletal syndrome which manifests as the excessive release of muscle fibre contents into the blood stream and can lead to fatal complications such as acute renal failure (Chang et al., 2004).

1.7 CLN6 Batten disease

1.7.1 Gene and protein

The human *CLN6* gene, first identified in 2002, is located on the long arm of chromosome 15 (15q23) and is composed of seven exons spanning ~22 kb of genomic DNA. It encodes a highly-conserved 27 kDa protein, CLN6, which is predicted to have seven transmembrane domains and localises in membrane of the endoplasmic reticulum (ER), as well as sub-domains of the ER membrane network which extend along the axons and dendrites of neural cells (Gao et al., 2002; Heine et al., 2007; Wheeler et al., 2002).

Until recently, very little was known about the function of the CLN6 protein, as it bears no homology to any other human protein and its complete structure has yet to be determined. In 2007, Heine et al. used differential permeabilizaton of transfected baby hamster kidney (BHK) cells and antibody binding assays to determine that CLN6 had a N-terminal cytoplasmic domain and a luminal C-terminus, and that a signalling region on the N-terminal, along with a dilysine motif located in the 6th and 9th transmembrane regions, dictated CLN6's localisation to the ER (Heine et al., 2007). Since then, clues to CLN6's role within the cell have come primarily from identifying binding partners and related signalling pathways. For instance, Benedict et al. (2009) determined that collapsin mediator response protein 2 (CRMP-2) interacts with CLN6's N-terminus and, using the Cln6^{nclf} mouse model and several Cln6^{nclf} neuronal co-cultures, found that CRMP-2 levels were significantly downregulated in specific regions of the brain, particularly the thalamus, in the absence of functional CLN6 (White et al., 2019). CRMP-2 is a protein implicated in axonal growth and development, playing several roles in neural microtubule dynamics, and is known to be highly expressed in the healthy, developing brain (Moutal et al., 2019). Aberrant Akt/GSK3 and ERK/MAPK cell signalling was

also identified in a Southern Hampshire sheep model (OCLN) of CLN6 BD, suggesting CLN6's involvement in cellular biometal homeostasis – as both of these pathways are biometal-regulated and increased accumulation of zinc, copper, manganese and cobalt had been previously identified in neural and non-neural OCLN and $CLN6^{-/-}$ Merino sheep tissues (Kanninen et al., 2013).

The biggest advance in our understanding of the biological role of the CLN6 protein, however, was only published in 2019. Bajaj et al (2019) used a series of biochemical assays to investigate the function of CLN6 in relation to that of another NCL-related protein, CLN8. CLN8's role as an ER cargo receptor had been elicited a year earlier, in 2018, by the same group, and the similarities between the clinical features of CLN6 BD and CLN8 BD, coupled with the fact that they are the only two known NCL-related proteins to be localised to the ER, lead the group to hypothesise that CLN6 was also involved in the ER-to-Golgi apparatus (Golgi) transport of lysosomal enzymes (Bajaj et al., 2018; Bajaj et al., 2019). Through the post-mortem analysis of brain tissue taken from $Cln6^{nclf}$ and $Cln8^{mnd}$ mice, Bajaj et al (2019) determined that CLN6 and CLN8 work as a complex that recruits newly synthesised lysosomal enzymes in the ER and transports them to the Golgi. They named this complex EGRESS (ER-to-Golgi relaying of enzymes of the lysosomal system). They determined that the complex forms at the ER membrane, and lysosomal enzymes are recruited via interaction with large luminal loops from both proteins. Absence of either protein appears to make the other unable to recruit the lysosomal enzymes and results in pathology. Once the enzymes have been recruited, they are packaged into a 'coat-protein' (COPI) vesicle with CLN8 and transported to the Golgi where they undergo further modification and packaging before being transported to the lysosome. CLN6, it appears, remains in the ER membrane once CLN8 has been packaged into a vesicle, preparing for the next round of transport (Bajaj et al., 2019).

While Bajaj et al's work represents a large leap forward in our understanding of (at least one of) CLN6's role(s) within the cell, there are many questions that remain unanswered. For example, expression levels of *CLN6* mRNA transcripts have been found to differ significantly across the lifespan in mouse models. These studies have shown *Cln6* expression to be amplified during prenatal development and for the first month after birth, demonstrating a similar murine expression profile to other NCL-related genes such as *Cln1* (*Ppt1*), *Cln3* and *Cln5*, and suggesting the importance of CLN6 in neurodevelopmental processes such as neurogenesis and maturation (Thelen et al, 2012; Isomppi et al., 1999; Holmberg et al., 2004; Eliason et al., 2007). This is further supported by region-specific differences in Cln6 transcript expression in mice, with the highest levels of expression found in the dentate gyrus, the hippocampus, the Purkinje cells of the cerebrellum and cortical layers II-VI (Thelen et al., 2012). The dentate gyrus is one of only two brain regions found to promote and maintain neurogenesis in adult human brains post-development (Gage, 2002), highlighting the protein's importance in this process. Why CLN6's role is so critical to these neuro-developmental processes, and why its absence or dysfunction seems to confer a targeted vulnerability to cells within the CNS remains an area of ongoing investigation and speculation.

1.7.2 Mutational spectrum

As of 2017, which is the last time the University College London's NCL mutation and patient database was updated, there were 71 unique CLN6 BD-causing mutations identified. These included substitutions, deletions, insertions, and duplications of both single nucleotides and longer sequences in all seven exons, two introns and the 5' upstream sequence (CLN6, *ucl.ac.uk/ncl-disease*). These mutations are known not only to cause classical CLN6 BD, but are

also implicated in Kufs disease Type A (Arsov et al., 2011) and several non-NCL diseases (**Table 1.1**) (Farqu, 2014).

The majority of NCL-causing mutations appear to affect amino acid residues that are located on the ER-exposed loops of the protein. Before Bajaj et al's (2019) paper, this 'clustering' of mutations was speculated to indicate an important functional role for these regions within the protein, which has now been confirmed by their work (Mole et al., 2004; Kousi et al., 2012; Bajaj et al., 2019).

1.7.3 Clinical presentation

CLN6 BD was first described in several families from Costa Rica. However, CLN6 BD has since been identified in patients with a wide range of different ethnicities and does not appear to be restricted geographically to any particular part of the world (Wheeler et al., 2002).

Symptom onset for CLN6 BD has been described as highly variable, with some cases reporting presentation as young as 8 months of age or as old as 8 years (Sharp et al., 2003; Alroy et al., 2011; Schulz et al., 2013). However, 'classical' CLN6 BD is traditionally seen as a variant of LINCL that presents between 3 and 5 years of age, with the first symptoms usually being vision loss and seizures (Goebel et al., 2004). Other symptoms experienced by CLN6 BD patients include progressive loss of speech and motor skills, developmental delays and intellectual decline, mood swings, personality changes and dementia. Complete loss of motor skills is usually observed between 4 and 10 years of age, with patients usually dying in their mid-to-late teens or early 20s. CT, MRI and autopsy usually reveal severe cortical and cerebellar atrophy (Goebel et al., 2004; Mole et al., 2004).

In 2011, Arsov et al determined that Kufs disease Type A, originally thought to be a rare adult onset variant of CLN4 BD, was also caused by mutations in CLN6 (Arsov et al., 2011).

Disease progression and clinical presentation seems to be significantly different in Kufs disease patients, with most presenting with symptoms in their late 20s. Patients with Kufs also seem to maintain their eyesight, with their first symptoms being cognitive and/or behavioural changes and ataxia – all of which seem to develop several years (3-8) before myoclonic seizures begin. Progressive ataxia and unrelenting seizures usually leads to patients being wheelchair bound approximately 12 years post-diagnosis, with premature death occuring 8 to 31 years after onset (Berkovic, 2019).

1.7.4 The Gray Foundation (Amicus Therapeutics) CLN6 BD clinical trial

In 2016, Amicus Therapeutics and the Gray Foundation funded the first ever clinical trial of AAV2/9-mediated gene therapy for CLN6 BD (Trial No. NCT02725580, *Clinicaltrials.gov*). Thirteen children, all diagnosed with CLN6 BD, received a single intrathecal dose of scAAV9.CB.*hCLN6.* While the trial is still ongoing, interim results suggest the treatment has been tolerated well by the participants and some of the younger children remain symptom-free despite reaching the age at which symptoms are expected to appear (Amicus Therapeutics, 2019). Unfortunately, however, some of the older participants, who were displaying symptoms before treatment, continue to decline. Whether their rate of decline has been slowed by the treatment is yet to be determined, but it highlights the need for supplementary therapeutics to augment the effects of the gene therapy in older, symptomatic patients. For this reason, the Gray Foundation enlisted the help of the Hughes lab to run a large-scale, longitudinal combination therapy trial in $Cln6^{nclf}$ mice, with the hopes of designing a safe and effective combination treatment involving both gene and small molecule (CBD and gemfibrozil) treatments (Stephanie Hughes, personal communication).

1.7.5 Animal model – the Cln6^{nclf} mouse

As has been the case with all forms of NCL (see **section 1.4**), the use of animal models has been critical to understanding of the pathophysiology of CLN6 BD and to attempts to develop effective therapeutic strategies against it. While there are several useful CLN6 animal models currently available, including two CLN6$^{-/-}$ ovine models and one canine, the practical component of this thesis used *the* Cln6^{nclf} murine model (Oswald et al., 2005; Katz et al., 2011; Best et al., 2017). The Cln6^{nclf} murine model was selected for several reasons:

First, the model is derived from the widely used and readily available C57 Black 6 (C57Bl/6) inbred strain of laboratory mice. These mice are well-studied, with the line first established in 1921, and there is a wealth of genetic, phenotypic and genomic data available on the strain, including a high-quality reference genome (GRCm38.p6). From this genome, it has been established that mice (*Mus muscularis*) have a homolog of the human *CLN6* gene, *Cln6*, on chromosome 9 and this homolog shares a 92% amino acid identity with its human counterpart (Huber et al., 2020). Originally identified in the Jackson Laboratory and described by Bronson et al in 1998, the Cln6^{nclf} murine model arose from a naturally occurring insertion mutation of a cysteine amino acid codon into exon 4 of the C57Bl/6 *Cln6* gene (Bronson et al., 1999). Also known as the 'nclf' mouse, the Cln6^{nclf} murine model is one of only two naturally occurring murine models for the NCLs, the other being the Cln8^{mnd} mouse, and lends itself – like most rodent models – to relatively inexpensive breeding, transportation, experimentation, housing and upkeep (Huber et al., 2020). The use of the Cln6^{nclf} mouse in the practical component of this thesis allowed for the use and maintenance of over 540 experimental animals, split into eighteen different experimental groups by gender, strain and therapy type, some of which were kept for almost two years – a feat that would be much more

difficult, and expensive, if one of the larger CLN6 animal models (ovine or canine) had been used instead.

Second, the Cln6^{nclf} mouse model was employed in the practical component of this thesis due to the fact that this work, and the overall trial it is part of, make up only one part of a larger international effort by several labs to investigate and improve upon the use of gene therapy to treat CLN6 BD. Several labs from around the world, including the Cooper and Weimer labs in the United States, are working on parallel projects and their data is currently being generated using the Cln6^{nclf} model (Cain et al., 2019; White et al., 2021). Using the Cln6^{nclf} mouse for this project ensures that any data generated will be relevant and hopefully translation when reported in the wider context of other labs' work. It also means that the data will be able to build upon a variety of key, published CLN6 BD preclinical studies – including several published by current and previous members of the Hughes Lab (Neverman, 2015; Best, 2017; Best et al., 2017; Linterman et al., 2011; Mole et al., 2019; Partridge, 2017).

Finally, and perhaps most importantly, the Cln6^{nclf} murine model has been independently validated as a reliable format for screening potential CLN6 BD therapeutics and found to have several key behavioural and pathological similarities to the human disease (Morgan et al., 2013). Early histological studies in the brains of these mice demonstrated progressive, selective regional and neuronal loss, as well as wide-spread astrocyte activation and microgliosis - both of which are considered key features of NCL pathophysiology in humans (see **section 1.5**; Bronson et al., 1999; Thelen et al., 2012). A 2013 study conducted by Jeremy Morgan from the Jill Weimer Lab found the Cln6^{nclf} mouse to demonstrate retinal degeneration (and blindness), motor deficits such as dysarthria and ataxia, and CLN6 BD-characteristic cortical thinning, brain atrophy and selective loss of GABAergic inhibitory interneurons from the cortex and hippocampus. All these features replicate, to different

degrees, the disease seen in humans and other animal models of CLN6 BD (Morgan et al., 2013). Taken together, these findings helped establish the Cln6^{nclf} mouse as a cornerstone tool for studying the pathology – both behavioural and histological – of CLN6 BD.

1.7.6 Comparing mice to 'men' (humans)

The practical component of this thesis involves screening several experimental therapeutics for efficacy against a progressive, and therefore time-dependent, neurodegenerative condition. It has long been proven that interventions such as gene therapy are only effective when administered during their specific 'therapeutic window' and failure to translate this 'window' from the lifespans of preclinical animal models to humans has been hypothesised as the reason many promising therapeutics end up failing to produce successful clinical outcomes, despite showing promise in the lab (Cabrera-Salazar et al., 2007; Sondhi et al., 2008). Despite the Cln6^{nclf} mouse having been proven to demonstrate several key features of human CLN6 BD, as well as sharing genes, organ systems and several aspects of systemic physiology with humans, it cannot be ignored that the morphometry, physiology and lifespan of a mouse differs significantly from that of a human (Agoston, 2017; Clancy et al., 2007; Zhao & Bhattacharyya, 2018). These differences should and will be taken into consideration when interpreting any data regarding the efficacy of a potential treatment and determining the optimal 'therapeutic window' for that treatment in humans.

Making a direct comparison between the lifespan of a rodent, in this case the Cln6^{nclf} mouse, and that of a human patient is a difficult endeavour. Various methods have been employed to correlate the ages of small mammals with human age. Perhaps the most successful, or at least most well-known, of these attempts is the standardized Carnegie staging system, which uses a 23-stage system to provide a unified developmental chronology of vertebral embryos, including those of humans and mice (DiCaglio, 2017). Unfortunately, this

system only extends from fertilization through to the 60th day of embryological development (in humans), after which the 'embryo' becomes known as a 'foetus' and the staging system ceases and cannot be used to compare foetal or post-natal mice to their human counterparts. Other methods used to compare later stages of life between humans and mice include determining and comparing changes in the weight of the eye lens, age and staging of epiphyseal closure, patterns of body weight change or tooth wear and, more recently, comparing the time it takes each mammal to reach 'keystone' stages of development: weaning, puberty, adulthood, reproductive senescence (menopause), and 'old age' (Dutta & Sengupta, 2016). In their 2016 paper, for example, Sulagna Dutta and Pallav Sengupta proposed that a precise correlation of age between mice and humans must be calculated at each key developmental stage over the lifespan – resulting in a changing relationship between 'mouse days' and 'human years' over the lifespan (see **Figure 1.8**)(Dutta & Sengupta, 2016).

Using Dutta and Sengupta's model, post-natal day 0 (P0) would reflect post-natal day 6 (P6) in human days, P28 in mice (weaning) would reflect approximately 6 human months, P42 in mice (puberty) would reflect 11.8 human years, P70 would reflect 27 human years and so on. This model is based on a simple calculation using the average lifespan of laboratory mice (24 months) and the average lifespan of humans (80 years):

$$(80 \times 365) \div (2 \times 365) = 40 \text{ human days} = 1 \text{ mouse day}$$

And/or

$$365 \div 40 = 9.125 \text{ mice days} = 1 \text{ human year.}$$

Thus, according to their calculation, one human year is equivalent to 9 mouse days when correlating to their entire lifespan. Recognising that this calculation is a little too simplistic, considering the different *rates* at which mice and humans develop and mature,

Dutta and Sengupta alter this calculation slightly for each developmental milestone, using the average ages at which mice and humans reach each milestone to determine a new relationship between ‘mice days’ and ‘human years’ (Dutta & Sengupta, 2016).

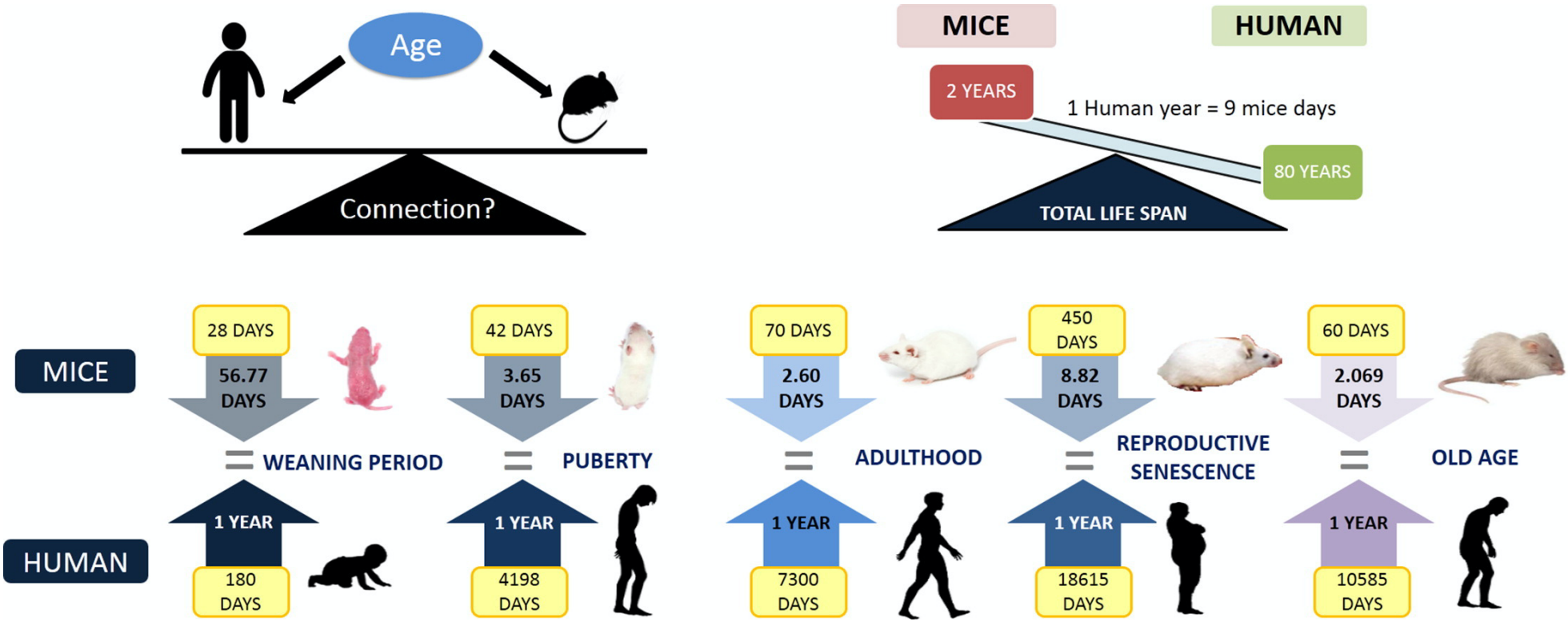

Figure 1.8 | Graphic abstract of Dutta and Sengupta's comparison model for human and mouse lifespans. Dutta and Sengupta proposed a proposed that a precise correlation of age between mice and humans must be calculated at each key developmental stage over the lifespan – resulting in a changing relationship between 'mouse days' and 'human years' over the lifespan. Image taken from *Dutta and Sengupta, 2016.*

While this model helps frame, in very simple terms, how the age of a mouse might be correlated to that of a human counterpart, it is flawed. For example, the model only works if you look at each developmental milestone in isolation: a mouse reaches puberty at P42, at which point you can divide 42 by 3.65 in order to calculate 11.5 human years (the approximate age that humans reach puberty). However, if you subtract 28 days from P42, to account for the fact that mice were ageing at a rate of 56.77 days = 1 human year for those first 28 days, you are only left with 14 days to divide by 3.65. This gives you 3.83 human years, to which you can add the 184 human days that mice are aged, roughly, at P28, and you have nowhere near the expected 11.5 human years. Therefore, it is evident that the authors intend for you to calculate the approximate age of your pubescent mouse, in human years, in isolation from the age you calculated at weaning, P28 (Dutta & Sengupta, 2016). This difference in calculation method could impact the way in which we interpret anatomical, physiological and behavioural changes that occur in a mouse between the two time points. The method used by the authors suggests a regular rate of development from P0 to P42, ignoring the accelerated rate you used to originally calculate age between P0 and P28. Using a calculation that acknowledges this rapid development between P0-28, however, would have to account for the mouse moving through the equivalent of 4013.5 days of human development over a period of just 14 days, and take this into account when interpreting changes in anatomy, physiology or behaviour between P28 and P42.

On top of this, Dutta and Sengupta's calculations seem to become less and less accurate as they progress through the lifespan of the ageing mouse, with their 'adult stage' equation correlating the age of a 6-month-old mouse (~180 days) to a 70-year-old human being. It becomes unclear whether they want readers to use this equation or revert to their original

'entire lifespan' equation above (in which a 180-day-old mouse would be equivalent to a 20 year old human), but in doing so this would contradict the equation they proposed for 'adulthood' (70 days in a mouse, ~25 years in a human) (Dutta & Sengupta, 2016). While Dutta and Sengupta's model provides a useful framework within which to consider and compare key reproductive 'milestones' between the human and mouse species, especially around the period of puberty, it is evident that the model requires evidence-based modification to improve its accuracy and relevancy to the practical component of this thesis.

In order to address Dutta and Sengupta's model's shortcomings when it comes to calculating later stages of life, the author of this project combined their original model with another, evidence-based (but far less detailed), model from the Jackson Laboratory (Flurkey et al., 2007). This model, shown in **Figure 1.9**, was developed from huge quantities of data using the C57Bl/6 mouse – the strain from which the $Cln6^{nclf}$ mouse was originally bred – and provides a much more reasonable estimation of 'human age' from animals at 6 and 12 months of age (both key ages for behavioural analysis in this project). The only reason this model wasn't adhered to completely in the first place is due to its lack of detail surrounding birth and early post-natal staging, which is a key consideration because of the early stage in which this project's animals were administered intracerebroventricular injections of gene therapy or a saline control (see **Chapter 2** for more information).

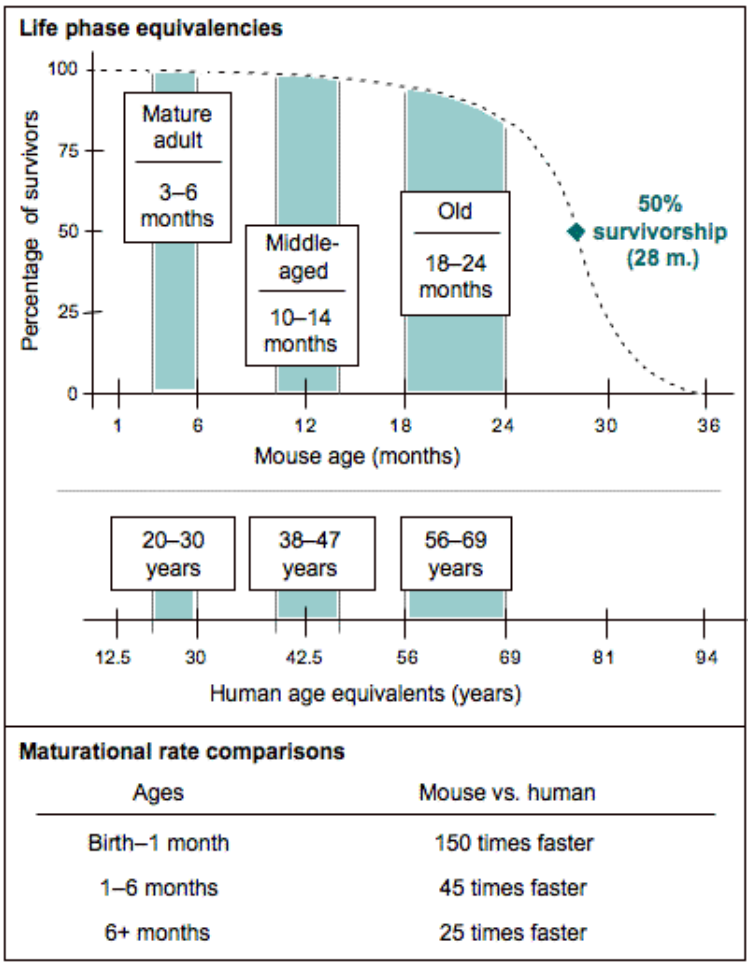

Figure 1.9| Life history stages in C57Bl/6J mice in comparison to human beings. Data Adapted from Figure 20-3: *Flurkey et al., 2007*. "The mouse in biomedical research" in James G. Fox (ed.), American College of Laboratory Animal Medicine series (Elsevier, AP: Amsterdam; Boston). Image and abstract taken from the Jackson Laboratory's website, "When are mice considered old?,", *jax.org*, 2020.

A second shortcoming of the Dutta and Sengupta model, shared by the model from the Jackson Laboratory, is the absence of correlation between stages of brain development in humans and mice, which could have significant implications for any study involving the CNS. The milestones chosen for calculation by Dutta and Sengupta's model are primarily hormonal ones, with the criteria for each stage of life explicitly described in terms of gonadal development and fertility by the authors (Dutta & Sengupta, 2016). There is, of course, some argument to be made regarding the close relationship between endocrinological and neurological development, with the hypothalamic-pituitary-gonadal (HPG) axis representing a direct connection between the two processes, but to directly correlate hormonal and

neurological development risks inaccurate staging of the key processes neurological studies are looking to characterise. A variety of different studies show that mouse and human brain development differs greatly over the lifespan, especially during gestation and the first few weeks of life (see **Figures 1.9** and **1.10**)(Chini & Hanganu-Opatz, 2021; Clancy et al., 2007). For example, a 'rule of thumb' that has been applied to most rodent models is that the rat neurodevelopment at postnatal days 1-10 equates to the third trimester in humans, or that rat neurodevelopment at day P7 is equivalent to that of humans at birth (Andrews & Fitzgerald, 1997; Clancy et al., 2007; Dobbing & Sands, 1979). The studies upon which this widely accepted approximation is based, however, are decades old, primarily conducted in rats, and several estimate neural development without empirical evidence (Dobbing & Smart, 1974; Dobbing, 1970, 1974; Dobbing & Sands, 1979).

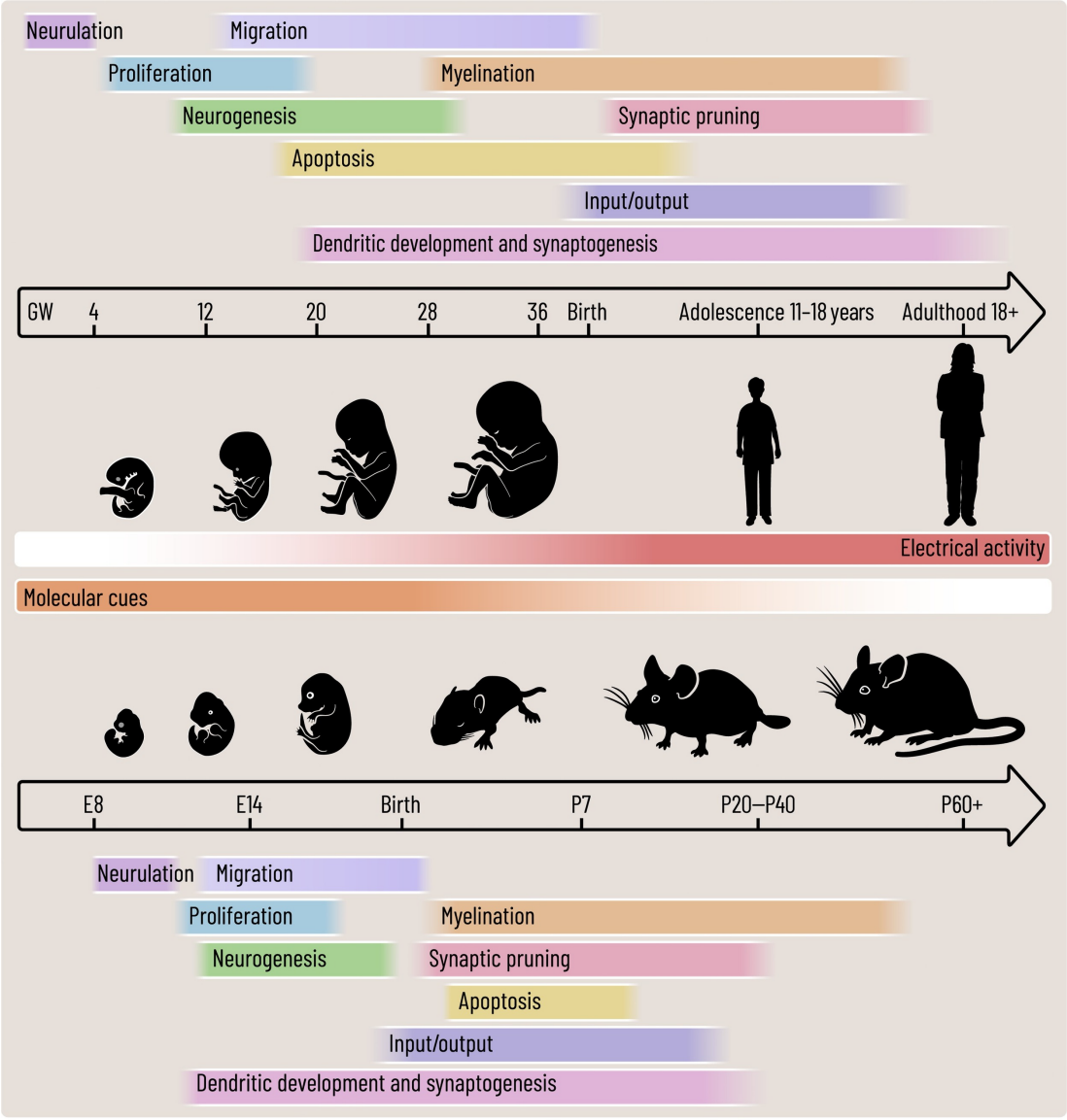

Figure 1.10 | Schematic representation of the processes guiding human and rodent brain (prefrontal) development. While overall brain development appears to be similar in the two species, individual processes occur at different relative time points and with different time courses. Not only are mice born at a more premature state but, even when accounting for this, some processes are less protracted than in humans and synaptic pruning occurs at an earlier stage. Image and abstract taken from *Chini and Hanganu-Opatz, 2021*.

Despite these shortcomings, the 'third trimester' hypothesis of brain development comparison is widely accepted and implemented in mouse laboratories around the world, including those of collaborators working on Gray Foundation preclinical and clinical trials running parallel with the practical component of this thesis (Best, 2017; Cain et al., 2019; Weimer et al., 2019; White et al., 2019). For this reason, a developmental comparison model used by Tseng et al. in their 2009 paper, looking at the impact of ventricular lesions on the

development of schizophrenia-like symptoms in rats, has also been incorporated into the final 'hybrid' development model used by this thesis to compare mouse and human ages (**Figure 1.12**)(Clancy et al., Flurkey et al., 2007; Tseng et al., 2009; Dutta & Sengupta, 2016; Chini et al., 2021). Tseng et al.'s model (2009; **Figure 1.11**) takes into account the differences in neural development, including neurulation, synaptic pruning and gliogenesis, between rodents in their first seven post-natal days of life and the third trimester of the human foetus.

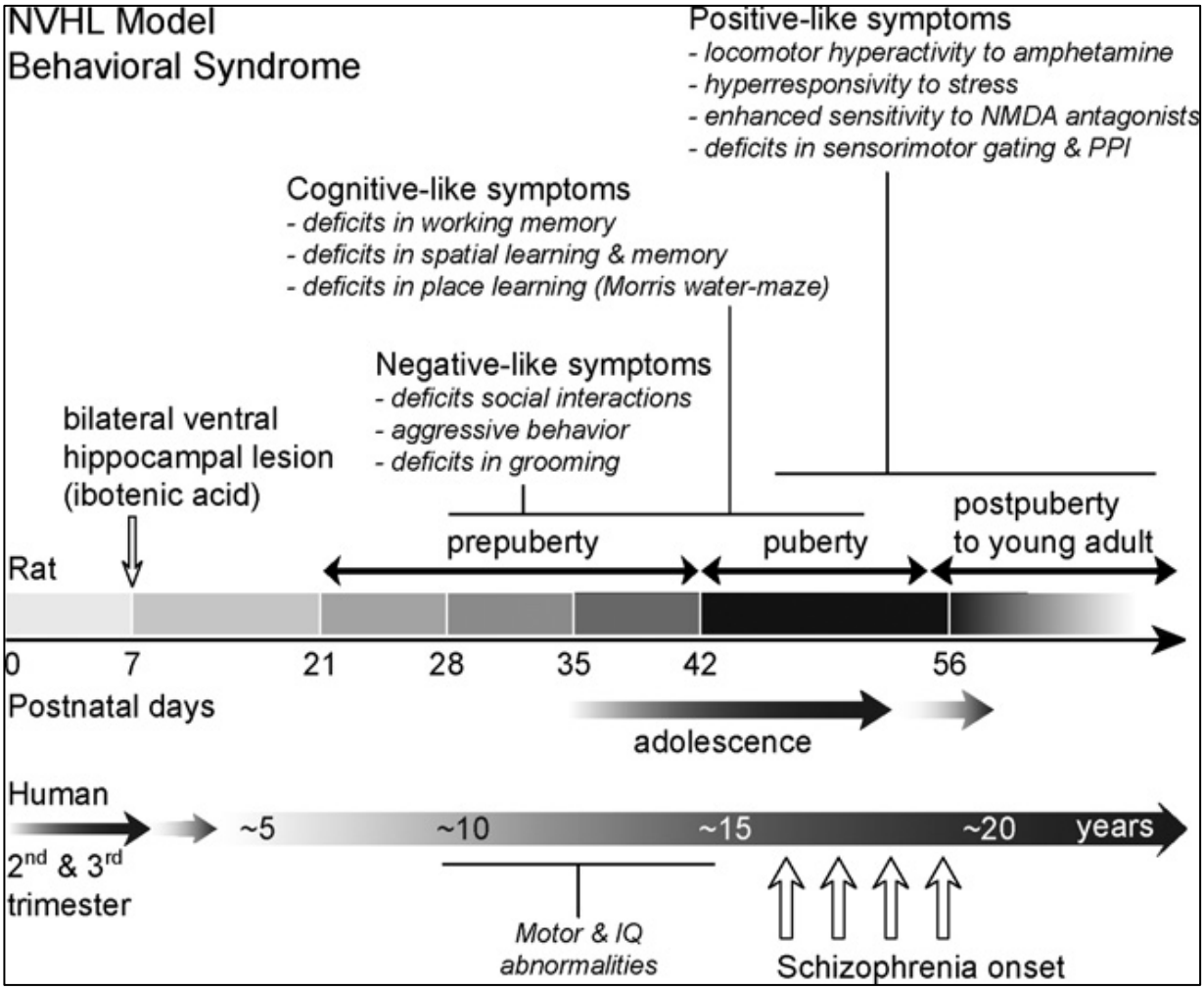

Figure 1.11 | Tseng et al.'s model comparing the timeline of the emergence of behavioural changes following the neonatal ventral hippocampal lesion in the rat and the timeline of the emergence of symptoms in schizophrenia in humans. While not a perfect model, Tseng et al's developmental model offers some critical insight into the differences in neural development, including the processes of neurulation, synaptic pruning, gliogenesis and brain plasticity in response to trauma or disease, between rodents in their first seven post-natal days of life and the third trimester of the human foetus. For this reason, it has been incorporated into the 'final' model used to compare mouse and human brain development in this project. Image and image caption title taken from *Tseng et al., 2009.*

The final, hybridised, model used in this project to conceptualised and compare the lifespans of healthy and CLN6 BD-affected murine and human lifespans is depicted in **Figure 1.12**. It takes into consideration the similarities and differences between the C57Bl/6 mouse, used in the practical component of this thesis as a healthy control and serving as the background strain from which the Cln6^{nclf} mice are bred, and a healthy human's lifespan (**Figure 1.12.A**). Despite obvous differences in length of life (with the average lifespan o a C57Bl/6 mouse being approximately 2 years and the average lifespan of a human being 75 years or older, depending on the country and socioeconomic class in which they are born), both lifespans share several key developmental events, such as weaning and puberty, and both species spend the majority of their life in the post-pubescent phase known as 'adulthood'. From this template, one can see how different therapeutics could be given to mice at specific ages in order to replicate the age at which they would be given to a human counterpart. For instance, if you were looking to give a teenager a certain medication, you might consider dosing mice in a preclinical trial for that medication at some point between 28 and 42 days of age.

The model goes on to contrast and compare the average lifespans of athe two strains of mice used in the practical component of this thesis – the Cln6^{nclf} (untreated) and C57Bl/6 mouse strains (**Figure 1.12.B**). One could argue that this is a somewhat 'easier' or more direct comparison to make, since both strains are the same species (*Mus muscularis*) and the Cln6^{nclf} mouse was originally bred from the C57Bl/6 strain by the Jackson Laboratory (Bronson et al., 1999). This comparison, based on previously published literature surrounding the Cln6^{nclf} mouse, is important to make as it highlights the behavioural deficits and truncated lifespan experienced by the Cln6^{nclf} mouse due to its naturally occurring insertion mutation in the *Cln6* gene. It also provides a timeline of key events over which the

practical component of this thesis was designed, allowing for the identification of practical points (6 months, 9 months and 12 months) to investigate efficacy of several small molecule therapies (gemfibrozil and CBD oil), alone and in combination with each other and AAV2/9-mediated *CLN6* gene therapy, in protecting Cln6^{nclf} mice against the CLN6 BD behavioural phenotype (see **section 1.8.1** for a summary of this project's aims and objectives).

Finally, the model compares the trunacted lifespan of an untreated Cln6^{nclf} mouse and the average lifespan of a patient diagnosed with CLN6 BD. While this comparison demonstrates that both human and mice experience significant behavioural deficits and shortened lifespans, it also highlights some concerning differences in the timing and progression of the disease in each species. For instance, this model shows us that Cln6^{nclf} mice tend to begin demonstrating motor deficits well into their adulthood, whereas humans classically start to show symptoms around 3 to 4 years of age. In fact, many human patients barely make it into their teenage years, the start of puberty, before reaching the end stages of the disease. These differences could prove problematic when trying to translate preclinical data into human trials – as what was successful in ameliorating or preventing disease in a mouse, presumably treated from birth or at least from puberty, could prove less efficacious when given to children who have already begun to show symptoms of motor decline (as most CLN6 BD patients are diagnosed post-symptom onset).

⇒**Figure 1.12 | A three part model comparing the average lifespans of (A) C57Bl/6 mice to healthy humans; (B) Cln6^{nclf} mice to C57Bl/6 mice; and (C) Cln6^{nclf} mice to human CLN6 BD patients (opposite page).** A. Despite significantly different lengths, healthy C57Bl/6 mice undergo many of the same key hormonal and developmental milestones as humans. The most complex period of life to compare between the two species is arguably, the early developmental stage – with the first 7 days of life for C57Bl/6 mice often being compared to the third trimester *in utero* for humans. B. Comparing the average lifespan of C57Bl/6 mice to that of untreated Cln6^{nclf} mice, as has been done in several studies prior to this project, highlights not only the truncated nature of the Cln6^{nclf} lifespan but also the early emergence of behavioural (motor and memory/learning) deficits in the Cln6^{nclf} strain when compared to C57Bl/6 controls (Poppens et al., 2019).This timeline also illustrates the observed differences in disease symptom onset between male and female Cln6^{nclf} mice, although the literature finds that the re is no significant difference in the overall average length of life between males and females – suggesting males experience later onset of symptoms but more rapid disease progression (Poppens et al., 2019). C. Making a direct comparison between the average lifespan of a Cln6^{nclf} mouse and a human patient with CLN6 BD highlights one of the biggest challenges to the development of efficacious therapies for CLN6 BD in humans: model systems, such as the Cln6^{nclf} mouse, display markedly different disease progression. Cln6^{nclf} mice, for example, don't start showing motor deficits until approximately 6 months of age – by which time they are considered, developmentally, to be in 'adulthood'. In stark comparison, human patients being showing motor symptoms between 3 and 4 years of age, and often don't even make it t puberty, let alone adulthood. This difference in disease progression could be significant when translating preclinical data from a Cln6^{nclf} model to clinical trials in humans. *Image created by author using elements of the Flurkey et al. 2007, Tseng et al. 2009's and Dutta and Sengupta's 2016 models.*

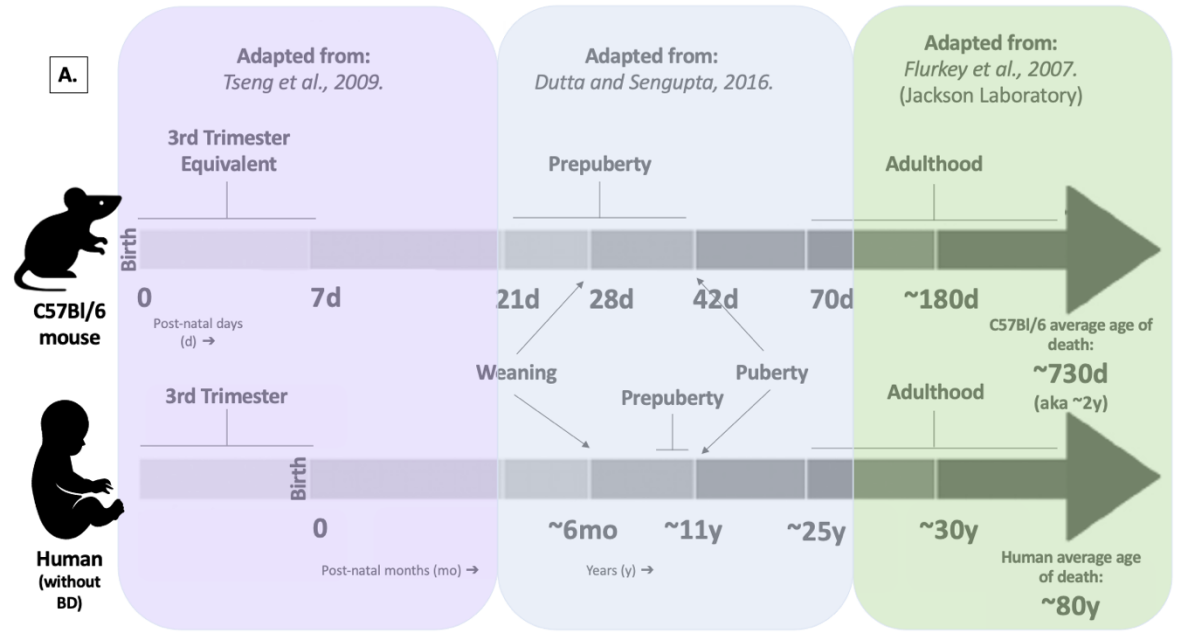
A.
Adapted from:
Tseng et al., 2009.
Adapted from:
Dutta and Sengupta, 2016.
Adapted from:
Flurkey et al., 2007.
(Jackson Laboratory)
3rd Trimester Equivalent
Prepuberty
Adulthood
Birth
C57Bl/6 mouse
0
7d
21d
28d
42d
70d
~180d
Post-natal days (d) →
C57Bl/6 average age of death:
~730d
(aka ~2y)
Weaning
Puberty
3rd Trimester
Prepuberty
Adulthood
Birth
Human (without BD)
0
~6mo
~11y
~25y
~30y
Post-natal months (mo) →
Years (y) →
Human average age of death:
~80y

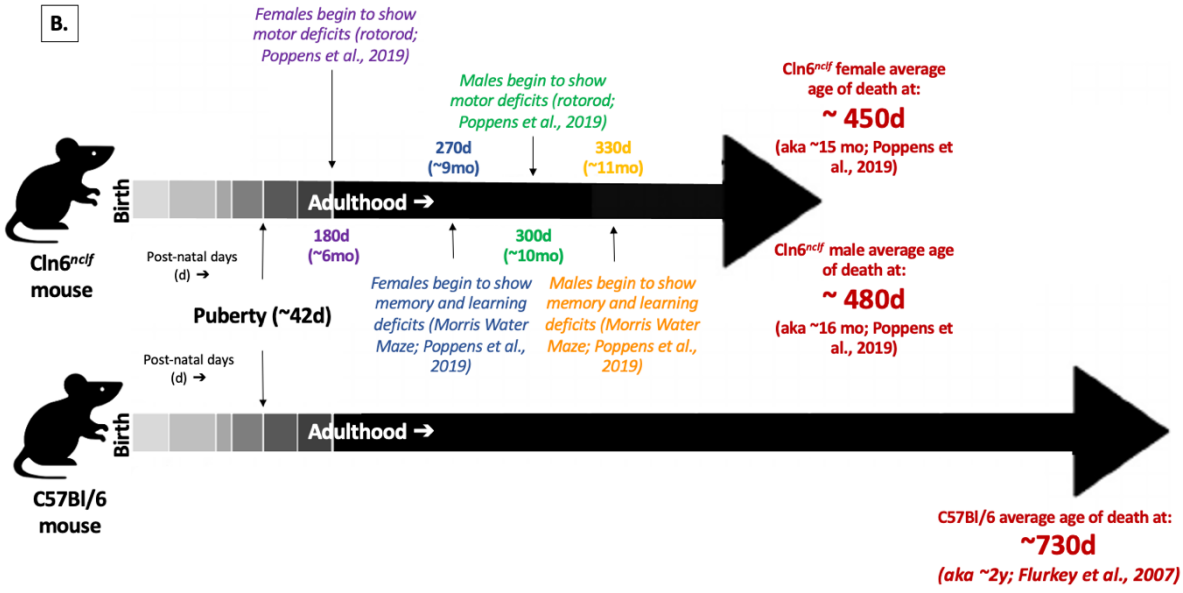
B.
Females begin to show motor deficits (rotorod; Poppens et al., 2019)
Males begin to show motor deficits (rotorod; Poppens et al., 2019)
270d (~9mo)
330d (~11mo)
Cln6nclf female average age of death at:
~ 450d
(aka ~15 mo; Poppens et al., 2019)
Birth
Adulthood →
Cln6nclf mouse
180d (~6mo)
300d (~10mo)
Post-natal days (d) →
Cln6nclf male average age of death at:
~ 480d
(aka ~16 mo; Poppens et al., 2019)
Puberty (~42d)
Females begin to show memory and learning deficits (Morris Water Maze; Poppens et al., 2019)
Males begin to show memory and learning deficits (Morris Water Maze; Poppens et al., 2019)
Post-natal days (d) →
Birth
Adulthood →
C57Bl/6 mouse
C57Bl/6 average age of death at:
~730d
(aka ~2y; Flurkey et al., 2007)

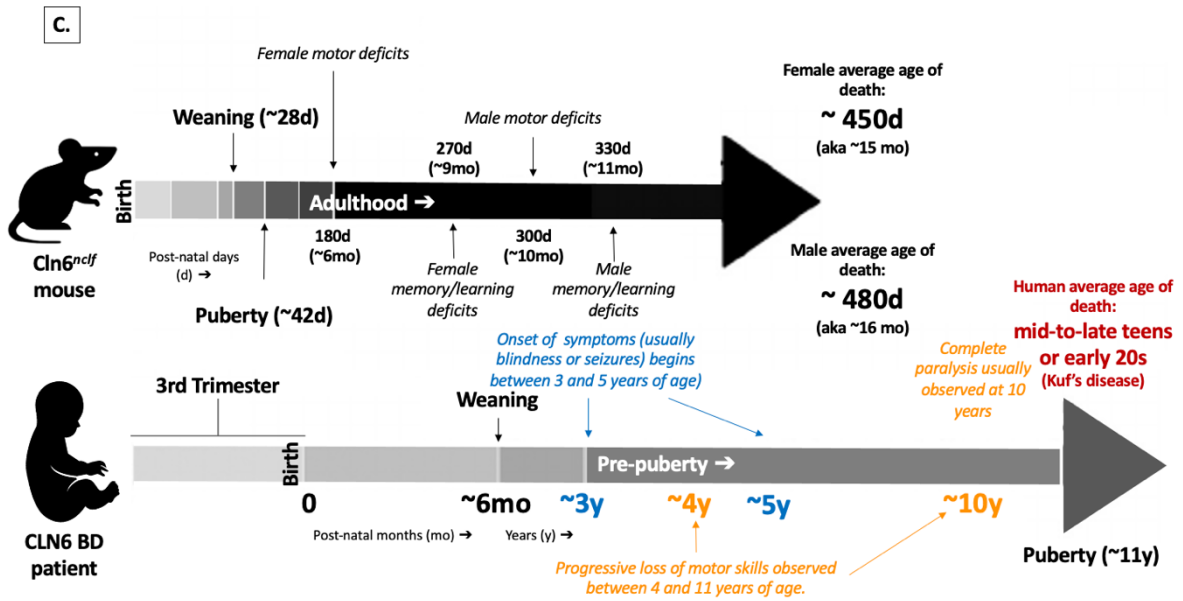
C.
Female motor deficits
Weaning (~28d)
Male motor deficits
270d (~9mo)
330d (~11mo)
Female average age of death:
~ 450d
(aka ~15 mo)
Birth
Adulthood →
Cln6nclf mouse
180d (~6mo)
300d (~10mo)
Post-natal days (d) →
Male average age of death:
~ 480d
(aka ~16 mo)
Female memory/learning deficits
Male memory/learning deficits
Puberty (~42d)
Onset of symptoms (usually blindness or seizures) begins between 3 and 5 years of age)
Human average age of death:
mid-to-late teens or early 20s
(Kuf's disease)
Complete paralysis usually observed at 10 years
3rd Trimester
Weaning
Birth
Pre-puberty →
CLN6 BD patient
0
~6mo
~3y
~4y
~5y
~10y
Post-natal months (mo) →
Years (y) →
Progressive loss of motor skills observed between 4 and 11 years of age.
Puberty (~11y)

1.8 Summary and experimental rationale

'Batten disease' refers to several heterogenous lysosomal-storage disorders (LSDs) of the nervous system known as the neuronal ceroid lipofuscinoses (NCLs). The NCLs are clinically characterized by debilitating neurological decline, progressive deterioration of vision and motor skills, personality and behavioural changes, dementia and myoclonic seizures (Haltia, 2006; Mole et al., 2011; Rider et al., 1988; Schulz et al., 2013). Thirteen NCL variants have been identified to date, with a fourteenth hypothesised, and all are currently considered fatal, with treatments focused primarily on palliative care and symptom amelioration. Patient life expectancy ranges from late teens to early 30's (Haltia, 2006; Mole & Cotman, 2015; Rider et al., 1988).

Despite their overlapping clinical symptoms and pathophysiology, each form of the disease is genetically distinct, caused by mutations in genes encoding a range of proteins involved in the endosomal-lysosomal-secretory compartment (Mole & Cotman, 2015). One NCL-related gene, located on chromosome 15q23, encodes a non-glycosylated ER membrane protein, known as CLN6 (Gao et al., 2002; Wheeler et al., 2002). CLN6 has been recently characterised as a key component in the transport of lysosomal enzymes from the ER to the Golgi, and its dysfunction or absence has been associated with two types of Batten disease: a variant of late infantile onset NCL (vLINCL or CLN6 BD), as well as Type A Kufs disease, one of the few NCLs characterized by adult-onset (Kay, 2011; Kufs, 1925; Lake & Cavanagh, 1978).

While there is currently no cure for any variant of Batten, including those caused by mutations in the *CLN6* gene, several promising experimental therapies are being developed (Johnson et al., 2019; Neverman et al., 2015). These include gene therapy, which involves the packaging of a healthy wild-type (WT) gene (e.g. *CLN6*) into either lentiviral or adeno-

associated viral (AAV) particles (Cain et al., 2019; Neverman et al., 2015; Weimer et al., 2019). These particles are then injected into the CNS of the CLN6 BD patient with the expectation that virally-transduced cells will begin to express the corrected WT gene. Gene therapy has been carried out, with promising results, in several preclinical trials using a variety of different NCL animal models (Best, 2017; Cain et al., 2019; Neverman et al., 2015). Preclinical, *CLN6*-specific gene therapy has been conducted by several groups using either $Cln6^{nclf}$ mice or $CLN6^{-/-}$ (OCLN6) South Hampshire sheep models. These studies involved the analysis of several pathological parameters, including CT scans, post-mortem histopathological analysis and behaviour assays, to help determine if viral-mediated over-expression of the *CLN6* gene will delay or halt disease progression *in vivo* (Best, 2017; Cain et al., 2019).

Small molecule or drug compound administration is another promising field of NCL therapy research, one that may prove to be complementary to gene/protein-restoration techniques such as gene therapy or enzyme replacement therapy (Johnson et al., 2019; Neverman et al., 2015). Cannabidiol (CBD) and gemfibrozil are two examples of small molecule compounds currently being investigated as potential Batten disease therapies. CBD is a compound extracted from the cannabis plant, *Cannabis sativa*, and has been found to have antiepileptic, analgesic, anxiolytic, antipsychotic, antioxidative and anti-inflammatory traits, amongst others, in both animal and human studies (Zuardi, 2008). These traits, combined with CBD's observed neuroprotective properties in Parkinson's disease models, identify CBD as a potential candidate for the amelioration of several of the symptoms associated with NCLs, such as seizures, neuroinflammation, pain and ataxia. Madison Partridge, from the Hughes' Lab, recently completed a master's project involving the 3-month voluntary oral dosing of $Cln6^{nclf}$ mice with cannabidiol. While her results were not definitive, they did suggest that a longer-term administration of the drugs might result in a more statistically significant

difference between CBD-dosed and control groups than the one observed during her three-month trial (Partridge, 2017).

Aside from CBD, some preliminary small molecule work has been done with the CLN6 BD phenotype using the lipid-lowering drug gemfibrozil (Best, 2017). Gemfibrozil is one of several fibrates being investigated as potential NCL therapies due to their anti-inflammatory and neuroprotective effect on neurons (Prahan, 2006). Preliminary data gathered from both *in vitro* and *in vivo* studies by the Hughes' laboratory has been promising, warranting further long-term investigation into the beneficial effects of gemfibrozil for the treatment of CLN6 BD (Best, et al., 2017).

To date, *in vitro* neural cultures and *in vivo* animal models have been invaluable in characterizing NCL disease pathologies and informing potential therapeutic strategies, such as those discussed above. For CLN6 BD , these have included ovine neural cultures from New Zealand South Hampshire sheep (OCLN6)(Best, et al., 2017; Best, 2017), mouse neural cultures ($Cln6^{nclf}$)(Best, 2017), and *in vivo* ovine, murine and canine models (Best, 2017; Best et al., 2017; Katz, et al., 2010; Morgan et al., 2013). Selecting an appropriate model with which to conduct further CLN6 BD research is essential. The $Cln6^{nclf}$ mouse was selected for the practical component of this thesis over larger animal models, such as sheep or dogs (which offer size and anatomy more similar to humans), due to the fact that this mouse, first identified by the Jackson Laboratory, has become recognized in the literature as an accurate, efficient and reliable model of human CLN6 BD and will allow for the cost-effective use of experimental group sizes large enough to provide statistically relevant results. The $Cln6^{nclf}$ model exhibits the key pathological features of its NCL human counterparts, including early retinal degeneration (~6 months of age), inflammation and associated microglial and astrocytic activation, the accumulation of autofluorescent cellular storage material, progressive cortical

atrophy and interneuron loss within the cerebral cortex and hippocampus (Morgan et al., 2013). Finally, the use of the Cln6^{nclf} murine model in the practical component of this thesis allows the work to remain consistent with past and current *in vivo* work being conducted by the Hughes lab and its collaborators (Best, 2017; Cain et al., 2019; Holthaus et al., 2019; Poppens et al., 2019).

1.8.1 Aims and objectives

The overall aim of this masters project was to investigate the efficacy of three experimental therapies, alone and in combination, as protection against the behavioural deficits experienced by untreated Cln6^{nclf} mice. In using a well-characterised murine model of CLN6 BD, the Cln6^{nclf} mouse, this project will build on the results of previous, smaller, pilot studies investigating the therapeutic potential of AAV2/9-mediated gene therapy, gemfibrozil and CBD against the CLN6 BD behavioural phenotype. This project also aims to replicate many of the parameters of an ongoing clinical phase I/II trial of gene therapy for CLN6 BD, with the intention of informing potential complementary therapeutic strategies that could be used to augment any therapeutic effects experienced by participants. This project was also designed to generate novel data, as a combination therapeutic approach involving gene therapy, gemfibrozil and CBD has not been attempted in Cln6^{nclf} mice, or any NCL animal model, before.

It should also be noted that the practical component of this thesis focuses solely on the analysis of behavioural data and the Cln6^{nclf} behavioural phenotype. Behavioural studies are only one important part of determining the efficacy of potential therapeutics and are best interpreted alongside post-mortem analyses. The amount of work required to conduct both the behavioural and post-mortem analyses would have been beyond the scope of a thesis-only masters, and so this thesis represents only a part of a larger preclinical study being conducted by multiple members of the Hughes (and associated) lab(s).

Specifically, this thesis aimed to achieve the following:

a) To characterise an untreated Cln6^{nclf} (UT^{Cln6nclf}) behavioural phenotype in both male and female animals at 6, 9 and 12 months of age, in order to distinguish a baseline UT^{Cln6nclf} control behavioural phenotype that could be used for comparisons when assessing the protective properties of gene therapy, gemfibrozil and CBD against CLN6 BD-related behavioural deficits.

b) To determine whether the small molecule therapeutics, gemfibrozil and CBD, provide any protection against the Cln6^{nclf} behavioural phenotype, on their own or in combination, without gene therapy. This will constitute the largest and most long-term study of the behavioural effects of either gemfibrozil or CBD in Cln6^{nclf} mice, and the first NCL study to combine the two.

c) To confirm the efficacy of AAV2/9-mediated gene therapy on its own, delivered via ICV injection on P0-2, in protecting against the UT^{Cln6nclf} behavioural phenotype in Cln6^{nclf} mice.

d) To characterise the effects of combining small molecule and gene therapies on the Cln6^{nclf} behavioural phenotype and compare these effects to UT^{Cln6nclf} and healthy WT (C57Bl/6) mice. This will be the first study to combine gene therapy with small molecule therapy in the Cln6^{nclf} mouse.

e) To assess whether any combination of gene therapy, gemfibrozil and/or CBD offers any therapeutic benefit, in terms of behavioural performance, over gene therapy alone.

f) To characterise any sex-based behavioural differences in response to the different therapeutic regimens.

Chapter 2: Materials and Methods

2.1 Materials

For a complete list of reagents, chemicals, lab-made solutions and equipment and software used, see ***Appendix A.***

2.2 Project overview

This project, originally designed by Stephanie Hughes and Hollie Wicky in consultation with the Weimer and Cooper labs and the Gray Foundation, involved the co-ordination, breeding, dosing, weighing and behavioural assessment of over 540 mice (see **section 2.3** for more information on the animals and associated ethics employed) for almost two years – from January 2018 through until December 2019.

The project was originally designed to have eighteen different experimental groups, each containing 30 animals (**Table 2.1**). Each experimental group was differentiated by strain (either C57Bl/6 or Cln6^{nclf}), sex (male or female), whether the animals in that group received gene therapy or not and which oral drug they were dosed with over their lifetime (vehicle, gemfibrozil, cannabidiol (CBD) or a combination of gemfibrozil and cannabidiol)(**Table 2.1**).

One to two days after birth (post-natal days 0-2), each mouse in every experimental group received an intracerebroventricular injection of either 4 µL of 'gene therapy' (scAAV9.CB.*hCLN6*; see **section 2.4.1** for more details) or 4 µL of 1x PBS ('no gene therapy'; **section 2.4**). Mice were then weaned at approximately 28 days and separated by their experimental group (**Table 2.1**) into enclosures that could contain up to 5 mice.

At approximately 30 days of age, mice began to be dosed with their allocated small molecule therapy via voluntary oral dosing (using strawberry flavoured jelly cubes or 'pellets'). Mice were dosed every second day for the rest of their natural lives or until they reached one of the experimental end-points outlined in **section 2.3**.

Ten mice from each experimental group (**Table 2.1**) were selected, at random, to undergo a battery of behavioural and motor skills assessments at 6 months of age (see **section 2.6** for more information on the beahvioural testing). These behavioural assays were conducted in a blinded manner to reduce experimenter bias. After testing, 5 of the original 10 animals were selected randomly to be euthanised for post-mortem analyses (not included in this thesis).

Similarly, 10 *different* mice from each experimental group (**Table 2.1**) were selected, at random, to undergo the same behavioural assays at 9 and 12 months of age (**Figure 2.1**). Further behavioural assessment was conducted on all remaining animals at 18 months of age but this data was not included in this thesis.

The above outline describes the original 'idealised' plan for this thesis's project. In reality, due to variations in litter birth timing and size, as well as the unexpected loss of some animals to humane end-points (see **section 2.3**), the number of mice that ultimately underwent behavioural testing in each experimental group at each time point varied somewhat (see **Tables 2.4** and **2.5** for exact group sizes for behavioural testing). Similarly, not every mouse was weaned at exactly 28 days of age, started dosing at 30 days of age or began behavioural testing at exactly 6, 9 or 12 months of age. The Hughes Lab managed, however, to keep these dates within a small margin (approximately 2 days either side), and used a 'staggered' approach to ensure all mice were treated and tested as close to the originally planned time points a possible (see **Figure 2.1**).

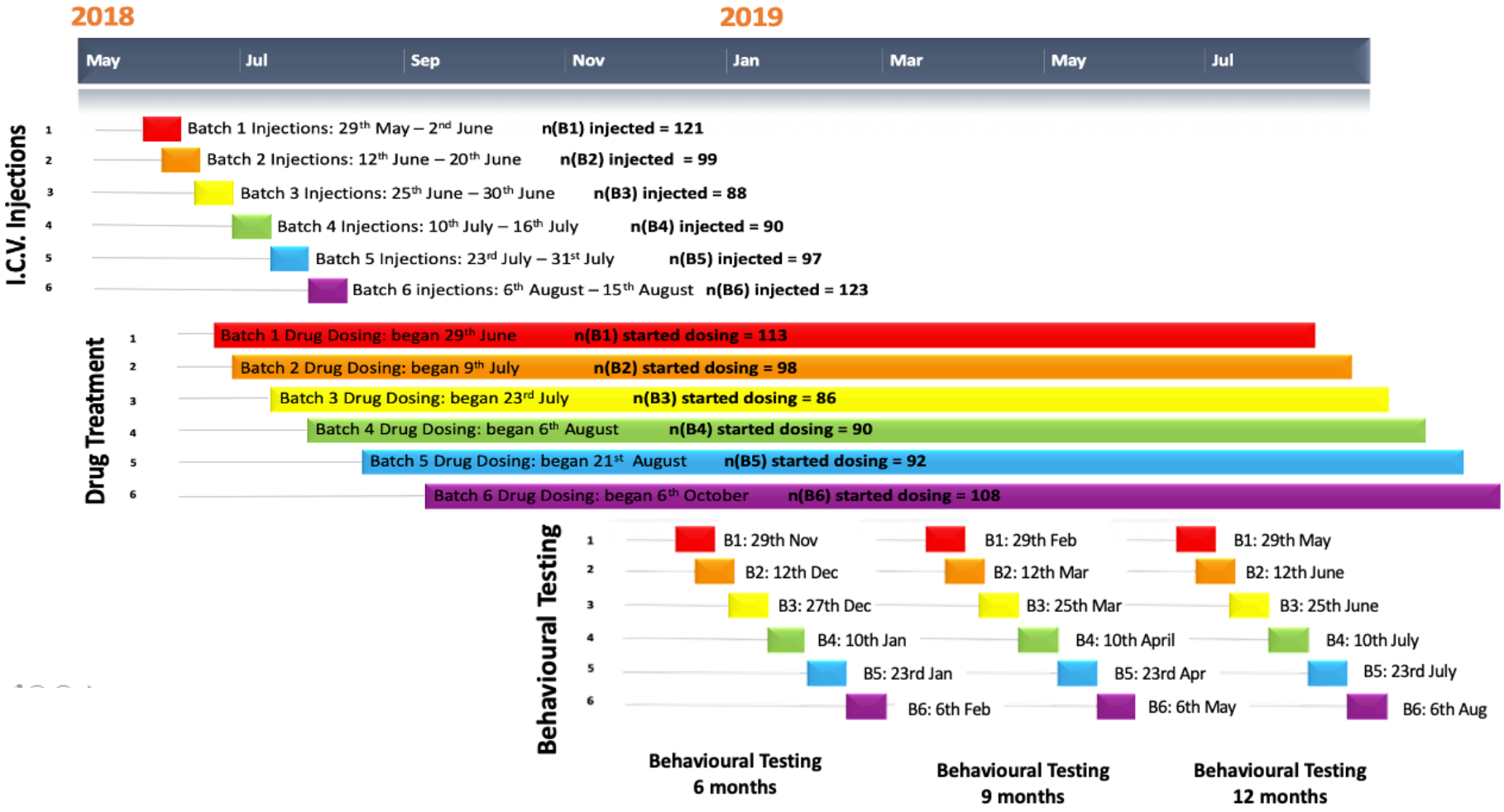
2018
2019
May
Jul
Sep
Nov
Jan
Mar
May
Jul
I.C.V. Injections
1 Batch 1 Injections: 29th May – 2nd June n(B1) injected = 121
2 Batch 2 Injections: 12th June – 20th June n(B2) injected = 99
3 Batch 3 Injections: 25th June – 30th June n(B3) injected = 88
4 Batch 4 Injections: 10th July – 16th July n(B4) injected = 90
5 Batch 5 Injections: 23rd July – 31st July n(B5) injected = 97
6 Batch 6 injections: 6th August – 15th August n(B6) injected = 123
Drug Treatment
1 Batch 1 Drug Dosing: began 29th June n(B1) started dosing = 113
2 Batch 2 Drug Dosing: began 9th July n(B2) started dosing = 98
3 Batch 3 Drug Dosing: began 23rd July n(B3) started dosing = 86
4 Batch 4 Drug Dosing: began 6th August n(B4) started dosing = 90
5 Batch 5 Drug Dosing: began 21st August n(B5) started dosing = 92
6 Batch 6 Drug Dosing: began 6th October n(B6) started dosing = 108
Behavioural Testing
1 B1: 29th Nov B1: 29th Feb B1: 29th May
2 B2: 12th Dec B2: 12th Mar B2: 12th June
3 B3: 27th Dec B3: 25th Mar B3: 25th June
4 B4: 10th Jan B4: 10th April B4: 10th July
5 B5: 23rd Jan B5: 23rd Apr B5: 23rd July
6 B6: 6th Feb B6: 6th May B6: 6th Aug
Behavioural Testing 6 months
Behavioural Testing 9 months
Behavioural Testing 12 months

⇐ **Figure 2.1 | Approximate timeline of the Hughes Lab's Gray Foundation preclinical trial dosing regimen (previous page)**. Mice were divided into breeding 'batches' of approximately 90 animals and underwent neonatal i.c.v injections and began voluntary oral drug dosing (via jelly pellets) every second day in a staggered fashion. This allowed for all mice to receive an i.c.v injection of either scAAV9.CB.*hCLN6* or 1x PBS at P0-2 and to be dosed every second day from 28 days of age. Similarly, mice were tested in a 'staggered' fashion to ensure all mice were 6, 9 or 12 months of age when they underwent testing. Image originally created by *Jasmine Lock from the Hughes Lab, edited by Madeline McIntyre Wilson (the author).*

Table 2.1 | Summary table of the different experimental groups used in the Gray Foundation trial. Each group had a unique combination of strain (C57Bl/6 or Cln6^{nclf}), sex (male or female), drug treatment (vehicle, gemfibrozil, CBD or a combination of gemfibrozil and CBD), and gene therapy treatment (received an injection of scAAV9.CB.*hCLN6* at P0-2 aka 'Yes' or received an injection of 1x PBS aka 'No').

Trial group	Genotype	Gene therapy?	Drug therapy	Sex	n for injections and dosing
A	C57Bl/6	Yes	Vehicle	F	30
B	C57Bl/6	Yes	Vehicle	M	30
C	Cln6^{nclf}	No	Vehicle	F	30
D	Cln6^{nclf}	No	Vehicle	M	30
E	Cln6^{nclf}	No	Gemfibrozil	F	30
F	Cln6^{nclf}	No	Gemfibrozil	M	30
G	Cln6^{nclf}	No	Cannabidiol (CBD)	F	30
H	Cln6^{nclf}	No	CBD	M	30
I	Cln6^{nclf}	No	Gemfibrozil and CBD	F	30
J	Cln6^{nclf}	No	Gemfibrozil and CBD	M	30
K	Cln6^{nclf}	Yes	Vehicle	F	30
L	Cln6^{nclf}	Yes	Vehicle	M	30
M	Cln6^{nclf}	Yes	Gemfibrozil	F	30
N	Cln6^{nclf}	Yes	Gemfibrozil	M	30
O	Cln6^{nclf}	Yes	CBD	F	30
P	Cln6^{nclf}	Yes	CBD	M	30
Q	Cln6^{nclf}	Yes	Gemfibrozil and CBD	F	30
R	Cln6^{nclf}	Yes	Gemfibrozil and CBD	M	30
				Total	540

2.3 Animals

All animal work was conducted in strict accordance with The Animal Welfare Act, 1999, and had the approval for animal husbandry, surgical procedures and use of animal tissue, granted by the University of Otago Animal Ethics Committee (AEC). The use of AAV *in vivo* in the mouse brain was approved by the New Zealand Environmental Protection Authority (EPA; ethics approval number GMD101718).

All animals used for experimentation were either affected $Cln6^{nclf}$ mice or healthy wild-type (WT) control animals from the background strain C57Bl/6. Animals were bred and supplied by the University of Otago's Hercus-Taieri Research Unit (HTRU).

After weaning at an age of ~28 days, animals were kept, in most cases, in same-sex group housing (2-5 mice) and monitored daily by trained HTRU staff for signs of health decline. Animals, when not being handled, had constant access to food, water and recreation (plastic cylinder and straw bedding) throughout the experiment and were kept on a strict 12-hour light/dark cycle.

Animals were euthanised at one of three end-points:

(1) at a planned, post-behavioural analysis time-point (6, 9 or 12 months)

(2) after losing 20% of their maximum weight or 10% of their maximum weight within a 7-day period

(3) for ethical and/or welfare reasons determined by the Animal Welfare Office (AWO) veterinarians

2.4 Neonatal intracerebroventricular (i.c.v) injections

This protocol was adapted, with consultation from the AWO veterinary team and University of Otago's AEC, from the protocols used by Cain et al., 2019 and *Kim et al., 2014*

2.4.1 Self-complementary (sc) adeno-associated virus (AAV) vector expressing human CLN6 (hCLN6) under the control of a CB promoter

The vector used for the work presented in this thesis was cloned and packaged by the Viral Vector Core at the Nationwide Ohio Children's Hospital (NWOCH) in Columbus, Ohio, USA.

The vector was a recombinant, self-complementary (sc) adeno-associated virus serotype 2/9 (AAV9) vector that expressed the human gene *CLN6* (*hCLN6*) under the control of the synthetic CAG (CB) promoter (scAAV9.CB.*hCLN6*).

The CAG promoter consists of three parts:

(1) the cytomegalovirus (CMV) early enhancer element

(2) the promoter, the first exon and the first intron of a chicken beta-actin gene

(3) the splice acceptor of the rabbit beta-globin gene (Hitoshi et al., 1991; Jun-ichi et al., 1989).

These elements were chosen to mirror the vector used in the 2016 Amicus Therapeutics CLN6 Batten disease trial (Trial No. NCT02725580, *Clinicaltrials.gov*). Subjects in that trial received a single-dose of AT-GTX-501 (scAAV9.CB.*hCLN6*) via intrathecal delivery.

2.4.2 Injection apparatus

The injection apparatus (**Figure 2.2**) used to deliver either AAV2/9 (NWOCH's Viral Vector Core, Nationwide Ohio Children's Hospital) or 1x PBS (Gibco™, Sigma-Aldrich NZ) was created

using a customised design adopted from the Weimer lab at Sanford Research, South Dakota, USA (Brandon Meyerink, personal communication).

The design consisted of a 1 mL disposable slip-lock syringe (BD Luer-Lock™, Medshop NZ; **Figure 2.2.C**) with a 2 – 20 µL pipette tip (**Figure 2.2.B**) attached to the slip-lock nozzle and secured in place with fast-drying adhesive (Selleys®, Mitre10 NZ). A short (1-2 cm) piece of surgical silicon tubing (1 mm inner diameter; **Figure 2.2.A**) was attached to the cut-off tip of this pipette and also secured in place. Finally, custom-made glass needle tips could be inserted into the free end of the silicon tubing (**Figure 2.2**).

After the injection protocol had taken place, the glass needle tips could be removed and disposed of appropriately. As the silicon tubing aged, it was either replaced or a small amount of fast-drying adhesive was used to secure the glass needle tips in place for each set of injections, to prevent the needle slipping out of the stretched tubing and to keep the connection air-tight.

The glass needle tips used for all injections were made from 15.2 cm borosil glass capillary tubes with filament with an original outer diameter of 1 mm (World Precision Instruments Inc). These tubes were pulled to 1 µm outer diameter points using the University of Otago's Department of Psychology's electrophysiology micropipette puller (Sutter Instruments #P-97) and snapped off at the other, non-pulled, end to shorten them into 2–3 cm lengths.

After being inserted into the injection apparatus's tubing and fixed into position, these tips were cut manually by the researchers approximately ½ cm from the point – creating a wider outer diameter. While the new outer diameter of the cut needle tip would vary slightly between needles, depending on the position at which the cut was made, the majority would

have been approximately 100 µm in outer diameter (Brandon Meyerink, personal communication). All needle tips used would have been finer than a 34 gauge (G) needle, hopefully reducing the amount of local tissue damage at the injection site caused by the insertion of the needle (Glascock et al., 2011).

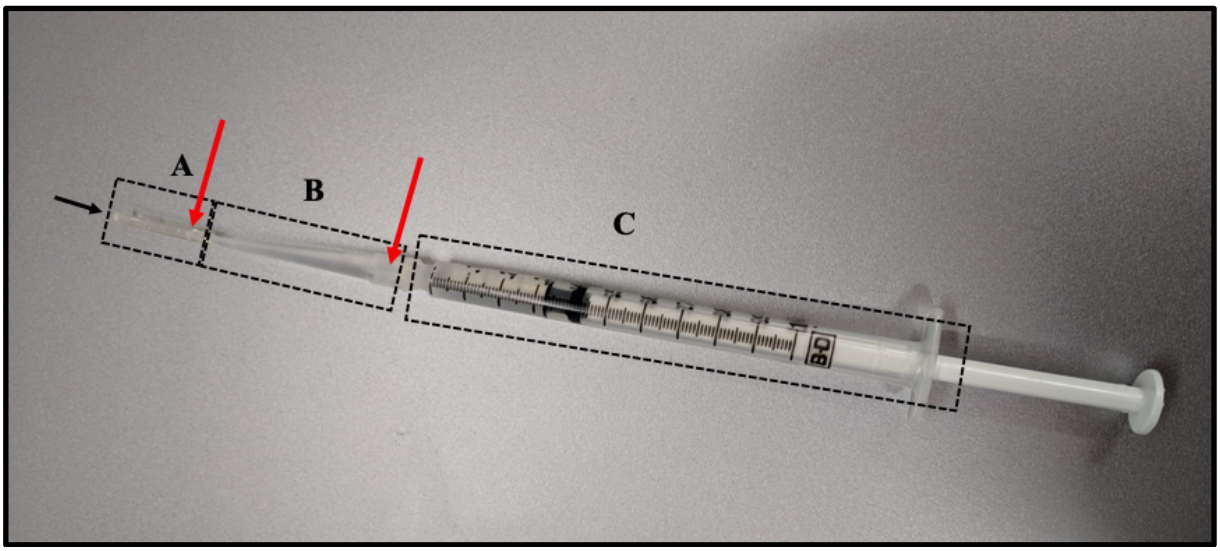

Figure 2.2 | Weimer laboratory neonate i.c.v Injection apparatus. Consists of (A) a short (1–2 cm) piece of surgical silicon tubing (1 mm inner diameter), attached to (B) a 2–20 µL pipette tip with a cut-off tip, which is fastened to the (C) slip-lock nozzle of a disposable 1 mL slip-lock syringe. Fast-drying fixative (Selleys®, Mitre10), was used to keep all components firmly attached (red arrows) and a manually pulled glass needle tip (2–3 cm in length) would be inserted into the silicon tubing (black arrow). Photograph taken and edited by the author.

2.4.3 Injection protocol

All injections were performed with the HTRU's Physical Containment Level 2 (PC2) biosafety bubble (BioBubble), with all surfaces and equipment wiped down with 10% TriGene (Merck, InVitro NZ) and 70% ethanol (Merck, LabSupply NZ) before and after the procedure. Personnel wore personal protective equipment (PPE), at all times within the BioBubble. This included plastic eyewear, disposable hair nets, filter masks, gloves, lab coats and shoe covers. Glass needle tips and any protective material that came into contact with the injection apparatus were disposed of in 10% TriGene after each injection session. The injection apparatus was cleaned thoroughly by aspiration of 70% ethanol, 10% TriGene and water after each session. The syringe of the injection apparatus (**Figure 2.2.C**) was stored with 1 mL of 3% hydrogen peroxide in the barrel between injection sessions.

Protocol training was conducted by Brandon Meyerink from the Weimer lab (Sanford Research, South Dakota, USA). PC2 safety training was provided by the University of Otago's Department of Biochemistry Health and Safety Officer, Jackie Daniels. Viral-handling and safety training was provided by Hollie Wicky and Alison Clare from the Hughes lab (Department of Biochemistry, University of Otago, Dunedin, NZ).

Six hundred and eighteen mouse pups, including both $Cln6^{nclf}$ and healthy WT controls, were injected on postnatal day 0-2 (P0, P1 or P2) with either 4 µL of AAV2/9 or 1x PBS. Due to the size of the study's animal cohort, litters were born in groups of ~90 pups, approximately 2 weeks apart (**Figure 2.1**). This ensured that all pups could be injected within the desired 2-day post-natal window.

Prior to injection, pups were removed from their home cage in small groups (half a litter at a time). Leaving some pups with the mother while their littermates were injected reduced the amount of stress experienced by the mother during this procedure, as measured by a reduction in post-injection maternal cannibalism rates.

Pups were originally going to be cryo-anaesthetised by being placed on a paper towel-covered aluminium plate that had been kept in a -80℃ freezer overnight, but this method – recommended by Kim et al., 2014 – proved to be unsuitable as it caused the mice to fall asleep too quickly (under 5 minutes) and reduced their core temperatures too low. This technique was also found to have a high risk of freeze burn-associated tissue damage.

For the pups welfare, this technique was modified and they were cryo-anaesthetised via placement on a damp paper towel in a Styrofoam box of ice. Pups were monitored closely and consistently throughout the anaesthesia process. This adapted method was slower than the original, with pups now requiring 7-10 min to reach a 'surgical plane of general

anaesthesia' (determined by an absence of the pedal withdrawal reflex), but pups revived quicker and the water in the towel appeared to be protective against freeze-related tissue damage. Post-procedural maternal cannibalism was also reduced after switching to this method.

Once pups had been anaesthetised, the top of their heads were cleaned using an autoclaved cotton-tip applicator and 70% ethanol (Merck, LabSupply). The injection site, for all pups, was approximately 1 mm lateral from the sagittal suture, halfway between lambda and bregma, on the left hemisphere of the skull (**Figure 2.3**). These landmarks are visible to the naked eye under a good light source in murine neonates. The glass needle tips on the injection apparatus (**Figure 2.2**) were marked, either with pen or a small amount of dried super adhesive, at 2 mm from the tip, to ensure the injection went no deeper than 2 mm into the left hemisphere of the pup's skull. This position and depth was chosen to maximise the chances of the AAV2/9 or 1x PBS being injected directly into the pup's left hemisphere ventricle. Injection of AAV vectors into this area has been previously shown to facilitate global spread and transduction of the virus throughout the murine CNS, an ideal outcome for potential therapies of a global neurodegenerative disorder like CLN6 BD (Lock, 2018).

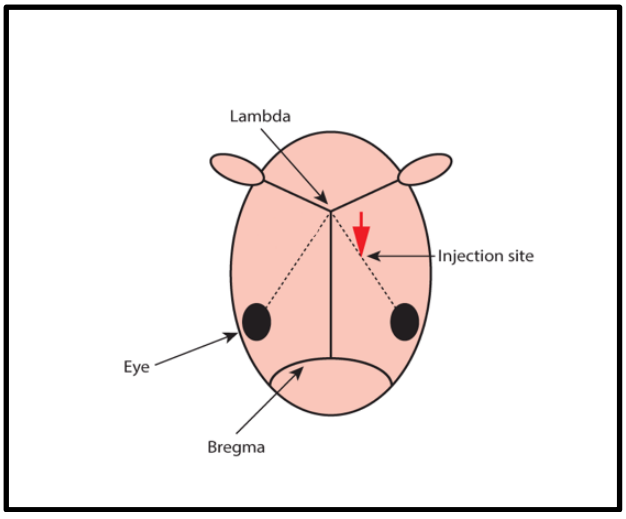

Figure 2.3| Schematic of neonatal i.c.v injection site. Mice received a single, unilateral i.c.v injection of either 4 uL of scAAV9.CB.*hCLN6* or 4 uL 1x PBS into the left hemisphere (red arrow) at P0-2. Image author's own.

Prior to injection, a small volume of liquid was released from the injection apparatus to remove any blockages and avoid the accidental injection of air bubbles. Each injection consisted of 4 uL of either AAV2/9 or 1x PBS, and each one was delivered to the left hemisphere by hand, as opposed to stereotaxic injection. The glass needle tip was left within the injection site for approximately 5 seconds post-delivery to reduce the amount of backflow. Pups were then placed on a heating pad (36.6°C, HTRU, University of Otago) with their littermates for 2-5 minutes in order to reverse anaesthesia.

After being revived and returned to their home cage, animals were monitored for 5 days post-injection for cannibalism, pain symptoms and maternal water consumption, as per the University of Otago's Animal Welfare guidelines.

It took approximately 3-8 days to inject all ~90 pups within each litter group (**Figure 2.1**) and injections were carried out primarily by Ben Bolton (assistant research fellow, Hughes lab) and Madeline McIntyre Wilson (author, Hughes lab), with some done by Jasmine Lock (assistant research fellow, Hughes lab) and Brandon Meyerink (assistant research fellow, Weimer lab).

2.5 Small molecule therapy

2.5.1 Weaning and jelly conditioning

Mouse pups were weaned between 23-28 days of age. Male and female pups were separated into same-sex group housing (mouse 'stock boxes'), with up to 5 mice per cage. Cln6^{nclf} mice were housed with other Cln6^{nclf} mice, and WT mice were housed with other WT mice.

In most cases, all 2-5 mice in one group cage would be receiving the same small molecule therapy regimen (**2.5.2** and **2.5.3** below), e.g. all mice in cage 'x' had been injected with the same treatment (AAV2/9 or 1x PBS) and would receive the same type of drug.

After weaning, mice were given 2-3 mL of plain strawberry jelly (Champion Jelly, Trents Wholesaler NZ; **Appendix A.2**) on a 'dosing platform' (30 mm-diameter plastic petri dishes; Thermo Fisher Scientific NZ) placed in the centre of the cage. The jelly was left overnight and any remaining in the morning was disposed of and replaced with fresh jelly. Mice were given jelly every day for up to a week, until each animal in the group cage had reached the age of at least 28 days. This conditioning was designed to help the mice overcome any neophobia and accustom them to jelly as a food-source. This 'conditioning' step was critical for the voluntary oral dosing protocol.

2.5.2 Voluntary oral dosing

This protocol was adapted from the protocol used by Zhang & Zhang, 2011

Each mouse began one of four small molecule therapy (drug) dosing regimens after weaning (approx. 1 month of age). Gemfibrozil, cannabidiol (CBD) oil, a combination of both drugs or a vehicle control were administered orally, suspended in a palatable, 1 mL gelatine (jelly) tablet. All mice were dosed every second day from weaning to their individual experimental end-

points. Due to the staggered nature of the litter breeding for i.c.v injections (**section 2.4**), dosing was also staggered (refer to **Figure 2.1**).

Table 2.2 | Summary table of gemfibrozil doses, based on mouse weight (in grams). Mouse weights (in grams) were split into 5 g ranges or 'bins' and all doses were calculated using the lowest weight in the range.

Gemfibrozil dose rate of 120 mg/kg (0.12 mg/g; adapted from *Best, 2017 and Mercer, unpublished thesis***)**			
Mouse weight ranges (g)	**Lowest weight in range (g)**	**Calculation**	**Gemfibrozil dose (mg) for all mice in this weight range**
5 - 9	5	0.12 x 5	0.6
10 - 14	10	0.12 x 10	1.2
15 - 19	15	0.12 x 15	1.8
20 - 24	20	0.12 x 20	2.4
25 - 29	25	0.12 x 25	3
30 - 34	30	0.12 x 30	3.6
35-39	35	0.12 x 35	4.2
40 - 44	40	0.12 x 40	4.8
45-49	45	0.12 x 45	5.4
50-54	50	0.12 x 50	6

Table 2.3 | Summary of CBD doses, based on mouse weight (in grams). Mouse weights (in grams) were split into 5 g ranges or 'bins' and all doses were calculated using the lowest weight in the range.

Cannabidiol dose rate of 5 mg/kg (0.005 mg/g; adapted from *personal communication with HERBA imports***)**			
Mouse weight ranges (g)	**Lowest weight in range (g)**	**Calculation**	**CBD dose (mg) for all mice in this weight range**
5 - 9	5	0.005 x 5	0.025
10 - 14	10	0.005 x 10	0.05
15 - 19	15	0.005 x 15	0.075
20 - 24	20	0.005 x 20	0.1
25 - 29	25	0.005 x 25	0.125
30 - 34	30	0.005 x 30	0.15
35-39	35	0.005 x 35	0.175
40 - 44	40	0.005 x 40	0.2
45-49	45	0.005 x 45	0.225
50-54	50	0.005 x 50	0.25

In order to determine the correct dosage for each mouse, mice were weighed weekly from weaning, with weights rounded to the nearest gram (g). The sheer size of the study cohort, once all mice had been weaned, meant that it wasn't feasible to dose mice using their individual, specific weights. Instead, weights were divided into a series of weight ranges, with each range allocated a drug-specific dose in mg (**Tables 2.2** and **2.3**). These doses were calculated using the different dose rates determined for each drug and the lightest weight in the weight range, producing a conservative dose for all mice with weights within that range.

On their allocated dosing day, mice were separated from their cage-mates (up to 5 mice per cage) by insertable dividers constructed from white corflute, a lightweight, durable polypropylene often used for industrial packaging. The design for these corflute dividers was based on a cardboard prototype created by HTRU technician Becci Gadbsy, which proved to be too flimsy (and edible) for long-term use. Madeline McIntyre Wilson and Ben Bolton from the Hughes lab, along with Peter Small, the property services manager of the University of Otago's Department of Biochemistry, designed, measured, cut and constructed the corflute dividers specifically for the HTRU group mouse stock boxes (**Figure 2.4**). Approximately 150 dividers in total were made and stored in the HTRU.

When inserted, the corflute dividers split the stock box into five spaces which could comfortably fit a mouse and its 'dosing platform'. The metal grate lid of the stock box could sit on top of the dividers, closing each mouse into its own enclosed space. Some stock boxes, due to warping and distortion caused by frequent autoclaving, required the use of bull clips to keep the lid firmly down on top of the divider and prevent mice climbing over the top and into their neighbour's space.

When the mice were younger and smaller, it was possible for the fifth mouse – left in the largest space (**Figure 2.4.E**) – to climb into the small space between the wall of the stock

box and the wall of the divider, and sometimes get stuck. To prevent this, large silicon tubing (2 cm-diameter; **Figure 2.4**) was cut into 10 cm strips and sliced vertically on one side, producing a circular 'bumper' that could be slid onto the corners of the divider, facing outwards into the fifth space and prevented animals moving into the small gap between the divider and stock box wall.

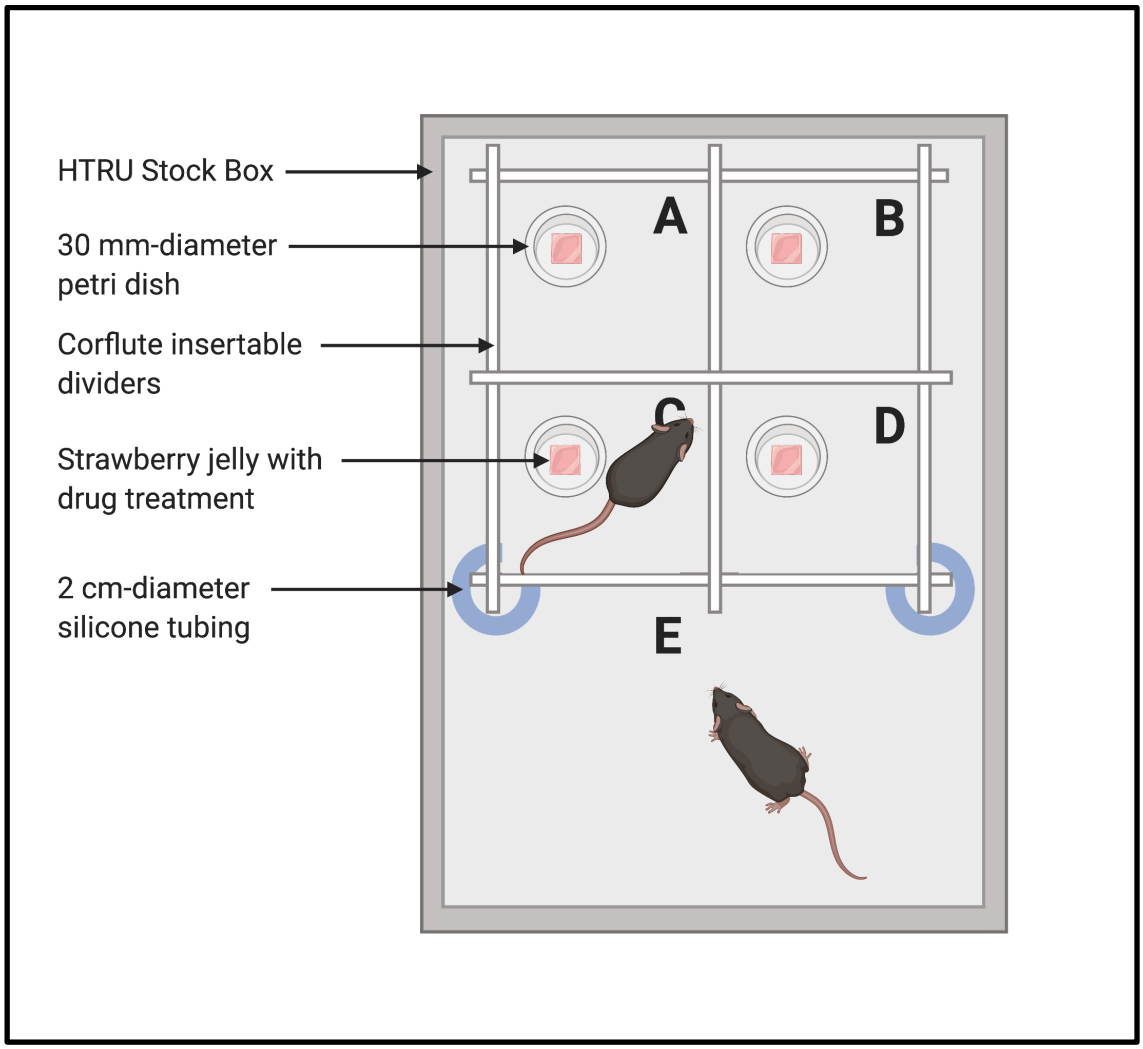

Figure 2.4 | Schematic of made-for-purpose dosing divider. Pictured in a HTRU stock box. The mae-for-purpose divider separated stock boxes into five different areas by a dividing structure made out of corflute and surgical silicon tubing (blue circles). Image author's own, *created using biorender.com*.

Once the mice were separated and given their correct dose, they would be left to consume their jelly for 45-120 min. They would then be released by the removal of the dividers

from the stock box. Records were kept of mice who failed to consume all of their jelly within that time period.

Dosing was carried out by Madeline McIntyre Wilson, Ben Bolton, Jasmine Lock, Janet Xu and Stephanie Hughes from the Hughes Lab, as well as by Becci, Jaye, Louise, Robyn, Fiona, and Matthew from the HTRU.

2.5.3 Jelly production

This protocol was adapted from the protocols used by Zhang & Zhang, 2011 and Mercer, unpublished thesis.

Jellies were made in bulk, with the production process taking up to two days a week. An Excel spreadsheet was used to calculate how many individual mice were in each weight range and therefore how many 1 mL jelly tablets, or cubes, needed to be made up using the doses associated with those ranges. If a mouse was fed every second day, then at least three jelly tablets needed to be made, per mouse, for one week of dosing.

If there were, for example, ten mice who all weighed between 15-19 g and were all receiving CBD oil only as their drug treatment regimen, then that meant that 30 jelly tablets needed to be made that week, with each tablet containing a CBD oil dose of 0.075 mg. This also meant that, for that particular group of mice, a minimum of 30 mL of jelly needed to be made to produce enough jelly tablets.

This was all calculated automatically by an Excel spreadsheet for all four treatment regimens and across all weight ranges. The only required input was the individual weights of each mouse, each week.

Jelly was made by heating one or more beakers-worth of distilled water (dH_2O) to 50℃ using an electric kettle (Breville, Briscoes NZ), and then placing the water in beakers on a

magnetic stirrer hotplate (Chiltern Scientific, Thermo Fisher Scientific NZ) and adding enough Splenda® sweetener (Splenda®, Trents Wholesale) to create a 20% solution. A magnetic stirring pill was used to help dissolve the Splenda®, after which an equivalent amount of strawberry jelly crystals (Champion Professional, Trents Wholesale) would be added, creating a thick, viscous liquid. 14% gelatin and 4% methylcelluose would then be added and dissolved, giving the jelly a more solid consistency when it set. A hand-held immersion blender (Bodum Bistro, Briscoes NZ) would be used, when necessary, to help completely dissolve the gelatin and methylcellulose into the solution.

Once all the components of the jelly were added and dissolved, this 'master mix' could be separated, using a measuring cylinder, into four smaller beakers: one for the gemfibrozil-only tablets, one for the CBD oil-only tablets, one for the combination tablets and one for the vehicle control tablets. Each beaker would contain the correct amount of jelly required to make enough tablets to dose all the mice taking that drug for at least a week, so at least three doses per mouse. Another, smaller measuring cylinder would be used to measure out the amount of jelly required to make enough tablets for mice within a weight range subset for a given drug and that liquid jelly would be mixed, still at a temperature of 50℃, with the correct volume of drug stock solution to ensure that every mL of that jelly would contain the correct dose for mice of a certain weight.

These sub-beakers of jelly, now each containing a specific drug at a specific concentration, would be poured liberally over silicon 160-well ice cube trays (12.1 cm x 23.8 cm, Amazon). Any excess liquid jelly would be scraped off the top with a kitchen scraper. The trays would then be placed between two pieces of baking paper, labelled to identify the concentration/dosage and type of drug in the jelly, and placed in a -20℃ freezer to set overnight – producing trays of 160x 1 mL jelly tablets with uniform drug concentration. If the

amount of jelly required for that week was less than 160 mL, then several of these trays had been cut into half, third, quarter and even eighth sizes, allowing some flexibility in the amount of jelly that could be produced at one time with one drug at a specific concentration.

All jelly was stored in containers labelled with their drug and concentration/dose at -20℃ until needed, and could be kept frozen for up to 2 weeks.

Twenty four-well, TC-treated, cell-culture plates (Corning® Costar®, Sigma-Aldrich NZ), were used and reused to distribute jelly containing the correct drug and dose to the correct animals (**Figure 2.5**). Each well in the plate was labelled with a mouse's individual identification number, which contained their ear tag and an arbitrary number relating to the trial, and a reference sheet was used to ensure these wells received the correct jelly. Jelly was removed from the 24-well plates using a metal spatula and placed onto the mouse's dosing platform within their divided stock box.

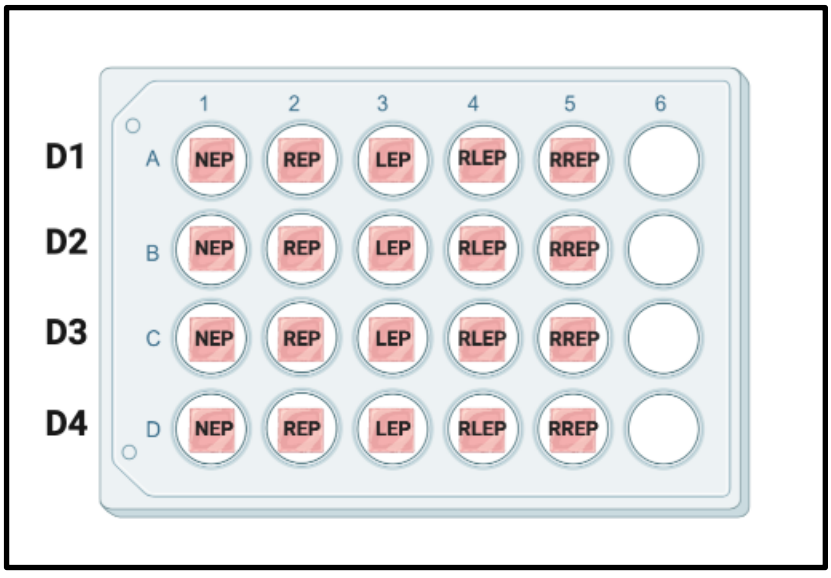

Figure 2.5| **24-well cell-culture plates for jelly storage and transportation**. 24-well cell-culture plates were used to store and transport jelly tablets from the Biochemistry department to the individual mice in the HTRU These plates were washed and reused after each shipment/dosing. All wells labelled 'NEP' would carry jelly with the correct dose for the mouse in cage x with the ear-tag 'NEP'. 'REP' would carry doses for the mouse with the ear-tag 'REP' etc. These plates could carry up to four doses (D1-D4) – four different days' worth of drug treatment - over to the HTRU at a time, so jelly tablets could be made in bulk. Image author's own, created using biorender.com.

A small subset of mice appeared to develop a jelly aversion during the study, refusing to eat some or – in the worst cases - any of their jelly. In order to transition these mice back into their planned drug therapy regimens, several alterations were made to the jelly making and dosing protocols:

(1) Drug-adverse mice were returned to plain strawberry jelly (as per **2.5.1**), to see if they were willing to eat the jelly without any drug. If they ignored the jelly, then it was replaced with a different flavour (e.g. lime) – also without any drug.

(2) Once the mice were consistently eating all of their plain strawberry or plain lime jelly (Value, Safeway Traders NZ) tablets (minimum of three dosings), their drug was reintroduced at the lowest dose (e.g. the concentration they would have received if they still weighed ~10 g).

(3) Once they were consistently eating this jelly (again, minimum of three dosings), then the dose was increased to the next weight range's concentration. This continued until the mice were consistently eating the correct dose in their jelly.

2.6 Behavioural Testing

Due to the staggered birth of the study cohort (**Figure 2.1**), all behavioural assays conducted at 6, 9 and 12 months (12 months only for rotarod) were also staggered, with ~30 mice being tested every 2 weeks over a total of 2 months, per time point (**Tables 2.4** and **2.5**).

The behavioural testing aspect of this study was designed to be between-subjects, meaning that the ~180 animals tested at each time point differed from those tested at other time points. ~540 animals were tested in total, across all three time points, though the mice and data from 12 months for ataxia is not included in this thesis due to the assessment being conducted by a different experimenter – Jasmine Lock. The subjective nature of the ataxia protocol meant that including Jasmine's data for analysis would have meant any results might be heavily influenced by experimenter-specific bias.

Table 2.4 | Population table for different experimental mouse groups tested for rotarod behaviour at 6, 9 and 12 months of age. (n)6 = number of mice tested at 6 months; (n)9 = number of mice tested at 9 months; (n)12 = number of mice tested at 12 months; WT = wildtype; UT^{Cln6nclf} = Cln6^{nclf} mice injected with 1x PBS and treated with vehicle jelly; Gemfib^{PBS} = Cln6^{nclf} mice injected with 1x PBS and treated with gemfibrozil; CBD^{PBS} = Cln6^{nclf} mice injected with 1x PBS and treated with CBD; Combo^{PBS} = Cln6^{nclf} mice injected with 1x PBS and treated with a combination of gemfibrozil and CBD; Gemfib^{AAV9} = Cln6^{nclf} mice injected with scAAV9.CB.*hCLN6* and treated with gemfibrozil; CBD^{AAV9} = Cln6^{nclf} mice injected with scAAV9.CB.*hCLN6* and treated with CBD; Combo^{AAV9} = Cln6^{nclf} mice injected with scAAV9.CB.*hCLN6* and treated with a combination of gemfibrozil and CBD; No Drug^{AAV9} = Cln6^{nclf} mice injected with scAAV9.CB.*hCLN6* and treated with vehicle jelly.

	Genotype	Treatment Group	Sex	(n)6	(n)9	(n)12
A	WT (C57Bl/6)	Vehicle (WT)	M	9	9	14
B	WT (C57Bl/6)	WT	F	8	9	9
C	Cln6^{nclf}	1x PBS + vehicle (UT^{Cln6nclf})	M	12	8	7
D	Cln6^{nclf}	UT^{Cln6nclf}	F	9	10	8
E	Cln6^{nclf}	1x PBS + gemfibrozil (Gemfib^{PBS})	M	10	9	7
F	Cln6^{nclf}	Gemfib^{PBS}	F	10	9	8
G	Cln6^{nclf}	1x PBS + cannabidiol (CBD^{PBS})	M	10	15	10
H	Cln6^{nclf}	CBD^{PBS}	F	9	8	9
I	Cln6^{nclf}	1x PBS + gemfibrozil and CBD (Combo^{PBS})	M	10	10	10
J	Cln6^{nclf}	Combo^{PBS}	F	8	8	9
K	Cln6^{nclf}	scAAV9.CB.*hCLN6* + vehicle (No Drug^{AAV9})	M	9	10	8
L	Cln6^{nclf}	No Drug^{AAV9}	F	10	10	10
M	Cln6^{nclf}	scAAV9.CB.*hCLN6* + gemfibrozil (Gemfib^{AAV9})	M	10	10	10
N	Cln6^{nclf}	Gemfib^{AAV9}	F	9	8	6
O	Cln6^{nclf}	scAAV9.CB.*hCLN6* + CBD (CBD^{AAV9})	M	9	8	6
P	Cln6^{nclf}	CBD^{AAV9}	F	10	7	6
Q	Cln6^{nclf}	scAAV9.CB.*hCLN6* + gemfibrozil and CBD (Combo^{AAV9})	M	9	10	8
R	Cln6^{nclf}	Combo^{AAV9}	F	10	9	12
			Totals	180	169	160

Table 2.5 | Population table for different experimental mouse groups tested for ataxia behaviour at 6, and 9 months of age. (n)6 = number of mice tested at 6 months; (n)9 = number of mice tested at 9 months; WT = wildtype; $UT^{Cln6nclf}$ = $Cln6^{nclf}$ mice injected with 1x PBS and treated with vehicle jelly; $Gemfib^{PBS}$ = $Cln6^{nclf}$ mice injected with 1x PBS and treated with gemfibrozil; CBD^{PBS} = $Cln6^{nclf}$ mice injected with 1x PBS and treated with CBD; $Combo^{PBS}$ = $Cln6^{nclf}$ mice injected with 1x PBS and treated with a combination of gemfibrozil and CBD; $Gemfib^{AAV9}$ = $Cln6^{nclf}$ mice injected with scAAV9.CB.*hCLN6* and treated with gemfibrozil; CBD^{AAV9} = $Cln6^{nclf}$ mice injected with scAAV9.CB.*hCLN6* and treated with CBD; $Combo^{AAV9}$ = $Cln6^{nclf}$ mice injected with scAAV9.CB.*hCLN6* and treated with a combination of gemfibrozil and CBD; No $Drug^{AAV9}$ = $Cln6^{nclf}$ mice injected with scAAV9.CB.*hCLN6* and treated with vehicle jelly.

	Genotype	Treatment Group	Sex	(n)6	(n)9
A	WT (C57Bl/6)	Vehicle (WT)	M	9	9
B	WT (C57Bl/6)	WT	F	8	9
C	$Cln6^{nclf}$	1x PBS + vehicle ($UT^{Cln6nclf}$)	M	12	8
D	$Cln6^{nclf}$	$UT^{Cln6nclf}$	F	9	10
E	$Cln6^{nclf}$	1x PBS + gemfibrozil ($Gemfib^{PBS}$)	M	10	9
F	$Cln6^{nclf}$	$Gemfib^{PBS}$	F	10	9
G	$Cln6^{nclf}$	1x PBS + cannabidiol (CBD^{PBS})	M	10	15
H	$Cln6^{nclf}$	CBD^{PBS}	F	9	8
I	$Cln6^{nclf}$	1x PBS + gemfibrozil and CBD ($Combo^{PBS}$)	M	10	10
J	$Cln6^{nclf}$	$Combo^{PBS}$	F	8	8
K	$Cln6^{nclf}$	scAAV9.CB.*hCLN6* + vehicle (No $Drug^{AAV9}$)	M	9	10
L	$Cln6^{nclf}$	No $Drug^{AAV9}$	F	10	10
M	$Cln6^{nclf}$	scAAV9.CB.*hCLN6* + gemfibrozil ($Gemfib^{AAV9}$)	M	10	10
N	$Cln6^{nclf}$	$Gemfib^{AAV9}$	F	9	8
O	$Cln6^{nclf}$	scAAV9.CB.*hCLN6* + CBD (CBD^{AAV9})	M	9	8
P	$Cln6^{nclf}$	CBD^{AAV9}	F	10	7
Q	$Cln6^{nclf}$	scAAV9.CB.*hCLN6* + gemfibrozil and CBD ($Combo^{AAV9}$)	M	9	10
R	$Cln6^{nclf}$	$Combo^{AAV9}$	F	10	9
			Totals	180	169

2.6.1 Ataxia phenotyping

This protocol was adapted from Guyenet et al's (2011) "Simple composite scoring system for evaluating mouse models of cerebella ataxia". A video explaining how scores are assigned for each test can be found at: https://www.ncbi.nlm.nih.gov/pmc/articles/PMC3121238/

Ataxia phenotyping is a subjective assay that allows the quantification of disease severity in mouse models of neurological diseases that demonstrate an ataxic phenotype (like CLN6 BD). Measurable tasks include a ledge test, hindlimb clasping and a gait test. Each task

is assigned a score on a scale of 0-3, with a combined or 'composite' score calculated for all three tasks. A score of 0 represented an absence of the diseased phenotype, while a score of 3 represented it's most severe manifestation (Guyenet et al., 2010).

The experimenter conducting the behavioural tests had no prior knowledge of the animals' genotypes (blinded study design).

Animals were run through all three tasks in sequence (one after the other), before being returned to their home cage and given a 15 to 20 minute break. After that break, they would repeat the sequence again. All animals would perform three sequences or trials, earning a total of 9 scores between 0-3 (3 score values per task).

2.6.1.a The ledge test

The ledge test is a measure of motor coordination and balance, which is traditionally impaired in ataxic neurological disorders like CLN6 BD.

Animals were lifted from their home cage and placed on the ledge of another, empty 'testing' cage. Unaffected mice will typically grasp the ledge with all four feet and walk along the ledge comfortably before lowering themselves to the cage floor, landing gracefully on their front paws. This behaviour is assigned a score of 0.

If an animal loses its footing briefly while walking along the edge, but otherwise seems coordinated, then it is assigned a score of 1. If it does not effectively use its hindlimbs, dragging them or clutching the sides of the cage wall with them, and/or lands on its head rather than its paws while lowering itself to the cage floor, then it is assigned a 2.

If the animal falls off the ledge completely, or almost does so, while walking or attempting to lower itself to the cage floor, or refuses to move along the ledge even when encouraged, then this warrants a score of 3. Scores were recorded on an Excel spreadsheet (Microsoft® Office).

2.6.1.b The hindlimb clasping test

Hindlimb clasping is a common marker of disease progression in many neurodegenerative disease mouse models, including Cln6^{nclf}. Unaffected mice will typically abduct their hindlimbs when held upside down by the base of their tail (**Figure 2.6**). This abduction is, presumably, to help them grasp onto nearby objects and/or balance themselves while they are suspended. Mice who display an ataxic phenotype have difficulty keeping their hindlimbs abducted out from their body, and involuntarily retract them in towards their midline (**Figure 2.6**).

Animals were lifted from their home cage by the base of their tail and lifted clear of surrounding objects (approximately 10 cm from a bench surface). The hindlimb position was observed by the experimenter for a total of 10 seconds, before the animal was place back in its cage. During that 10 second interval, if the hindlimbs were consistently abducted laterally, away from the abdomen, then the animal was assigned a score of 0.

If one hindlimb was retracted towards the abdomen for more than 50% of the 10 second window, then the animal was assigned a score of 1.

If both hindlimbs were partially retracted towards the abdomen for more than 50% of the time then the animal was assigned a score of 2.

Finally, if both hindlimbs were completely retracted in towards the abdomen or 'clasping' then the animal was assigned a score of 3 (**Figure 2.6**). Scores were recorded in an Excel spreadsheet (Microsoft® Office).

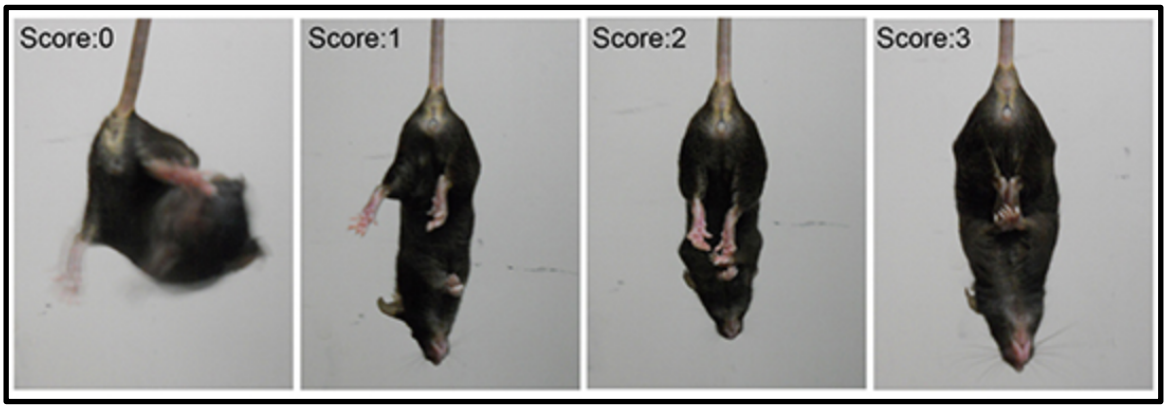

Figure 2.6 | Hindlimb clasping phenotype scoring system. Image adapted from *Zhu et al., 2016.*

2.6.1.c The gait test

The gait test subjectively assesses muscle co-ordination and function. In this test, the experimenter observes the animal's hindlimbs as it walks around on a flat surface. Unaffected mice will walk normally, distributing weight on all four paws, with their belly close to – but not touching – the ground. Mice experiencing neurological symptoms may display limping, dragging, tremors, or uneven weight distribution on their hindlimbs, or may be unwilling to move around at all.

Animals were removed from their home cage and placed on a clean, flat surface (a stainless steel bench in the University of Otago HTRU). The animals were encouraged to walk away from the experimenter, so that their hindlimb movements could be observed. If the animal walked normally, with a confident, fluid gate absent of any tremors or limping, then it was assigned a score of 0. If it showed a tremor or appeared to limp while walking, it was assigned a score of 1. If the animal had a severe tremor, severe limp, lowered pelvis or "duck feet" (feet pointing away from the midline of the body during movement), then it was assigned a score of 2. If the animal had difficulty moving forward and/or dragged its abdomen on the ground, it was assigned a score of 3.

2.6.1.d A quick note about ataxia statistical analyses

The data collected from these three tests, as well as the subsequently calculated composite phenotype score that was scored between 0 and 9, are presented as averaged means with ± standard error of the mean (±SEM)**.** This is a divergence from standard statistical protocol, which usually requires ordinal data – that is, data that is ranked or has an inherent *order* to it – to be presented using median scores as a measure of central tendency and the data set's range or a confidence interval (CI) of 95% as the measure of spread.

The decision to present our ataxia phenotyping data using the mean and ±SEM was based on several factors: first, the original protocol from which our behavioural assay was adapted, published by Guyenet et al. (2010), presents their example data using mean and ±SEM, rather than the more traditional median and range.

Second, our collaborators – namely the Weimer lab from Sanford Research in Sioux Falls, SD – used mean and ±SEM in two of their most recently published BD papers, both of which examined the ataxic phenotypes of $Cln6^{nclf}$ mice under various experimental conditions (Cain et al., 2019; White et al., 2019). Discrepancies in statistical methodology between our work and theirs would make drawing meaningful comparisons difficult, if not impossible.

Finally, a brief foray into statistical literature revealed that the statistical community has not reached a consensus when it comes to the application of parametric or 'metric' analyses to ordinal data. While many of the more 'conservative' statisticians insist on ordinal data should *always* be analysed using either a median or mode and non-parametric testing, there is a growing community of statisticians who argue that many forms of ordinal data – such as the data presented in this thesis – have inherent 'interval' like qualities that lend themselves to accurate analyses using parametric testing and a mean measure of central tendency (Carifio & Perla, 2008; Norman, 2010).

Taking these factors into consideration, data for ataxia phenotyping in this thesis will be presented using mean and ± SEM and analysed via parametric testing, where normality allows.

2.6.1.e Repeated measures

As mentioned above, all the tasks in **2.6.1.1**-**3** were repeated three times on the testing day. These tasks were also recorded and the video was analysed at a later date by the same experimenter who conducted the ataxia tasks. This meant that each individual animal ended up having 6 repeated measures for each task, 3 taken on the day, and 3 given from the recording.

Since three composite scores (0-9) were calculated by adding the triad of task scores (0-3) from the three trials on the day, an extra three composite scores were also produced by the scoring of the three trials of the three tasks via video at a later date.

All scores for each task were averaged for analysis (**Appendix A.4**), including the composite scores. Data was then imported into GraphPad Prism (v8) for statistical analysis. The data presented in **Chapter 3** (Results) represents the average (mean) scores for each task (and the composite ataxia scores) for each experimental group, ± SEM.

2.6.2 Rotarod performance testing

This protocol was adapted from a protocol provided by the Weimer lab at Sanford Research, Sioux Falls, SD, USA (personal communication).

The rotarod performance test is a classic assay used in the psychological and neurosciences to assess motor co-ordination, balance and endurance in rodents. The parameters measured are typically 'latency to fall' (sometimes also referred to as 'duration') and an associated 'rotations per minute (RPM) at fall.

In this study sub-cohorts of ~180 different mice (~10 from each experimental group listed in **Table 2.4**) were assessed at 6, 9 and 12 months. The protocol was split into two parts: training and testing. Each part consisted of three trials per animal, with the data collected from the testing trials used for statistical analysis. All trials were conducted using Med Associates Inc's Five Lane Rota-Rod for Mice and Rota-Rod 2 Software (**Appendices A.3** and **A.4**).

In each trial, up to five animals were placed on the rod while it was stationary. Once all animals had been 'loaded', the rod would begin to rotate at a constant acceleration of 0.2 rpm/s from 0 to 48 rpm. Each trial had a maximum duration of 300 seconds, meaning that once the rod had reached 48 rpm at 240 seconds, the rod would continue to rotate at maximum speed for a further 60 seconds. During the trial, each animal's latency to fall (in seconds) would be recorded automatically by the Rotarod, along with the associated rpm of the rod at the time the animal fell.

Three training trials would be conducted in the morning, with animals receiving an hour break in between trials. The three testing trials would then occur in the afternoon on the same day, also separated by rest intervals of an hour.

Only the afternoon (testing) trials data and the latency to fall (in seconds) parameter were used for statistical analysis. Each animal had three repeated measures of latency to fall, which were averaged. For each trial, an individual animal could receive a continuous latency to fall score between 0 and 300 sec, with a higher score representing an indirect measure of superior motor co-ordination compared to lower scores.

Averaged data from all mice was imported into GraphPad Prism (v.8) for statistical analysis, with the data presented in **Chapter 3** representing the mean behavioural scores of each experimental group, ± SEM (**Appendix A.4**).

Chapter 3: Results

3.1 Untreated Cln6^{nclf} mice demonstrate expected behavioural deficits by 9 to 12 months of age

Previous behavioural studies using the Cln6^{nclf} murine model have identified a characteristic decline in motor co-ordination and development of hindlimb ataxia analogous to the motor symptoms experienced by human CLN6 BD patients (Best, 2017; Cain et al., 2019; Morgan et al., 2013). Since some genetic mouse models have been known to experience phenotypic discrepancies due to genetic drift after too many generations of inbreeding (Benavides et al., 2019; Stevens et al., 2007; Zeldovich, 2017), it was critical to replicate and confirm the presence of this Cln6^{nclf} behavioural phenotype in this study's cohort of Cln6^{nclf} mice. Characterising the untreated Cln6^{nclf} (UT^{Cln6nclf}) behavioural phenotype in this study also lent itself to the development of a 'diseased' baseline overall, which was invaluable for further comparisons to the treated Cln6^{nclf} groups and eliciting any protective effects of the various therapeutics being tested (**sections 3.2** to **3.5**).

Four different tests were used to assess mice for motor skill and co-ordination, as well as screen them for ataxic behaviours, at 6, 9 and 12 months of age: the rotarod, the ledge test, the hindlimb clasping test and the gait test (see **Chapter 2** for more info). In order to determine whether a diseased phenotype was present in UT^{Cln6nclf} mice (defined as Cln6^{nclf} mice that received 1x PBS injection at P0-2 and were only dosed with vehicle jelly), their behavioural scores were compared and contrasted with those of healthy, age- and sex-matched 'wildtype' (WT; C57Bl/6s) controls at each time point.

Sex differences in UT^{Cln6nclf} scores were also assessed, due to recent studies using the Cln6^{nclf} mouse model that indicate females experience accelerated disease progression

compared to males (Cialone et al., 2012; Poppens et al., 2019). Identifying sex differences in pathology is important, and historically overlooked, when considering the translation of preclinical mouse studies into clinical applications (reviewed in Beery & Zucker, 2011 and Jazin & Cahill, 2010).

3.1.1 The Cln6^{nclf} disease(d) phenotype: ***rotarod***

The overall rate of decline in UT^{Cln6nclf} rotarod scores, and the range over which this decline occurred – known as the 'elevation' – was assessed and compared to the scores of their age-matched WT counterparts across the 6, 9 and 12 month time points using linear regression (**Table 3.1**; **Appendices B.2** and **B.3**). Multiple unpaired student t-tests (**Appendices B.4.1-B.2**) were also used to separately assess differences between age- and sex-matched experimental groups within each time point (**Figures 3.1 B** and **C**).

Parametric testing was found to be suitable for these analyses as the data collected – scores measured as latency to fall (seconds) - is nominal and the experimental groups being assessed were found to have a normal (Gaussian) distribution at all three time points (D'Agostino-Pearson test; **Appendix B.1.1**). Data for the rotarod are presented as mean scores ± SEM (**Figure 3.1 A-C**).

The mean rotarod scores of both UT^{Cln6nclf} and WT mice – for both sexes – demonstrate a decline in motor co-ordination and balance over the three time points assessed, with each experimental group producing a negative gradient (m) in their linear equations (**Appendix B.2.2**). This was to be expected, irrespectve of genetic background or sex, due to an increase in age being associated with declining motor skills, even in 'healthy' C57Bl/6 mice (Barreto et al., 2010; Shoji et al., 2016).

While male and female UT^{Cln6nclf} mice had lower mean scores than their WT counterparts at every time point measured, the difference between the overall rates of decline in male and female UT^{Cln6nclf} mice compared to WT were found to be not significant (linear regression; male p = .0607; female p = .0629; **Appendices B.2.1** and **B.3**).

The use of multiple t-tests (**Appendices B.4.1-4.2**) to compare mean scores of male and female UT^{Cln6nclf} mice against their WT counterparts at each individual time point supported this non-significant result until 12 months of age, at which point the difference between mean Cln6^{nclf} scores was found to be significantly lower (worse) than their WT counterparts for both sexes (**Figure 3.1 B** and **C;** male p = .0041; female $p \leq .001$; **Appendices B.4.1-4.2**).

Despite the overall rate of decline of UT^{Cln6nclf} mice being statistically indistinguishable from their WT counterparts, the overall elevations of both male and female UT^{Cln6nclf} mean scores were found to be significantly lower than WT (**Figure 3.1**; male p = .0014; female p = .0104; **Appendices B.2.2**). This could either indicate a task learning deficiency in UT^{Cln6nclf} mice at each individual time point, or simply reflect their inability to achieve equivalent motor co-ordination scores to WT at any tested age due to disease-related sensorimotor deficiencies. Either scenario would be consistent with previously described cognitive and motor deficits in the UT^{Cln6nclf} mouse model (Cain et al., 2019; Gao et al., 2002; Morgan et al., 2013; Poppens et al., 2019; Wheeler et al., 2002).

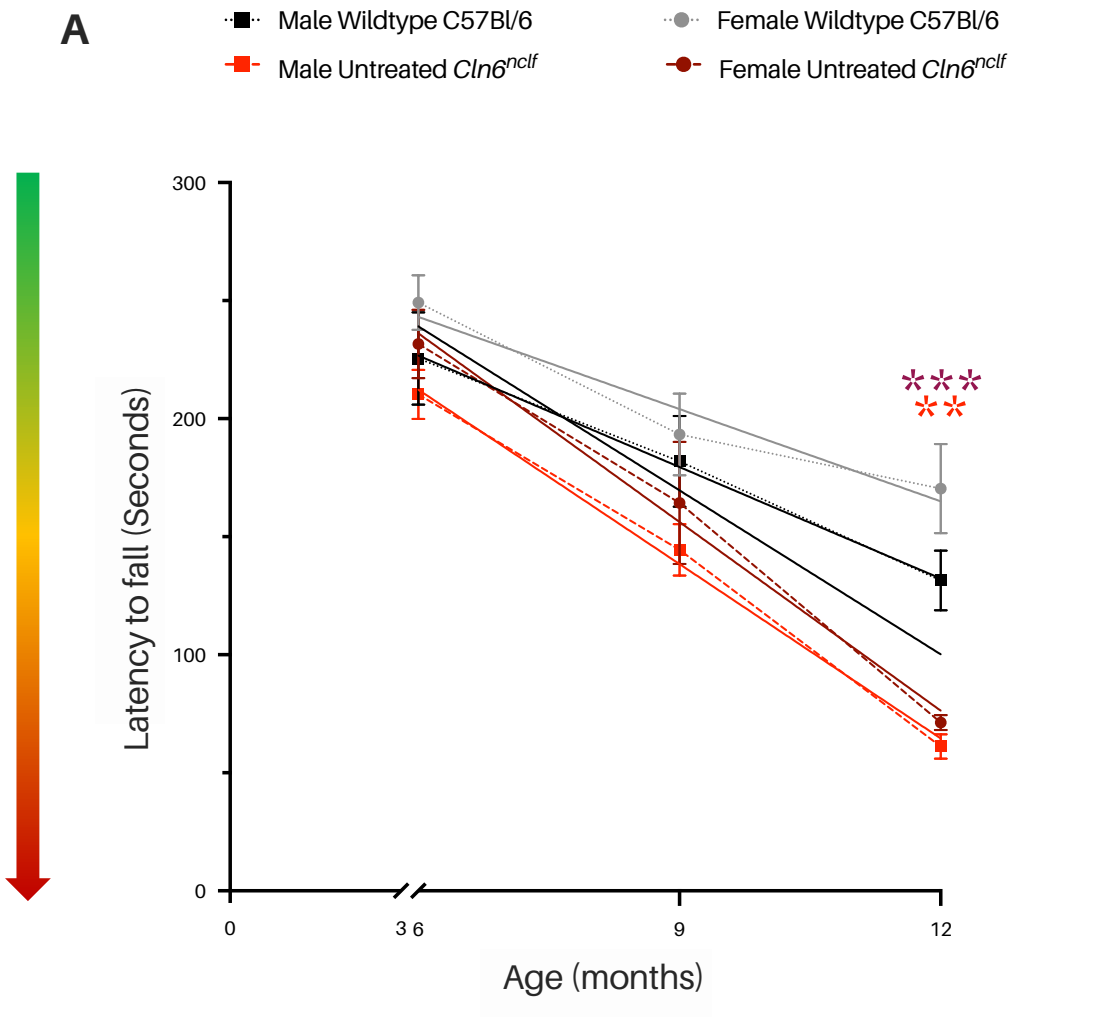
A
Male Wildtype C57Bl/6
Female Wildtype C57Bl/6
Male Untreated Cln6nclf
Female Untreated Cln6nclf
Latency to fall (Seconds)
300
200
100
0
0
3 6
9
12
Age (months)
B
Male rotarod 12 months
Male 12 month latency to fall (seconds)
**
WT
Untreated Cln6nclf
Treatment Group
C
Female rotarod 12 months
Female 12 month latency to fall (seconds)
***
WT
Untreated Cln6nclf
Treatment Group

⇐ **Figure 3.1 Establishing the Cln6^{nclf} disease(d) phenotype: rotarod scores (opposite page)**. *Lower mean rotarod scores compared to wildtype (WT; C57Bl/6) are present across all three tested time points in the untreated Cln6^{nclf} (UT^{Cln6nclf})mouse model, for both genders, but not significant until 12 months of age.* **A.** Rotarod behavioural testing was performed on female and male UT^{Cln6nclf} and WT mice at three different time points. Testing was conducted using Med Associates Inc's Five-Lane RotaRod for Mice (**Appendix A.3**). Averaged means of latency to fall (in seconds; line graph) are presented for male and female WT (male = black squares; female = grey circles) and UT^{Cln6nclf} (male = red squares; female = maroon circles) animals at 6, 9 and 12 months of age, with error bars = ± SEM). Different groups of mice were tested at each time point (between-subjects study design). A high score (~300) indicates a high level of motor co-ordination as measured by the rotarod, while lower scores correlate to increasing levels of motor dysfunction (coloured arrow on the left). No significant differences in mean rotarod score were found between UT^{Cln6nclf} mice and their WT age- and sex-matched WT counterparts until 12 months of age. Analyses at each time point between gender-matched WT and UT^{Cln6nclf} groups were performed using multiple paired student t-tests (**Appendices B.4.1-4.2**). Linear regression analysis (solid lines; **Appendices B.2-3**) showed progressive decline in motor performance for all mice, irrespective of sex or strain, as summarised in **Appendix B.2.2.** No significant difference in overall rate of decline between UT^{Cln6nclf} mice and their sex-matched WT counterparts was found (male p = .0607; female p = .0629; **Appendices B.2-3**), but elevations for both male and female UT^{Cln6nclf} animals were determined to be significantly lower (male p = .0014; female p = .0104; **Appendix B.2.2**). n = 25-32. **B.** Histogram of mean rotarod scores (latency to fall; in seconds) of male UT^{Cln6nclf} mice (red bar on right) and their age- and sex-matched WT (white bar on left) controls at 12 months of age – the only time point measured where a significant difference was seen between the two groups' scores. Error bars = ± SEM. Clear circles indicate individual animal rotarod scores (averaged from three trials). Male UT^{Cln6nclf} animals showed significantly reduced ability to stay on the rotarod at 12 months of age (unpaired student t-test; UT^{Cln6nclf} mean = 61.14 seconds; WT mean = 131.5 seconds; ** p = .0012; **Appendix B.4.1**). n = 7-14. **C.** Histogram of mean rotarod scores (latency to fall; in seconds) of female UT^{Cln6nclf} mice (maroon bar on right) and their age- and sex-matched WT (C57Bl/6; grey patterned bar on left) controls at 12 months of age – the only time point measured where a significant difference was seen between the two groups' scores. Error bars = ± SEM. Clear circles indicate individual animal rotarod scores (averaged from three trials). Female UT^{Cln6nclf} animals also showed significantly reduced ability to remain on the rotarod at 12 months of age (unpaired student t-test; Cln6^{nclf} mean = 71.25 seconds; WT mean = 170.4 seconds; *** p = .002; **Appendix B.4.2**). n = 7-8.

*3.1.2 The Cln6^{nclf} disease(d) phenotype: **ataxia***

Three separate tasks, performed sequentially, were used to assess mice for the presence or absence of ataxia: the ledge test, the hindlimb clasping test, and the gait test (**Figure 3.3**). Ataxia, defined as 'the loss of full control of bodily movements' (from the Greek *a-* meaning 'without' and *taxis* meaning 'order'), is a commonly observed phenotype in the Cln6^{nclf} mouse model and mirrors ataxic symptoms experienced by many human CLN6 BD patients (Cannelli et al., 2009; Morgan et al., 2013).

In these tests, unlike the rotarod (**section 3.1.1**), a 'high score' indicates an increase in expression of the diseased phenotype. Each task was scored from 0 to 3, with a score of 0 indicating an animal demonstrated no ataxic behaviour, while a score of 3 indicated a fully penetrant ataxic phenotype. The data collected from these three tests, as well as the

subsequently calculated composite phenotype score that was scored between 0 and 9 (**Figure 3.2**), are presented as averaged means with ± SEM (**Figures 3.2 – 3.3**).

3.1.2.a Composite ataxia phenotype scores

Calculating a composite ataxia phenotype score for each mouse not only allows for greater statistical power when analysing results (Guyenet et al., 2010), but also lets researchers develop a more comprehensive overview of an individual animal's or experimental group's ataxic phenotype. Each assay is used to assess a different facet of ataxia and the composite score reduces the likelihood of a false positive or negative from one assay causing an animal or group to be misinterpreted as 'healthy' or 'ataxic'. Twelve-month data for each experimental group in this study was also collected by a different experimenter (J. Lock) but excluded from this analysis due to the subjective nature of scoring and the inconsistencies this could create when looking at trends over time.

Mean composite scores were calculated by averaging the mean scores of individual ataxia assays (ledge, hindlimb clasping and gait) – these scores, in turn, had been calculated by averaging the scores of six trials for each assay (3 conducted in-person, 3 conducted via watching footage of the original trials). The experimenter was blinded at the time of scoring for both in-person and footage assessments.

Comparisons between mean composite scores of UT^{Cln6nclf} and WT mice were made using unpaired student t-tests, with separate analyses being conducted for each sex (**Appendices B.5.1-5.2**). Parametric testing was found to be suitable for these analyses as the despite the data collecting being ordinal (see discussion regarding ordinal data in **Chapter 2**), and the experimental groups being assessed were found to have a normal (Gaussian)

distribution at both time points (D'Agostino-Pearson test; **Appendix B.1.2**). Data are presented as mean composite scores ± SEM.

No significant difference in mean composite ataxia score was observed between UT^{Cln6nclf} and WT controls for either sex at 6 months of age (**Figure 3.2.Ai**), though the mean score of UT^{Cln6nclf} was non-significantly higher (worse) than WT for both 6 month males and females.

At 9 months, however, both male and female UT^{Cln6nclf} mice (male UT^{Cln6nclf} = 4.833 ± 0.321; female UT^{Cln6nclf} = 5.00 ± 0.243) demonstrated significantly worse (higher) mean composite scores than their WT counterparts (male WT = 2.574 ± 0.222; $p \leq .0001$; female WT = 2.407 ± 0.499; $p = .0002$; **Figure 3.2.Bi**).

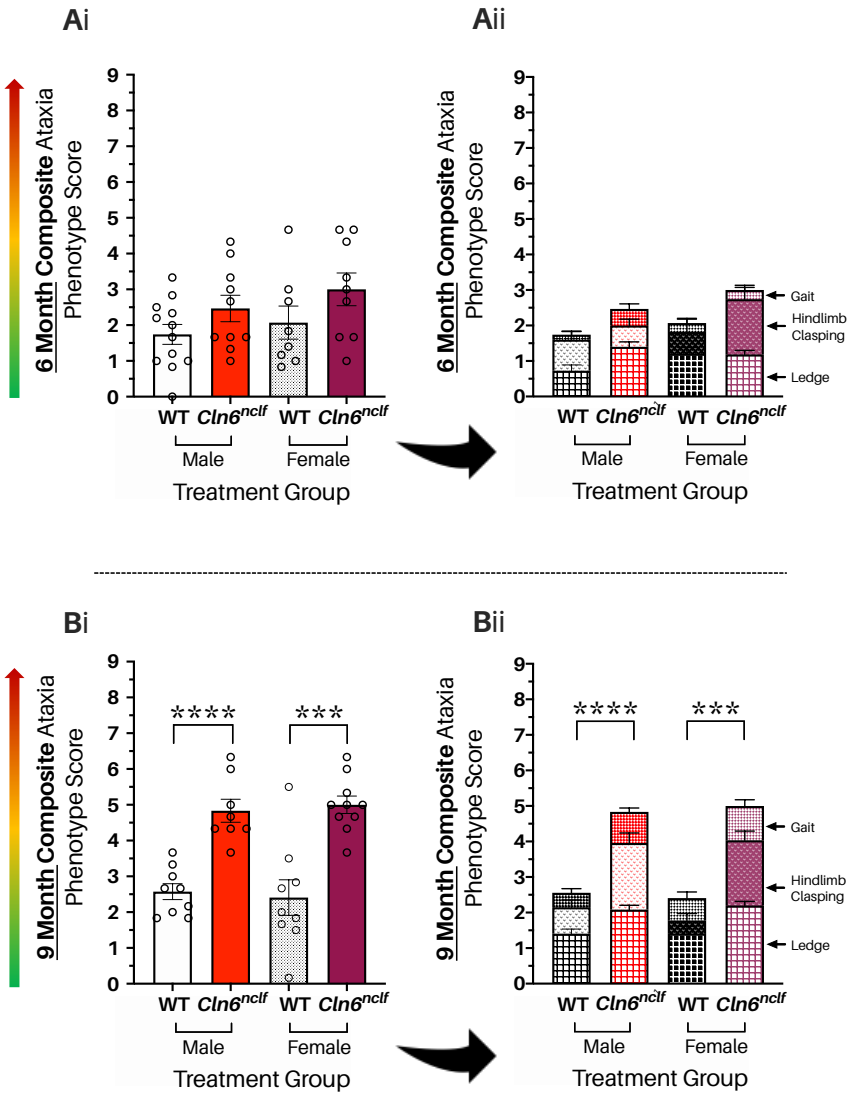

Figure 3.2 | Establishing the Cln6^{nclf} disease(d) phenotype: composite ataxia scores. *Significant motor co-ordination deficits, as measured by composite ataxia phenotyping, are present in both male and female untreated Cln6^{nclf} (UT^{Cln6nclf}) mice by 9 months of age.* Mean composite ataxia phenotype scores were calculated using mean scores from three trials each of ledge, hindlimb clasping and gait tests for male and female UT^{Cln6nclf} and wildtype (WT; C57Bl/6) mice at two different time points: 6 months (**Ai-ii**) and 9 months (**Bi-ii**). Different mice were tested at each time point (between-subjects study design). Averaged means of composite ataxia scores for WT (male = plain white bars; female = patterned grey bars) and UT^{Cln6nclf} (male = plain red; female = plain maroon) animals are presented in histograms for 6 (**Ai-ii**) and 9 (**Bi-ii**) months of age. A low score (close to 0) indicates an absence of the ataxic phenotype as measured by the composite scoring system, while higher scores, closer to 9, indicate increasing levels of ataxic behaviour (coloured arrow on the left). The overall mean composite scores illustrated in **Ai** and **Bi** are further broken down into the average ledge (bottom), hindlimb clasping (middle) and gait (top) scores that comprise them in segmented bar graphs (**Aii** and **Bii**). Individual mouse composite scores are shown as clear circles in **Ai** and **Bi,** and error bars = ± SEM. Analyses between UT^{Cln6nclf} and their age- and sex-matched WT (C57Bl/6) controls were conducted via unpaired student t-tests at each time point for each sex (**Appendices B.5.1-5.2**). n(per group per time point) = 8-10. **Ai-ii** No significant difference was observed between the average composite scores of UT^{Cln6nclf} mice and their age- and sex-matched WT counterparts for either males or females at 6 months of age (unpaired student t-test; **Appendices B.5.1-5.2**), though UT^{Cln6nclf} animals appear to have (non-significantly) higher (worse) mean scores for both sexes. **Bi-ii.** Both male and female UT^{Cln6nclf} mice perform significantly worse than their age- and sex-matched WT counterparts at 9 months of age (unpaired student t-test; male WT mean =2.574 ; male UT$^{Cln6nclf\ lf}$ mean = 4.833 ; **** male $p \leq .0001$; female WT mean = 2.407 ; female UT^{Cln6nclf} mean = 5.0 ; *** female $p = .0002$; **Appendices B.5.1-5.2**).

3.1.2.b Ledge test

Mice were placed on the ledge of their home cage's wall and were assigned a grade between 0 and 3 based on their ability to (a) walk along the ledge, (b) lower themselves gracefully to the cage floor or (c) a combination of the two activities (see **Chapter 2** for a more detailed description of the grading criteria). The ledge test is purported to assess behaviours in murine models that are most similar or representative of human ataxias, and is designed to measure co-ordination, balance and fine motor control, all of which are known to be compromised in human CLN6 BD patients (Cannelli et al., 2009; Guyenet et al., 2010).

In male mice, a series of paired student t-tests[†] (**Appendix B.6.1)** revealed that UT^{Cln6nclf} mice performed significantly worse at the ledge test than their age-matched WT counterparts at both the 6 (p = .0062) and 9 month (p = .0017) time points (**Figure 3.3.A**). Several previous studies using the Cln6^{nclf} murine model have indicated that diseased mice should not yet be demonstrating significant behavioural deficits at 6 months of age, though this is by no means a consistent finding across all CLN6 BD animal studies and could also be assay-dependent, with some tests being higher resolution and/or more subjective than others.

UT^{Cln6nclf} female mice, on the other hand, only begin to perform significantly worse than WT (female WT = 1.407 ± 0.204) in the ledge test at 9 months of age (female UT^{Cln6nclf} = 2.200 ± 0.113; p = .0028; **Figure 3.3.B; Appendix B.6.2**). This finding is consistent with studies across several variants of BD that suggest females experience disease onset later than males, but consequently experience accelerated disease progression (Cialone et al., 2012).

[†] All ledge, hindlimb clasping, and gait ataxia test data for the experimental groups being analysed in this section demonstrated normal (Gaussian) distribution (**Appendices B.1.3-1.5**), with three exceptions (see **Appendices**), so parametric testing was deemed appropriate in both this instance and when looking at the individual ataxic assays. The exceptions were treated as parametric/normal on advice of a statistician. If the majority of experimental group's scores had been found to have non-normal distribution, then a non-parametric test, the Mann-Whitney test, would have been used instead of the unpaired student t-test.

3.1.2.c Hindlimb clasping test

Aberrant clasping of the hindlimbs is a well characterised ataxic marker of disease progression in several neurodegenerative murine models, including Cln6^{nclf} (Guyenet et al., 2010; Lalonde & Strazielle, 2011). Comparisons between experimental groups were made at different time points using unpaired student t-tests (**Appendices B.7.1-7.2**). Different mice were measured at each time point, making this assay between-subjects in design. Data are mean hindlimb clasping scores ± SEM.

While all UT^{Cln6nclf} hindlimb clasping scores were statistically indistinguishable from healthy WT scores at 6 months of age, both male and female UT^{Cln6nclf} mice in this study demonstrated a marked hindlimb clasping phenotype, in comparison to WT controls, by 9 months (**Figure 3.3 C-D**).

At 9 months, UT^{Cln6nclf} males had an average clasping score of 1.875 ± 0.178 (**Figure 3.3.C**) and females had an average of 1.950 ± 0.259 (**Figure 3.3.D**) . This indicated, that, on average, male and female UT^{Cln6nclf} mice were involuntarily retracting at least one limb in towards the midline of their body for over 50% of the 30 seconds they were suspended by their tail. Healthy WT controls, in comparison, were averaging 0.370 ± 0.196 (males) or 0.741 ± 0.206 (females) – average scores that were significantly lower than their sex-matched UT^{Cln6nclf} counterparts (male p = .0048; female p = .002; **Appendices B.7.1-7.2**).

3.1.2.d Gait test

In humans, gait disturbance is a common and early symptom of cerebellar ataxia in a wide range of neurological conditions – including BD (Cannelli et al., 2009; Schulz et al., 2013). In rodent models, gait is often used to assess general motor co-ordination and muscle function as an indirect measure of cerebellar ataxia (Guyenet et al., 2010). Comparisons between

experimental groups were made at different time points using unpaired student t-tests (**Appendices B.8.1-8.2**). Different mice were measured at each time point, making this assay between-subjects in design. Data are mean gait ataxia scores ± SEM.

In male mice, the first significant difference in mean gait scores was seen at 9 months, with UT^{Cln6nclf} mice demonstrating a more obvious ataxic gait phenotype (0.875 ± 0.108) than WT (0.407 ± 0.118; p = .0111; **Appendix B.8.1**). Female UT^{Cln6nclf} mice did not demonstrate a significantly different mean gait score from sex-matched WT at either time point measured.

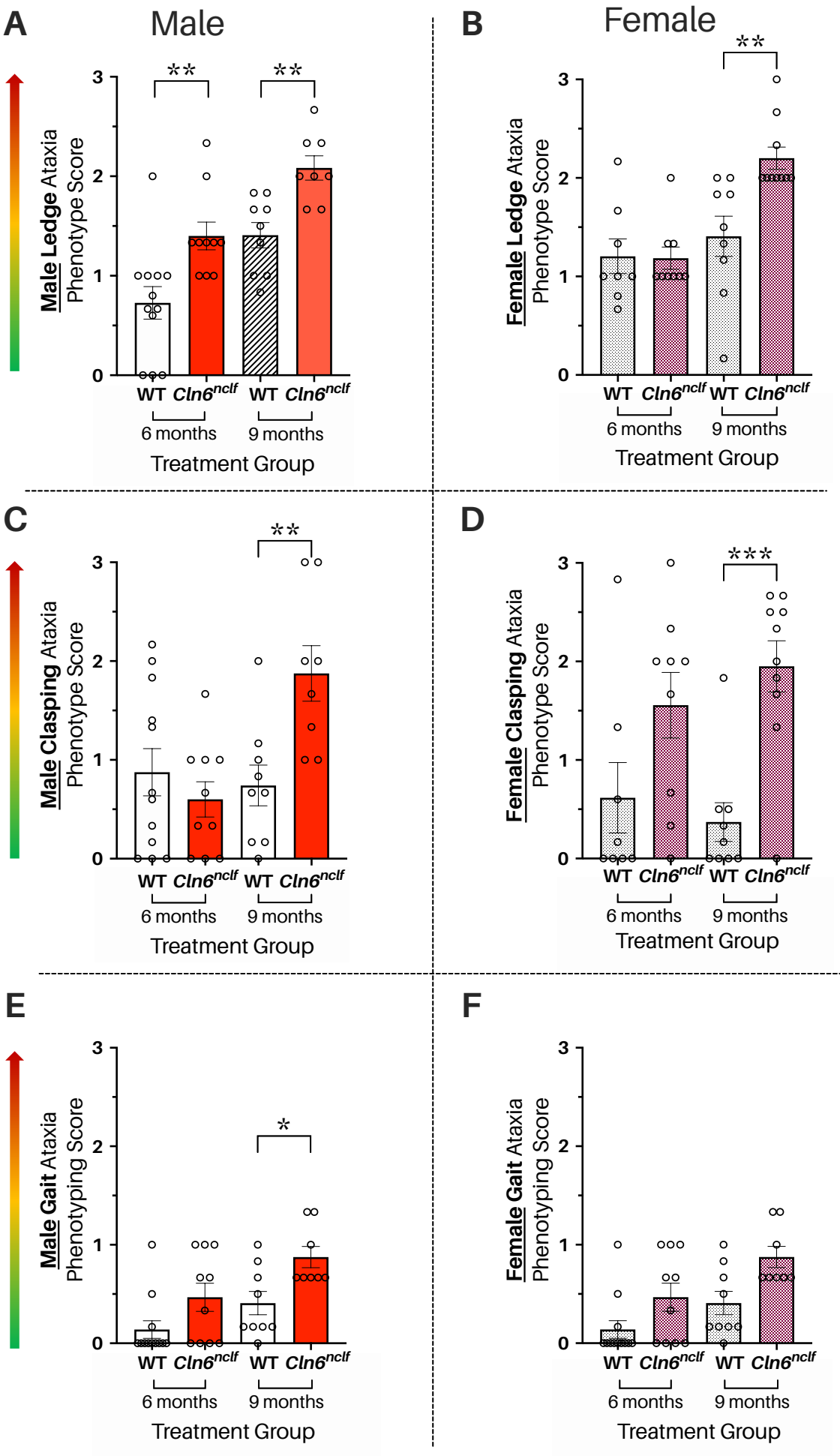
A
Male
B
Female
C
D
E
F
Male Ledge Ataxia Phenotype Score
Female Ledge Ataxia Phenotype Score
Male Clasping Ataxia Phenotype Score
Female Clasping Ataxia Phenotype Score
Male Gait Ataxia Phenotyping Score
Female Gait Ataxia Phenotyping Score
WT Cln6nclf WT Cln6nclf
6 months 9 months
Treatment Group

⇐ **Figure 3.3 | Establishing the Cln6^{nclf} disease(d) phenotype: ataxia phenotyping scores (opposite page)**. *Both male and female untreated Cln6^{nclf} (*UT^{Cln6nclf}*) mice demonstrate significant ataxic phenotypes by 9 months of age.* Mice underwent three trials of a sequence three different ataxia assays – the ledge test, the hindlimb clasping test and the gait test (adapted from *Guyenet et al., 2010*) – in order to determine the presence or absence of an ataxic phenotype at 6 and 9 months of age. Different mice were assessed at each time point, making the experiment between-subjects in design. For each assay, a mouse could be assigned a score between 0 and 3, with 0 indicating a complete absence of the ataxic phenotype and 3 indicating a completely penetrant ataxic phenotype (coloured arrows on the left). All data (A-F) are presented as the mean of averaged (3 trials; scored from 0-3) individual mouse scores, with clear circles representing the individual averaged scores. Error bars = ± SEM. All analyses were conducted using unpaired student t-tests between sex and age matched experimental groups (**Appendices B.6.1-8.2**). **A** and **B.** Histograms of mean ledge test scores. Male (**A**) and female (**B**) UT^{Cln6nclf} (male = plain red bars; female = patterned maroon bars) and WT (C57Bl/6; male = plain white bars; females = patterned black and white bars) mice were placed on top of the wall of their home cage and allowed to walk along this ledge and/or lower themselves to the cage floor. Male UT^{Cln6nclf} mice demonstrated significantly more ataxic behaviour (higher score) compared to WT (black) at both 6 months (WT mean = 0.7278; UT^{Cln6nclf} mean = 1.40; ** p = .0062; **Appendix B.6.1**) and 9 months (WT mean = 1.407; UT^{Cln6nclf} mean = 2.083; ** p = .0017; **Appendix B.6.1**) of age. Female UT^{Cln6nclf} mice, however, only begin to demonstrate significant deficits compared to WT at 9 months (WT mean = 1.407; UT^{Cln6nclf} mean = 2.200; ** p = .0028; **Appendix B.6.2**). n(per group per time point) = 8-12. **C** and **D.** Hindlimb clasping test scores. Mice were suspended for 30 seconds and their hindlimb positions assessed according to Guyenet et al. (2010). Both male and female UT^{Cln6nclf} only begin to show a significant ataxic phenotype (when compared to WT) at 9 months of age (male WT mean = 0.7407; male UT^{Cln6nclf} mean = 1.875; ** p = .0048; **Appendix B.7.1**; female WT mean = 0.3704; female UT^{Cln6nclf} mean =1.950; ***p = .0002; **Appendix B.7.2**). n(per group per time point) = 8-12. **E** and **F.** Gait test scores. Only 9-month-old male UT^{Cln6nclf} mice demonstrated a significantly more ataxic phenotype than their age- and sex-matched WT counterparts in the gait test, with a significantly higher (worse) mean score at 9 months of age (WT mean = 0.4074; UT^{Cln6nclf} mean = 0.8750; * p = .0111; **Appendix B.8.1**). Female UT^{Cln6nclf} mice did not produce a significantly different mean score from their age- and sex-matched WT counterparts at either 6 (WT mean = 0.2500; UT^{Cln6nclf} mean = 0.2500; p = .9612; **Appendix B.8.2**) or 9 months (WT mean = 0.6296; UT^{Cln6nclf} mean = 0.9667; p = 0.1905; **Appendix B.8.2**) of age. n(per group per time point) = 8-12 ➢

3.1.3 The Cln6^{nclf} disease(d) phenotype: ***survival and weight***

Survival curves and median lifespan were generated from euthanasia records for each experimental group. Mice would be euthanised once they reached one of the three humane end-points stipulated by the Animal Ethics Committee (AEC; see **Chapter 2** for details). Data are presented here up until 14 months – even though the trial continued on until past the 16 month time point for some mice – due to the time limits of a MSc. Survival data are presented as percentage of the original cohort n, with curve comparisons between sex-matched Cln6^{nclf} and WT conducted via separate log-rank (Mantel-Cox) tests for each sex (**Appendices B.9.1-9.2**). Small 'tick' marks indicating planned removals of mice from the experiment for post-mortem analysis. Weight data are presented as mean weights, in grams, ± SEM.

Both male and female UT^{Cln6nclf} mice had significantly shortened lifespans compared to their WT counterparts. This was to be expected, as a significantly shortened lifespan has previously been characterised as part of the Cln6^{nclf} phenotype (Gao et al., 2002; Morgan et al., 2013b; Wheeler et al., 2002). Male UT^{Cln6nclf} mice had a median survival of 13.29 months, while their WT counterparts hadn't even reached a median survival point at 14 months (WT survival was undefined at 14 months; $p = 0.0005$; **Appendix B.9.1**). Female UT^{Cln6nclf} mice had, on average, slightly shorter lifespans than males with a median survival of 12.50 months. Female WT survivals were also undefined at 14 months ($p \leq .0001$).

Body weights for all male and female UT^{Cln6nclf} and WT mice (n = 24-35) were recorded weekly as a means of monitoring general health. Weights taken prior to behavioural assays at 6, 9 and 12 months of age have been averaged and used for analysis. Unpaired student t-tests were used to compare the weights of sex-matched UT^{Cln6nclf} and WT mice (**Appendices B.10.1-10.2**). Female UT^{Cln6nclf} mice were found to be significantly lighter than WT at 6 (UT^{Cln6nclf} = 24.11 g; WT = 27.04; $p = .0041$) and 9 months of age (Cln6^{nclf} = 26.0 g; WT = 28.9 g; $p = .0228$). At 12 months, however, while still lighter (26.86 g), their mean weight was no longer significantly less than that of WT (30.23 g) . Male UT^{Cln6nclf} demonstrated the opposite trend – with non-significantly lighter weights at 6 and 9 months, followed by a significantly lighter average weight at 12 months (UT^{Cln6nclf} = 37.76 g; WT = 41.49; $p \leq .0001$; **Appendix B.10.1**).

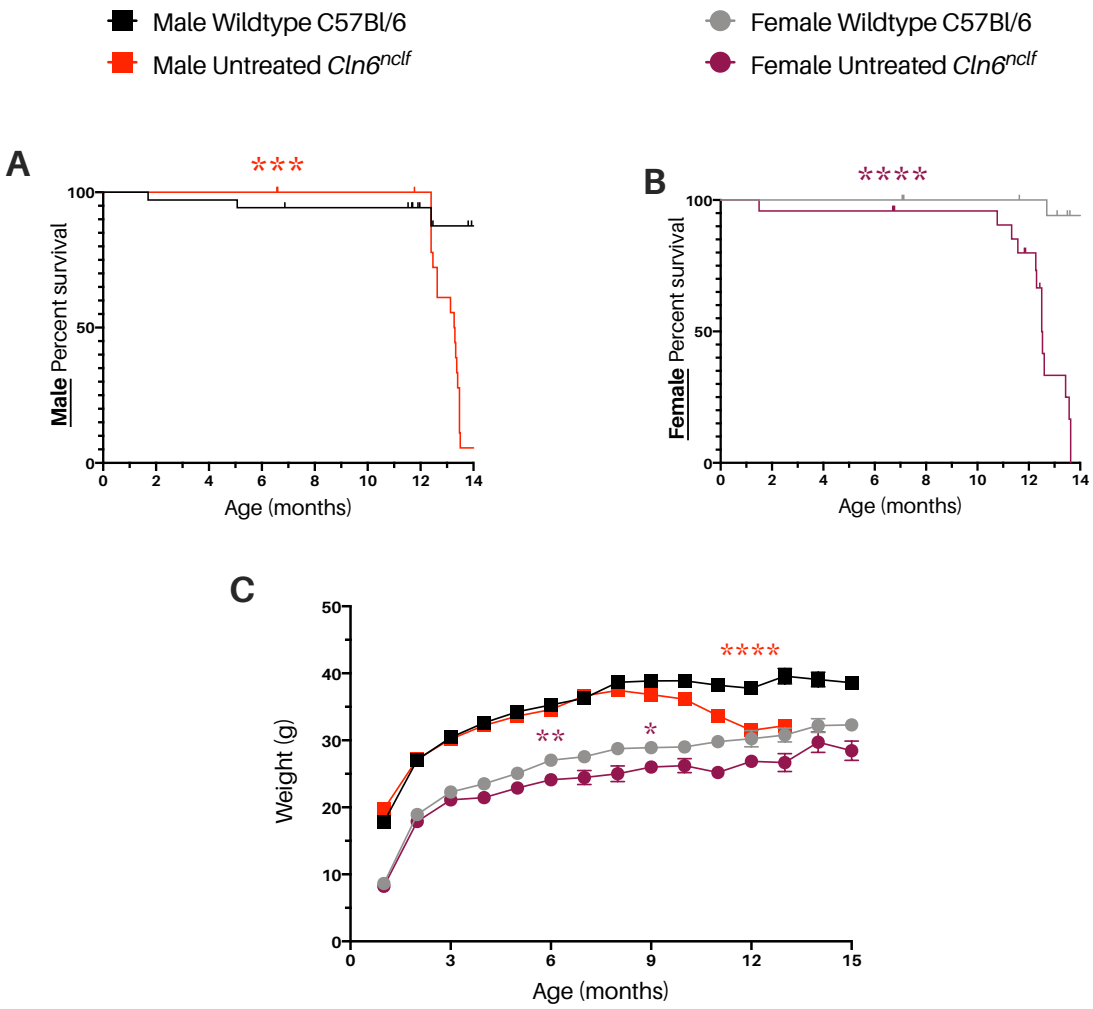

Figure 3.4 | Establishing the Cln6^{nclf} disease(d) phenotype: survival and weight. *Untreated Cln6^{nclf} (UT^{Cln6nclf}) mice demonstrated variable significant differences across their lifespan but had a significantly decreased lifespan, overall, compared to healthy WT (C57Bl/6) controls.* Survival and weights were only recorded up until 14 months of age due to the time limitations of a MSc thesis, however, survival and weights continued to be recorded for the larger Gray Foundation trial - until all animals had reached one of the three humane endpoints outlined in **Chapter 2**. Almost all male and female UT^{Cln6nclf} mice had reached one of these endpoints by 14 months. **A.** Kaplan-Meier plot of male mouse survival (%). UT^{Cln6nclf} mice (red lines; median survival = 13.3 months) had significantly shorter lifespans than sex-matched WT controls (black lines; median survival undefined at 14 months; *** p = .0005). Survival curve comparison conducted via log-rank (Mantel-Cox) test (**Appendix B.9.1**). Planned deaths (for post-behavioural post-mortem analysis) are indicated by small 'tick' marks on the lines. Starting n = 28-35 per group. **B.** Kaplan-Meier plot of female mouse survival (%). UT^{Cln6nclf} mice (maroon lines; median survival = 12.5 months) had significantly shorter lifespans than sex-matched WT controls (grey lines; median survival undefined at 14 months; **** p = ≤.0001). Survival curve comparison conducted via log-rank (Mantel-Cox) test (**Appendix B.9.2**). Starting n = 24-27 per group. C. Line graph of mean weights (in grams) of male UT^{Cln6nclf} (red squares), male WT (C57Bl/6; black squares), female UT^{Cln6nclf} (maroon circles) and female WT (C57Bl/6; grey circles) mice over 15 months. Female UT^{Cln6nclf} mice weighed significantly less than their age- and sex-matched WT counterparts at 6 (6 month female WT mean weight = 27.040 g ; 6 month female UT$^{Cln6nclf\ f}$ mean weight = 24.11 g; ** p = .0041) and 9 (9 month female WT mean weight = 28.9 g; 9 month female Cln6^{nclf} mean weight = 26.0 g; * p = .0228) months of age, while male UT^{Cln6nclf} mice only began to show a significant difference in weight from their WT counterparts at 12 months of age (12 month male WT mean weight = 37.76 g; 12 month male UT^{Cln6nclf} mean weight = 31.49 g; **** p ≤ .0001). n = 24-35. Analyses at individual time points conducted using unpaired student t-tests (**Appendices B.10.1-10.2**).

3.1.4 The Cln6^{nclf} disease(d) phenotype: ***sex differences***

Sex differences in disease progression is historically overlooked in the life sciences, with the use of a single sex (typically male) in animal model studies being a commonplace practice. This tradition has begun to be viewed as problematic as our understanding of how biological sex, and the associated physiological differences between the sex, influences a patient's experience of disease – from symptoms to rate of progression – and can dictate their response to potential therapies. These differences could be particularly pertinent for the development of potential therapies for the NCLs as differences in male and female experiences of these diseases is underinvestigated. With this in mind, the practial component of this thesis included both male and female mice for every treatment combination, to ensure any sex-based differences in response to the three therapies being investigated (gene therapy, gemfibrozil and CBD) would be accounted for and characterised. Here, the mean behaviour scores of male and female UT^{Cln6nclf} mice are compared across the lifespan (6, 9 and 12 months for rotarod; 6 and 9 months for ataxia and up to 14 months for survival and weight), in an effort to better characterise any differences in male and female experiences of untreated CLN6 BD.

3.1.4.a Rotarod sex differences

Male and female UT^{Cln6nclf} mice demonstrated no significant differences in mean rotarod scores (**Figure 3.5.A**) at 6, 9 or 12 months of age (unpaired t-tests; **Appendix B.11**), though females had non-significantly better (higher) scores at each time point. Similarly, there was no significant difference in male and female overall rate of score decline across the lifespan (simple linear regression; **Appendix B.12**).

3.1.4.b Composite ataxia sex differences

Male and female UT^{Cln6nclf} mice demonstrated no significant differences in mean composite ataxia scores (**Figure 3.5.B**) at 6 or 9 months of age (unpaired t-tests; **Appendix B.13**), though females had non-significantly worse (higher) scores than their male counterparts at 6 months of age.

3.1.4.c Ledge ataxia sex differences

Male and female UT^{Cln6nclf} mice demonstrated no significant differences in mean ledge ataxia scores (**Figure 3.5.C**) at 6 or 9 months of age (unpaired t-tests; **Appendix B.14**).

3.1.4.d Hindlimb clasping ataxia sex differences

Female UT^{Cln6nclf} had significantly higher (worse) hindlimb clasping scores (**Figure 3.5.D**) than their age-matched male counterparts at 6 months of age (male mean score = 0.6; female mean score = 1.556; *p = .0185; **Appendix B.15**).

3.1.4.e Gait ataxia sex differences

Male and female UT^{Cln6nclf} mice demonstrated no significant differences in mean gait ataxia scores (**Figure 3.5.E**) at 6 or 9 months of age (unpaired t-tests; **Appendix B.16**).

3.1.4.f Survival sex differences

Male and female UT^{Cln6nclf} mice demonstrated no significant differences in median survival (**Figure 3.5.F**, log-rank (Mantel-Cox) test; **Appendix B.25**).

⇒ **Figure 3.5 | Establishing the Cln6^{nclf} disease(d) phenotype: sex differences (opposite page).** *No significant sex differences were observed in mean behavioural scores or lifespan between male and female untreated Cln6^{nclf} (UT^{Cln6nclf}) mice at any age point except for mean hindlimb clasping scores at 6 months of age.* Mean behavioural scores for rotarod (**A**; latency to fall in seconds) at 6, 9 and 12 months of age, composite ataxia (**B**; score 0-9), the ledge ataxia test (**C**; score 0-3), the hindlimb clasping ataxia test (**D**; score 0-3), the gait ataxia test (E; score 0-3) at 6 and 9 months of age, and survival (**F**; %) up to 14 months were compared between male and female UT^{Cln6nclf} mice. **A.** Female UT^{Cln6nclf} mice (maroon circles) appear to have, on average, higher rotarod scores than males (red squares) at all three time points measured. None of these differences, however, are statistically significant. Dotted lines between time points represent assumed trajectory of average scores between measured time points. Higher scores (~300) indicate a higher level of motor co-ordination and balance as measured by the rotarod (coloured arrow on the left). Lower scores represent increasing levels of motor dysfunction. Data are presented as average scores and error bars represent ± SEM. n(per group per time point) = 7-12. Comparisons between average scores at each time point were conducted using unpaired student t-tests (**Appendix B.11**). A simple linear regression analysis (**Appendix B.12**) of the overall rate of decline between male and female UT^{Cln6nclf} mean scores showed that there was no significant difference in slope (rate of decline; p = .6896) or elevation (range of time over which the decline occurred; p = .1327). **B.** Mean composite ataxia scores for male (red) and female (maroon) UT^{Cln6nclf} mice at 6 (dark) and 9 (lighter) months of age. Females appear to have slightly higher average composite scores at both age points, though this difference is not significant at either time point. Higher scores (~9) in this behavioural assay, unlike the rotarod, represent a more ataxic/diseased phenotype. Scores closer to 0 represent an absence of this disease phenotype (coloured arrow on the left). Analysis was conducted using unpaired student t-tests (**Appendix B.11**). Data are presented as average scores and error bars represent ±SEM. Individual averaged (3 trials) composite ataxia phenotype scores are presented as clear circles. n(per group per time point) = 8-10. **C.** Averaged ledge ataxia test scores of male (red) and female (maroon) UT^{Cln6nclf} mice at 6 and 9 months. No significant difference was found at either time point, although females demonstrated non-significantly lower ledge scores at 6 months and then ns higher at 9 months. Analysis was conducted using unpaired student t-tests (**Appendix B.14**). Data are presented as average scores and error bars represent ±SEM. Individual averaged (3 trials) ledge ataxia phenotype scores are presented as clear circles. n(per group per time point) = 8-10. **D.** Averaged hindlimb clasping scores of males (red) and females (maroon) at 6 and 9 months of age. Females demonstrated a significantly more ataxic (higher; coloured arrow on left) score (female mean score =1..556) at 6 months than their male counterparts (male mean score = 0.6; p = .0185. Analysis was conducted using unpaired student t-tests (**Appendix B.15**). This significant difference was no longer present at 9 months. Data are presented as average scores and error bars represent ±SEM. Individual averaged (3 trials) hindlimb clasping ataxia phenotype scores are presented as clear circles. n(per group per time point) = 8-10. **E.** Averaged gait scores of males (red) and females (maroon) at 6 and 9 months of age. Females appear to perform better, with lower scores, than males at 6 months and then have worse scores than their male counterparts at 9 months – but neither of these differences in averaged gait score produced a statistically significant result. Analysis was conducted using unpaired student t-tests (**Appendix B.16**). Data are presented as average scores and error bars represent ±SEM. Individual averaged (3 trials) gait ataxia phenotype scores are presented as clear circles. n(per group per time point) = 8-10. **F.** Kaplan-Meier survival curve (%) of male (red) and female (maroon) UT^{Cln6nclf} mice. Small 'tick' marks on lines represent the planned removal of mice (~5 per time point, per experimental group) from the study for post-mortem analysis after behavioural testing at 6 and 12 months of age. No significant difference in average lifespan was observed between the sexes (Mantel-Cox test; p = .5129; **Appendix B.17**). Starting n =24-28.

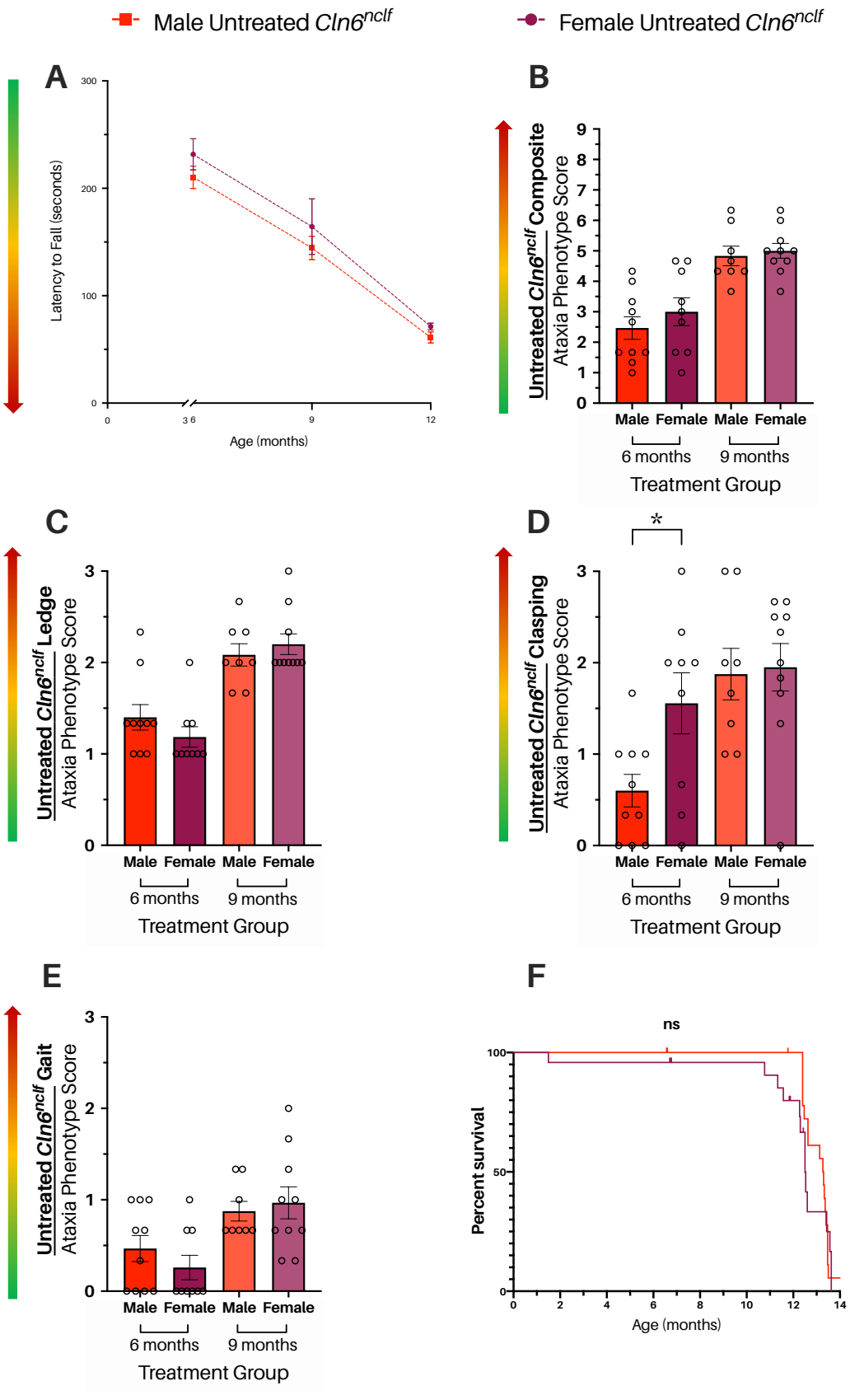
Male Untreated Cln6nclf
Female Untreated Cln6nclf
A
Latency to Fall (seconds)
Age (months)
B
Untreated Cln6nclf Composite Ataxia Phenotype Score
Male Female Male Female
6 months 9 months
Treatment Group
C
Untreated Cln6nclf Ledge Ataxia Phenotype Score
Male Female Male Female
6 months 9 months
Treatment Group
D
*
Untreated Cln6nclf Clasping Ataxia Phenotype Score
Male Female Male Female
6 months 9 months
Treatment Group
E
Untreated Cln6nclf Gait Ataxia Phenotype Score
Male Female Male Female
6 months 9 months
Treatment Group
F
ns
Percent survival
Age (months)

3.1.5 The Cln6^{nclf} disease(d) phenotype: ***summary***

All UT^{Cln6nclf} mice, regardless of gender, had significantly shorter lifespans and demonstrated some form of significant behavioural deficit compared to WT by 9 months of age – though these deficits were not consistently present across the range of behavioural assays. Male UT^{Cln6nclf} mice began demonstrating significant behavioural deficits earlier than UT^{Cln6nclf} females, with significantly worse average composite ataxia and ledge test scores than sex-matched WT at 6 months of age. Female UT^{Cln6nclf} behavioural scores at this age were not significantly different from WT but their weights were significantly lower. At 9 months, however, UT^{Cln6nclf} males continued to demonstrate significantly worse scores than WT only in the composite and ledge assays, while UT^{Cln6nclf} females performed significantly worse across all ataxia assays and continued to have significantly lower weights than WT.

By 12 months of age both males and females were performing significantly worse than WT on the rotarod (**Tables 3.1** and **3.2**). No ataxia measurements were analysed at 12 months for this thesis, due to the fact that another reseacher, Jasmine Lock, had taken over the practical component of behavioural testing by this time point, and the subjective nature of the ataxia grading system means that the relationship between the 6 and 9 months scores and her 12 month scoring might be compromised by experimenter bias. Previous studies characterising the behavioural deficits of Cln6^{nclf} mice up to this age point, coupled with the significant deficit in rotarod scores for both genders at 12 months, could lead one to extrapolate that any 12 month ataxia scores would be worse, if not significantly so, than WT at this age point. Without actually analysing the data, however, this can only remain as conjecture.

Overall, the behavioural scores of UT^{Cln6nclf} mice paint a picture of progressive behavioural deficits in co-ordination, balance, endurance (rotarod) and motor control (ataxia)

over their significantly shortened lifespans. Females appear to experience later onset of behavioural deficits than males, but ataxic symptoms are more apparent/penetrant at this later time point. There were no significant differences in behavioural scores or lifespan between male and female UT^{Cln6nclf}, even for 6 month composite and ledge ataxia scores – where males were significantly worse than their sex-matched WT and females were not – with the exception of mean hindlimb clasping scores at 6 months. Here, UT^{Cln6nclf} females performed significantly worse than than UT^{Cln6nclf} males (**Table 3.3**).

Table 3.1 | Establishing the Cln6^{nclf} disease(d) phenotype: summary table of untreated Cln6^{nclf} (UT^{Cln6nclf}) males. *Summary table of behavioural scores (rotarod and ataxia), survival and weight comparisons carried out between male* UT^{Cln6nclf} *and age-matched male WT (C57Bl/6) mice at 6, 9 and 12 months of age.* All behavioural score and weight comparisons were conducted using unpaired student t-tests (**Appendices B.1.-8.2 and B.10.1**), while survival curves were compared using log rank (Mantel-Cox) tests (**Appendix B.9.1**). nsd = no significant difference.

Untreated Cln6^{nclf} Males				
Behavioural Test	**Comparison Group**	**6 months**	**9 months**	**12 months**
Rotarod	WT	nsd	nsd	**Worse (s)**
Composite	WT	**Worse (s)**	**Worse (s)**	-
Ledge	WT	**Worse (s)**	**Worse (s)**	-
Hindlimb	WT	nsd	nsd	-
Gait	WT	nsd	nsd	-
Survival	WT	**Reduced survival (s)**		
Weight	WT	nsd	nsd	**Weigh less(s)**

Table 3.2 | Establishing the Cln6^{nclf} disease(d) phenotype: summary table of untreated Cln6^{nclf} (UT^{Cln6nclf}) females. *Summary table of behavioural scores (rotarod and ataxia), survival and weight comparisons carried out between female* UT^{Cln6nclf} *and age-matched female WT (C57Bl/6) mice at 6, 9 and 12 months of age.* All behavioural score and weight comparisons were conducted using unpaired student t-tests (**Appendices B.1.-B.8.2 and B.10.2**), while survival curves were compared using log rank (Mantel-Cox) tests (**Appendix B.9.2**). nsd = no significant difference.

Untreated Cln6^{nclf} Females				
Behavioural Test	**Comparison Group**	**6 months**	**9 months**	**12 months**
Rotarod	WT	nsd	nsd	Worse (s)
Composite	WT	nsd	**Worse (s)**	-
Ledge	WT	nsd	**Worse (s)**	-
Hindlimb	WT	nsd	**Worse (s)**	-
Gait	WT	nsd	**Worse (s)**	-
Survival	WT	**Reduced survival (s)**		
Weight	WT	**Weigh less (s)**	**Weigh less (s)**	nsd

Table 3.3 | Establishing the Cln6^{nclf} disease(d) phenotype: summary table of untreated Cln6^{nclf} (UT^{Cln6nclf}) males versus females. *Summary table of behavioural score (rotarod and ataxia), survival and weight comparisons carried out between male and female* UT^{Cln6nclf} *mice at 6, 9 and 12 months of age.* All behavioural score and weight comparisons were conducted using unpaired student t-tests (**Appendices B.11-16**), while survival curves were compared using log rank (Mantel-Cox) tests (**Appendix B.17**). nsd = no significant difference.

Untreated Cln6^{nclf} Males vs Females			
Behavioural test	**6 months**	**9 months**	**12 months**
Rotarod	nsd	nsd	nsd
Composite	nsd	nsd	-
Ledge	nsd	nsd	-
Hindlimb	**Males performed sig. better**	nsd	-
Gait	nsd	nsd	-
Survival	nsd		

3.2 Sustained small molecule therapy, when administered without gene therapy, did not protect against motor or survival deficits in Cln6^{nclf} mice

Gemfibrozil, an FDA-approved fibrate commonly used to treat high cholesterol, and cannabidiol (CBD), a cannabinoid with polymorphic pharmaceutical properties that has shown some promising neuroprotective qualities in a wide range of neurodegenerative conditions, were selected for investigation due to the Gray Foundation's interest in supplementary small molecule therapies and their potential to augment the efficacy of gene therapy in CLN6 BD patients.

Gemfibrozil has previously shown promise in several NCL *in vitro* systems. It was found to upregulate CLN2 activity in a CLN2$^{-/-}$ mouse model (Ghosh et al., 2012), inhibit apoptosis of lymphoblast cells via autophagy recovery in CLN3$^{-/-}$ cell culture and has demonstrated positive effects on the autophagic processes and lysosomal acidity of CLN6$^{-/-}$ cells *in vitro* (Best, 2017; Best et al., 2017). Preliminary studies conducted by the Hughes lab have also indicated that gemfibrozil is well tolerated at 30 kg/mg and 120 kg/mg doses in WT (C57Bl/6) mice and appears to have promising effects on lysosomal clearance and autophagy markers in the Cln6^{nclf} mouse brain (Stephanie Mercer, Isaiah Cheong, Cliff Abrahams and Stephanie Hughes, unpublished work, 2016; Best, 2017).

CBD, in comparison, has yet to be validated as having therapeutic benefits in any form of BD. A preliminary investigation of it's effect on the behaviour and post-mortem pathophysiology of Cln6^{nclf} mice yielded inconclusive results, though this might be due to the short time frame of the study (Partridge, 2017). Despite this, CBD has been shown to have antiepileptic, sedative, analgesic, anti-inflammatory, anxiolytic and anti-oxidant properties in a wide range of healthy and pathological animal models and human clinical trials (Devinsky et al., 2016; Johnson et al., 2010; Russo et al., 2007; Turkanis et al., 1974; Zuardi, 2008), indicating

that it may offer benefits to CLN6 BD patients – though the way in which those benefits manifest and to what it extent has yet to be characterised. This project aims to build on the successful preliminary studies of gemfibrozil *in vivo* in a large-scale, long-term study and to better characterise the effects, if any exist, of CBD on the behavioural phenotype of Cln6^{nclf} mice.

Viral-mediated gene therapy has been previously established as being incredibly effective, both *in vitro* and *in vivo*, and has even been known to produce hyperactivity in Cln6^{nclf} mice (aka higher behavioural scores than healthy controls)(Cain et al., 2019; Weimer et al., 2019). Such results would make interpreting the effects of complementary therapies, especially subtle effects, much more difficult, as they may be phenotypically masked by the overwhelming effects of gene therapy. Therefore, in order to properly characterise the effects of gemfibrozil and CBD, alone and in combination, on the Cln6^{nclf} phenotype, they were also investigated here *without* gene therapy.

3.2.1 Small molecule therapy in PBS-treated Cln6^{nclf} mice: ***rotarod***

Ten different experimental groups were assessed with the rotarod at 6, 9 and 12 months of age. These included male and female (M/F) WT controls, M/F Cln6^{nclf} mice treated with gemfibrozil (Gemfib^{PBS}) M/F Cln6^{nclf} mice treated with CBD (CBD^{PBS}), M/F Cln6^{nclf} mice treated with a combination of gemfibrozil and CBD (Combo^{PBS}) and M/F UT^{Cln6nclf} controls. All groups, including controls, were injected with 1x PBS at P0-2, rather than scAAV9.CB.*hCLN6* (**section 2.3**). Gemfib^{PBS} mice received 120 mg/kg of gemfibrozil in strawberry jelly every second day from weaning until individual end points of the trial. CBD^{PBS} mice received 5 mg/kg of CBD in strawberry jelly every second day from weaning until the end of the trial. Finally, Combo^{PBS} mice received a combination of 120 mg/kg gemfibrozil and 5 mg/kg CBD every day from weaning until individual end points of the trial (see **sections 2.3** and **2.4** for more details

regarding i.c.v injections and dosing). Rotarod scores for the drug-only Cln6^{nclf} experimental groups were found to have normal (Gaussian) distributions using D'Agostino & Pearson normality tests, so all subsequent statistical analyses were conducted using parametric testing (**Appendix B.18**).

Linear regression was used to compare the overall rate of decline of mean rotarod scores over time and the associated elevation (range over which the decline occurred) of each drug treated group versus sex-matched WT controls and UT^{Cln6nclf} counterparts (**Figure 3.6**; **Appendices B.19-21**). To compare differences in rotarod score between groups at each individual time point, 1-way analysis of variances (ANOVAs) were used, complemented by Tukey's multiple comparison post-hoc testing when significant differences were found to be present (**Appendices B.21-22**). The rotarod assay showed a steady decline in motor performance over time for all mice, as to be expected due to age, and this decline was mathematically confirmed by the negative line equations of each group (**Figure 3.6**; **Appendix B.21**). None of the drug treated groups (M/F Gemfib^{PBS}, M/F CBD^{PBS} or M/F Combo^{PBS}) overall rate of decline or elevation differed significantly from sex-matched UT^{Cln6nclf} mice, indicating that while the drugs may not be improving rotarod performances in diseased mice, they are at least not performing worse than the UT^{Cln6nclf} controls.

In male mice, Gemfib^{PBS} and Combo^{PBS} animals declined at a significantly greater rate than healthy male WT controls (simple linear regression; WT vs Gemfib^{PBS} adjusted p = .0033; WT vs Combo^{PBS} adjusted p = .0362; **Appendices B.19** and **B.21**), as is to be expected since their mean rotarod scores were not significantly different from those of male UT^{Cln6nclf} mice. The overall rate of decline in male CBD^{PBS} mice, however, was not significantly different from that of WT (p = .1299; B.21). Male Cln6^{nclf} mice were also the first to present with significant motor deficits in the rotarod task, with Gemfib^{PBS} mice scoring significantly lower (mean =

111.4 seconds) than WT (mean = 181.9 seconds; *p = .0358) at 9 months of age (1-way ANOVA with Tukey's multiple comparisons post-hoc testing; **Figure 3.7.B; Appendix B.22**). By 12 months, all three male drug-only groups were performing significantly worse than WT (**Figure 3.7.C**; ****p(Gemfib^{PBS}) ≤ .0001; ****p(CBD^{PBS}) ≤ .0001; ****p(Combo^{PBS}) ≤ .0001; **Appendix B.22**) and their mean scores are not significantly different from those of male UT^{Cln6nclf}, indicating that small molecule therapy does not appear to protect male Cln6^{nclf} mice from a diseased behavioural phenotype on the rotarod by 12 months of age.

For females, mice on single-drug regimens declined at a significantly greater rate than WT controls (simple linear regression; **p(Gemfib^{PBS}) = .0048; *p(CBD^{PBS}) = .0262; **Figure 3.6; Appendices B.20-21**), while female Combo^{PBS} Cln6^{nclf} mice appear to decline at a rate not significantly different from WT (p = .0629; **Figure 3.6**). Combo^{PBS} female mice, while having a statistically similar rate of decline to WT, had a significantly different elevation (p = .0104; **Appendix B.21**)– indicating that, at every time point measured, the Combo^{PBS} mice had a lower (worse) rotarod score than WT. This could indicate a learning deficit when it came to learning the rotarod task or be indicative of a motor deficit, either of which would indicate that the combined drug treatment may be influencing the slowing of decline in Cln6^{nclf} female mice to a rate similar to WT, but is not eliminating the presence of a diseased phenotype altogether. Unlike males, where Gemfib^{PBS} mice started to show deficits at 9 months of age, no drug-only female group showed significant deficits until the 12 month time point. At this stage, all three drug treated groups performed significantly worse than WT (**Figure 3.7.C**; 1-way ANOVA with Tukey's multiple comparisons post-hoc texts; ****p(Gemfib^{PBS}) ≤ .0001 ; ****p(CBD^{PBS}) ≤ .0001;*** p(Combo^{PBS}) = .0008; **Appendix B.22**).

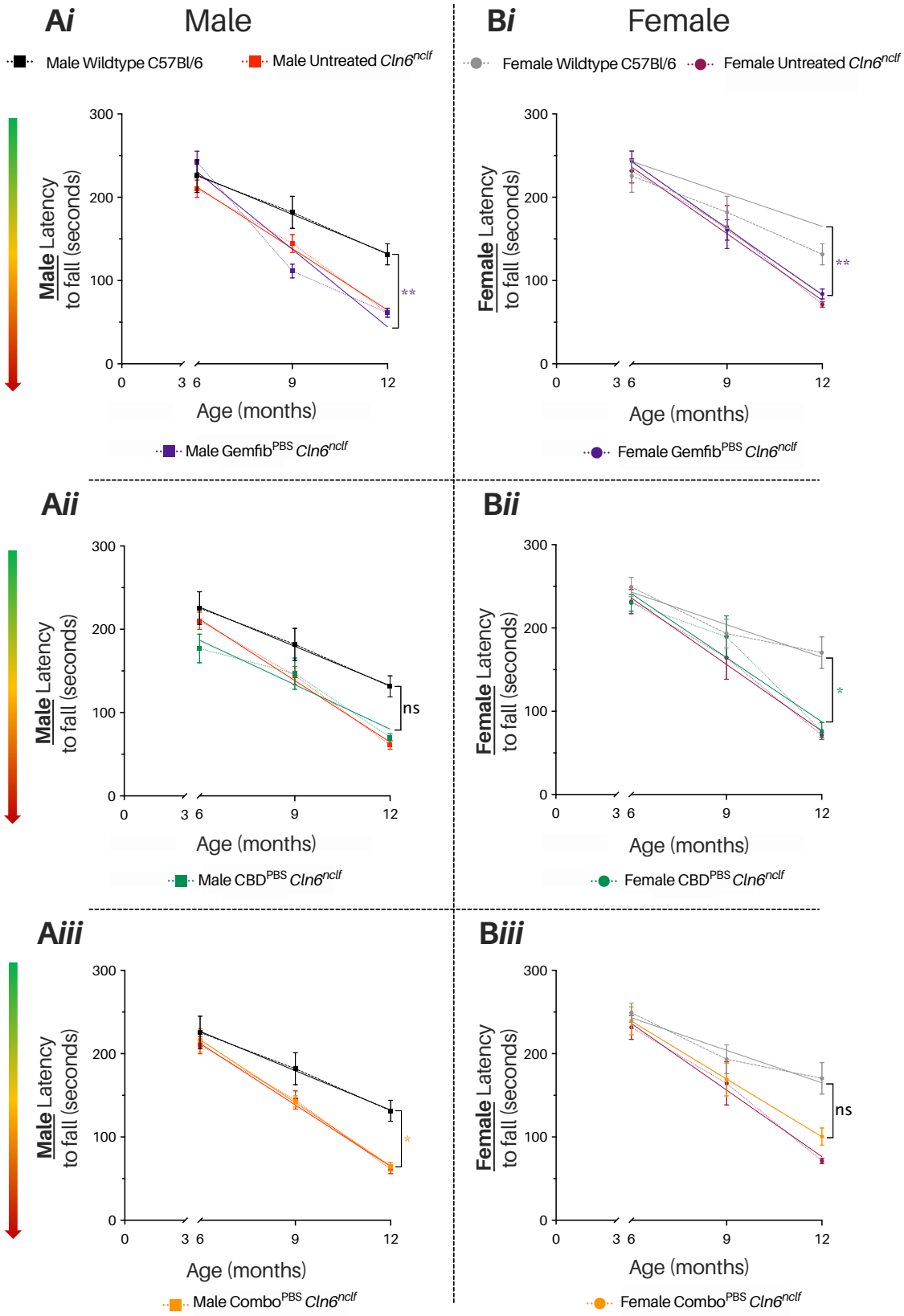
Ai
Male
Male Wildtype C57Bl/6
Male Untreated Cln6nclf
Male Latency to fall (seconds)
Age (months)
Male GemfibPBS Cln6nclf
Bi
Female
Female Wildtype C57Bl/6
Female Untreated Cln6nclf
Female Latency to fall (seconds)
Age (months)
Female GemfibPBS Cln6nclf
Aii
Male Latency to fall (seconds)
ns
Age (months)
Male CBDPBS Cln6nclf
Bii
Female Latency to fall (seconds)
*
Age (months)
Female CBDPBS Cln6nclf
Aiii
Male Latency to fall (seconds)
*
Age (months)
Male ComboPBS Cln6nclf
Biii
Female Latency to fall (seconds)
ns
Age (months)
Female ComboPBS Cln6nclf

⇐ Figure 3.6 | Small molecule therapy in PBS-treated Cln6^{nclf} mice: rotarod scores (line graphs; previous page). *Overall rate of decline in motor skills, as determined by a rotarod assay, appears to be sexually dimorphic in Cln6^{nclf} mice treated with one of the three different drug regimens (gemfibrozil, CBD and a combination of the two aka 'Combo^{PBS}') and no gene therapy at P0-2 (1x PBS instead).* **Ai-iii.** Mean male rotarod scores (square points) recorded at 6, 9 and 12 months of age. Data are presented as a line graph of mean scores (latency to fall, in seconds), with error bars = ± SEM. Dotted lines indicate the expected mean score trajectory for an experimental group between measured time points. Solid lines represent the regression lines of each experimental group, as calculated via simple linear regression. A high score (~300) indicates a high level of motor co-ordination as measured by the rotarod, while lower scores correlate to increasing levels of motor dysfunction (coloured arrow on the left). n(per group per time point) = 26-35. **Ai.** Male Cln6^{nclf} mice treated with gemfibrozil only (Gemfib^{PBS}; purple lines and squares) declined at a significantly greater rate (simple linear regression; ** p = .0033; **Appendix B.21**) than 'healthy' WT controls (WT C57Bl/6; black lines and squares) and showed no significant difference in overall rate of decline from UT^{Cln6nclf} counterparts (red lines and squares; p = .0919). n(per group per time point) = 26-32 **Aii.** Male Cln6^{nclf} mice treated only with CBD (CBD^{PBS}, green lines and squares) showed no significant (ns) difference in overall rate of decline from either the WT controls or their UT^{Cln6nclf} counterparts (simple linear regression, p(WT) = .1299; p(UT^{Cln6nclf}) = .1854; **Appendix B.21**). n(per group per time point) = 32-35. **Aiii**. Male Cln6^{nclf} mice treated with a combination of gemfibrozil and CBD (Combo^{PBS}; orange squares and lines) demonstrated a significantly greater rate of decline, overall, than WT controls (simple linear regression; * p = .0362; **Appendix B.21**). n = ranging between 30-32**. Bi-iii.** Mean female rotarod scores (circle points) recorded at 6, 9 and 12 months of age. n(per group per time point) = 25-27**. Bi.** Female Cln6^{nclf} mice treated with gemfibrozil only (Gemfib^{PBS}; purple lines and circles) declined at a significantly greater rate (simple linear regression; ** p = .0048; **Appendix B.21**) than 'healthy' WT controls (WT C57Bl/6; grey lines and circles) and showed no significant difference in overall rate of decline from UT^{Cln6nclf} counterparts (maroon lines and circles; p = .9984; **Appendix B.21**). n(per group per time point) = 26-27. **Bii.** Female Cln6^{nclf} treated with CBD only (CBD^{PBS}; green lines and circles) demonstrated a significantly greater rate of decline, overall, than WT controls (simple linear regression; * p = .0262; **Appendix B.21**). Comparison between the CBD-treated females and their UT^{Cln6nclf} counterparts, however, showed no significant difference in slope (simple linear regression; p = .8664; **Appendix B.21**). n = 26. **Biii.** Female Cln6^{nclf} mice treated only with a combination of gemfibrozil and CBD (Combo^{PBS}; orange lines and circles) showed no significant (ns) difference in overall rate of decline from either the WT controls or their UT^{Cln6nclf} counterparts (simple linear regression, p(WT) = .0629; p(UT^{Cln6nclf}) = .5487; **Appendix B.21**). n(per group per time point) = 25-26.

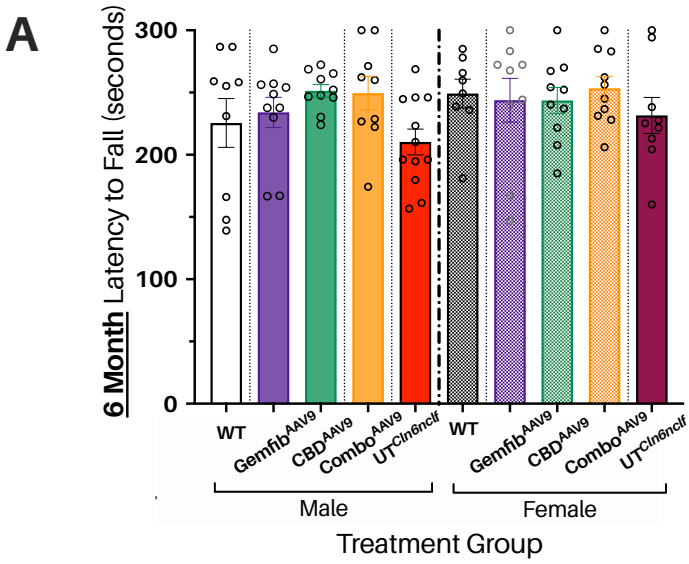
A
6 Month Latency to Fall (seconds)
300
200
100
0
WT
GemfibAAV9
CBDAAV9
ComboAAV9
UTCln6ncl
WT
GemfibAAV9
CBDAAV9
ComboAAV9
UTCln6ncl
Male
Female
Treatment Group

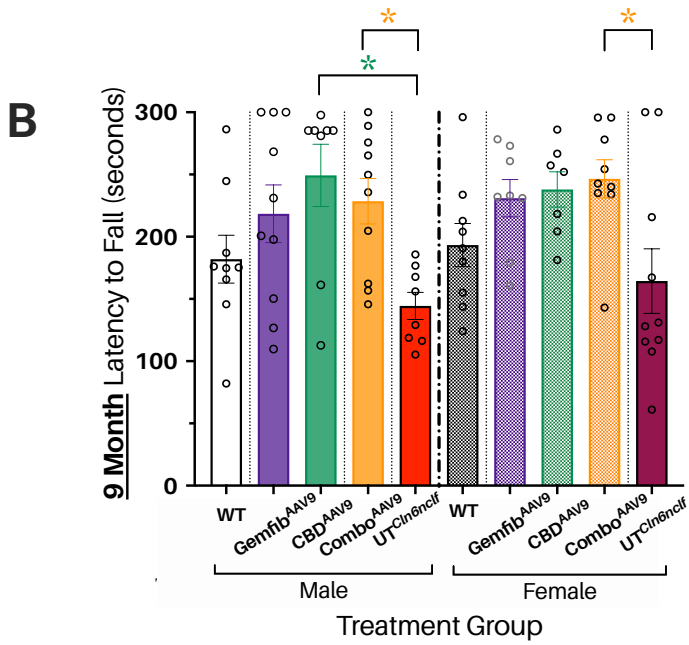
B
9 Month Latency to Fall (seconds)
300
200
100
0
*
*
*
WT
GemfibAAV9
CBDAAV9
ComboAAV9
UTCln6ncl
WT
GemfibAAV9
CBDAAV9
ComboAAV9
UTCln6ncl
Male
Female
Treatment Group

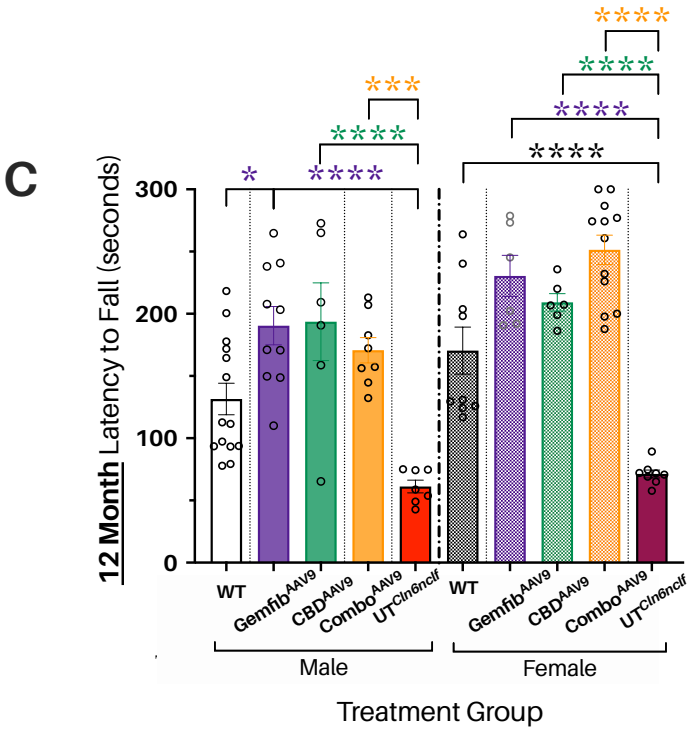
C
12 Month Latency to Fall (seconds)
300
200
100
0
*
****
***
****
****
****
****
WT
GemfibAAV9
CBDAAV9
ComboAAV9
UTCln6ncl
WT
GemfibAAV9
CBDAAV9
ComboAAV9
UTCln6ncl
Male
Female
Treatment Group

⇐ **Figure 3.7| Small molecule therapy in PBS-treated Cln6^{nclf} mice: rotarod scores (histograms; previous page).** *Male and female Cln6^{nclf} mice who received one of the three drug treatments - gemfibrozil, CBD or a combination of the two ('combo')- without gene therapy at P0-2 (were treated with 1x PBS instead; drug-only) were not protected against untreated Cln6^{nclf} (UT^{Cln6nclf}) rotarod deficiencies by 12 months of age.* Histograms presenting mean rotarod scores (latency to fall in seconds) of male (left; plain coloured bars) and female (right; patterned bars) Cln6^{nclf} mice treated only with either: gemfibrozil (Gemfib^{PBS}), CBD (CBD^{PBS}), or a combination of the two (Combo^{PBS}) and their age- and gender-matched UT^{Cln6nclf} and WT (C57Bl/6) counterparts at 6 (**A**), 9 (**B**) and 12 (**C**) months of age. Data are presented as mean scores with error bars = ± SEM. Different mice were tested at each of the different time points, making the experiment between-subjects in design. All analyses were conducted using 1-way ANOVAs with Tukey's post-hoc comparisons used to elicit specific significant differences between experimental groups (**Appendix B.22-23**). Individual mean mouse rotarod scores indicated by clear circles. **A.** Mean male (left; plain coloured bars) and female (right; patterned coloured bars) rotarod scores (latency to fall in seconds) at 6 months. No differences, for either gender, were observed between the three different drug-only treated Cln6^{nclf} groups (Gemfib^{PBS}, CBD^{PBS} or Combo^{PBS}) and 'healthy' WT controls or UT^{Cln6nclf} counterparts at 6 months of age. n(per group per time point) = 25-35. **B.** Mean male (left; plain coloured bars) and female (right; patterned, coloured bars) rotarod scores (latency to fall in seconds) at 9 months. Male Cln6^{nclf} mice treated only with gemfibrozil (Gemfib^{PBS}; plain purple bar) began to show significant deficits (coloured arrow on the left) compared to WT controls (plain white bar; male WT mean =181.9 s; male Gemfib^{PBS} mean = 111.4 s; * p = .0358; **Appendix B.22**) n = 9. No other drug-only treated group, male or female, demonstrated significant differences when compared to age- and sex-matched either WT (male WT = plain white bar; female WT = patterned black and white bar) or UT^{Cln6nclf} (male UT^{Cln6nclf} = plain red bar; female UT^{Cln6nclf} = plain maroon bar) groups at 9 months. n(per group per time point) = 8-15. **C.** Mean male (left; plain coloured bars) and female (right; patterned, coloured bars) rotarod scores (latency to fall in seconds) at 12 months. Error bars ± SEM. Individual mean mouse rotarod scores indicated by clear circles. Mean of male Cln6^{nclf} mice in all three drug-only groups (Gemfib^{PBS}, CBD^{PBS}, Combo^{PBS}) were significantly worse than WT at 12 months of age (WT mean = 131.5 s; Gemfib^{PBS} mean = 61.14 s; CBD^{PBS} mean = 70.33 s; Combo^{PBS} mean = 64.60 s; **** $p \leq 0.0001$; **Appendix B.22**). n(per group per time point) = 7-14. None of these three groups, however, demonstrated a significant difference in average score with their age matched UT^{Cln6nclf} counterparts. Significant differences in rotarod scores were also observed at 12 months between the female Cln6^{nclf} mice treated only with gemfibrozil, only with CBD, only with a combination of both drugs and the WT control (WT mean = 170.4 s; Gemfib^{PBS} mean = 83.88 s; CBD^{PBS} mean = 76.33 s; Combo^{PBS} mean = 100.4 s; *** $p \leq 0.001$; **** $p \leq 0.0001$; **Appendix B.23**). None of these three female drug-only groups demonstrated a significant difference in mean score from their UT^{Cln6nclf} counterparts at 12 months. n(per group per time point) = 8-9.

3.2.2 Small molecule therapy in PBS-treated Cln6^{nclf} mice: ***ataxia***

In order to characterise the effects gemfibrozil, CBD or a combination of the two drugs might have on the Cln6^{nclf} ataxic behavioural phenotype, without gene therapy, ten different experimental groups were assessed for signs of cerebellar ataxia at 6 and 9 months of age. Ataxia phenotyping scores for the drug-only Cln6^{nclf} experimental groups were found to have normal (Gaussian) distributions using D'Agostino & Pearson normality tests, so all subsequent statistical analyses were conducted using parametric testing (**Appendix B.18**).

3.2.2.a Composite ataxia phenotype scores

Composite ataxia scores (0-9) for each mouse were calculated by adding together it's mean ledge, hindlimb clasping and gait ataxia phenotyping scores (0-3). Individual mouse composite

ataxia scores were then averaged for each experimental group and presented as mean score (0-9) ± SEM. Comparisons between mean composite scores of age- and sex-matched Gemfib^{PBS}, CBD^{PBS}, Combo^{PBS} treated and UT^{Cln6nclf} and WT (C57Bl/6) mice were made using 1-way ANOVAs, with Tukey's post-hoc multiple comparisons tests conducted when significant differences were found to occur (**Appendices B.24-25**).

No significant differences in mean composite score were detected at 6 months of age for male mice, regardlesss of strain or treatment group (**Figure 3.8.Ai-ii; Appendix B.24**). At 9 months, however, all three male drug-only Cln6^{nclf} treatment groups were demonstrating significantly higher (worse) scores than their WT counterparts (WT mean = 2.574; Gemfib^{PBS} mean =5.0; **** $p \leq .0001$; CBD^{PBS} mean = 4.6; **** $p \leq .0001$; Combo^{PBS} mean = 5.067; **** $p \leq .0001$; **Appendix B.24**). None of these drug-only treatment groups demonstrated a significant difference in mean composite score from their age-matched UT^{Cln6nclf} counterparts (UT^{Cln6nclf} mean = 4.833), suggesting that, by 9 months of age, gemfibrozil and/or CBD small molecule therapy fails to protect male Cln6^{nclf} mice from the diseased Cln6^{nclf} ataxic phenotype.

In females, however, gemfibrozil-only treated mice (Gemfib^{PBS}) demonstrated a significantly improved (lower) mean composite score (**Figure 3.8.Bi-ii**; Gemfib^{PBS} mean = 1.0) at 6 months of age compared to their age- and sex-matched UT^{Cln6nclf} counterparts (UT^{Cln6nclf} mean = 3.0; ** $p = .0099$; **Appendix B.25**). This score was even (non-significantly) lower than the mean score of 6 month female WT mice (WT mean = 2.071). No other female drug-only treatment group demonstrated a significant difference in mean composite score at 6 months of age compared to either UT^{Cln6nclf} or WT mice. At 9 months of age, female Gemfib^{PBS} treated Cln6^{nclf} mice continued to do well – with the mean Gemfib^{PBS} composite score remaining statistically indistinguishable from age- and sex-matched WT (**Figure 3.8.Bi-ii**; WT mean =

2.407; Gemfib^{PBS} mean = 3.933; p = .075; **Appendix B.25**). It should be noted, however, that the mean composite score of the Gemfib^{PBS} treated mice was also not significantly different from the 9 month UT^{Cln6nclf} mean composite ataxia score (UT^{Cln6nclf} mean =5.0; p = .3215; **Appendix B.25**). In comparison, female mice treated with CBD-only (CBD^{PBS}) or a combination of gemfibrozil and CBD (Combo^{PBS}) both performed significantly worse than age- and sex-matched WT counterparts at 9 months (**Figure 3.8.Bi-ii**; CBD^{PBS} mean = 4.583; ** p = .0071; Combo^{PBS} mean = 5.375; ***p = .0001 ; **Appendix B.25**) and were statistically indistinguishable from female UT^{Cln6nclf} mice at that time point. In fact, the mean composite score for Combo^{PBS} female mice was higher (non-significantly) than that of UT^{Cln6nclf} at 9 months.

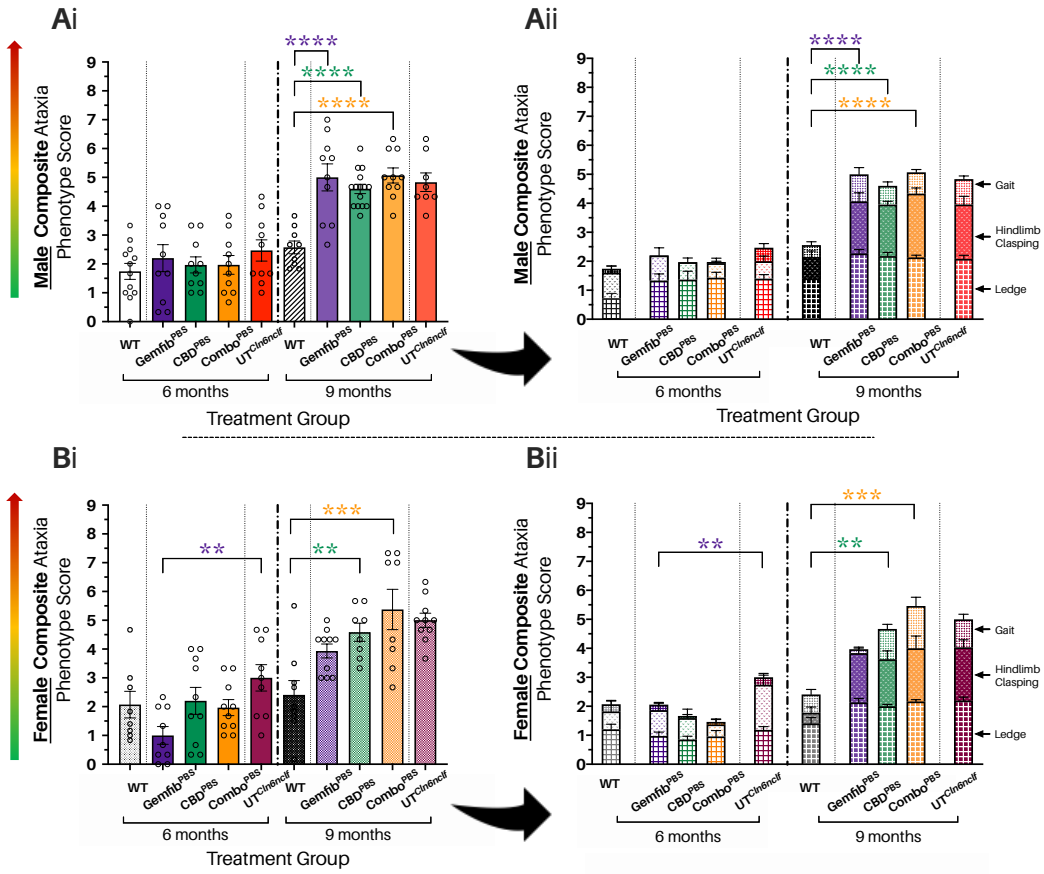

Figure 3.8 | Small molecule therapy in PBS-treated Cln6^{nclf} mice: composite ataxia scores. *CBD (CBD^{PBS}) and combination small molecule therapy (Combo^{PBS}), without gene therapy, fail to protect male and female mice from the diseased Cln6^{nclf} composite ataxia phenotype by 9 months of age. Gemfib^{PBS}, however, appears to protect female Cln6^{nclf} mice against the diseased Cln6^{nclf} composite ataxia phenotype at both 6 and 9 months of age.* Mean composite ataxia phenotype scores (0 to 9) were calculated using averaged ataxia test individual scores (ledge, hindlimb clasping and gait) for male (**Ai-ii**) and female (**Bi-ii**) Cln6^{nclf} mice treated with one of three drug regimens: gemfibrozil (Gemfib^{PBS}), CBD (CBD^{PBS}) or a combination of gemfibrozil and CBD (Combo^{PBS}), and their UT^{Cln6nclf} and wildtype (WT) C57Bl/6 counterparts across two different time points: 6 months (left) and 9 months (right). Different mice were tested at each time point (between-subjects study design). A low score (close to 0) indicates an absence of the ataxic phenotype as measured by the composite scoring system, while higher scores, closer to 9, indicate increasing levels of ataxic behaviour (coloured arrow on the left). The overall mean composite scores illustrated in **Ai** and **Bi** are further broken down into the average ledge (bottom segment), hindlimb clasping (middle segment) and gait (top segment) scores in segmented bar graphs (Aii and Bii). Individual, averaged composite scores are shown as clear circles in Ai and Bi, error bars = ± SEM. Analyses were conducted via 1-way ANOVAs and subsequent Tukey's multiple comparison post-hoc tests (**Appendices B.24-25**). n(per group per time point) = 8-15**.** **Ai-ii.** Histogram presenting the mean composite ataxia scores of male mice at 6 (left) and 9 (right) months of age. No significant differences were observed between the mean composite ataxia scores of any of the male drug treated Cln6^{nclf} groups and their UT^{Cln6nclf} or WT counterparts at 6 months of age; (left; **Appendix B.24**). At 9 months of age, however, Gemfib^{PBS}, CBD^{PBS} and Combo^{PBS} male mice all performed worse (higher score) than the WT control (WT mean = 2.574; Gemfib^{PBS} mean = 5.0; CBD^{PBS} mean = 4.6; Combo^{PBS} mean = 5.067; **** $p \leq 0.0001$; Appendix B.24). **Bi-ii**. Histogram presenting the mean composite ataxia scores of female mice at 6 (left) and 9 (right) months of age. Female Cln6^{nclf} mice treated only with gemfibrozil (Gemfib^{PBS}) performed better (significantly lower composite ataxia score) than UT^{Cln6nclf} mice at 6 months of age (UT^{Cln6nclf} mean = 3.00; Gemfib^{PBS} mean = 1.0; ** p = .0099; **Appendix B.25**). There was no significant difference in the composite scores of CBD^{PBS} or Combo^{PBS} female mice and their UT^{Cln6nclf} and WT counterpoints at 6 months. At 9 months (left), female CBD^{PBS} mice and Combo^{PBS} mice performed significantly worse than WT controls (WT mean = 2.407; CBD^{PBS} mean = 4.583; Combo^{PBS} mean = 5.375; ** p = .0071; *** $p \leq .0001$; **Appendix B.25**).

3.2.2.b Ledge test

Gemfibrozil, CBD and a combination of gemfibrozil and CBD, without gene therapy, failed to protect Cln6^{nclf} mice from the Cln6^{nclf} diseased ledge ataxia phenotype by 9 months of age (**Figure 3.9A** and **Figure 3.9B**).

For males, a 1-way ANOVA (**Appendix B.26**) indicated that there were no significant differences between Gemfib^{PBS}, CBD^{PBS}, Combo^{PBS} and WT in mean ledge scores at 6 months, but by 9 months all three drug-only treatment groups demonstrated a significantly higher (worse) score than WT (**Figure 3.9A**; WT mean = 1.407; Gemfib^{PBS} mean = 2.267; *** p = .0002 ; CBD^{PBS} mean = 2.178; *** p = .0003 ; Combo^{PBS} mean = 2.133; **p = .0023). No significant difference between the male drug-treated groups and their age-matched UT^{Cln6nclf} counterparts was observed at this time point, indicating the small molecule therapies did little to alleviate or protect against the Cln6^{nclf} ledge phenotype established in **section 3.1.2b**.

This result was mirrored by female mice (**Figure 3.9B**), where all three drug-only groups also ended up performing comparably to sex-matched UT^{Cln6nclf} mice by 9 months of age and demonstrating mean scores that differed significantly from healthy WT controls (WT mean = 1.407; Gemfib^{PBS} mean = 2.133; ** p = .0023; CBD^{PBS} mean = 2.00; * p = .0278; Combo^{PBS} = 2.167; ** p = .0026; **Appendix B.27**).

3.2.2.c Hindlimb clasping test

Mice treated with gemfibrozil, CBD or a combination of the two drugs, without gene therapy, had their muscle function and control assessed via the hindlimb clasping test. Different mice were measured at each time point, making this assay between-subjets in design. Data are mean hindlimb clasping scores ± SEM.

In male mice (**Figure 3.9C**), the first significant difference in hindlimb clasping scores was observed at 9 months, with all three drug treatment groups ($Gemfib^{PBS}$, CBD^{PBS} and $Combo^{PBS}$) retracting their limbs to the abdomen more often and more consistently than age and sex-matched WT controls, which was reflected in significantly higher hindlimb clasping scores (1-way ANOVA, WT mean = 0.7407; $Gemfib^{PBS}$ mean = 1.800; * p = .0107 ; CBD^{PBS} mean = 0.7407; ** p = .0056; $Combo^{PBS}$ mean = 2.200; *** p = .0002; **Appendix B.28**).

Female mice (**Figure 3.9.D**) recapitulated the trend demonstrated by males, with no significant differences in mean hindlimb score observed until the 9 month time point. Here, female $Gemfib^{PBS}$, CBD^{PBS} and $Combo^{PBS}$ treated mice all demonstrated significantly higher (worse) hindlimb clasping scores than their sex- and age-matched WT controls, but were statistically indistinguishable from $UT^{Cln6nclf}$ (WT mean = 0.3704; $Gemfib^{PBS}$ mean = 1.700; ** p = .0077; CBD^{PBS} mean = 1.625; * p = .0217; $Combo^{PBS}$ mean = 1.833; ** p = .0052; **Appendix B.29**).

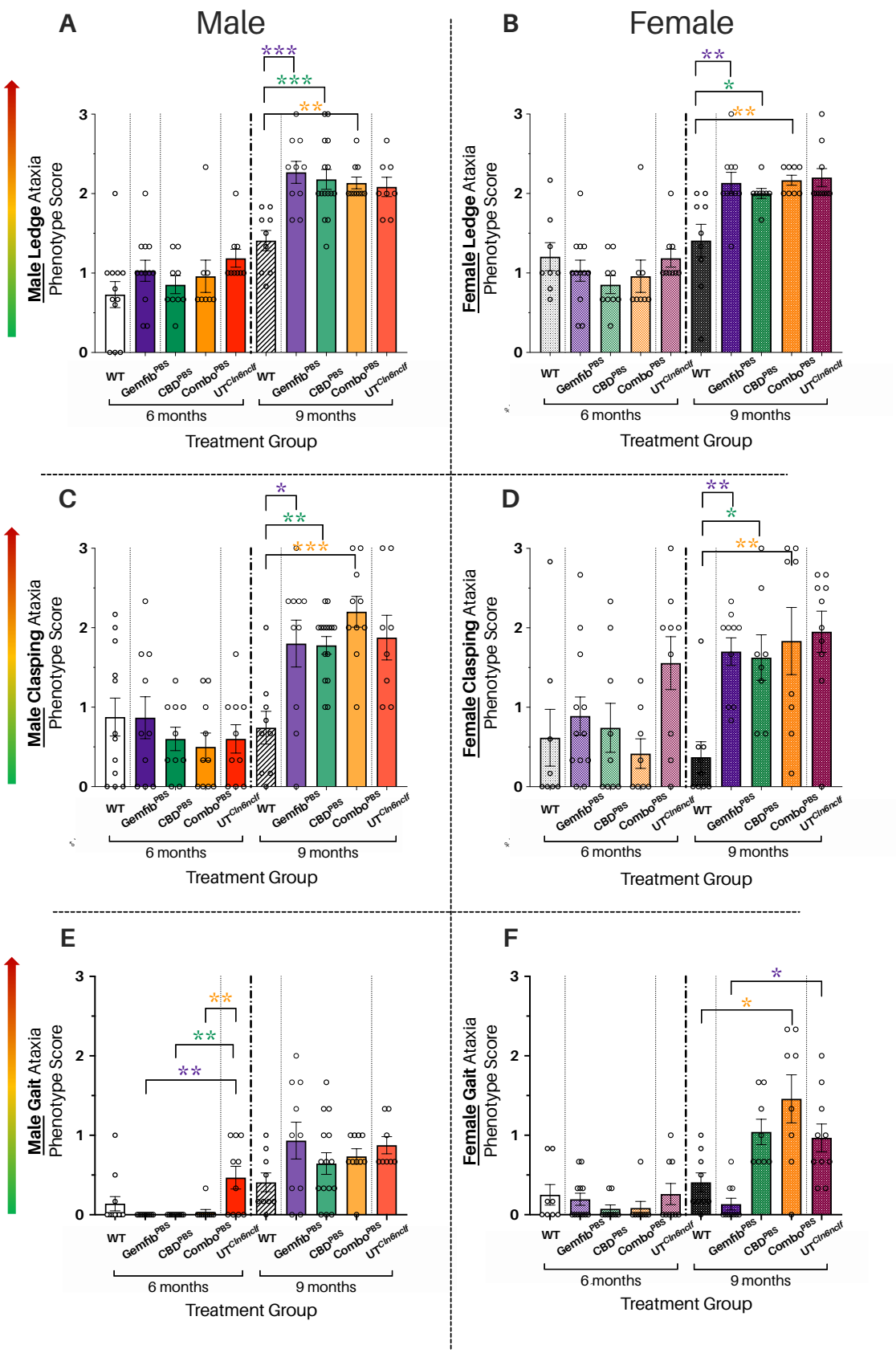
A
Male
B
Female
Male Ledge Ataxia Phenotype Score
Female Ledge Ataxia Phenotype Score
C
D
Male Clasping Ataxia Phenotype Score
Female Clasping Ataxia Phenotype Score
E
F
Male Gait Ataxia Phenotype Score
Female Gait Ataxia Phenotype Score
WT
GemfibPBS
CBDPBS
ComboPBS
UTCln6ncl
6 months
9 months
Treatment Group

⇐ Figure 3.9 | Small molecule therapy in PBS-treated Cln6^{nclf} mice: ataxia phenotyping scores (opposite page). *Small molecule therapy, when administered without gene therapy, does not appear to protect Cln6^{nclf} mice against the untreated Cln6^{nclf} (UT^{Cln6nclf}) ledge and hindlimb clasping ataxia phenotypes. The mean gait test scores of all three drug-treated experimental groups, however, were not significantly different from those of healthy wildtype (WT) scores at 9 months for both sexes.* Ataxia scoring criteria and methodology can be found in **Chapter 2**, adapted from *Guyenet et al. 2010*. Different mice were assessed at each time point, making the experiment between-subjects in design. For each assay, a mouse could be assigned a score between 0 and 3, with 0 indicating a complete absence of the ataxic phenotype and 3 indicating a completely penetrant ataxic phenotype (coloured arrows on the left). Data are presented as mean scores, with error bars representing ± SEM. Individual (averaged) mouse scores are presented as clear circles. All analyses were conducted using 1-way ANOVAs (**Appendices B.26-27**), followed by Tukey's multiple comparisons post-hoc tests. **A.** Histogram presenting mean male ledge scores for 6 months (left; darker coloured bars) and 9 months (right; lighter coloured bars) of age. No significant difference in ledge score was detected between the male drug treated Cln6^{nclf} groups (Gemfib^{PBS}, purple; CBD^{PBS}, green; Combo^{PBS}, orange) and their UT^{Cln6nclf} (red) and WT (C57Bl/6, white) counterparts at 6 months of age. At 9 months, however, significant differences in ledge scores are observed between all three of the drug treated groups and WT (WT mean = 1.407; Gemfib^{PBS} mean = 2.267; *** p = .0002; CBD^{PBS} mean = 2.178; *** p = .0003; Combo^{PBS} mean = 2.133; ** p = .0023; **Appendix B.26**), with all three drug groups performing significantly worse (higher scores; coloured arrow on the left) than WT. n(per group per time point) = 8-10. **B.** Histogram presenting mean female ledge scores for 6 months (left; lighter patterned bars) and 9 months (right; darker patterned bars). No significant difference was observed between the mean ledge scores of any of the drug treated female groups and WT control or *UT^{Cln6nclf}* at 6 months. All three drug groups (Gemfib^{PBS}, CBD^{PBS} and Combo^{PBS}), however, had significantly worse ledge scores than WT at 9 months of age (WT mean = 1.407; Gemfib^{PBS} mean = 2.133; ** p = .0023; CBD^{PBS} mean = 2.00; * p = .0278; Combo^{PBS} = 2.167; ** p = .0026; **Appendix B.27**). No significant differences were found between the 9-month drug-only treated groups and their UT^{Cln6nclf} counterparts. n(per group per time point) = 8-12 **C.** Histogram presenting mean male hindlimb clasping scores for 6 (left; darker coloured bars) and 9 months (right; lighter coloured bars). No significant difference between the mean hindlimb clasping scores of drug-only treated groups and their age- and sex-matched WT and UT^{Cln6nclf} counterparts was detected at 6 months. All three male drug-only groups (Gemfib^{PBS}, CBD^{PBS} and Combo^{PBS}) performed significantly worse (higher mean scores) than WT at 9 months of age (WT mean = 0.7407; Gemfib^{PBS} mean = 1.800; * p = .0107 ; CBD^{PBS} mean = 0.7407; ** p = .0056; Combo^{PBS} mean = 2.200; *** p = .0002; **Appendix B.28**), but their scores were not significantly different from UT^{Cln6nclf} counterparts. n(per group per time point) = 8-15. **D.** Histogram presenting mean female hindlimb clasping scores for 6 (left, lighter patterned bars) and 9 months (right; darker patterned bars). No significant difference between the mean hindlimb clasping scores of drug-only treated groups and their age- and sex-matched WT and UT^{Cln6nclf} counterparts was detected at 6 months. All three female drug-only groups (Gemfib^{PBS}, CBD^{PBS} and Combo^{PBS}) performed significantly worse (higher mean scores) than WT at 9 months of age (WT mean = 0.3704; Gemfib^{PBS} mean = 1.700; ** p = .0077; CBD^{PBS} mean = 1.625; * p = .0217; Combo^{PBS} mean = 1.833; ** p = .0052; **Appendix B.29**), but their scores were not significantly different from UT^{Cln6nclf} counterparts. n(per group per time point) = 8-12. **E.** Histogram presenting mean male gait scores for 6 (left, darker coloured bars) and 9 months (right; lighter coloured bars). At 6 months, all three drug-only treated groups produce mean gait scores significantly better (lower) than their UT^{Cln6nclf} counterparts (UT^{Cln6nclf} mean = 0.4667; Gemfib^{PBS} mean = 0.0; ** p = .0012; CBD^{PBS} mean = 0.0; ** p = .0012; Combo^{PBS} mean = 0.033; ** p = .0031; **Appendix B.30**). At 9 months, however, none of the male drug-only Cln6^{nclf} show significant differences in mean gait score from either the healthy WT control or their UT^{Cln6nclf} counterparts. n(per group per time point) = 10-12. **F.** Histogram presenting mean female gait scores for 6 (left, lighter patterned bars) and 9 months (right; darker patterned bars). At 6 months of age, no significant differences in mean scores could be detected between any of the experimental groups. At 9 months, however, gemfibrozil-only treated female mice (Gemfib^{PBS}) performed significantly better (lower mean score) than their age-matched UT^{Cln6nclf} counterparts (UT^{Cln6nclf} mean = 0.9667; Gemfib^{PBS} mean = 0.1333; * p = .0123) while mice treated with a combination of gemfibrozil and CBD performed significantly worse (higher mean score) than WT controls (WT mean = 0.6296; Combo^{PBS} mean =1.458 ; * p = .0261; **Appendix B.31**). n(per group per time point) = 8-12.

3.2.2.d Gait test

Motor co-ordination and control, as determined by a low score in the gait test, was assessed in Cln6^{nclf} mice treated with gemfibrozil, CBD or a combination of the two drugs, without gene therapy (**Figures 3.9.E** and **3.9.F**). Different mice were assessed at each time point (6 and 9 months), making the assay between subjects in design. Data are mean gait ataxia scores ± SEM.

Unlike the ledge and hindlimb clasping tests, which illustrated a clear trend of motor skill degeneration over time, the gait test results were more varied. Male drug-only groups, for instance, actually demonstrated significantly better (lower) gait scores than UT^{Cln6nclf} mice at 6 months (UT^{Cln6nclf} mean = 0.4667; Gemfib^{PBS} mean = 0.0; ** p = .0012; CBD^{PBS} mean = 0.0; ** p = .0012; Combo^{PBS} mean = 0.033; ** p = .0031; **Appendix B.30).** Why this is the case is unclear, but could either be an indication of early-acting efficacy from the drug treatments or, perhaps more likely, could be to do with the more subjective nature of gait assessment versus ledge or hindlimb (ledge and hindlimb criteria are more clearly divided into scores of 0, 1, 2 and 3). Either way, drug only males did well at 6 months and while their scores did increase by 9 months, they remained statistically indistinguishable from WT controls (**Appendix B.30**).

Female drug-treated mice, however, demonstrated a more linear trend – with no significant differences in mean gait score present for any experimental group at 6 months, similar to the ledge and hindlimb tests. At 9 months Combo^{PBS} females had, on average, a significantly more ataxic gait phenotype than their age- and sex-matched WT controls, indicating that this treatment does not protect female Cln6^{nclf} mice from the UT^{Cln6nclf} gait phenotype (WT mean = 0.6296; Combo^{PBS} mean =1.458 ; * p = .0261; **Appendix B.31**).

Gem^{PBS} females, however, demonstrated significantly better (lower) gait scores than UT^{Cln6nclf} mice at 9 months of age (UT^{Cln6nclf} mean = 0.9667; Gemfib^{PBS} mean = 0.1333; * p = .0123), perhaps indicative of a sex-based difference in response to the drug, since male mice of the same age and treated with the same drug did not demonstrate a significantly better gait score than male UT^{Cln6nclf}.

3.2.3 Small molecule therapy in PBS-treated Cln6^{nclf} mice: ***survival and weight***

The survival curves (and median survival) of gemfibrozil, CBD and combination treated Cln6^{nclf} mice were compared to WT and UT^{Cln6nclf} controls. Mice would be euthanised once they reached one of the three humane end-points stipulated by the Animal Ethics Committee (AEC; see **Chapter 2** for details). Data are presented here up until 14 months – even though the trial continued on until past the 16 month time point for some mice – due to the time limits of a MSc. Survival data are presented as percentage of the original cohort n, with curve comparisons between sex-matched Cln6^{nclf} and WT conducted via separate log-rank (Mantel-Cox) tests for each sex (**Appendices B.32-43**).

The median survival of male WT mice was undefined at 14 months, meaning that there had not been enough 'unplanned' deaths to determine a median survival. This meant that all the drug treated groups, in comparison, had significantly shorter survival curves – with Gemfib^{PBS} treated male mice having a median survival of 12.5 months, CBD^{PBS} male mice having a median survival of 12.9 months and Combo^{PBS} male mice having a median survival of 12.6 months (**Figure 3.10. A**; WT median survival aka 'ms' = undefined at 14 months; Gemfib^{PBS} ms = 12.5 months; **** $p \leq .0001$; CBD^{PBS} ms = 12.9 months; **** $p \leq .0001$ Combo^{PBS} ms = 12.6; * p = .0478; **Appendices B.32 - 37**). A dramatic drop off in population numbers around 12 months resulted in the Combo^{PBS} median survival being significantly shorter than UT^{Cln6nclf} mice as well, all Combo^{PBS} mice met a human endpoint before 14 months of age.

Female survival demonstrated a similar trend (**Figure 3.10.B**). All drug-only treatment groups had significantly shorter lifespans that WT controls (WT ms = undefined at 14 months; Gemfib^{PBS} ms = 12.9 months; CBD^{PBS} ms = 12.97 months; Combo^{PBS} ms = 12 months; **** $p \leq$ .0001; **Appendices B.38-40**), suggesting a failure to protect against the characteristically shortened lifespan phenotype of Cln6^{nclf} mice.

Weights were also kept, as a measure of overall health, and body weight was recorded weekly (in grams). Average weights for each experimental group are presented in monthly increments, as it gives a clearer overview of weight progression throughout the lifespan. Simple linear regression was conducted to determine the overall rate of weight gain and/or loss over the first 14 months of the trial, but no differences were detected in the slopes of any experimental group. A series of 1-way ANOVA analyses were also used to compare the mean weights of gemfibrozil treated, CBD treated and combination treated Cln6^{nclf} mice to age-matched WT and UT^{Cln6nclf} controls at 6, 9 and 12 months – which felt appropriate, as this is when behavioural assessments were carried out. Data are presented here as average weights, in grams ± SEM (**Figure 3.11**).

Male Cln6^{nclf} mice, both treated and untreated, gain weight until approximately 7 months of age – at which point all weights began to plateau or decline. CBD^{PBS} males demonstrate significantly lower weights than WT as early as 9 months (**Figure 3.11.E**; CBD^{PBS} mean weight = 35.4 g; WT mean weight = 38.87 g; ** p = .0067; **Appendix B.44**), and by 12 months all three male drug-only groups are significantly lighter than WT controls (WT mean weight = 37.76 g; Gemfib^{PBS} mean weight = 33.93 g; ** p = .0055; CBD^{PBS} mean weight = 30.83 g; p ≤ .0001; Combo^{PBS} mean weight = 33.86 ; p = .0273; **Appendix B.44**).

Female drug-treated Cln6^{nclf} mice, on the other hand, are significantly lighter than WT at 6 months (1-way ANOVA; WT mean weight = 27.04 g; Gemfib^{PBS} mean weight = 24.67 g;

**** p = ≤ .0001; CBD^{PBS} mean weight = 25.29 g; * p = .0137; $Combo^{PBS}$ mean weight = 25.04; ** p = .0016; **Appendix B.45**), and at 9 months (WT mean weight = 28.90 g; $Gemfib^{PBS}$ mean weight = 25.79 g; *** p = .0007; CBD^{PBS} mean weight = 26.44 g; * p = .0307; $Combo^{PBS}$ mean weight = 25.85 g; p = .0017; **Appendix B.45**). Unexpectedly, however, CBD^{PBS} and $Combo^{PBS}$ treated females appear to either gain weight or experience a reduction in overall rate of weight loss by 12 months, as their average weights are no longer statistically indistinguishable from WT. Only $Gemfib^{PBS}$ treated females remain significantly lighter than WT at 12 months of age ($Gemfib^{PBS}$ mean weight = 23.66 g; WT mean weight = 30.23 g; *** p = .0001; **Appendix B.45**).

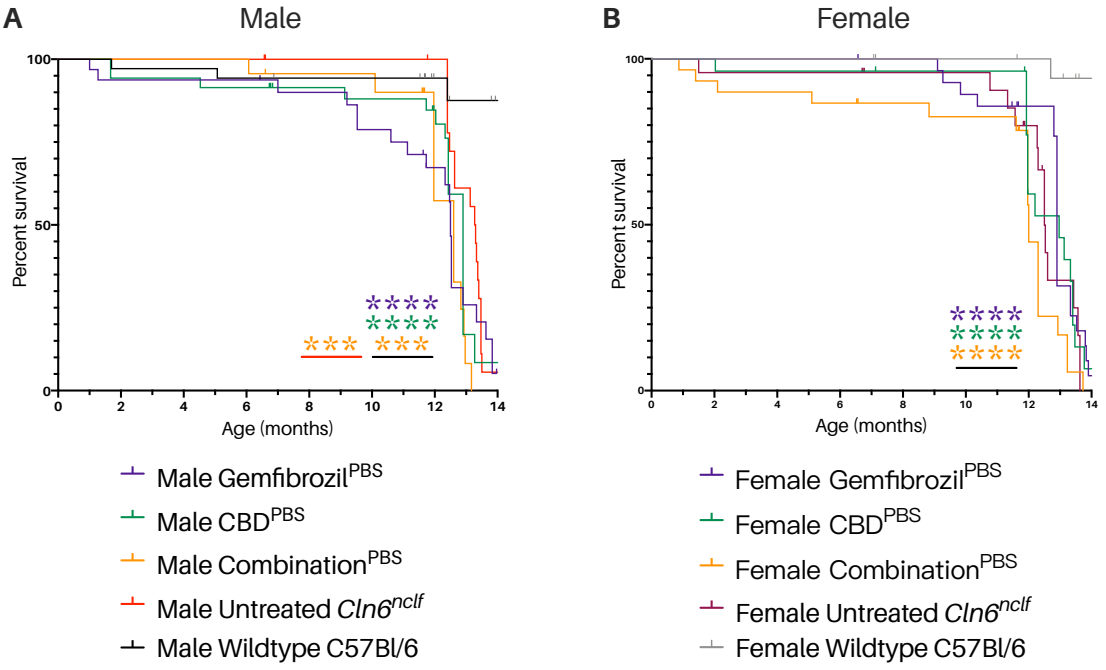

Figure 3.10 | Small molecule therapy in PBS-treated Cln6^{nclf} mice: survival curves *Small molecule therapy alone, without gene therapy, fails to rescue Cln6^{nclf} mice from characteristically shortened lifespans.* Kaplan-Meier survival plots (%) comparing the survival curves of wildtype (WT; C57Bl/6; male = black lines; female = grey lines) and UT^{Cln6nclf} mice (male = red lines; female = maroon lines) to Cln6^{nclf} mice treated with one of three small molecule therapy regimens (gemfibrozil = purple lines; CBD = green lines; Combo = orange lines), without gene therapy (1x PBS at P0-2). All survival curve comparisons were conducted using a log rank (Mantel-Cox) test in GraphPad Prism 8 (**Appendices B.32-43**). **A.** Male survival curves (%) from birth to 14 months of age. All three male small molecule treatment groups (Gemfib^{PBS}, CBD^{PBS} and Combo^{PBS}) had significantly shorter survival curves than WT control (WT median survival aka 'ms' = undefined at 14 months; Gemfib^{PBS} ms = 12.5 months; **** $p \leq .0001$; CBD^{PBS} ms = 12.9 months; **** $p \leq .0001$ Combo^{PBS} ms = 12.6; * $p = .0478$; **Appendices B.32 - 37**) with all Combo^{PBS} mice reaching a humane end-point before 14 months of age. This meant that not only was the average survival age of male Combo^{PBS} mice significantly younger than WT, it was also significantly younger than UT^{Cln6nclf} counterparts (UT^{Cln6nclf} ms =; *** $p = .0005$; **Appendices B.34 and B.37**). Starting n = 23-35. **B.** Female survival curves (%) from birth to 14 months of age. All three female small molecule treatment groups (Gemfib^{PBS}, CBD^{PBS} and Combo^{PBS}) had, on average, significantly shorter lives than WT controls (WT ms = undefined at 14 months; Gemfib^{PBS} ms = 12.9 months; CBD^{PBS} ms = 12.97 months; Combo^{PBS} ms = 12 months; **** $p \leq .0001$; **Appendices B.38-40**). Their average lifespan was statistically indistinguishable from their UT^{Cln6nclf} counterparts (Cln6^{nclf} ms = 12.5 months; **Appendices B.41-43**). n = 24-34.

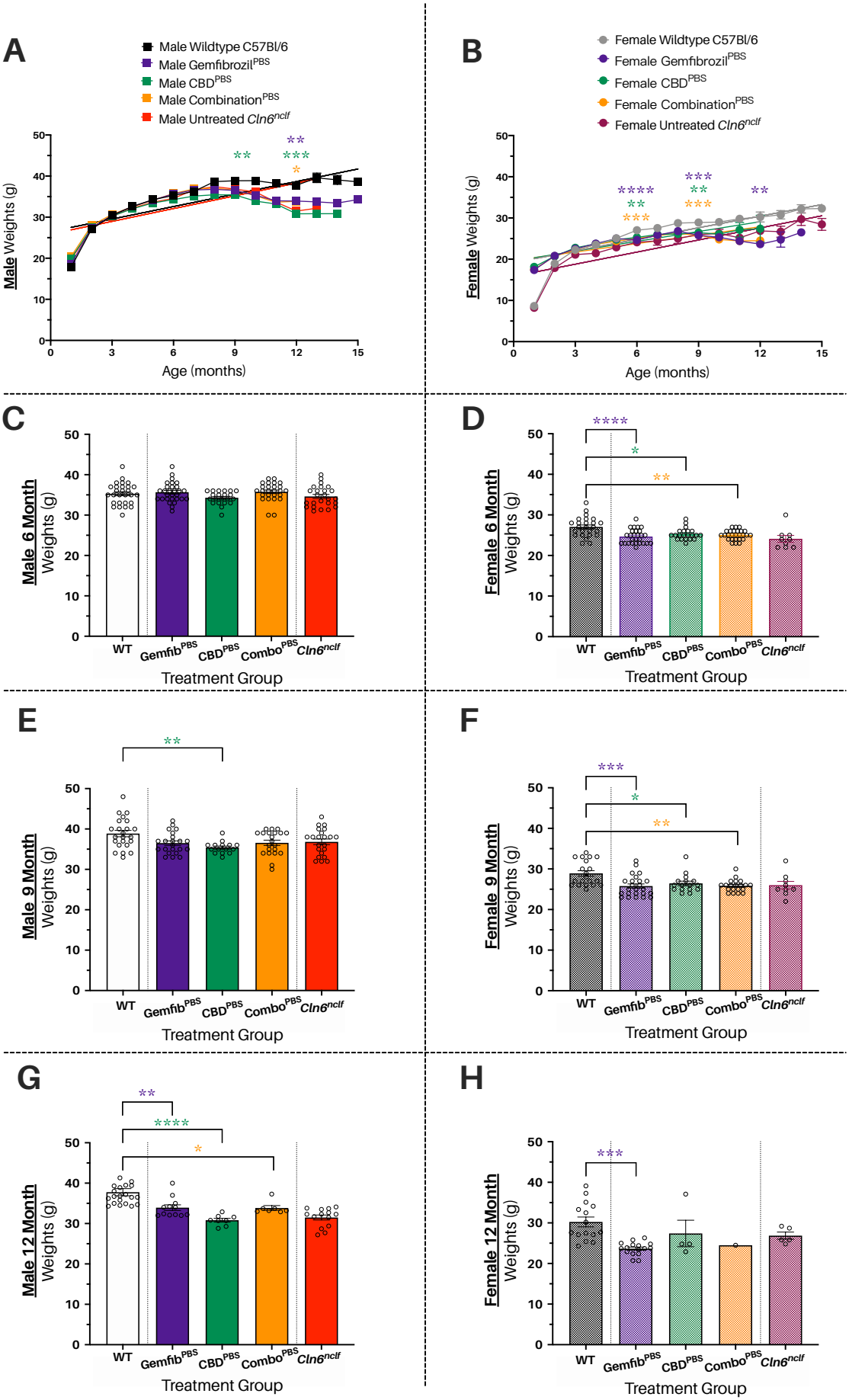
A
Male Wildtype C57Bl/6
Male Gemfibrozil PBS
Male CBD PBS
Male Combination PBS
Male Untreated Cln6 nclf
Male Weights (g)
Age (months)
B
Female Wildtype C57Bl/6
Female Gemfibrozil PBS
Female CBD PBS
Female Combination PBS
Female Untreated Cln6 nclf
Female Weights (g)
Age (months)
C
Male 6 Month Weights (g)
WT
Gemfib PBS
CBD PBS
Combo PBS
Cln6 nclf
Treatment Group
D
Female 6 Month Weights (g)
Treatment Group
E
Male 9 Month Weights (g)
Treatment Group
F
Female 9 Month Weights (g)
Treatment Group
G
Male 12 Month Weights (g)
Treatment Group
H
Female 12 Month Weights (g)
Treatment Group

⇐ **Figure 3.11 | Small molecule therapy in PBS-treated Cln6^{nclf} mice: weights (previous page)**. *Small molecule therapy appears to have sexually dimorphic effects on the weights of Cln6^{nclf} mice during the first fifteen months of life.* Mice were weighed weekly from weaning (~28 days) to determine drug dosage and as a measure of general health. Weights are shown here from weaning to 15 months due to the time constraints of an MSc (weights continued to be tracked for the entire duration of the trial). Data are presented as average weights, in grams error bars = ± SEM. Analyses conducted via 1-way ANOVA with Tukey's multiple comparisons post-hoc tests where applicable. **A.** Average male weights, in grams, over 14 months (line graph). 1-way ANOVA analyses conducted between male WT (black squares and lines), Gemfib^{PBS} (purple squares and lines), CBD^{PBS} (green squares and lines), Combo^{PBS} (orange squares and lines) and UT^{Cln6nclf} (red squares and lines) mice at 6, 9 and 12 months of age. n = 24-29. **B.** Average female weights, in grams, over 15 months (line graph). 1-way ANOVA analyses conducted between female WT (grey circles and lines), Gemfib^{PBS} (purple circles and lines), CBD^{PBS} (green circles and lines), Combo^{PBS} (orange circles and lines) and UT^{Cln6nclf} (maroon circles and lines) mice at 6, 9 and 12 months of age. n = 22-33. **C.** Histogram of average weights (in grams) of male WT (white bar), Gemfib^{PBS} (purple bar), CBD^{PBS} (green bar), Combo^{PBS} (orange bar) and UT^{Cln6nclf} (red bar) mice at 6 months of age. Clear circles represent individual mouse weights at 6 months. No significant differences in average weight were found between any of the experimental groups at this time point (1-way ANOVA; **Appendix B.44**). There were no significant differences between the three drug treated groups and UT^{Cln6nclf} weights. n = 21-29. **D.** Histogram of average weights (In grams) of female WT (black patterned bar), Gemfib^{PBS} (purple patterned bar), CBD^{PBS} (green patterned bar), Combo^{PBS} (orange patterned bar) and UT^{Cln6nclf} (maroon patterned bar) mice at 6 months of age. Clear circles represent individual mouse weights at 6 months. All three drug treated experimental groups were significantly lighter, on average, than age-matched WT (1-way ANOVA; WT mean weight = 27.04 g; Gemfib^{PBS} mean weight = 24.67 g; **** p = ≤ .0001; CBD^{PBS} mean weight = 25.29 g; * p = .0137; Combo PBS mean weight = 25.04; ** p = .0016;**Appendix B.45**). There were no significant differences between the three drug treated groups and UT^{Cln6nclf} weights. n = 21-27. **E.** Histogram of male average weights at 9 months of age. CBD^{PBS} (green bar; mean weight = 35.40 g) treated Cln6^{nclf} mice demonstrate significantly lower weights, on average, than WT (WT mean weight = 38.87 g; ** p = .0067; **Appendix B.44**) at 9 months. There were no significant differences between the three drug treated groups and UT^{Cln6nclf} weights. n = 15-22. **F.** Histogram of female average weights at 9 months of age. All three drug treatment groups remain significantly lighter, on average, than WT at 9 months (WT mean weight = 28.90 g; Gemfib^{PBS} mean weight = 25.79 g; *** p = .0007; CBD^{PBS} mean weight = 26.44 g; * p = .0307; Combo^{PBS} mean weight = 25.85 g; p = .0017; **Appendix B.45**). There were no significant differences between the three drug treated groups and UT^{Cln6nclf} weights. n = 9-24. **G.** Histogram of average male weights, in grams, at 12 months of age. All three drug treated groups demonstrated lighter weights, on average, than WT at 12 months (WT mean weight = 37.76 g; Gemfib^{PBS} mean weight = 33.93 g; ** p = .0055; CBD^{PBS} mean weight = 30.83 g; p = ≤.0001; Combo^{PBS} mean weight = 33.86 ; p = .0273; **Appendix B.44**). There were no significant differences between the three drug treated groups and UT^{Cln6nclf} weights. n = 8-21. **H.** Histogram of average female weights, in grams, at 12 months of age. Female mice dosed only with gemfibrozil (Gemfib^{PBS}; purple patterned bar) showed significantly lower weights (Gemfib^{PBS} mean weight = 23.66 g) , on average, than WT (WT mean weight = 30.23 g; *** p = .0001; **Appendix B.45**). No other drug treatment group showed significant differences in weight from either WT or Cln6^{nclf} and Gemfib^{PBS} weights were not statistically different from UT^{Cln6nclf} either. n = 4-16.

3.2.4 Small molecule therapy in PBS-treated Cln6^{nclf} mice: ***sex differences***

Sex differences are particularly pertinent to small molecule therapy development due to the well-documented differences in male and female responses to different drugs. Women have been determined to be more susceptible to the toxicity of many compounds, with an increased risk of negative side-effects such as inflammation, nausea and alopecia (Nicolson et al., 2010; Soldin et al., 2011). Here, the mean behaviour scores, survival data and weights of

male and female Cln6^{nclf} mice treated with either gemfibrozil (Gemfib^{PBS}), CBD (CBD^{PBS}) or a combination of the two drugs (Combo^{PBS}) are compared across the lifespan in an effort to determine any sex-based differences in response to the small molecule therapies.

3.2.4.a Rotarod sex differences

Simple linear regression analyses revealed that there was no significant difference in the overall rate of motor skill decline, as determined by the rotarod, between male and female animals for any of the drug only groups (**Figures 3.12.A-C**). Despite this, however, a series of unpaired student t-test analyses at 6, 9 and 12 months detected several significant differences in mean rotarod score beween the sexes (**Figures 3.12.E-G**).

Male and female Gemfib^{PBS} mice have comparable mean rotarod scores at 6 months of age (**Figure 3.12.E**). By 9 months, however, females are staying on the rotarod significantly longer than males (**Figure 3.12.F;** 9 month Gemfib^{PBS} male mean rotarod score = 111.4 seconds; 9 month Gemfib^{PBS} female mean rotarod score = 160.7 seconds; ***p* =.0041; **Appendix B.46**) and maintain this significant difference at 12 months (**Figure 3.12.G;** 12 month male Gemfib^{PBS} mean rotarod score = 61.14 seconds; 12 month female Gemfib^{PBS} mean rotarod score = 83.88 seconds; * *p* = .0312; **Appendix B.48**).

Female CBD^{PBS} mice presented with a significantly higher rotarod score than their age-matched male counterparts at 6 months (**Figure 3.12.E;** 6 month male CBD^{PBS} mean rotarod score = 177 seconds; 6 month female CBD^{PBS} mean rotarod score = 230.1 seconds; * *p* = .0193; **Appendix B.47**). While females continued to have a higher rotarod score at 9 months, the difference between scores was no longer significant and by 12 months it appears negligible (**Figures 3.12.F** and **G;** 12 month male CBD^{PBS} mean rotarod score = 70.33 seconds; 12 month female CBD^{PBS} mean rotarod score = 76.33 seconds; **Appendix B.48**).

Male and female Combo^{PBS} treated mice have statistically similar scores until 12 months of age (**Figures 3.12.E-G**). At 12 months, however, females perform significantly better than age-matched male counterparts (**Figure 3.12.G;** 12 month male Combo^{PBS} mean rotarod score = 64.60 seconds; 12 month Combo^{PBS} female mean rotarod score = 100.4 seconds; ** p = .0048; **Appendix B.48**).

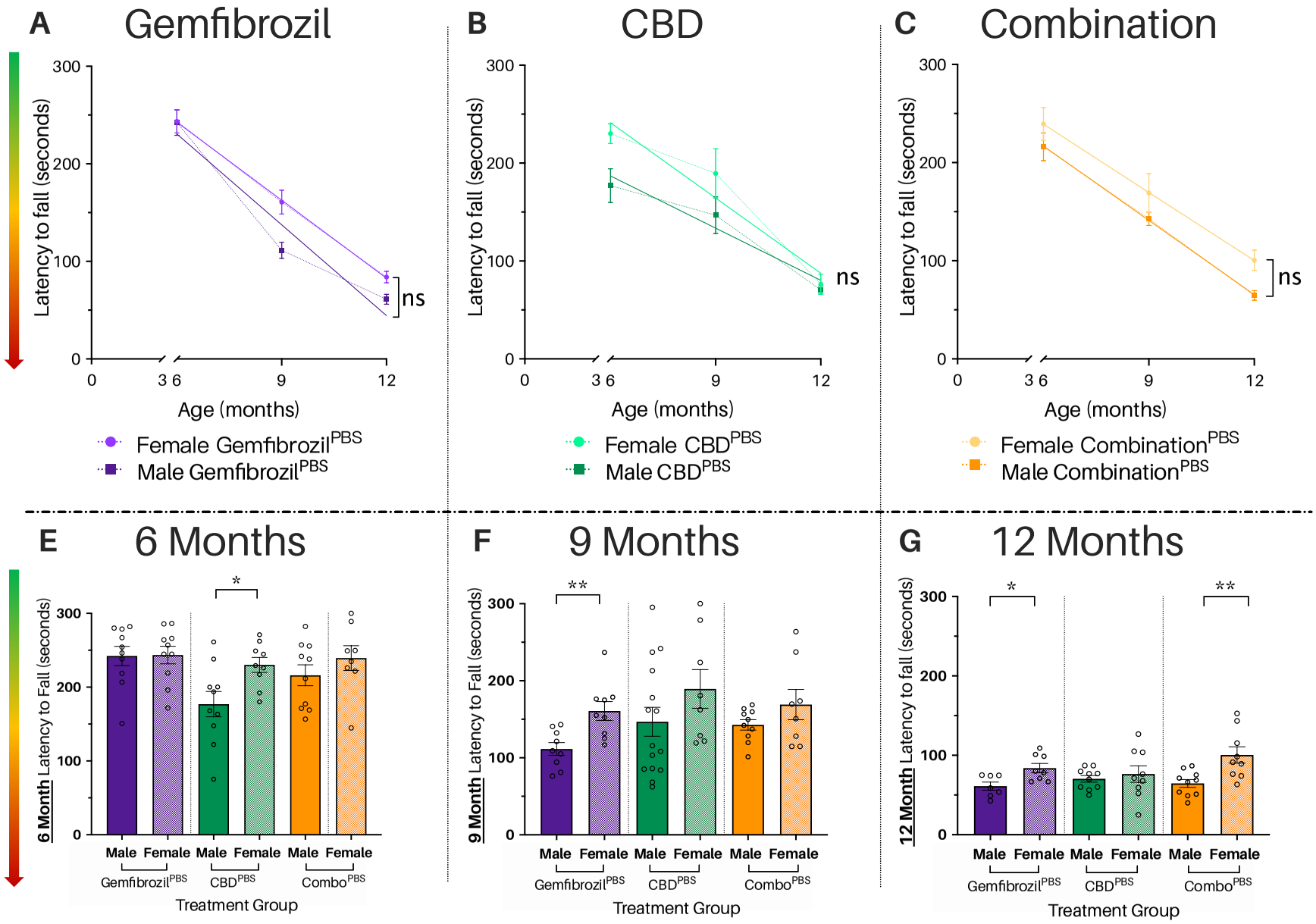
A
Gemfibrozil
B
CBD
C
Combination
Latency to fall (seconds)
300
200
100
0
0
3 6
9
12
Age (months)
ns
Female Gemfibrozil^PBS
Male Gemfibrozil^PBS
Female CBD^PBS
Male CBD^PBS
Female Combination^PBS
Male Combination^PBS
E
6 Months
F
9 Months
G
12 Months
6 Month Latency to Fall (seconds)
9 Month Latency to Fall (seconds)
12 Month Latency to fall (seconds)
*
**
Male
Female
Gemfibrozil^PBS
CBD^PBS
Combo^PBS
Treatment Group

⇐ **Figure 3.12 | Small molecule therapy in PBS-treated Cln6^{nclf} mice: sex differences in rotarod scores (previous page).** *Male and female mice treated with either gemfibrozil (Gemfib^{PBS}), cannabidiol (CBD^{PBS}) or a combination of gemfibrozil and cannabidiol (Combo^{PBS}) demonstrated similar overall rates of decline in rotarod performance over time but showed statistically significant differences in average rotarod score at the three different time points measured.* **A-C.** Line graphs presenting data as mean rotarod scores measured in latency to fall (seconds) for male (squares) and female (circle) Cln6^{nclf} mice, treated either with gemfibrozil (**A**; male = dark purple; female = light purple), CBD (**B**; male = dark green; female = light green) or a combination of the two (**C**; male = orange; female = yellow). Error bars represent ± SEM. Dotted lines indicate the expected trajectory of rotarod scores between measured time points (6, 9 and 12 months). Linear regression lines are represented by solid coloured lines (simple linear regression; **Appendices B.44-45**). **E-G**. Histograms presenting data as mean rotarod scores measured in latency to fall (seconds) for male (dark, solid coloured bars) and female (light, patterned bars) Cln6^{nclf} mice treated with either gemfibrozil (purple), CBD (green) or a combination of the two drugs (orange) at 6 (**E**), 9 (**F)** and 12 (**G**) months of age. Error bars represent ± SEM. Individual mouse scores are represented by clear circles. Analyses between male and female mean scores for each treatment group (Gemfib^{PBS}, CBD^{PBS} and Combo^{PBS}) were conducted using unpaired student t-tests (**Appendices B.46-48**). **A.** Both male (dark purple squares and lines) and female (light purple lines and circles) Gemfib^{PBS} treated Cln6^{nclf} mice demonstrated a decline in ability to stay on the rotarod from 6 to 12 months of age (negative slope gradients in line equations for both; **Appendix B.45**). Simple linear regression (solid lines) revealed that there was no significant difference between the overall rate of decline in motor performance between Gemfib^{PBS} treated males and females, though elevation differed significantly (p = .0133; **Appendix B.45**). **B.** Both male (dark green lines and squares) and female (light green lines and circles) CBD^{PBS} treated Cln6^{nclf} mice demonstrated a decline in ability to stay on the rotarod from 6 to 12 months of age (negative slope gradients in line equations for both; **Appendix B.45**). Simple linear regression (solid lines) revealed that there was no significant difference between the overall rate of decline in motor performance between CBD^{PBS} treated males and females, though elevation differed significantly (p = .0319; **Appendix B.45**).. **C.** Both male (orange lines and squares) and female (yellow lines and circles) Combo^{PBS} treated Cln6^{nclf} mice demonstrated a decline in ability to stay on the rotarod between 6 and 9 months of age (negative slope gradients in line equations for both; **Appendix B.45**). Simple linear regression (solid lines) revealed that there was no significant difference in the overall rate of decline in motor performance between Combo^{PBS} treated males and females, though elevation differed significantly (*p* = .0057; **Appendix B.45**). **E.** Histogram presenting average rotarod scores (latency to fall in seconds) of male (dark coloured bars) and female (light coloured bars) drug-only treated Cln6^{nclf} mice at 6 months of age. No significant difference was found between male and female Gemfib^{PBS} scores, and no significant difference was found between male and female Combo^{PBS} scores. There was, however, a significant difference between the scores of male and female CBD^{PBS} treated mice, with females, on average, scoring higher than their male counterparts (male mean score = 177 seconds; female mean score = 230.1 seconds; * *p* = .0193; **Appendix B.47**). n(per group) = 8-10. **F.** Histogram presenting average rotarod scores (latency to fall in seconds) of male (dark coloured bars) and female (light coloured bars) drug-only treated Cln6^{nclf} mice at 9 months of age. No significant differences between male and female average scores were found for either CBD^{PBS} treated or Combo^{PBS} treated mice at this age. There was, however, a significant difference in average score between male Gemfib^{PBS} (mean = 111.4 seconds) and Gemfib^{PBS} female (mean = 160.7 seconds) scores (***p* =.0041; **Appendix B.46**). n(per group) = 8-15.. **G.** Histogram presenting average rotarod scores (latency to fall in seconds) of male (dark coloured bars) and female (light coloured bars) drug-only treated Cln6^{nclf} mice at 12 moths of age. No significant difference was found between male and female CBD^{PBS} scores. There were, however, significant differences found between male and female scores for both Gemfib^{PBS} (male mean score = 61.14 seconds; female mean score = 83.88 seconds; * *p* = .0312) and Combo^{PBS} treated mice (male mean score = 64.60 seconds; female mean score = 100.4 seconds; ** *p* = .0048; **Appendix B.48**), with females performing better (higher score) in both cases.. n(per group) = 7-10.

3.2.4.b Composite ataxia sex differences

Male and female Cln6^{nclf} mice demonstrated no significant difference in mean composite ataxia scores (**Figure 3.13**) at 6 or 9 months of age (unpaired t-tests; **Appendices B.49-51**), regardless of drug treatment.

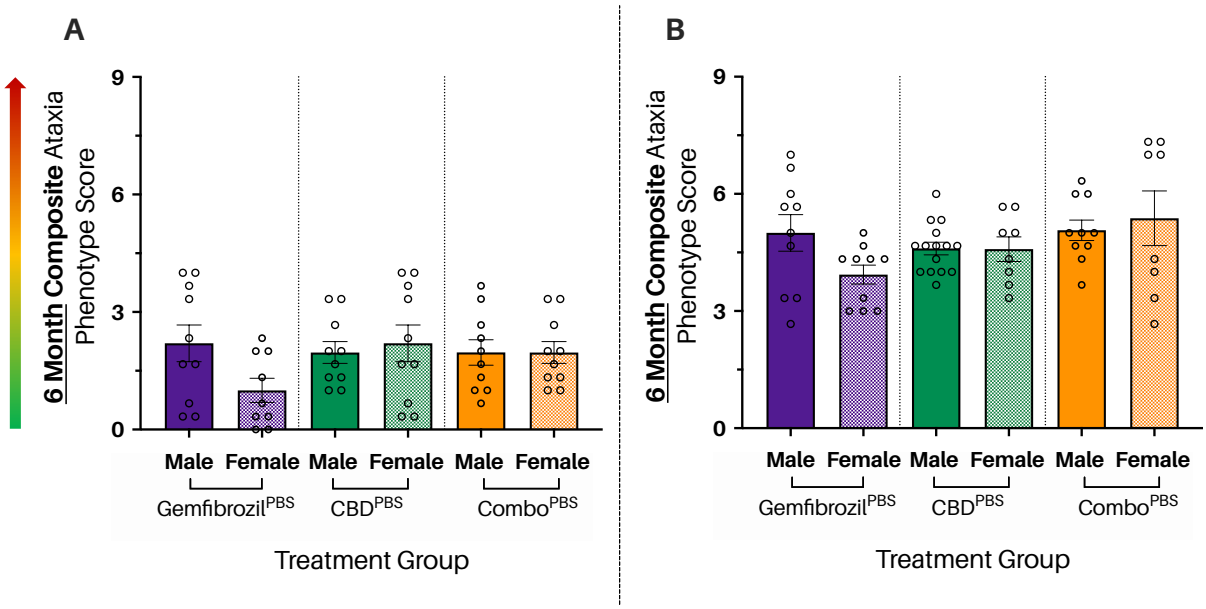

Figure 3.13 | Small molecule therapy in PBS-treated Cln6^{nclf} mice: sex differences in composite ataxia scores. *Male and female mice treated with either gemfibrozil (Gemfib^{PBS}), cannabidiol (CBD^{PBS}) or a combination of gemfibrozil and cannabidiol (Combo^{PBS}) demonstrated statistically similar composite ataxia scores (0-9) at both 6 and 9 months of age.* Histograms demonstrating mean composite ataxia scores for male (dark coloured bars) and female (light, patterned bars) Cln6^{nclf} mice treated with either gemfibrozil (gemfibrozil^{PBS}; purple), cannabidiol (CBD; CBD^{PBS}; green) or a combination of gemfibrozil and CBD (Combo^{PBS}), without gene therapy, at 6 (**A**) and 9 (**B**) months of age. Different mice were tested at each time point (between-subjects study design). A low score (close to 0) indicates an absence of the ataxic phenotype as measured by the composite scoring system, while higher score (close to 9) indicate increasing levels of ataxic behaviour (arrow on the left). Individual mouse composite scores are shown as clear circles and error bars = ± SEM. Analyses between male and female mean scores for each treatment group at each time point were conducted via unpaired student t-tests (**Appendices B.49-51**). n(per group per time point) = 8-15. **A.** No significant differences were observed between mean male and female composite ataxia scores at 6 months, regardless of drug treatment regimen (unpaired student t-tests; **Appendices B.49-51**), though Gemfib^{PBS} males appear to have (non-significantly) higher (worse) mean scores than age-matched Gemfib^{PBS} females. **B.** No significant differences were observed between mean male and female composite ataxia scores at 9 months, regardless of drug treatment regimen (unpaired student t-tests; **Appendices B.49-51**).

3.2.4.c Ledge ataxia sex differences

Male and female Cln6^{nclf} mice demonstrated no significant difference in mean ledge ataxia scores (**Figure 3.14.A** and **B**) at 6 or 9 months of age (unpaired t-tests; **Appendices B.52-60**), regardless of drug treatment.

3.2.4.d Hindlimb clasping ataxia sex differences

Male and female Cln6^{nclf} mice demonstrated no significant difference in mean hindlimb clasping ataxia scores (**Figure 3.14.C** and **D**) at 6 or 9 months of age (unpaired t-tests; **Appendices B.52-60**), regardless of drug treatment.

3.2.4.e Gait ataxia sex differences

Gemfib^{PBS} female mice performed significantly worse (higher ataxia score) in the gait ataxia test than age-matched male counterparts at 6 months of age (female Gemfib^{PBS} mean gait ataxia score = 0.1944; male Gemfib^{PBS} mean gait ataxia score = 0.0; *p = .312 ; **Appendix B.58)**, though this difference was reversed at 9 months – with Gemfib^{PBS} males performing significantly worse (mean score of 0.9333) than females (mean score of 0.1333; ** p = .0041; **Appendix B.58**).

Neither CBD^{PBS} or Combo^{PBS} treated Cln6^{nclf} demonstrated any sex differences in mean gait ataxia score at 6 months of age. At 9 months, however, female Combo^{PBS} mice demonstrated significantly more ataxic gaits, on average, than their age-matched male counterparts (12 month Combo^{PBS} male mean gait ataxia score = 0.7333; 12 month Combo^{PBS} female mean gait ataxia score = 1.458; * p = 0.233; **Appendix B.60**). The gait scores of M/F CBD^{PBS} mice at 9 months remained statistically indistinguishable.

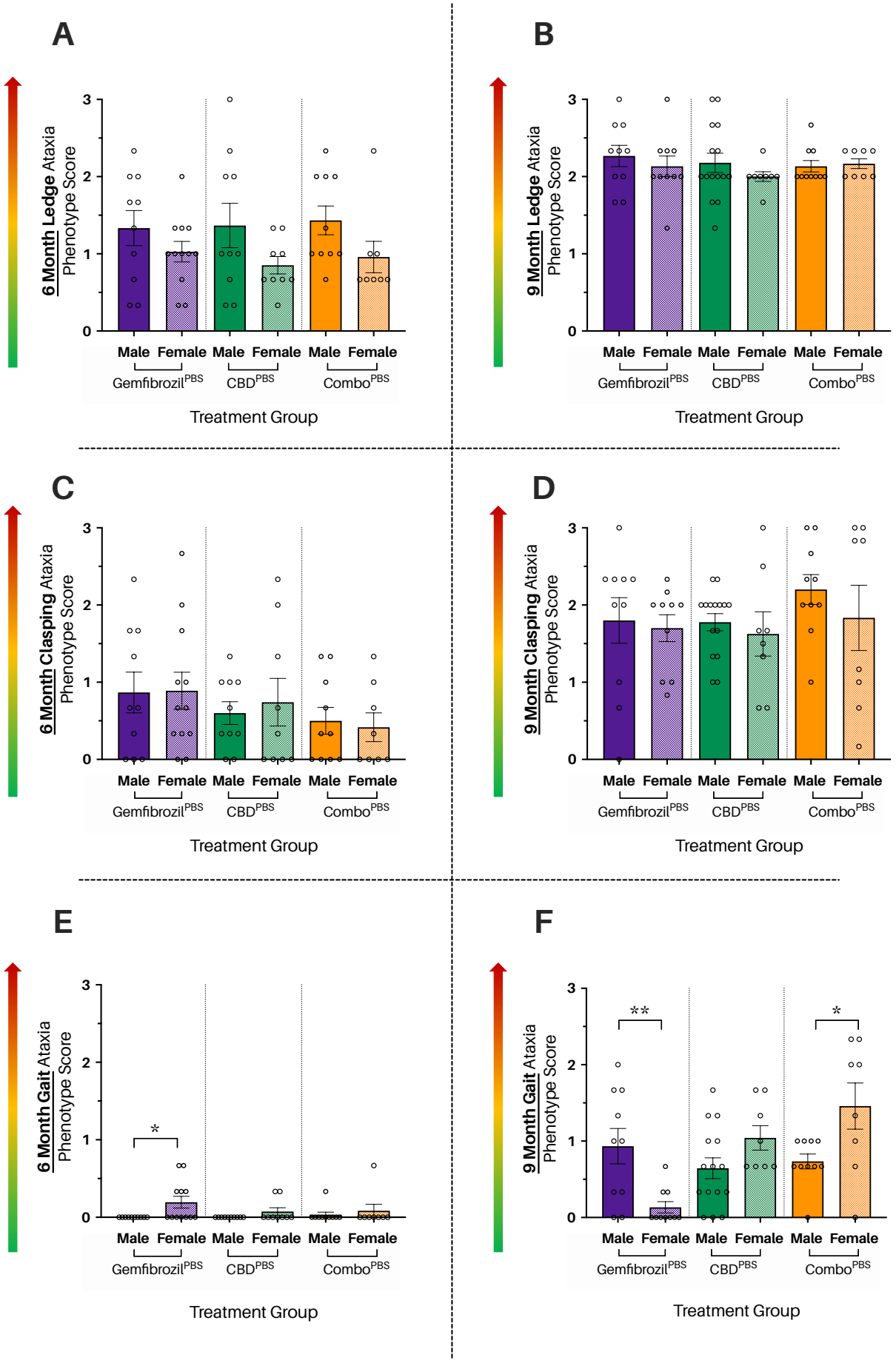
A
6 Month Ledge Ataxia Phenotype Score
B
9 Month Ledge Ataxia Phenotype Score
C
6 Month Clasping Ataxia Phenotype Score
D
9 Month Clasping Ataxia Phenotype Score
E
6 Month Gait Ataxia Phenotype Score
F
9 Month Gait Ataxia Phenotype Score
0
1
2
3
Male Female Male Female Male Female
GemfibrozilPBS CBDPBS ComboPBS
Treatment Group
*
**
*

⇐ **Figure 3.14 | Small molecule therapy in PBS-treated Cln6^{nclf} mice: sex differences in ataxia phenotyping scores (previous page)**. *Male and female Cln6^{nclf} mice treated with either gemfibrozil (Gemfib^{PBS}), cannabidiol (CBD^{PBS}) or a combination of gemfibrozil and cannabidiol (Combo^{PBS}) demonstrated statistically similar ledge and hindlimb clasping ataxia scores at both 6 and 9 months of age, while mean gait ataxia scores presented with several statistically significant sex differences at both time points.* Mice underwent three trials of a sequence three different ataxia assays – the ledge test, the hindlimb clasping test and the gait test (adapted from *Guyenet et al., 2010*) – in order to determine the presence or absence of an ataxic phenotype at 6 and 9 months of age. Different mice were assessed at each time point, making the experiment between-subjects in design. For each assay, a mouse could be assigned a score between 0 and 3, with 0 indicating a complete absence of the ataxic phenotype and 3 indicating a completely penetrant ataxic phenotype (coloured arrows on the left). All data (**A-F**) are presented as the mean of averaged (3 trials; scored from 0-3) individual mouse scores, with clear circles representing the individual averaged scores. Error bars = ± SEM. All analyses between male and female mean ataxia scores were conducted using unpaired student t-tests (**Appendices B.52 - 60**). **A** and **B.** Histograms of mean ledge test scores at 6 (A) and 9 (B) months of age for male (dark coloured bars) and female (light coloured, patterned bars) Cln6^{nclf} mice treated with either gemfibrozil (Gemfib^{PBS}; purple), CBD (CBD^{PBS}; green) or a combination of gemfibrozil and CBD (Combo^{PBS}; orange) without gene therapy. No significant differences were observed between the mean ledge scores of treatment- and age-matched male and female Cln6^{nclf} mice, regardless of drug treatment regimen. **C** and **D.** Histograms of mean ledge hindlimb clasping scores at 6 (**C**) and 9 (**D**) months of age for male (dark coloured bars) and female (light coloured, patterned bars) Cln6^{nclf} mice treated with either gemfibrozil (Gemfib^{PBS}; purple), CBD (CBD^{PBS}; green) or a combination of gemfibrozil and CBD (Combo^{PBS}; orange) without gene therapy. No significant differences were observed between the mean hindlimb clasping scores of treatment- and age-matched male and female Cln6^{nclf} mice, regardless of drug treatment regimen. **E** and **F.** Histograms of mean ledge gait clasping scores at 6 (**E**) and 9 (**F**) months of age for male (dark coloured bars) and female (light coloured, patterned bars) Cln6^{nclf} mice treated with either gemfibrozil (Gemfib^{PBS}; purple), CBD (CBD^{PBS}; green) or a combination of gemfibrozil and CBD (Combo^{PBS}; orange) without gene therapy. **E.** Female Gemfib^{PBS} mice demonstrated significantly higher (worse) gait scores than their age-matched Gemfib^{PBS} male counterparts at 6 months of age (Female Gemfib^{PBS} mean = 0.1944; Male Gemfib^{PBS} mean = 0.0; *p = .312 ; **Appendix B.58**). No other significant differences in mean gait scores were observed between treatment-matched male and female Cln6^{nclf} drug-only groups at 6 months. **F.** At 9 months of age Gemfib^{PBS} treated male Cln6^{nclf} mice were performing significantly worse (higher score) than their treatment- and age-matched female counterparts (female Gemfib^{PBS} mean = 0.1333; male Gemfib^{PBS} mean = 0.9333; ** p = .0041; **Appendix B.58**). A significant difference in mean scores was also observed between Combo^{PBS} treated male (mean = 0.7333) and female (mean = 1.458; * p = 0.233; **Appendix B.60**) Cln6^{nclf} mice at this time point. No significant difference was observed between male and female CBD^{PBS} Cln6^{nclf} mice at 9 months.

3.2.4.f Survival and weight gain sex differences

Male and female Cln6^{nclf} mice demonstrated no sex-based differences in survival, regardless of what small molecule therapy they received (**Figure 3.15**; **Appendices B.61-63**).

In terms of weight gain (**Figure 3.16**), however, male Gemfib^{PBS} and male Combo^{PBS} mice gained and lost weight at a greater rate than their female counterparts.

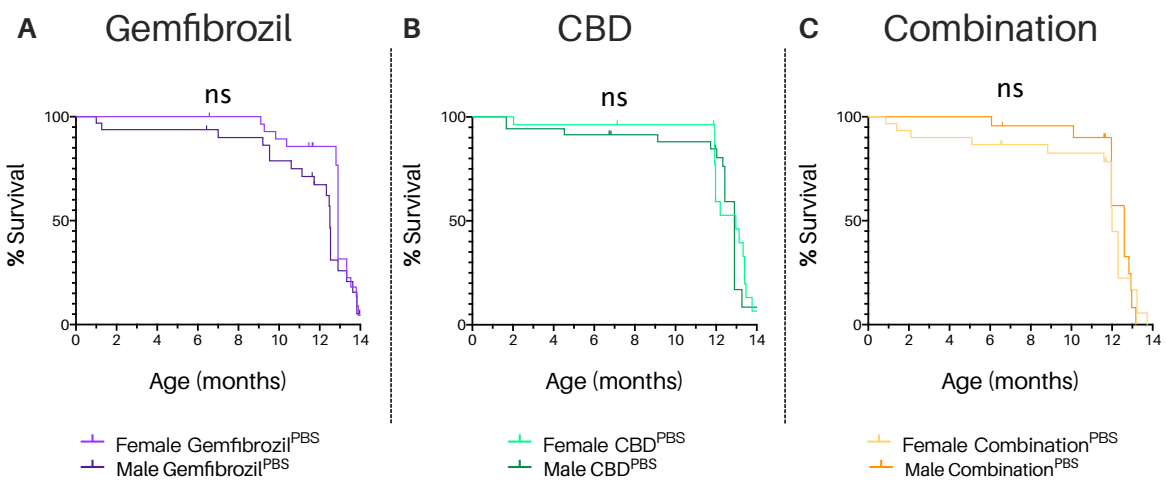

Figure 3.15 | Small molecule therapy in PBS-treated Cln6^{nclf} mice: sex differences in survival. *.Male and female Cln6^{nclf} mice treated with either gemfibrozil (Gemfib^{PBS}), cannabidiol (CBD^{PBS}) or a combination of gemfibrozil and cannabidiol (Combo^{PBS}) had similar survival curves, regardless of drug treatment.* Kaplan-Meier survival plots (%) comparing the survival curves of male and female Gemfib^{PBS} treated Cln6^{nclf} mice (**A**), male and female CBD^{PBS} treated Cln6^{nclf} mice (**B**), and male and female Combo^{PBS} treated Cln6^{nclf} mice (**C**). All survival curve comparisons were conducted using log-rank (Mantel-Cox) tests in GraphPad Prism 8 (**Appendices B.61-63**). **A.** Male (dark purple) and female (light purple) Gemfib^{PBS} treated Cln6^{nclf} survival curves from birth to 14 months of age. No significant difference was found between the median survival of male and female Gemfib^{PBS} treated mice (**Appendix B.61**). Starting n = 32-34. . **B.** Male (dark green) and female (light green) CBD^{PBS} treated Cln6^{nclf} survival curves from birth to 14 months of age. No significant difference was found between the median survival of male and female CBD^{PBS} treated mice (**Appendix B.62**). Starting n = 27-35. **C.** Male (orange) and female (yellow) Combo^{PBS} treated Cln6^{nclf} survival curves from birth to 14 months of age. No significant difference was found between the median survival of male and female Combo^{PBS} treated mice (**Appendix B.63**). Starting n = 23-30.

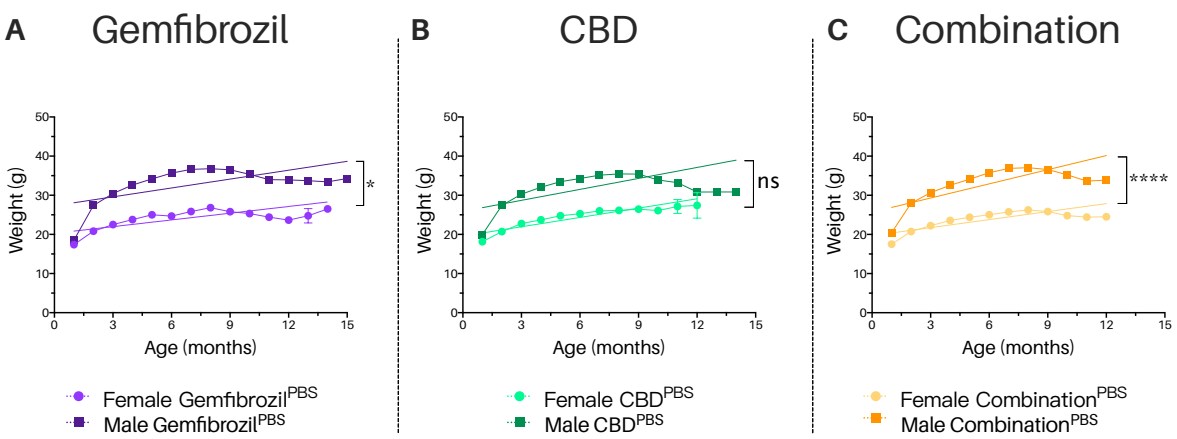

Figure 3.16 | Small molecule therapy in PBS-treated Cln6^{nclf} mice: sex differences in rate of weight gain. *.Male and female Gemfib^{PBS}- and CBD^{PBS}- treated Cln6^{nclf} mice gained weight (g) over their lifespan at similar rates, while the overall rate of weight gain in Combo^{PBS} treated male and female Cln6^{nclf} mice differed significantly.* Mice were weighed weekly from weaning (~28 days) to determine drug dosage and as a measure of general health. Weights are shown here from weaning to 15 months due to the time constraints of an MSc (weights continued to be tracked for the entire duration of the trial). Data are presented as average weights, error bars ± SEM. Comparisons between male and female weights were conducted via simple linear regression only, as there is always an expected dispairty between male and female mice. A. Average male (dark purple) and female (light purple) Gemfib^{PBS} treated Cln6^{nclf} weights (in grams) plotted every month from weaning until 14 months of age (line graph). A significant difference in rate of weight gain was observed between male and female Gemfib^{PBS} mice (simple linear regression; *p = .0219; **Appendix B.67**). B. Average male (dark green) and female (light green) CBD^{PBS} treated Cln6^{nclf} weights (in grams) plotted every month from weaning until 14 months of age (line graph). No significant difference in rate of weight gain was observed between male and female CBD^{PBS} mice (simple linear regression; **Appendix B.67**).

3.2.5 Small molecule therapy in PBS-treated Cln6^{nclf} mice: ***summary***

All Cln6^{nclf} mice, regardless of which small molecule therapy group they were in, demonstrated significantly shorter lifespans and some form of behavioural deficit compared to WT by either 9 months (for ataxia) or 12 months (for rotarod). This was confirmed by the fact that these scores were also statistically indistinguishable from the scores of age- and sex-matched UT^{Cln6nclf} at each time point. The only exceptions were Gemfib^{PBS} treated female mice who did not demonstrate a significantly worse composite ataxia score compared to WT by 9 months of age and CBD^{PBS} treated female mice who did not demonstrate a significantly worse gait ataxia score compared to WT by 9 months either. It can be concluded from this data that, overall, small molecule therapy alone does little to protect Cln6^{nclf} mice from the diseased Cln6^{nclf} phenotype established in **section 3.1**.

Interestingly, however, the use of small molecule therapy, on its own without gene therapy, does seem to delay symptom onset in male Cln6^{nclf} mice. As established in **section 3.1**, male UT^{Cln6nclf} mice started demonstrating significant behavioural deficits compared to WT in the ledge and composite ataxia assays by 6 months of age. These behavioural deficits are absent in all three drug-only groups (**Tables 3.4, 3.7** and **3.10**).

Finally, female Cln6^{nclf} mice appear to demonstrate subtle behavioural improvements when treated with gemfibrozil alone – improvements which are not present in male Cln6^{nclf} mice (**Table 3.5**). Gemfib^{PBS} treated female mice, for instance, not only maintain behavioural scores that are similar to WT in the 6 month composite and 9 month gait ataxia assays, but also demonstrate scores that are significantly better (lower) than age- and sex-matched UT^{Cln6nclf}. Female Gemfib^{PBS} mice also have significantly better rotarod scores than their male Gemfib^{PBS} counterparts at 9 and 12 months of age, indicating a sex-based difference in response to the drug (**Table 3.6**).

Table 3.4 | Small molecule therapy in PBS-treated Cln6^{nclf} mice: summary table of Gemfib^{PBS} males. *Summary table of behavioural score (rotarod and ataxia), survival and weight comparisons carried out between male gemfibrozil (Gemfib^{PBS}) treated Cln6^{nclf} mice and their age- and sex-matched WT and untreated Cln6^{nclf} (UT^{Cln6nclf}) counterparts at 6, 9 and 12 months of age.* All behavioural score and weight comparisons were conducted using 1-way ANOVAs (**Appendices B.22, 24, 26, 28, 30** and **44**), with Tukey's post-hoc multiple comparisons tests where appropriate, while survival curves were compared using log rank (Mantel-Cox) tests (**Appendices B.32** and **35**). nsd = no significant difference; s = significant.

Gemfib^{PBS} Cln6^{nclf} Males				
Behavioural Test	**Comparison Group**	**6 months**	**9 months**	**12 months**
Rotarod	UT^{Cln6nclf}	nsd	nsd	nsd
	WT	nsd	**Worse (s)**	**Worse (s)**
Composite	UT^{Cln6nclf}	nsd	nsd	-
	WT	nsd	**Worse (s)**	-
Ledge	UT^{Cln6nclf}	nsd	nsd	-
	WT	nsd	**Worse (s)**	-
Hindlimb Clasping	UT^{Cln6nclf}	nsd	nsd	-
	WT	nsd	**Worse (s)**	-
Gait	UT^{Cln6nclf}	**Better (s)**	nsd	-
	WT	nsd	nsd	-
Survival	UT^{Cln6nclf}	nsd		
	WT	**Reduced survival (s)**		
Weight	UT^{Cln6nclf}	nsd	nsd	nsd
	WT	nsd	nsd	**Weigh less (s)**

Table 3.5 | Small molecule therapy in PBS-treated Cln6^{nclf} mice: summary table of Gemfib^{PBS} females. *Summary table of behavioural score (rotarod and ataxia), survival and weight comparisons carried out between female gemfibrozil (Gemfib^{PBS}) treated Cln6^{nclf} mice and their age- and sex-matched WT and untreated Cln6^{nclf} (UT^{Cln6nclf}) counterparts at 6, 9 and 12 months of age.* All behavioural score and weight comparisons were conducted using 1-way ANOVAs (**Appendices B.23, 25, 27, 29, 31** and **45**), with Tukey's post-hoc multiple comparisons tests where appropriate, while survival curves were compared using log rank (Mantel-Cox) tests (**Appendix B.38** and **41**). nsd = no significant difference; s = significant.

Gemfib^{PBS} Cln6^{nclf} Females				
Behavioural Test	**Comparison Group**	**6 months**	**9 months**	**12 months**
Rotarod	UT^{Cln6nclf}	nsd	nsd	nsd
	WT	nsd	nsd	**Worse (s)**
Composite	UT^{Cln6nclf}	**Better (s)**	nsd	-
	WT	nsd	nsd	
Ledge	UT^{Cln6nclf}	nsd	nsd	-
	WT	nsd	**Worse (s)**	
Hindlimb Clasping	UT^{Cln6nclf}	nsd	nsd	-
	WT	nsd	**Worse (s)**	
Gait	UT^{Cln6nclf}	nsd	**Better (s)**	-
	WT	nsd	nsd	
Survival	UT^{Cln6nclf}	nsd		
	WT	**Reduced survival (s)**		
Weight	UT^{Cln6nclf}	nsd	nsd	nsd
	WT	**Weigh less (s)**	**Weigh less (s)**	**Weigh less (s)**

Table 3.6 | Small molecule therapy in PBS-treated Cln6^{nclf} mice: summary table of Gemfib^{PBS} males versus Gemfib^{PBS} females. *Summary table of behavioural score (rotarod and ataxia), survival and weight comparisons carried out between male and female gemfibrozil (Gemfib^{PBS}) treated Cln6^{nclf} mice at 6, 9 and 12 months of age.* All behavioural score and weight comparisons were conducted using unpaired student t-tests (**Appendices B44, 46, 49, 55, 58** and **66**), while survival curves were compared using log rank (Mantel-Cox) tests (**Appendix 61**). nsd = no significant difference.

Gemfib^{PBS} Cln6^{nclf} Males vs Females			
Behavioural test	**6 months**	**9 months**	**12 months**
Rotarod	nsd	**Females perform better (s)**	**Females perform better (s)**
Composite	nsd	nsd	-
Ledge	nsd	nsd	-
Hindlimb	nsd	nsd	-
Gait	**Females perform better (s)**	**Males perform better (s)**	-
Survival	nsd		

Table 3.7 | Small molecule therapy in PBS-treated Cln6^{nclf} mice: summary table of CBD^{PBS} males. *Summary table of behavioural score (rotarod and ataxia), survival and weight comparisons carried out between male CBD (CBD^{PBS}) treated Cln6^{nclf} mice and their age- and sex-matched WT and untreated Cln6^{nclf} (UT^{Cln6nclf}) counterparts at 6, 9 and 12 months of age.* All behavioural score and weight comparisons were conducted using 1-way ANOVAs (**Appendices B.22, 24, 26, 28, 30** and **44**), with Tukey's post-hoc multiple comparisons tests where appropriate, while survival curves were compared using log rank (Mantel-Cox) tests (**Appendices B.33** and **36**). nsd = no significant difference; s = significant.

CBD^{PBS} Cln6^{nclf} Males				
Behavioural Test	**Comparison Group**	**6 months**	**9 months**	**12 months**
Rotarod	UT^{Cln6nclf}	nsd	nsd	nsd
	WT	nsd	nsd	**Worse (s)**
Composite	UT^{Cln6nclf}	nsd	nsd	-
	WT	nsd	**Worse (s)**	-
Ledge	UT^{Cln6nclf}	nsd	nsd	-
	WT	nsd	**Worse (s)**	-
Hindlimb Clasping	UT^{Cln6nclf}	nsd	nsd	-
	WT	nsd	**Worse (s)**	-
Gait	UT^{Cln6nclf}	**Better (s)**	nsd	-
	WT	nsd	nsd	-
Survival	UT^{Cln6nclf}	nsd		
	WT	**Reduced survival (s)**		
Weight	UT^{Cln6nclf}	nsd	nsd	nsd
	WT	nsd	**Weigh less (s)**	**Weigh less (s)**

Table 3.8 | Small molecule therapy in PBS-treated Cln6^{nclf} mice: summary table of CBD^{PBS} females. *Summary table of behavioural score (rotarod and ataxia), survival and weight comparisons carried out between female CBD (CBD^{PBS}) treated Cln6^{nclf} mice and their age- and sex-matched WT and untreated Cln6^{nclf} (UT^{Cln6nclf}) counterparts at 6, 9 and 12 months of age.* All behavioural score and weight comparisons were conducted using 1-way ANOVAs (**Appendices B.23, 25, 27, 29, 31** and **45**), with Tukey's post-hoc multiple comparisons tests where appropriate, while survival curves were compared using log rank (Mantel-Cox) tests (**Appendix B.39** and **B.42**). nsd = no significant difference; s = significant.

CBD^{PBS} Cln6^{nclf} Females				
Behavioural Test	**Comparison Group**	**6 months**	**9 months**	**12 months**
Rotarod	UT^{Cln6nclf}	nsd	nsd	nsd
	WT	nsd	nsd	**Worse (s)**
Composite	UT^{Cln6nclf}	nsd	nsd	-
	WT	nsd	**Worse (s)**	
Ledge	UT^{Cln6nclf}	nsd	nsd	-
	WT	nsd	**Worse (s)**	
Hindlimb Clasping	UT^{Cln6nclf}	nsd	nsd	-
	WT	nsd	**Worse (s)**	
Gait	UT^{Cln6nclf}	nsd	nsd	-
	WT	nsd	nsd	
Survival	UT^{Cln6nclf}	nsd		
	WT	**Reduced survival (s)**		
Weight	UT^{Cln6nclf}	nsd	nsd	nsd
	WT	**Weigh less(s)**	**Weigh less(s)**	nsd

Table 3.9 | Small molecule therapy in PBS-treated Cln6^{nclf} mice: summary table of CBD^{PBS} males versus CBD^{PBS} females. *Summary table of behavioural score (rotarod and ataxia), survival and weight comparisons carried out between male and female CBD (CBD^{PBS}) treated Cln6^{nclf} mice at 6, 9 and 12 months of age.* All behavioural score and weight comparisons were conducted using unpaired student t-tests (**Appendices B.44, 47, 50, 53, 56, 59** and **66**), while survival curves were compared using log rank (Mantel-Cox) tests (**Appendix B.62**). nsd = no significant difference.

CBD^{PBS} Cln6^{nclf} Males vs Females			
Behavioural test	**6 months**	**9 months**	**12 months**
Rotarod	**Females perform better (s)**	nsd	nsd
Composite	nsd	nsd	-
Ledge	nsd	nsd	-
Hindlimb	nsd	nsd	-
Gait	nsd	nsd	-
Survival	nsd		

Table 3.10 | Small molecule therapy in PBS-treated Cln6^{nclf} mice: summary table of Combo^{PBS} males. *Summary table of behavioural score (rotarod and ataxia), survival and weight comparisons carried out between male combination drug (Combo^{PBS}) treated Cln6^{nclf} mice and their age- and sex-matched WT and untreated Cln6^{nclf} (UT^{Cln6nclf}) counterparts at 6, 9 and 12 months of age.* All behavioural score and weight comparisons were conducted using 1-way ANOVAs (**Appendices B.22, 24, 26, 28, 30** and **44**), with Tukey's post-hoc multiple comparisons tests where appropriate, while survival curves were compared using log rank (Mantel-Cox) tests (**Appendix B.34** and **37**). nsd = no significant difference; s = significant.

Combo^{PBS} Cln6^{nclf} Males				
Behavioural Test	**Comparison Group**	**6 months**	**9 months**	**12 months**
Rotarod	UT^{Cln6nclf}	nsd	nsd	nsd
	WT	nsd	nsd	**Worse (s)**
Composite	UT^{Cln6nclf}	nsd	nsd	-
	WT	nsd	**Worse (s)**	-
Ledge	UT^{Cln6nclf}	nsd	nsd	-
	WT	nsd	**Worse (s)**	-
Hindlimb Clasping	UT^{Cln6nclf}	nsd	nsd	-
	WT	nsd	**Worse (s)**	-
Gait	UT^{Cln6nclf}	Better (s)	nsd	-
	WT	nsd	nsd	-
Survival	UT^{Cln6nclf}	**Reduced survival (s)**		
	WT	**Reduced survival (s)**		
Weight	UT^{Cln6nclf}	nsd	nsd	nsd
	WT	nsd	nsd	**Weigh less (s)**

Table 3.11 | Small molecule therapy in PBS-treated Cln6^{nclf} mice: summary table of Combo^{PBS} females. *Summary table of behavioural score (rotarod and ataxia), survival and weight comparisons carried out between female combination drug (Combo^{PBS}) treated Cln6^{nclf} mice and their age- and sex-matched WT and untreated Cln6^{nclf} (UT^{Cln6nclf}) counterparts at 6, 9 and 12 months of age.* All behavioural score and weight comparisons were conducted using 1-way ANOVAs (**Appendices B.23, 25, 27, 29, 31** and **45**), with Tukey's post-hoc multiple comparisons tests where appropriate, while survival curves were compared using log rank (Mantel-Cox) tests (**Appendix B.40** and **43**). nsd = no significant difference; s = significant.

Combo^{PBS} Cln6^{nclf} Females				
Behavioural Test	**Comparison Group**	**6 months**	**9 months**	**12 months**
Rotarod	UT^{Cln6nclf}	nsd	nsd	nsd
	WT	nsd	nsd	**Worse (s)**
Composite	UT^{Cln6nclf}	nsd	nsd	-
	WT	nsd	**Worse (s)**	
Ledge	UT^{Cln6nclf}	nsd	nsd	-
	WT	nsd	**Worse (s)**	
Hindlimb Clasping	UT^{Cln6nclf}	nsd	nsd	-
	WT	nsd	**Worse (s)**	
Gait	UT^{Cln6nclf}	nsd	nsd	-
	WT	nsd	**Worse (s)**	
Survival	UT^{Cln6nclf}	nsd		
	WT	**Reduced survival (s)**		
Weight	UT^{Cln6nclf}	nsd	nsd	nsd
	WT	**Weigh less (s)**	**Weigh less (s)**	nsd

Table 3.12 | Small molecule therapy in PBS-treated Cln6^{nclf} mice: summary table of Combo^{PBS} males versus females. *Summary table of behavioural score (rotarod and ataxia), survival and weight comparisons carried out between male and female combination drug (Combo^{PBS}) treated Cln6^{nclf} mice at 6, 9 and 12 months of age*. All behavioural score and weight comparisons were conducted using unpaired student t-tests (**Appendices 50, 53, 56, 59, 62** and **66**), while survival curves were compared using log rank (Mantel-Cox) tests (**Appendix B.65**). nsd = no significant difference.

Combo^{PBS} Cln6^{nclf} Males vs Females			
Behavioural test	**6 months**	**9 months**	**12 months**
Rotarod	nsd	nsd	**Females performed better (s)**
Composite	nsd	nsd	-
Ledge	nsd	nsd	-
Hindlimb	nsd	nsd	-
Gait	nsd	**Females performed better (s)**	-
Survival	nsd		

3.3 A single i.c.v injection of scAAV9.CB.*hCLN6* at P0-2 significantly improves behavioural scores and survival in Cln6^{nclf} mice

AAV2/9-mediated gene transfer of the *CLN6* gene as a potential treatment for CLN6 BD has been investigated in several preclinical studies and is the subject of an ongoing clinical trial (Cain et al., 2019; Holthaus et al., 2019; Poppens et al., 2019; Trial No. NCT02725580, *Clinicaltrials.gov* 2016). However, the use of AAV2/9-mediated gene therapy for CLN6 BD is still very much in its infancy, and lessons from completed gene therapy trials in other metabolic disorders have suggested that gene therapy, as it exists right now, will not offer CLN6 BD patients a complete cure. For that reason, the investigtion, validation and improvement of gene therapy technologies must continue. This thesis aims to do that, primarily by combining gene therapy with several small molecule therapies and determining whether this combination results in improved behavioural outcomes, but also by validating Cln6^{nclf} behavioural results from previous studies that used gene therapy alone. This section contributes to both those aims by examining the behaviour, survival and weights of Cln6^{nclf} mice who received a single, unilateral i.c.v injection of scAAV9.CB.*hCLN6* at P0-2 and were only dosed with strawberry jelly containing a vehicle solution as a control for small molecule therapy. In establishing a 'No Drug^{AAV9}' behavioural phenotype, for male and female Cln6^{nclf} mice, it is possible to not only validate and expand upon previous gene therapy studies, but also allow for later comparisons between a series of combined therapeutic strategies and gene therapy on its own. The true value of a combined therapeutic regimen can't be fully understood without direct comparison to the strategy we are seeking to improve.

*3.3.1 scAAV9.CB.hCLN6 treatment protects against the Cln6^{nclf} phenotype: **rotarod***

While UT^{Cln6nclf} mice began to show a decline in rotarod performance at 12 months of age (s**ection 3.1**), neonatal injection of scAAV9.CB.*hCLN6* appears to prevent this decline in both male and female animals (**Figure 3.17**).

Male No Drug^{AAV9} mice demonstrate statistically indistinguishable mean rotarod scores from their age- and sex-matched WT controls at 6 and 9 months, and demonstrate a significantly higher rotarod score than both WT and UT^{Cln6nclf} mice at 12 months (**Figures 3.17.A** and **C**; No Drug^{AAV9} mean =192.9 seconds; WT mean = 131.5 seconds; ** p = .009 ; UT^{Cln6nclf} mean = 61.14 seconds; **** $p \leq .0001$; **Appendix B.72**).

Female No Drug^{AAV9} mice also exhibited excellent motor co-ordination and endurance across all three time points, and achieved a statistically significant difference in scores from UT^{Cln6nclf} mice by 9 months of age (**Figure 3.7.D**; No Drug^{AAV9} mean score = 257.7 seconds; UT^{Cln6nclf} mean score = 164.3 seconds; ** p = .005 ; **Appendix B.73**). At 12 months of age, female No Drug^{AAV9} mice outperformed both UT^{Cln6nclf} and WT controls (No Drug^{AAV9} mean score = 234.4 seconds; UT^{Cln6nclf} mean score = 71.25 seconds; **** $p \leq .0001$; WT mean score = 170.4 seconds; ** p =.0058; **Appendix B.73).**

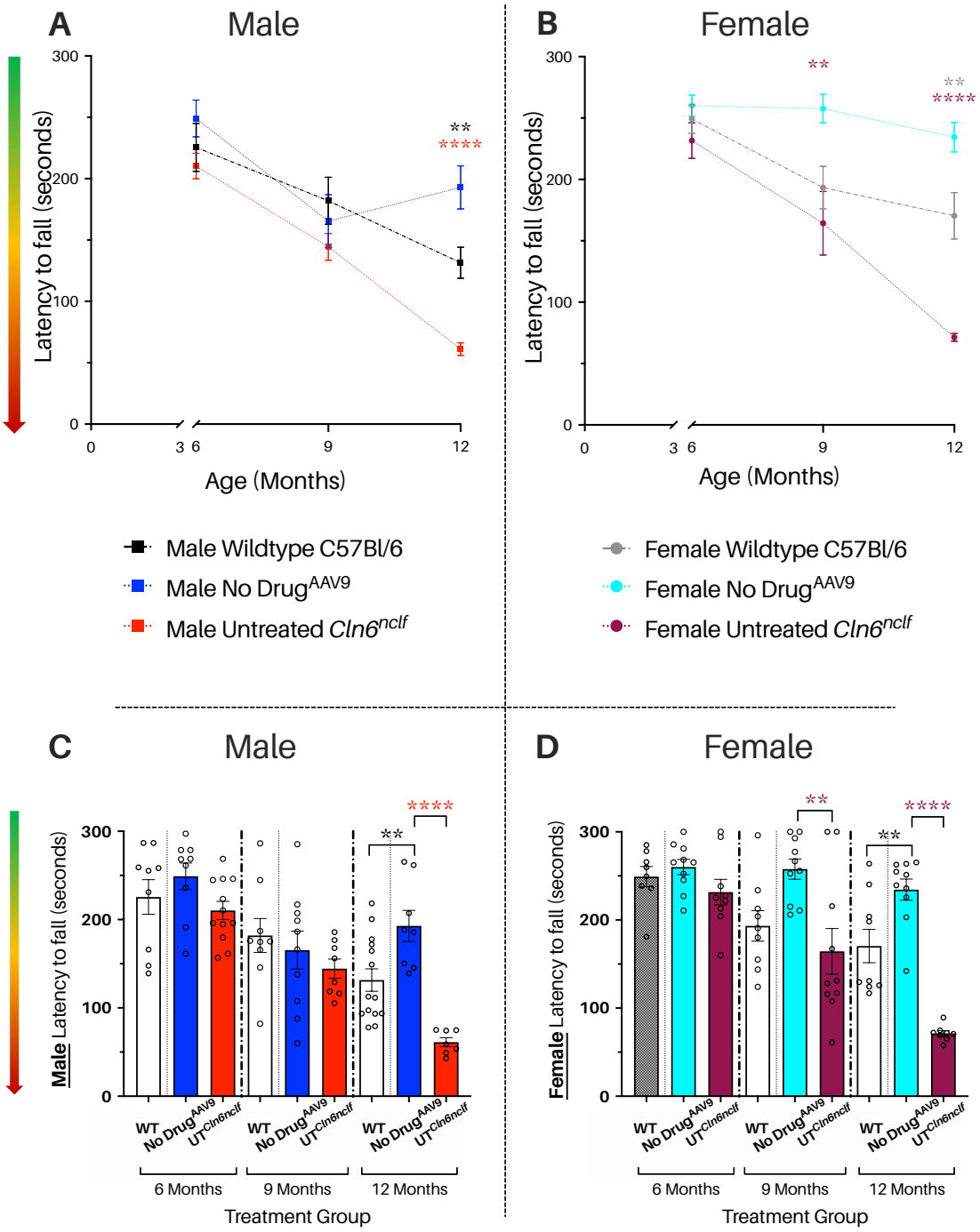
A
Male
B
Female
Latency to fall (seconds)
300
200
100
0
0
3
6
9
12
Age (Months)
**
****
Male Wildtype C57Bl/6
Male No Drug AAV9
Male Untreated Cln6 nclf
Female Wildtype C57Bl/6
Female No Drug AAV9
Female Untreated Cln6 nclf
C
Male
D
Female
Male Latency to fall (seconds)
Female Latency to fall (seconds)
WT
No Drug AAV9
UT Cln6nclf
6 Months
9 Months
12 Months
Treatment Group

⇐ **Figure 3.17 | scAAV9.CB.*hCLN6* treatment protects against the Cln6^{nclf} phenotype: rotarod scores (prevous page).** *A single, neonatal injection of scAAV9.CB.hCLN6 significantly improves Cln6^{nclf} rotarod scores at later stages of disease progression compared to untreated Cln6^{nclf} (UT^{Cln6nclf}) mice.* **A** and **B.** Line graphs presenting mean rotarod scores (latency to fall in seconds) of male (**A**) and female (**B**) WT (C57Bl/6; male = black lines and squares; female = grey lines and circles) gene therapy-treated (No Drug^{AAV9}; male = blue lines and squares; female = light blue lines and circles) and UT^{Cln6nclf} (male = red lines and squares; females = maroon lines and squares) mice across 6, 9 and 12 months of age. Error bars = ± SEM. Dotted lines indicate the expected mean score trajectory for an experimental group between measured time points. A high score (~300) indicates a high level of motor co-ordination as measured by the rotarod, while lower scores correlate to increasing levels of motor dysfunction (coloured arrow on the left). Analyses between groups at each time point were conducted via 1-way ANOVA, with Tukey's post-hoc multiple comparisons tests used when a difference was detected. **C** and **D.** Histograms presenting mean rotarod scores of male (**C**) and female (**D**) WT (C57Bl/6; male = white bars; female = black patterned bars) gene therapy-treated (No Drug^{AAV9}; male = blue bars; female = light blue bars) and UT^{Cln6nclf} (male = red bars; female = maroon bars). Data are presented as mean scores ± SEM. Individual mouse rotarod scores (averaged from 3 trials) are represented by clear circles. All analyses conducted by 1-way ANOVA and Tukey's post-hoc multiple comparisons tests. **A.** and **C.** Line graph (**A**) and histogram (**B**) of male rotarod scores. Male No Drug^{AAV9} mice demonstrate no significant difference in mean rotarod score from their age- and sex-matched WT and UT^{Cln6nclf} counterparts until 12 months of age, at which point the mean No Drug^{AAV9} rotarod score is significantly higher (better) than both WT and UT^{Cln6nclf} (No Drug^{AAV9} mean =192.9 seconds; WT mean = 131.5 seconds; ** p = .009 ; UT^{Cln6nclf} mean = 61.14 seconds; **** $p \leq .0001$; **Appendix B.72**). n(per group per time point) = 8-14. **B** and **D.** Line graph (**B**) and histogram (**D**) of female rotarod scores. Female No Drug^{AAV9} mice demonstrated a significantly better (higher) mean rotarod score than age- and sex-matched UT^{Cln6nclf} mice at 9 months of age (No Drug^{AAV9} mean score = 257.7 seconds; UT^{Cln6nclf} mean score = 164.3 seconds; ** p = .005 ; **Appendix B.73**). Female No Drug^{AAV9} mean rotarod scores reamined significantly higher than UT^{Cln6nclf} at 12 months (No Drug^{AAV9} mean score = 234.4 seconds; UT^{Cln6nclf} mean score = 71.25 seconds; **** $p \leq .0001$), but were also significantly higher than WT at this time point as well (WT mean score = 170.4 seconds; ** p =.0058; **Appendix B.73**). n(per group per time point) = 8-10.

*3.3.2 scAAV9.CB.hCLN6 treatment protects against the Cln6^{nclf} phenotype: **ataxia***

In order to characterise the effects neonatal gene therapy might have on the Cln6^{nclf} ataxic behavioural phenotype, six different experimental groups were assessed for signs of cerebellar ataxia at 6 and 9 months of age. These included male and female (M/F) WT (C57Bl/6) controls, M/F UT^{Cln6nclf} mice and M/F No Drug^{AAV9} mice. WT and UT^{Cln6nclf} mice were injected with 1x PBS at P0-2 and then given strawberry jelly with vehicle in it every second day from weaning as a control for small molecule therapy. No Drug^{AAV9} mice received a dose of scAAV9.CB.*hCLN6* via i.c.v at P0-2 and also received vehicle jelly after weaning. Ataxia phenotyping scores for the drug-only Cln6^{nclf} experimental groups, along with their UT^{Cln6nclf} and WT controls, were found to have normal (Gaussian) distributions using D'Agostino & Pearson normality tests, so all subsequent statistical analyses were conducted using parametric testing (**Appendix B.68**).

3.3.2.a Composite ataxia phenotype scores

Composite ataxia scores (0-9) for each mouse were calculated by adding together it's mean ledge, hindlimb clasping and gait ataxia phenotyping scores (0-3). Scores were then averaged for each experimental group and presented as mean score (0-9) ± SEM. Comparisons between mean composite scores of age- and sex-matched No Drug^{AAV9} treated and UT^{Cln6nclf} and WT (C57Bl/6) mice were made using 1-way ANOVAs, with Tukey's post-hoc multiple comparisons tests conducted when significant differences were found to occur (**Appendices B.74-75**).

Male No Drug^{AAV9} mice demonstrated significantly reduced composite scores compared to age- and sex-matched UT^{Cln6nclf} at both 6 (6 month male UT^{Cln6nclf} mean composite ataxia score = 2.467; male 6 month No Drug^{AAV9} mean composite ataxia score = 1.0; $^{**}p$ = .0113; **Appendix B.75**). and 9 months of age (male 9 month UT^{Cln6nclf} mean composite ataxia score = 4.833; male 9 month No Drug^{AAV9} mean composite ataxia score = 3.10; *** p = .0009; **Appendix B.24**). No Drug^{AAV9} mice demonstrated no significant difference in score from healthy WT controls at either time point (**Figure 3.18Ai-ii**).

Female No Drug^{AAV9} mice also demonstrated significantly improved composite ataxia scores compared to UT^{Cln6nclf} counterparts at 6 (female 6 month UT^{Cln6nclf} mean composite ataxia score = 2.467; No Drug^{AAV9} mean composite ataxia score = 1.0; **p = .0113; **Appendix B.75)** and 9 months of age (**Figure 3.18.Bi-ii**; female 9 month UT^{Cln6nclf} mean composite ataxia score = 5.0; female 9 month No Drug^{AAV9} mean composite ataxia score = 1.633; **** $p \leq .0001$; **Appendix B.76).**

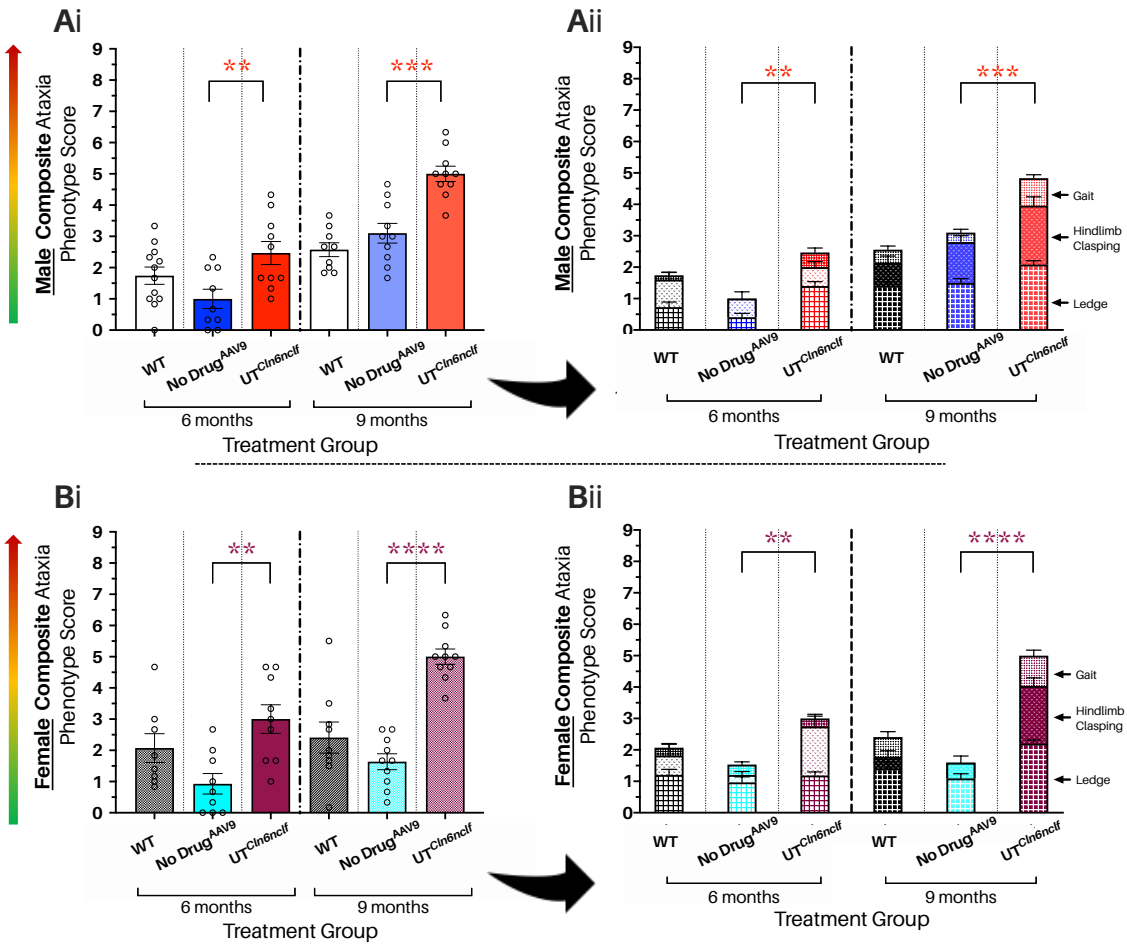

Figure 3.18 | scAAV9.CB.*hCLN6* treatment protects against the Cln6^{nclf} phenotype: composite ataxia scores. *Male and female Cln6^{nclf} mice who received a single injection of scAAV9.CB.hCLN6 at P0-2 and only received a vehicle drug treatment (No Drug^{AAV9}) have significantly improved composite ataxia scores compared to sex-matched untreated Cln6^{nclf} (UT^{Cln6nclf}) mice at both 6 and 9 months of age.* Mean composite ataxia phenotype scores (0 to 9) were calculated using averaged ataxia test individual scores (ledge, hindlimb clasping and gait) for male (**Ai-ii**) and female (**Bi-ii**) Cln6^{nclf} mice treated with a single injection of scAAV9.CB.*hCLN6* at P0-2 and vehicle drug treatment (No Drug^{AAV9}), and their UT^{Cln6nclf} and wildtype (WT) C57Bl/6 counterparts across two different time points: 6 months (left) and 9 months (right). Different mice were tested at each time point (between-subjects study design). A low score (close to 0) indicates an absence of the ataxic phenotype as measured by the composite scoring system, while higher scores, closer to 9, indicate increasing levels of ataxic behaviour (coloured arrow on the left). The overall mean composite scores illustrated in Ai and Bi are further broken down into the average ledge (bottom segment), hindlimb clasping (middle segment) and gait (top segment) scores in segmented bar graphs (**Aii** and **Bii**). Individual, averaged composite scores are shown as clear circles in **Ai** and **Bi**, error bars = ± SEM. Analyses were conducted via 1-way ANOVAs and subsequent Tukey's multiple comparison post-hoc tests (**Appendices B.75-76**). n(per group per time point) = 8-10. **Ai-ii.** Histogram presenting the mean composite ataxia scores of male mice at 6 (left) and 9 (right) months of age. No Drug^{AAV9} mice performed significantly better (lower score) than their age- and sex-matched UT^{Cln6nclf} counterparts at 6 months of age (left; UT^{Cln6nclf} mean = 2.467; No Drug^{AAV9} mean = 1.0; ** p = .0113; **Appendix B.75**). This was also the case at 9 months of age (UT^{Cln6nclf} mean = 4.833; No Drug^{AAV9} mean = 3.10; *** p = .0009; **Appendix B.24**). **Bi-ii**. Histogram presenting the mean composite ataxia scores of female mice at 6 (left) and 9 (right) months of age. Female No Drug^{AAV9} mice performed better (significantly lower composite ataxia score) than UT^{Cln6nclf} at 6 months of age (UT^{Cln6nclf} mean = 3.00; No Drug^{AAV9} mean = 0.9259; ** p = .0044; **Appendix B.76**). There was also a significant difference in the composite scores of No Drug^{AAV9} and UT^{Cln6nclf} female mice at 9 months (left; UT^{Cln6nclf} mean = 5.0; No Drug^{AAV9} mean = 1.633; **** $p \leq .0001$; **Appendix B.76**).

3.3.2.b Ledge test

A single unilateral injection of scAAV9.CB.*hCLN6* at P0-2 appears to protect against the diseased Cln6^{nclf} ledge ataxia phenotype by 9 months of age (**Figure 3.19.A** and **3.19.B**).

For males, a 1-way ANOVA (**Appendix B.76**) indicated that there was a significant difference between the mean ledge score of No Drug^{AAV9} and UT^{Cln6nclf} mice at 6 months of age (**Figure 3.19.A**; No Drug^{AAV9} mean score = 0.4074; UT^{Cln6nclf} mean score = 1.4; *** p = .0003; **Appendix B.76**), with No Drug^{AAV9} achieving a significantly lower (better) score than their UT^{Cln6nclf} counterparts. This trend continued at 9 months, with male No Drug^{AAV9} once again achieving a significantly lower mean ledge ataxia score than UT^{Cln6nclf} mice (No Drug^{AAV9} mean score = 1.5; UT^{Cln6nclf} mean score = 2.083; * p = .0112; **Appendix B.76**). Male No Drug^{AAV9} mean scores for both time points remained statistically indistinguishable from the mean scores of healthy WT mice, indicating that gene therapy effectively protected male Cln6^{nclf} mice from the Cln6^{nclf} ledge phenotype established in **section 3.1.**

Female No Drug^{AAV9} mice, on the other hand, do not demonstrate a significant difference in mean ledge score from either WT or UT^{Cln6nclf} counterparts at 6 months of age (**Figure 3.19.B**). It is only at 9 months that No Drug^{AAV9} begin to perform significantly better at the ledge test than age- and sex-matched UT^{Cln6nclf} counterparts (female 9 month No Drug^{AAV9} mean ledge score = 2.2; female 9 month UT^{Cln6nclf} mean score = 2.2; **** $p \leq .0001$; **Appendix B.77**). This may be due to sex based timing differences in response to the gene therapy, or, possibly more likely, due to the absence of a clear Cln6^{nclf} phenotype at 6 months for female mice (see **section 3.1**).

3.3.2.c Hindlimb clasping test

Cln6^{nclf} mice treated with gene therapy alone were assessed for muscle function and control via the hindlimb clasping test. Different mice were measured at each time point, making this assay between-subjects in design. Data are mean hindlimb clasping scores ± SEM.

Male No Drug^{AAV9} mice did not demonstrate any significant difference in hindlimb clasping score from age- and sex-matched WT controls and UT^{Cln6nclf} counterparts, at either 6 or 9 months (**Figure 3.19.C**).

Female No Drug^{AAV9} mice performed significantly better (lower score) at the hindlimb clasping ataxia assay than age- and sex-matched Cln6^{nclf} counterparts at both 6 (**Figure 3.19.D;** female 6 month No Drug^{AAV9} mean score = 0.2333; female 6 month UT^{Cln6nclf} mean score = 1.556; ** p = .0051; **Appendix B.79**) and 9 months of age (UT^{Cln6nclf} mean score = 0.9667; *** p = .0001; **Appendix B.81**).

3.3.2.d Gait test

Male No Drug^{AAV9} mice produced significantly better (lower) mean gait scores than UT^{Cln6nclf} mice at 6 (male 6 month No Drug^{AAV9} mean score = 0.0; male 6 month UT^{Cln6nclf} mean gait ataxia score = 0.4667; ** p = .0099; **Appendix B.80**) and 9 months of age (**Figure 3.19.E**; male 9 month No Drug^{AAV9} mean score = 0.3; male 9 month UT^{Cln6nclf} mean score = 0.8750; ** p = .0035; **Appendix B.80**). These scores were statistically indistinguishable from WT at both time points.

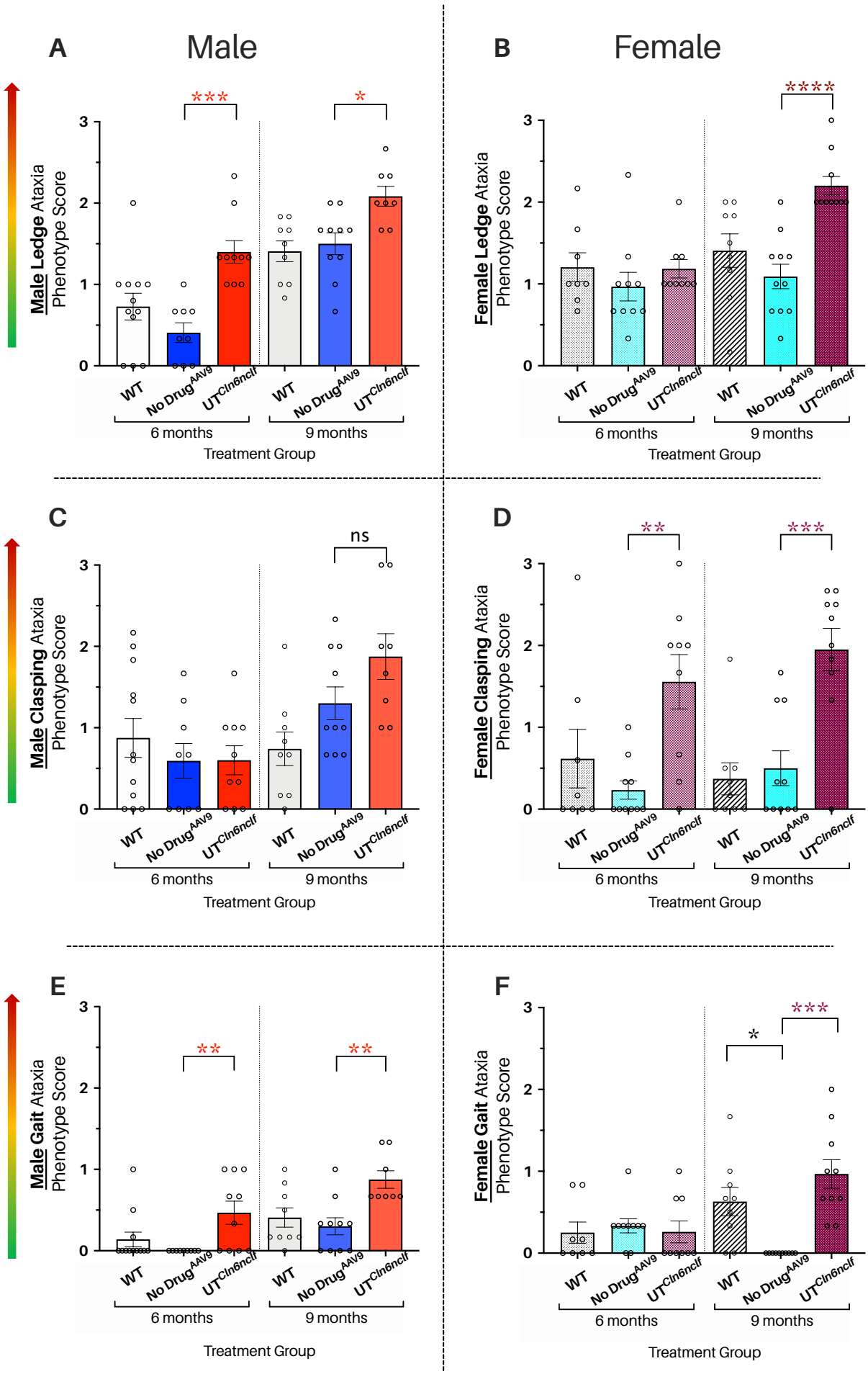
A
Male
B
Female
C
D
E
F
Male Ledge Ataxia Phenotype Score
Female Ledge Ataxia Phenotype Score
Male Clasping Ataxia Phenotype Score
Female Clasping Ataxia Phenotype Score
Male Gait Ataxia Phenotype Score
Female Gait Ataxia Phenotype Score
***
*
****
ns
**
***
WT
No Drug AAV9
UT Cln6nclf
6 months
9 months
Treatment Group

⇐ **Figure 3.19 | scAAV9.CB.*hCLN6* treatment protects against the Cln6^{nclf} phenotype: ataxia phenotyping scores (previous page).** *A single neonatal i.c.v injection of scAAV9.CB.hCLN6 significantly reduces ataxic phenotype in Cln6^{nclf} mice*. **A-F.** Histograms presenting mean ataxia scores (0-3) of individual ataxia assays: ledge (**A**; males; **B**; females), hindlimb clasping (**C**; males; **D**; females), and gait (**E**; males; **F**; females). Scoring criteria and methodology can be found in **Chapter 2**, adapted from *Guyenet et al. 2010*. Different mice were assessed at each time point, making the experiment between-subjects in design. For each assay, a mouse could be assigned a score between 0 and 3, with 0 indicating a complete absence of the ataxic phenotype and 3 indicating a completely penetrant ataxic phenotype (coloured arrows on the left). Data are presented as mean scores, with error bars representing ± SEM. Individual (averaged) mouse scores are presented as clear circles. All analyses were conducted using 1-way ANOVAs (**Appendices B.76-81**), followed by Tukey's multiple comparisons post-hoc tests. **A.** Histogram presenting mean male ledge ataxia scores for 6 months (left) and 9 months (right) of age. Male Cln6^{nclf} mice who received a single injection of scAAV9.CB.*hCLN6* at P0-2 and only received a vehicle drug treatment (No Drug^{AAV9}; blue bars) performed significantly better at the ledge ataxia task than their age- and sex-matched UT^{Cln6nclf} counterparts (red bars) at both 6 (No Drug^{AAV9} mean score = 0.4074; UT^{Cln6nclf} mean score = 1.4; *** p = .0003; **Appendix B.76**) and 9 months (No Drug^{AAV9} mean score = 1.5; UT^{Cln6nclf} mean score = 2.083; * p = .0112; **Appendix B.76**). perform significantly better at three different ataxia tasks, the ledge, hindlimb clasping and gait tests, than their age- and sex-matched UT^{Cln6nclf} counterparts by 9 months of age. n(per group per time point) = 8-12. **B.** Histogram presenting mean female ledgea ataxia scores for 6 (left) and 9 (right) months of age. Female Cln6^{nclf} mice who received a single injection of scAAV9.CB.*hCLN6* at P0-2 and only received a vehicle drug treatment (No Drug^{AAV9}; light blue bars) showed no significant difference in mean ledge score from their age- and sex-matched WT (C57Bl/6; black patterned bars) and UT^{Cln6nclf} (maroon bars) counterparts at 6 months of age (**Appendix B.77**). At 9 months, however, female No Drug^{AAV9} mice performed significantly better than their age- and sex-matched UT^{Cln6nclf} counterparts (No Drug^{AAV9} mean score = 2.2; UT^{Cln6nclf} mean score = 2.2; **** $p \leq .0001$; **Appendix B.77**). n(per group per time point) = 8-11. **C.** Histogram presenting mean male hindlimb clasping ataxia scores for 6 (left) and 9 (right) months of age. No significant difference in score was observed between No Drug^{AAV9} scores and those belonging to WT or UT^{Cln6nclf} at either time point (**Appendix B.78**).). n(per group per time point) = 8-12 **D.** Histogram presenting mean female hindlimb clasping ataxia scores at 6 (left) and 9 (right) months of age. Female No Drug^{AAV9} demonstrated a significantly better (lower) mean hindlimb clasping ataxia score than UT^{Cln6nclf} at both 6 (No Drug^{AAV9} mean score = 0.2333; UT^{Cln6nclf} mean score = 1.556; ** p = .0051; **Appendix B.79**) and 9 months of age (No Drug^{AAV9} mean score = 0.5; UT^{Cln6nclf} mean score = 1.95 ; *** p = .0003; **Appendix B.79**).). n(per group per time point) = 8-11. **E.** Histogram presenting mean male gait scores at 6 (left) and 9 (right) months of age. No Drug^{AAV9} mean scores were significantly better (lower) than UT^{Cln6nclf} scores at both 6 (No Drug^{AAV9} mean score = 0.0; UT^{Cln6nclf} mean score = 0.4667; ** p = .0099; **Appendix B.80**) and 9 months of age (No Drug^{AAV9} mean score = 0.3; UT^{Cln6nclf} mean score = 0.8750; ** p = .0035; **Appendix B.80**). n(per group per time point) = 8-12. **F.** Histogram presenting mean female gait scores at 6 (left) and 9 (right) months of age. No Drug^{AAV9} mean scores were statistically indistinguishable from age- and sex-matched UT^{Cln6nclf} and WT counterparts at 6 months of age (**Appendix B.81**). At 9 months, however, female No Drug^{AAV9} demonstrated a significantly better (lower; No Drug^{AAV9} mean score = 0.0) mean score than both WT (WT mean score = 0.6296; * p = .0110) and UT^{Cln6nclf} mice (UT^{Cln6nclf} mean score = 0.9667; *** p = .0001; **Appendix B.81**).). n(per group per time point) = 8-11.

*3.3.3 scAAV9.CB.hCLN6 treatment protects against the Cln6^{nclf} phenotype: **survival and weight***

A single injection of scAAV9.CB.*hCLN6* at P0-2, without any drug therapy, rescues Cln6^{nclf} mice, of both sexes, from characteristically shortened lifespans and improves survival significantly compared to untreated Cln6^{nclf} (UT^{Cln6nclf}) mice. Survival and weights were only recorded up until 14 months of age due to the time limitations of a MSc thesis, however, survival and weights continued to be recorded for the larger Gray Foundation trial - until all animals had

reached one of the three humane endpoints outlined in **Chapter 2**. Survival curve comparisons were conducted using a series of log-rank (Mantel-cox) tests (**Appendices B.82-85**) and weights were compared using simple linear regression (**Appendices B.86-87** and **B.89-90**) and 1-way ANOVAs (**Appendices B.88** and **B.91**).

⇒ **Figure 3.20 | scAAV9.CB.*hCLN6* treatment protects against the Cln6^{nclf} phenotype: survival and weight (following page)**. *A single injection of scAAV9.CB.hCLN6 at P0-2, without any drug therapy, rescues Cln6^{nclf} mice, of both sexes, from characteristically shortened lifespans and improves survival significantly compared to untreated Cln6^{nclf} (UT^{Cln6nclf}) mice.* Survival and weights were only recorded up until 14 months of age due to the time limitations of a MSc thesis, however, survival and weights continued to be recorded for the larger Gray Foundation trial - until all animals had reached one of the three humane endpoints outlined in **Chapter 2**. Survival curve comparisons were conducted using a series of log-rank (Mantel-cox) tests (**Appendices B.82-85**) and weights were compared using simple linear regression (**Appendices B.86-87** and **B.89-90**) and 1-way ANOVAs (**Appendices B.88** and **B.91**) **A.** Kaplan-Meier plot of male mouse survival (%). Male mice treated with a single dose of scAAV9.CB.*hCLN6* at P0-2 and vehicle drug (No Drug^{AAV9}; blue lines; median survival = undefined at 14 months) had significantly longer lifespans than UT^{Cln6nclf} mice (red lines; median survival = 13.3 months; **** p ≤ .0001; **Appendix B.83**). No significant difference in median survival could be detected between mal No Drug^{AAV9} and WT by 14 months. Starting n =28-35. **B.** Kaplan-Meier plot of female mouse survival (%). Female mice treated with a single dose of scAAV9.CB.*hCLN6* at P0-2 and vehicle drug (No Drug^{AAV9}; light blue lines; median survival = undefined at 14 months) had significantly longer lifespans than UT^{Cln6nclf} mice (maroon lines; median survival =12.50 months; **** $p \leq .0001$; **Appendix B.85**). No significant difference in median survival could be detected between female No Drug^{AAV9} and WT mice by 14 months. Starting n =24-27. **C.** Line graph of mean weights (in grams) of male No Drug^{AAV9} (blue lines and squares), UT^{Cln6nclf} (red lines and squares) and WT (C57Bl/6; black lines and squares) mice over a period of 15 months. Simple linear regression analysis (solid lines)revealed that there was a significant difference in the overall rate of weight gain and loss over the 15 month period between male No Drug^{AAV9} and UT^{Cln6nclf} mice (*** $p = .0008$; **Appendix B.87**) and between No Drug^{AAV9} and WT (**** $p \leq .0001$; **Appendix B.86**). 1-way ANOVA analyses conducted on data from at 6, 9 and 12 months revealed that at 9 months No Drug^{AAV9} mice weighed, on average, significantly less than WT (No Drug^{AAV9} mean weight = 35.95 g; WT mean weight = 38.87 g; ** $p = .0093$; **Appendix B.88**). At 12 months, however, the difference in mean weight between No Drug^{AAV9} and WT was no longer significant (**Appendix B.88**). No Drug^{AAV9} mice weighed significantly more, on average, than UT^{Cln6nclf} mice at 12 months of age (No Drug^{AAV9} mean weight = g; UT^{Cln6nclf} mean weight =; ** $p = .0012$; **Appendix B.88**). n(per group per time point) =14-28. D. Line graph of mean weights (in grams) of female No Drug^{AAV9} (light blue lines and circles), UT^{Cln6nclf} (maroon lines and circles) and WT (C57Bl/6; grey lines andcircles) mice over a period of 15 months. Simple linear regression analysis (solid lines)revealed that there was a significant difference in the overall rate of weight gain and loss over the 15 month period between female No Drug^{AAV9} and UT^{Cln6nclf} mice (*** $p = .0066$; **Appendix B.90**) and between No Drug^{AAV9} and WT (*** $p = .0026$; **Appendix B.89**). No significant differences in mean weight were detected between No Drug^{AAV9}, UT^{Cln6nclf} and WT weights at 6, 9 or 12 months of age via 1-way ANOVA (**Appendix B.91**).

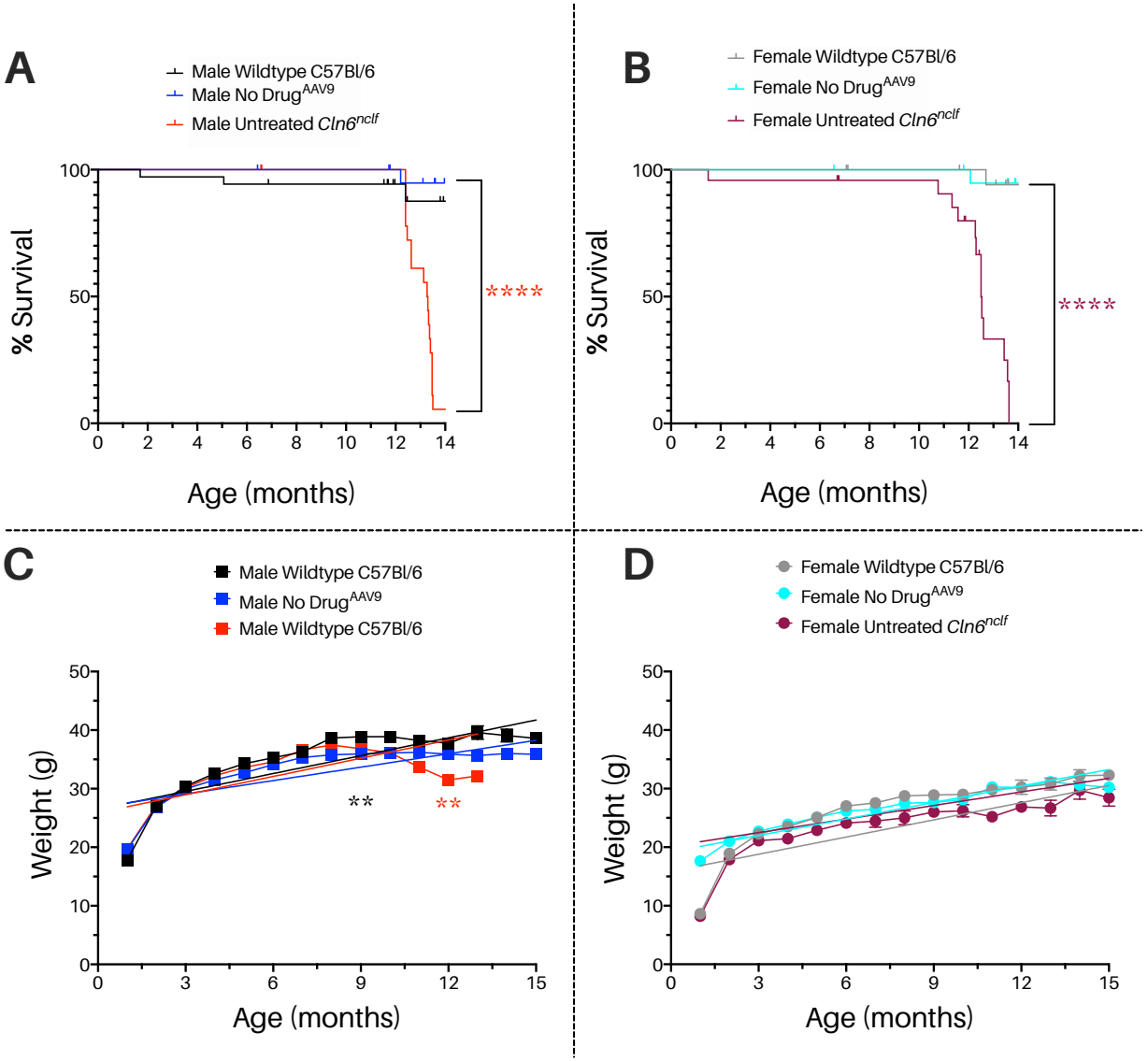
A
Male Wildtype C57Bl/6
Male No Drug AAV9
Male Untreated Cln6 nclf
% Survival
100
50
0
0 2 4 6 8 10 12 14
****
Age (months)
B
Female Wildtype C57Bl/6
Female No Drug AAV9
Female Untreated Cln6 nclf
% Survival
100
50
0
0 2 4 6 8 10 12 14
****
Age (months)
C
Male Wildtype C57Bl/6
Male No Drug AAV9
Male Wildtype C57Bl/6
Weight (g)
50
40
30
20
10
0
0 3 6 9 12 15
**
**
Age (months)
D
Female Wildtype C57Bl/6
Female No Drug AAV9
Female Untreated Cln6 nclf
Weight (g)
50
40
30
20
10
0
0 3 6 9 12 15
Age (months)

3.3.4 scAAV9.CB.hCLN6 treatment protects against the Cln6^{nclf} phenotype: ***sex differences***

Many host factors can help determine the success or failure of gene therapy. These include, but are not limited to, the innate immune reaction generated by administration of the therapy, differing gene expression profiles between tissues, organs and individuals, and hormonal attenuation or exacerbation of downstream symptoms (Amur et al., 2012; Duffy et al., 2012). It is now well understood that biological sex can play a huge role in all of these areas, with an individual's sex dictating what hormones are secreted and when, the speed, size and specificity of an immune response to foreign material and the ability of viral vectors to transduce specific tissues (Calcedo & Wilson, 2013; Dane et al., 2013; Dodge et al., 2005; Wells & Goldspink, 1992; Yan et al., 2005). CLN6 BD, like all variants of NCL, is not a sex-specific disease. For this reason it is critical to assess the efficacy and safety of every potential therapy in both male and female animal models and to compare results to identify and characterise any sex-dependent differences in response. For these reasons, this section compares the behaviour scores, survival data and weights of both male and female Cln6^{nclf} mice treated with gene therapy alone (No Drug^{AAV9}).

3.3.4.a Rotarod sex differences

No Drug^{AAV9} male and female Cln6^{nclf} mice experienced statistically similar rates of decline in rotarod score over 6, 9 and 12 months (simple linear regression; **Appendices B.92-93**). Despite this, however, a series of unpaired student t-test analyses at 6, 9 and 12 months revealed a significant difference in mean rotarod score beween the sexes at 9 months of age (**Figures 3.21.A; Appendix B.94**). At 9 months, female No Drug^{AAV9} mice demonstrated significantly higher levels of motor co-ordination, balance and endurance (as measured by the rotarod) compared to their age-matched male counterparts (9 month male mean score = 165.4 seconds; 9 month female male mean score = 257.7; ** p = .0014; **Appendix B.94**). This

disparity appears to be transient, however, with male and female scores becoming statistically indistinguishable at 12 months of age (**Figure 3.21.B**).

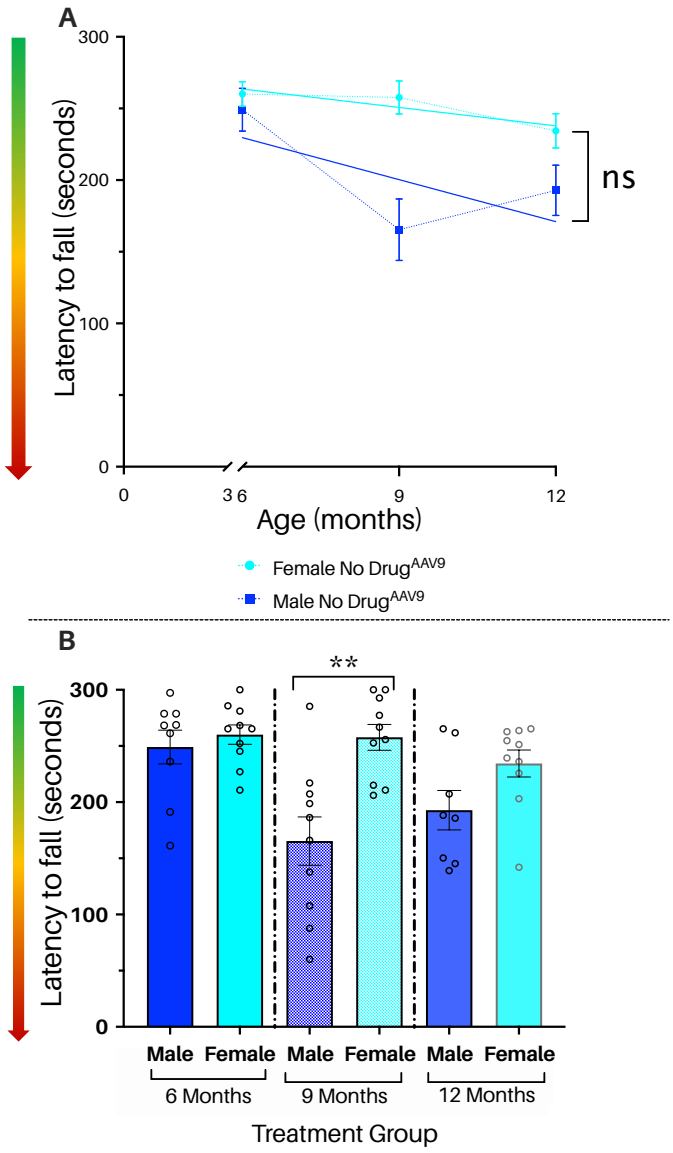

Figure 3.21 | scAAV9.CB.*hCLN6* treatment protects against the Cln6^{nclf} phenotype: sex differences in rotarod scores. *Male and female Cln6^{nclf} mice treated with a single injection of scAAV9.CB.hCLN6 at P0-2 and a vehicle drug (No Drug^{AAV9}) demonstrated similar overall rates of decline in rotarod performance over time but showed statistically significant differences in average rotarod score at 9 months of age.* **A.** Line graph presenting data as mean rotarod scores measured in latency to fall (seconds) for male (dark blue squares) and female (light blue circles) Cln6^{nclf} mice who received a single, neonatal i.c.v injection of scAAV9.CB.*hCLN6* at P0-2 (No Drug^{AAV9}). Error bars represent ± SEM. Dotted lines indicate the expected trajectory of rotarod scores between measured time points (6, 9 and 12 months). Linear regression lines are represented by solid coloured lines (simple linear regression; **Appendices B.92-93).** No significant difference in overall rate of motor decline, as measured by the rotarod, was detected between male and female No Drug^{AAV9} mice. **B.** Histogram presenting data as mean rotarod scores (latency to fall in seconds) for male (dark blue bars) and female (light blue bars) No Drug^{AAV9} mice at 6, 9 and 12 months of age. A series of unpaired student t-tests were used to assess differences in scores between male and female mice at each time point (**Appendix B.94**). No significant difference in mean rotarod scores were detected between male and female scores at 6 and 12 months of age. At 9 months, however, female No Drug^{AAV9} demonstrated a significantly higher (better) score than males (9 month male mean score = 165.4 seconds; 9 month female male mean score = 257.7; ** p = .0014; **Appendix B.94**) n(per group, per time point) = 8-10.

3.3.4.b Composite ataxia sex differences

Male and female No Drug^{AAV9} mice demonstrated no significant difference in mean composite ataxia scores (**Figure 3.22**) at 6 or 9 months of age (unpaired t-tests; **Appendix B.95**).

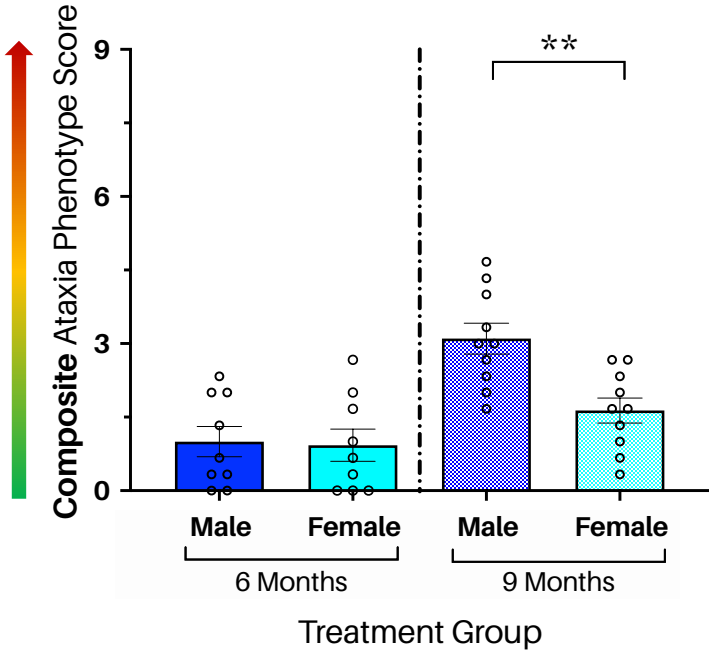

Figure 3.22 | scAAV9.CB.*hCLN6* treatment protects against the Cln6^{nclf} phenotype: sex differences in composite ataxia scores. *Male and female Cln6^{nclf} mice who received a single injection of scAAV9.CB.hCLN6 at P0-2 and only received a vehicle drug treatment (No Drug^{AAV9}) have significantly improved composite ataxia scores compared to sex-matched untreated Cln6^{nclf} (UT^{Cln6nclf}) mice at both 6 and 9 months of age.* Mean composite ataxia phenotype scores (0 to 9) were calculated using averaged ataxia test individual scores (ledge, hindlimb clasping and gait) for male (**Ai-ii**) and female (**Bi-ii**) Cln6^{nclf} mice treated with a single injection of scAAV9.CB.*hCLN6* at P0-2 and vehicle drug treatment (No Drug^{AAV9}), and their UT^{Cln6nclf} and wildtype (WT) C57Bl/6 counterparts across two different time points: 6 months (left) and 9 months (right). Different mice were tested at each time point (between-subjects study design). A low score (close to 0) indicates an absence of the ataxic phenotype as measured by the composite scoring system, while higher scores, closer to 9, indicate increasing levels of ataxic behaviour (coloured arrow on the left). The overall mean composite scores illustrated in Ai and Bi are further broken down into the average ledge (bottom segment), hindlimb clasping (middle segment) and gait (top segment) scores in segmented bar graphs (**Aii** and **Bii**). Individual, averaged composite scores are shown as clear circles in Ai and Bi, error bars = ± SEM. Analyses were conducted via 1-way ANOVAs and subsequent Tukey's multiple comparison post-hoc tests (**Appendices B.75-76**). n(per group per time point) = 8-10. **Ai-ii.** Histogram presenting the mean composite ataxia scores of male mice at 6 (left) and 9 (right) months of age. No Drug^{AAV9} mice performed significantly better (lower score) than their age- and sex-matched UT^{Cln6nclf} counterparts at 6 months of age (left; UT^{Cln6nclf} mean = 2.467; No Drug^{AAV9} mean = 1.0; ***p* = .0113; **Appendix B.75**). This was also the case at 9 months of age (UT^{Cln6nclf} mean = 4.833; No Drug^{AAV9} mean = 3.10; *** *p* = .0009; **Appendix B.24**). **Bi-ii**. Histogram presenting the mean composite ataxia scores of female mice at 6 (left) and 9 (right) months of age. Female No Drug^{AAV9} mice performed better (significantly lower composite ataxia score) than UT^{Cln6nclf} at 6 months of age (UT^{Cln6nclf} mean = 3.00; No Drug^{AAV9} mean = 0.9259; ** *p* = .0044; **Appendix B.76**). There was also a significant difference in the composite scores of No Drug^{AAV9} and UT^{Cln6nclf} female mice at 9 months (left; UT^{Cln6nclf} mean = 5.0; No Drug^{AAV9} mean = 1.633; **** *p* ≤ .0001; **Appendix B.76**).

3.3.4.c Ledge ataxia sex differences

Female No Drug^{AAV9} mice demonstrate a significantly higher ledge ataxia score than age-matched males at 6 months of age (**Figure 3.23.A**; unpaired student t-test; 6 month male mean score = 0.4074; 6 month female mean score = 0.9667; * *p* = .0201; **Appendix B.96).** This difference is only temporary, however, as there was no significant difference observed between the mean ledge ataxia score of male and female No Drug^{AAV9} mice at 9 months of age (**Figure 3.2.A**).

3.3.4.d Hindlimb clasping ataxia sex differences

In the hindlimb clasping ataxia assay, no differences were observed between male and female No Drug^{AAV9} mice until 9 months of age – at which point males demonstrated a significantly higher hindlimb clasping score (**Figure 3.23.B**; 9 month male mean score = 1.3; 9 month female mean score = 0.5; * p = .0137; **Appendix B.97**).

3.3.4.e Gait ataxia sex differences

Sex-specific differences in AAV2/9-mediated gene therapy's effect on the Cln6^{nclf} gait phenotype seems to be somewhat age-dependent, as No Drug^{AAV9} females peform poorly compared to male mice at 6 months of age (**Figure 3.23.C**; 6 month male mean score = 0.0; 6 month meanataxia score = 0.333; ** p = .0019; **Appendix B.98**) but then appear to recover at 9 months, producing a very low hindlimb score. No Drug^{AAV9} males decline in a more traditional manner, performing well at 6 months, and then becoming significantly worse than females by 9 months (**Figure 3.23.C**; 9 month male mean score = 0.3; 9 month female mean score = 0.0; * *p* = .0104; **Appendix B.98)**. It is difficult to intrepret these trends, however, due to the fact that separate groups of mice were assessed at each time point – leaving open the possibility that the scores are biased by individual differences between the different mice used.

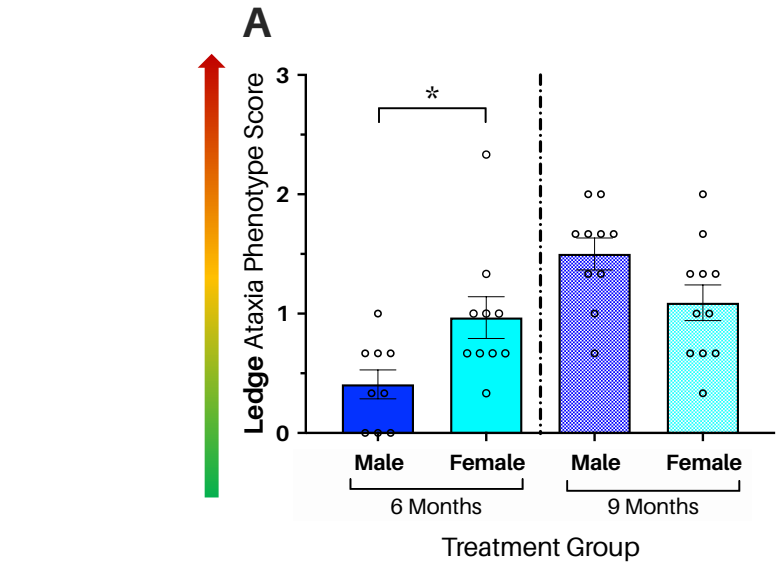
A
Ledge Ataxia Phenotype Score
3
2
1
0
*
Male
Female
Male
Female
6 Months
9 Months
Treatment Group

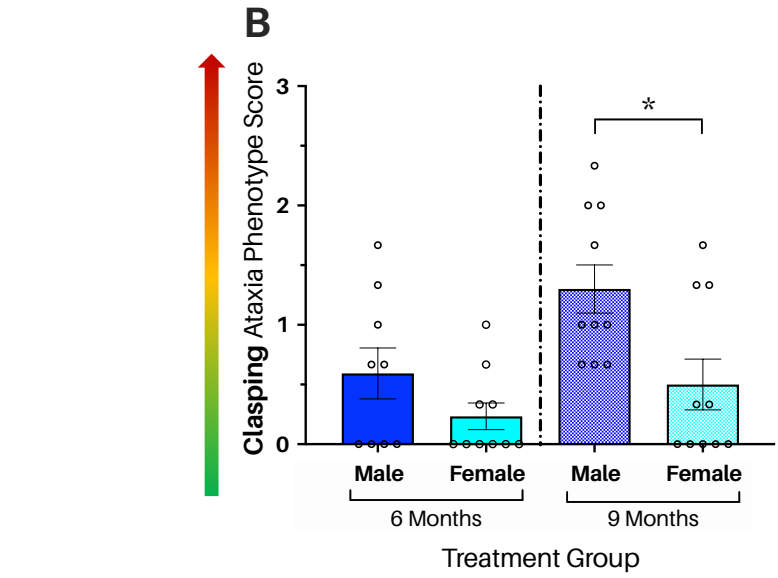
B
Clasping Ataxia Phenotype Score
3
2
1
0
*
Male
Female
Male
Female
6 Months
9 Months
Treatment Group

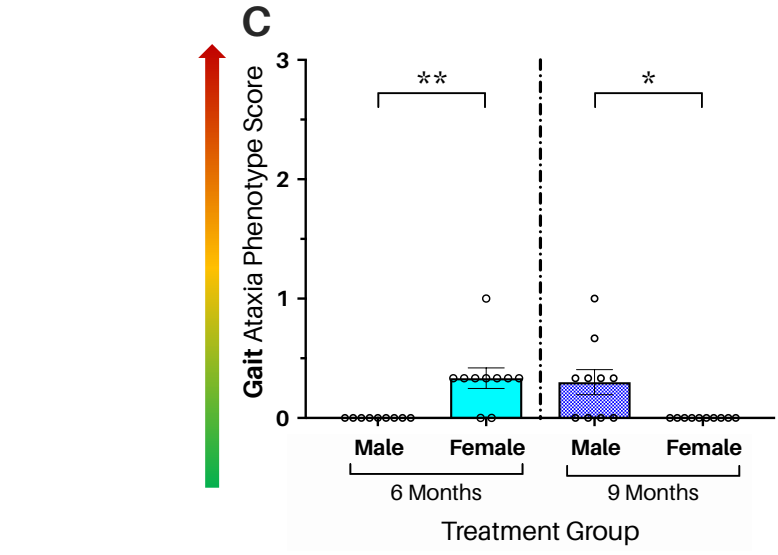
C
Gait Ataxia Phenotype Score
3
2
1
0
**
*
Male
Female
Male
Female
6 Months
9 Months
Treatment Group

⇐ **Figure 3.23 | scAAV9.CB.*hCLN6* treatment protects against the Cln6^{nclf} phenotype: sex differences in ataxia phenotyping scores (opposite page).** *Female mice who received a single scAAV9.CB.hCLN6 injection at P0-2 and vehicle drug (No Drug^{AAV9}) appear to perform better across three different ataxia behavioural assays (the ledge, hindlimb clasping and gait tests)than their male No Drug^{AAV9} counterparts during early stages of disease progression. This trend, however, is completely reversed by 9 months, with male No Drug^{AAV9} mice achieving consistently better ataxia scores than females in all three tests.* Mice underwent three trials of a sequence three different ataxia assays – the ledge test, the hindlimb clasping test and the gait test (adapted from *Guyenet et al., 2010*) – in order to determine the presence or absence of an ataxic phenotype at 6 and 9 months of age. Different mice were assessed at each time point, making the experiment between-subjects in design. For each assay, a mouse could be assigned a score between 0 and 3, with 0 indicating a complete absence of the ataxic phenotype and 3 indicating a completely penetrant ataxic phenotype (coloured arrows on the left). All data (**A-C**) are presented as the mean of averaged (3 trials; scored from 0-3) individual mouse scores, with clear circles representing the individual averaged scores. Error bars = ± SEM. All analyses between male and female mean ataxia scores were conducted using unpaired student t-tests (**Appendices B.96 -98**) **A.** Histogram of mean ledge ataxia scores for male (dark blue bars) and female (light blue bars) No Drug^{AAV9} treated Cln6^{nclf} mice at 6 (left) and 9 (right) months of age. Data are presented as mean scores ± SEM. Clear circles represent individual averaged mouse scores (3x trials per mouse). At 6 months of age females demonstrated a significantly higher (worse) ledge score than their male counterparts (6 month male mean ledge ataxia score = 0.4074; 6 month female mean ledge ataxia score = 0.9667; * p = .0201; **Appendix B.96**). This significant difference, however, in mean ledge scores no longer present at 9 months. n(per group, per time point) = 9-11. **B.** Histogram of mean hindlimb clasping scores for male (dark blue bars) and female (light blue bars) No Drug^{AAV9} treated Cln6^{nclf} mice at 6 (left) and 9 (right) months of age. Data are presented as mean scores ± SEM. Clear circles represent individual averaged mouse scores (3x trials per mouse). No significant difference was detected between male and female scores at 6 months of age. At 9 months, however, male No Drug^{AAV9} were performing significantly worse than females (9 month male hindlimb clasping ataxia score = 1.3; 9 month female hindlimb clasping ataxia score = 0.5; * p = .0137; **Appendix B.97**) n (per group, per time point) = 9-10. **C.** Histogram of mean gait ataxia scores for male (dark blue bars) and female (light blue bars) No Drug^{AAV9} treated Cln6^{nclf} mice at 6 (left) and 9 (right) months of age. Data are presented as mean scores ± SEM. Clear circles represent individual averaged mouse scores (3x trials per mouse). At 6 months, female No Drug^{AAV9} mice performed significantly worse than male counterparts (6 month male gait ataxia score = 0.0; 6 month female gait ataxia score = 0.333; ** p = .0019; **Appendix B.98**). At 9 months, however, this trend reverses and male mice perform significantly worse than female (9 month male gait ataxia score = 0.3; 9 month female gait ataxia score = 0.0; * p = .0104; **Appendix B.98**). n (per group, per time point) = 9-10.

3.3.4.f Survival and weight sex differences

Male and female No Drug^{AAV9} mice demonstrated no significant difference in median survival (**Figure 3.24.A**) or rate of weight change over a 14 month period (**Figure 3.24.B**).

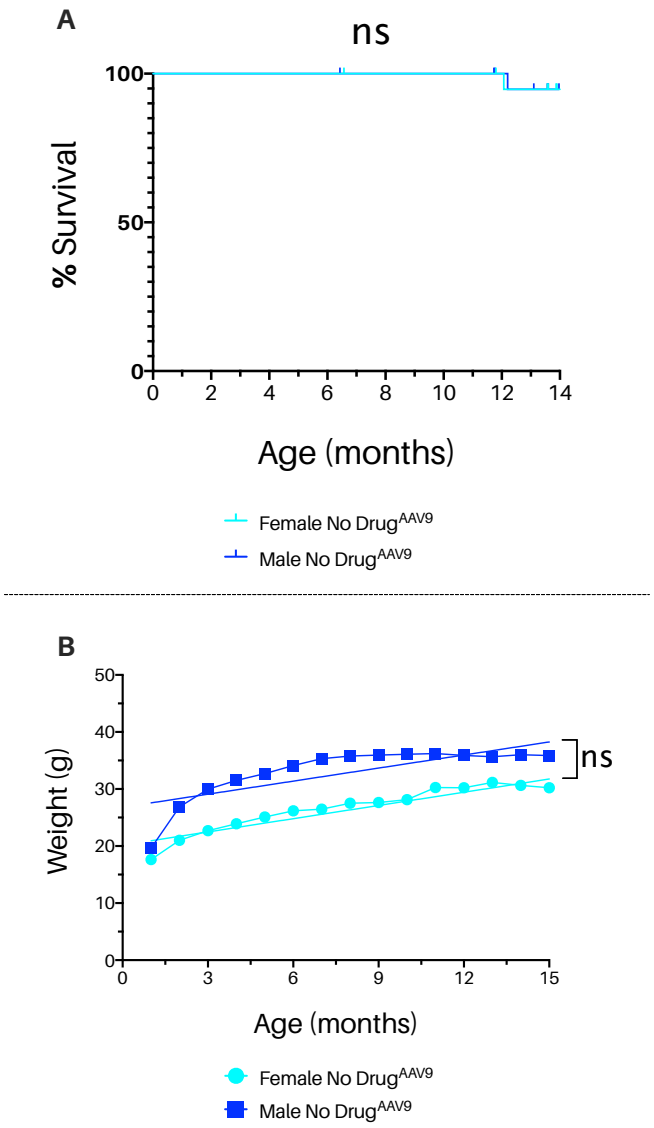

Figure 3.24 | scAAV9.CB.*hCLN6* treatment protects against the Cln6^{nclf} phenotype: sex differences in survival and weight. *Male and female Cln6^{nclf} mice treated with a single injection of scAAV9.CB.hCLN6 at P0-2 and vehicle drug (No Drug^{AAV9}) show statistically similar survival curves (A) and rates of weight gain over fourteen months (B).* **A.** Kaplan-Meier survival plot (%) comparing the survival curves of male (dark blue) and female (light blue) No Drug^{AAV9} mice over a period of 14 months. No significant difference in median survival was detected by 14 months (**Appendix B.99**). Starting n = 29. **B.** Line graph presenting the mean weights of male (dark blue squares) and female (light blue circles) No Drug^{AAV9} mice over a 14 month period – from weaning until 15 months of age. Simple linear analysis revealed no significant difference in overall rate of weight gain and loss during this period (**Appendix B.100**). No analyses were conducted directly between mean weights at 6, 9 and 12 months as there is an expected difference in male and female weights for mice due to sex-based differences in morphology. Starting n = 29.

3.3.5 scAAV9.CB.hCLN6 treatment protects against the Cln6^{nclf} phenotype: ***summary***

Analysis of No Drug^{AAV9} behavioural scores, survival and weights indicates that a single, unilateral i.c.v injection of scAAV9.CB.*hCLN6* at P0-2 potentially protects Cln6^{nclf} mice from the several key deficits associated with the Cln6^{nclf} behavioural phenotype.

Male No Drug^{AAV9} performed significantly better than UT^{Cln6nclf} mice at 6 months for both the composite and ledge ataxia assays, which were the two assays and time point at which the Cln6^{nclf} diseased behaviour phenotype was first observed in UT^{Cln6nclf} mice (**section 3.1**). This, coupled with the fact that their 6 month composite and ledge ataxia scores were also statistically indistinguishable from WT, indicates a potential protection against the Cln6^{nclf} phenotype at this time point. Male No Drug^{AAV9} also demonstrated significantly improved behavioural scores for all other assays, except 6 and 9 month rotarod and gait, and significantly improved survival by 15 months of age, compared to UT^{Cln6nclf} mice (**Table 3.13**).

Females treated with AAV2/9-mediated therapy also did well, with significantly improved behavioural scores seen at at least one time point per behavioural test when compared to age and sex-matched UT^{Cln6nclf} (**Table 3.14**).

Direct comparison between the sexes revealed that females, overall, seem to have higher scores in behaviour, possibly indicating a sex-based predisposition to AAV2/9-mediated gene therapy - though there were no significant sex differences observed in survival or rate of weight gain (**Table 3.15**).

Table 3.13 | scAAV9.CB.*hCLN6* treatment protects against the Cln6^{nclf} phenotype: summary table of No Drug^{AAV9} males. *Summary table of behavioural score (rotarod and ataxia), survival and weight comparisons carried out between male Cln6^{nclf} treated only with gene therapy (a single injection of scAAV9.CB.hCLN6 at P0-2) and vehicle drug (No Drug^{AAV9}) and their age- and sex-matched WT and untreated Cln6^{nclf} (*UT^{Cln6nclf}*) counterparts at 6, 9 and 12 months of age.* All behavioural score and weight comparisons were conducted using 1-way ANOVAs (**Appendices B.72, 74, 76, 78, 80** and **B.88**), with Tukey's post-hoc multiple comparisons tests where appropriate, while survival curves were compared using log rank (Mantel-Cox) tests (**Appendices B.82** and **83**). nsd = no significant difference; s = significant.

No Drug^{AAV9} Cln6^{nclf} Males				
Behavioural Test	**Comparison Group**	**6 months**	**9 months**	**12 months**
Rotarod	UT^{Cln6nclf}	nsd	nsd	**Better (s)**
	WT	nsd	nsd	**Better (s)**
Composite	UT^{Cln6nclf}	**Better (s)**	**Better (s)**	-
	WT	nsd	nsd	-
Ledge	UT^{Cln6nclf}	**Better (s)**	**Better (s)**	-
	WT	nsd	nsd	-
Hindlimb Clasping	UT^{Cln6nclf}	nsd	nsd	-
	WT	nsd	nsd	-
Gait	UT^{Cln6nclf}	**Better (s)**	**Better (s)**	-
	WT	nsd	nsd	-
Survival	UT^{Cln6nclf}	**Increased survival (s)**		
	WT	nsd		
Weight	UT^{Cln6nclf}	nsd	nsd	**Weigh more (s)**
	WT	nsd	**Weigh less (s)**	nsd

Table 3.14 | scAAV9.CB.*hCLN6* treatment protects against the Cln6^{nclf} phenotype: summary table of No Drug^{AAV9} females. *Summary table of behavioural score (rotarod and ataxia), survival and weight comparisons carried out between female Cln6^{nclf} treated only with gene therapy (a single injection of scAAV9.CB.hCLN6 at P0-2) and vehicle drug (No Drug^{AAV9}) and their age- and sex-matched WT and untreated Cln6^{nclf} (UT^{Cln6nclf}) counterparts at 6, 9 and 12 months of age.* All behavioural score and weight comparisons were conducted using 1-way analysis of variances ANOVAs (**Appendices B.73, 75, 77, 79, 81** and **B.91**), with Tukey's post-hoc multiple comparisons tests where appropriate, while survival curves were compared using log rank (Mantel-Cox) tests (**Appendices B.84** and **B.85**). nsd = no significant difference; s = significant.

No Drug^{AAV9} Cln6^{nclf} Females

Behavioural Test	Comparison Group	6 months	9 months	12 months
Rotarod	UT^{Cln6nclf}	nsd	Better (s)	**Better (s)**
	WT	nsd	nsd	**Better (s)**
Composite	UT^{Cln6nclf}	**Better (s)**	**Better (s)**	-
	WT	nsd	nsd	
Ledge	UT^{Cln6nclf}	nsd	**Better (s)**	-
	WT	nsd	nsd	
Hindlimb Clasping	UT^{Cln6nclf}	**Better (s)**	**Better (s)**	-
	WT	nsd	nsd	
Gait	UT^{Cln6nclf}	nsd	**Better (s)**	-
	WT	nsd	**Better (s)**	
Survival	UT^{Cln6nclf}	**Increased survival (s)**		
	WT	nsd		
Weight	UT^{Cln6nclf}	nsd	nsd	nsd
	WT	nsd	nsd	nsd

Table 3.15 | scAAV9.CB.*hCLN6* treatment protects against the Cln6^{nclf} phenotype: summary table of No Drug^{AAV9} males versus No Drug^{AAV9} females. *Summary table of behavioural score (rotarod and ataxia), survival and weight comparisons carried out between male and female Cln6^{nclf} mice treated only with gene therapy (a single injection of scAAV9.CB.hCLN6 at P0-2) and vehicle drug (No Drug^{AAV9}) at 6, 9 and 12 months of age.* All behavioural score and weight comparisons were conducted using unpaired student t-tests (**Appendices B.94, 95, 96, 97** and **98**), while survival curves were compared using log rank (Mantel-Cox) tests (**Appendix B.99**). nsd = no significant difference.

No Drug^{AAV9} Cln6^{nclf} Males vs Females

Behavioural test	6 months	9 months	12 months
Rotarod	nsd	**Females perform better (s)**	nsd
Composite	nsd	**Females perform better (s)**	-
Ledge	nsd	nsd	-
Hindlimb	nsd	**Females perform better (s)**	-
Gait	**Males perform better (s)**	**Females perform better (s)**	-
Survival	nsd		

3.4 Combined gene and small molecule therapy protects against the CLN6 BD behavioural phenotype in Cln6^{nclf} mice

It has become commonplace in the medical and research community to target several aspects of a disease's pathology in order to maximise therapeutic outcome. In diseases such as CLN6 BD, which are of genetic origin and therefore affect a wide range of cell and tissue types, a single treatment – even one as promising as AAV2/9-mediated gene therapy – is unlikely to address all clinical presentations or endure throughout a patient's lifetime. Several combination therapies have been trialled in the NCLs, including ibuprofen with lamotrigene in Cln3$^{-/-}$ mice and gene therapy coupled with a bone marrow transplant in Ppt1$^{-/-}$ mice, with varying levels of success (Cooper et al., 2018; Macauley et al., 2012). So far the most successful studies have involved multiple injections of AAV-mediated gene therapy (PPT1 in Ppt1$^{-/-}$ mice), administered at several different sites throughout the CNS . While promising, multiple injections into the brain and spine of children is not what most would consider an 'ideal' therapeutic strategy – so the search continues for treatment combinations that can improve therapeutic outcomes without sacrificing quality of life or creating unjustifiable risk to the patient. Here, the effects of several different combined gene and small molecule therapies on the Cln6^{nclf} behavioural phenotype are investigated, in the hopes of identifying a synergystic combination that can inform future therapeutic strategies and maximise clinical outcomes.

3.4.1 Functional improvements in combination therapy mice: ***rotarod***

Ten different experimental groups were assessed with the rotarod at 6, 9 and 12 months of age. Six of these groups represented three unique combinations of gene and small molecule therapy. Gemfib^{AAV9} mice (separated into male and female cohorts) received a single i.c.v injection of scAAV9.CB.*hCLN6* at P0-2 and were dosed with 120 mg/kg of gemfibrozil every second day from weaning until individual end points of the trial. CBD^{AAV9} mice (M/F) also received a neonatal i.c.v injection of AAV2/9-mediated gene therapy and were dosed with 5

mg/kg of CBD every second day from weaning until individual end points of the trial. Finally, Combo^{AAV9} mice (M/F) received AAV2/9-mediated gene therapy shortly after birth via unilateral i.c.v injection and were dosed with a combination of 120 mg/kg and 5 mg/kg CBD every second day from weaning until individual end points of the trial (see **sections 2.3** and **2.4** for more details regarding i.c.v injections and dosing). Rotarod scores for the combination therapy Cln6^{nclf} experimental groups were found to have normal (Gaussian) distributions using D'Agostino & Pearson normality tests, so all subsequent statistical analyses were conducted using parametric testing (**Appendix B.102**).

Linear regression was used to compare the overall rate of decline in mean rotarod scores over time and the associated elevation (range over which the decline occurred) of each combination therapy treated group versus sex-matched WT controls and UT^{Cln6nclf} mice (**Appendices B.104-107**). To compare differences in rotarod score between groups at each individual time point, 1-way ANOVAs were used, complemented by Tukey's multiple comparison post-hoc testing when significant differences were found to be present (**Appendices B.108-109**). The rotarod assay showed a steady decline in motor performance over time for all mice, as to be expected due to age, and this decline was mathematically confirmed by the negative line equations of each group (**Figure 3.25**; **Appendix B.106**).

In male mice, all three combination therapy (Gemfib^{AAV9}, CBD^{AAV9} and Combo^{AAV9}) groups declined at a significantly slower rate than male UT^{Cln6nclf} animals, an all three declined at a rate statistically indistinguishable from healthy WT controls (**Figures 3.25.A, C** and **E**; **Appendices 103** and **107**). Male CBD^{AAV9} and Combo^{AAV9} treated mice were the first male combination treatment groups to demonstrate a significant difference in mean rotarod score, with both performing significantly better (higher score) than UT^{Cln6nclf} counterparts at 9 months of age (**Figure 3.26.B**; male 9 month UT^{Cln6nclf} mean score = 144.4 seconds; male 9

month CBD^{AAV9} mean score = 249.2 seconds; * p = .0105; male 9 month Combo^{AAV9} mean score = 228.5 seconds; * p = .0418; **Appendix B.108**). At this time point the mean scores of Gemfib^{AAV9} and healthy WT controls remained statistically indistinguishable from UT^{Cln6nclf} – suggesting hyperactivity or over performance on the behalf of male CBD^{AAV9} and Combo^{AAV9} mice. By 12 months of age, however, all male combination treatment groups were demonstrating significantly higher rotarod scores than age- and sex-matched UT^{Cln6nclf} counterparts, indicating all three combination therapies potentially offer protection against the Cln6^{nclf} rotarod behavioural phenotype at this age point in male mice (**Figure 32.6.C;** male 12 month UT^{Cln6nclf} mean rotarod score = 61.14 seconds; male 12 month Gemfib^{AAV9} mean score = 190.4 seconds; **** $p \leq .0005$; male 12 month CBD^{AAV9} mean score = 193.6 seconds; **** $p \leq .0001$; male 12 month Combo^{AAV9} mean score = 170.7 seconds; *** p = .0001**,** **Appendix B.108**).

In terms of linear regression, female combination therapy groups demonstrated a similar trend to males, with female Gemfib^{AAV9}, CBD^{AAV9} and Combo^{AAV9} animals declining at a significantly slower rate than female UT^{Cln6nclf} animals (**Figures 3.25.B, D** and **F**; **Appendices 104** and **107**). Combo^{AAV9} females were the first to demonstrate a significant difference from UT^{Cln6nclf} mice, with a significantly increased mean rotarod score at 9 months (Figure 3.26.B; female 9 month UT^{Cln6nclf} mean score = seconds; female 9 month Combo^{AAV9} mean score = seconds; * p = ; **Appendix B.109**). By 12 months of age, however, all three treatment groups were demonstrating significantly better mean rotarod scores than UT^{Cln6nclf} (female 12 month UT^{Cln6nclf} mean score = 71.25 seconds; female 12 month Gemfib^{AAV9} mean score = 230.4 seconds; **** $p \leq .0001$; female 12 month CBD^{AAV9} mean score = 209.2 seconds; **** $p \leq .0001$; female 12 month Combo^{AAV9} mean score = 251.4 seconds; **** $p \leq .0001$, **Appendix B.109**).

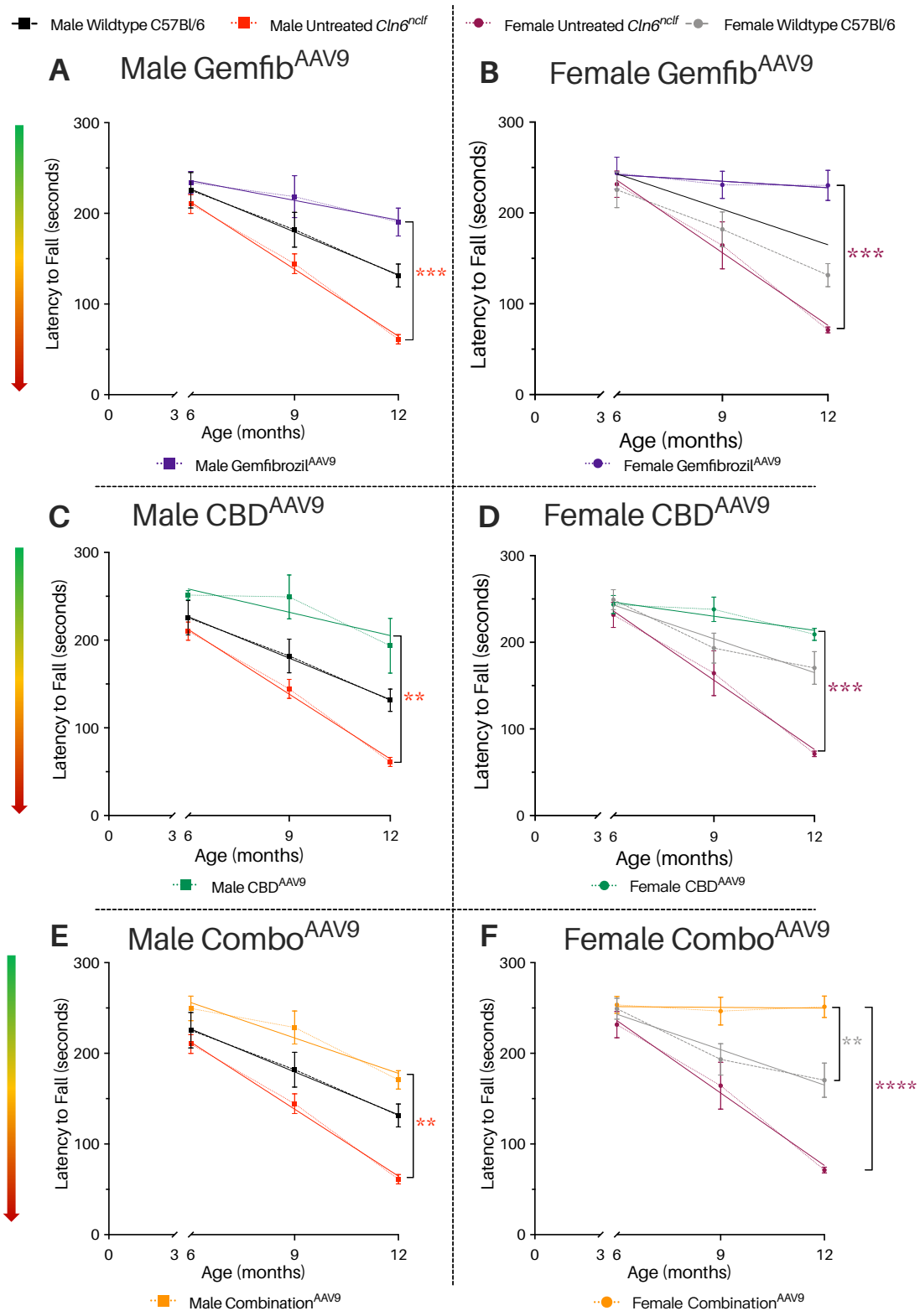
Male Wildtype C57Bl/6
Male Untreated Cln6nclf
Female Untreated Cln6nclf
Female Wildtype C57Bl/6
A Male GemfibAAV9
B Female GemfibAAV9
C Male CBDAAV9
D Female CBDAAV9
E Male ComboAAV9
F Female ComboAAV9
Latency to Fall (seconds)
Age (months)
0
3
6
9
12
100
200
300
***
**
****
Male GemfibrozilAAV9
Female GemfibrozilAAV9
Male CBDAAV9
Female CBDAAV9
Male CombinationAAV9
Female CombinationAAV9

⇐ **Figure 3.25 | Functional improvements in combination therapy mice: rotarod scores (line graphs; previous page).** *Cln6^{nclf} mice treated with a combination of gene and small molecule therapy (Gemfib^{AAV9}, CBD^{AAV9}, and Combo^{AAV9}) demonstrated significantly slower rates of motor co-ordination decline, as determined by rotarod scores, over a 12 month period than their age-matched untreated Cln6^{nclf} (UT^{Cln6nclf}) counterparts at 6, 9 and 12 months of age, regardless of gender and which type of small molecule therapy they received. Female Gemfib^{AAV9} and Combo^{AAV9} treatment groups even declined at a significantly slower rate than the age- and sex-matched WT (C57Bl/6) controls.* Data are presented as a line graph of mean scores (latency to fall, in seconds), with error bars = ± SEM. Different mice were tested at different time points, making this experiment between-subjects in design. Dotted lines indicate the expected mean score trajectory for an experimental group between measured time points. Solid lines represent the regression lines of each experimental group, as calculated via simple linear regression (**Appendices B.105-107**). A high score (~300) indicates a high level of motor co-ordination as measured by the rotarod, while lower scores correlate to increasing levels of motor dysfunction (coloured arrow on the left). **A.** Line graph presenting male mean Gemfib^{AAV9} (purple), UT^{Cln6nclf} (red) and WT (C67Bl/6; black) rotarod scores over 6, 9 and 12 months of age. Male mice treated with a combination of gene therapy and gemfibrozil had a significantly reduced rate of motor decline compared to UT^{Cln6nclf} counterparts (*** p =.0007; **Appendix B.107**). Starting n (per group) = 27-30. **B.** Line graph presenting female mean Gemfib^{AAV9} (purple), UT^{Cln6nclf} (maroon) and WT (C57Bl/6; black) rotarod scores over 6, 9 and 12 months of age. Female mice treated with a combination of gene therapy and gemfibrozil had a significantly reduced rate of motor decline compared to UT^{Cln6nclf} counterparts (*** p =.0002; **Appendix B.107**). Starting n (per group) = 23-32. **C.** Line graph presenting male mean CBD^{AAV9} (green), UT^{Cln6nclf} and WT rotarod scores over 6, 9 and 12 months of age. Male mice treated with gene therapy and CBD had a significantly reduced rate of motor decline compared to UT^{Cln6nclf} counterparts (** p = .0035; **Appendix B.107**). Starting n (per group) = 24-32. **D.** Line graph presenting female mean CBD^{AAV9} (green), UT^{Cln6nclf} and WT rotarod scores over 6, 9 and 12 months of age. Female mice treated with gene therapy and CBD had a significantly reduced rate of motor decline compared to UT^{Cln6nclf} counterparts (*** p = .0003; **Appendix B.107**). Starting n (per group) = 23-31. **E.** Line graph presenting male mean Combo^{AAV9} (orange), UT^{Cln6nclf} and WT rotarod scores over 6, 9 and 12 months of age. Male mice treated with gene therapy and a combination of gemfibrozil and CBD had a significantly reduced rate of motor decline compared to UT^{Cln6nclf} counterparts (** p = .0096; **Appendix B.107**). Starting n (per group) = 27-32. **F.** Line graph presenting female mean Combo^{AAV9} (orange), UT^{Cln6nclf} and WT rotarod scores over 6, 9 and 12 months of age. Feale mice treated with gene therapy and a combination of gemfibrozil and CBD had a significantly reduced rate of motor decline compared to UT^{Cln6nclf} counterparts (**** $p \leq .0001$; **Appendix B.107**). Starting n (per group) = 26-32.

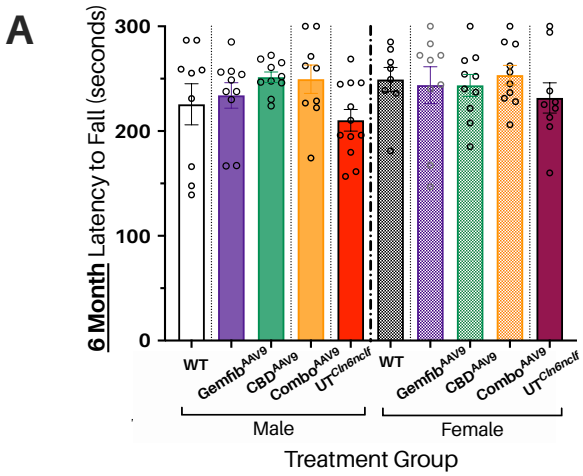
A
6 Month Latency to Fall (seconds)
300
200
100
0
WT
GemfibAAV9
CBDAAV9
ComboAAV9
UTCln6ncl
WT
GemfibAAV9
CBDAAV9
ComboAAV9
UTCln6ncl
Male
Female
Treatment Group

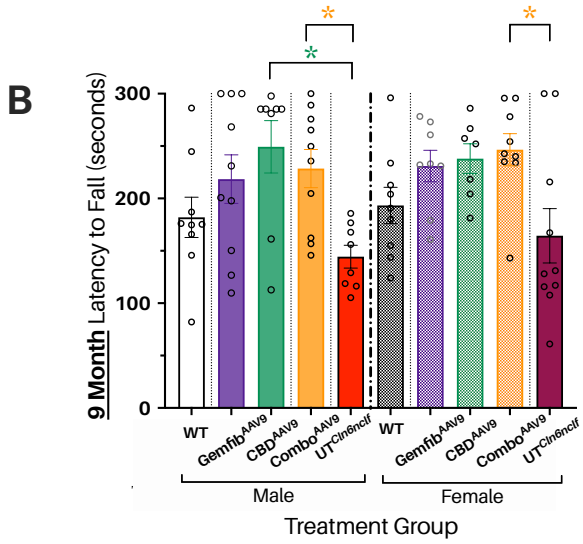
B
9 Month Latency to Fall (seconds)
300
200
100
0
*
*
*
WT
GemfibAAV9
CBDAAV9
ComboAAV9
UTCln6ncl
WT
GemfibAAV9
CBDAAV9
ComboAAV9
UTCln6ncl
Male
Female
Treatment Group

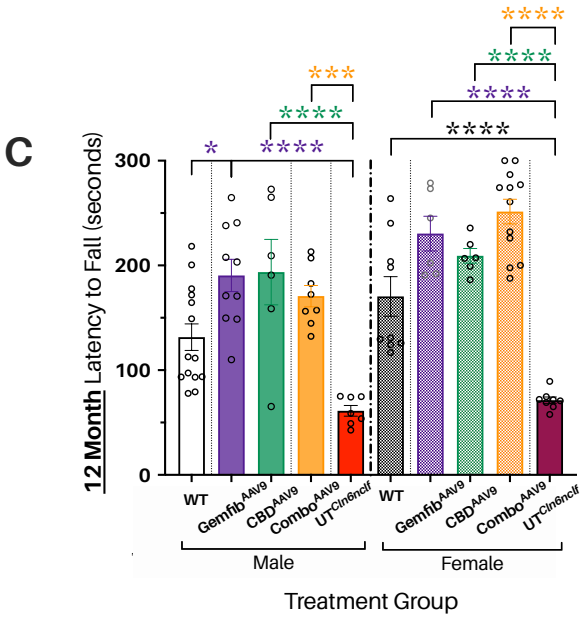
C
12 Month Latency to Fall (seconds)
300
200
100
0
***
****
*
****
****
****
****
WT
GemfibAAV9
CBDAAV9
ComboAAV9
UTCln6ncl
WT
GemfibAAV9
CBDAAV9
ComboAAV9
UTCln6ncl
Male
Female
Treatment Group

⇐ **Figure 3.26 | Functional improvements in combination therapy mice: rotarod scores (histograms; previous page).** *All three combinations of gene and small molecule therapy (Gemfib^{AAV9}, CBD^{AAV9} and Combo^{AAV9}) appear to protect both male and female Cln6^{nclf} mice from the diseased Cln6^{nclf} rotarod behavioural phenotype by 12 months of age.* Histograms presenting mean rotarod scores (latency to fall in seconds) of male (left; plain coloured bars) and female (right; patterned bars) *Cln6^{nclf}* mice treated a combination of gene therapy and either: gemfibrozil (Gemfib^{AAV9}), CBD (CBD^{AAV9}), or a combination of the two (Combo^{AAV9}) and their age- and gender-matched UT^{Cln6nclf} and WT (C57Bl/6) counterparts at 6 (**A**), 9 (**B**) and 12 (**C**) months of age. Data are presented as mean scores with error bars = ± SEM. Different mice were tested at each of the different time points, making the experiment between-subjects in design. All analyses were conducted using 1-way ANOVAs with Tukey's post-hoc comparisons used to elicit specific significant differences between experimental groups (**Appendix B.108-109**).Clear circles represent averaged individual mouse scores (3x trials per mouse). **A.** Mean male (left; plain coloured bars) and female (right; patterned coloured bars) rotarod scores (latency to fall in seconds) at 6 months. No differences, for either gender, were observed between the three different combination therapy *Cln6^{nclf}* groups (Gemfib^{AAV9}, CBD^{AAV9} or Combo^{AAV9}) and 'healthy' WT controls or UT^{Cln6nclf} counterparts at 6 months of age. n(per group per time point)= 6-12. **B.** Histogram presenting mean male (left; plain coloured bars) and female (right; patterned coloured bars) rotarod scores (latency to fall in seconds) at 9 months. Male CBD^{AAV9} and Combo^{AAV9} mice demonstrated significantly better rotarod scores than UT^{Cln6nclf} (male UT^{Cln6nclf} mean rotarod score = 144.4 seconds; male CBD^{AAV9} mean rotarod score = 249.2 seconds; * p = .0105; male Combo^{AAV9} mean rotarod score = 228.5 seconds; * p = .0418; **Appendix 108**). Female Combo^{AAV9} mice also demonstrated significantly better rotarod scores than UT^{Cln6nclf} at 9 months (female UT^{Cln6nclf} mean rotarod score = seconds; female Combo^{AAV9} mean rotarod score = seconds; * p = ; **Appendix B.109**). No other significant differences were present between groups at 9 months. n(per group) = 7-10. **C.** Histogram presenting mean male (left; plain coloured bars) and female (right; patterned coloured bars) rotarod scores (latency to fall in seconds) at 12 months. All three combination therapy experimental groups were demonstrating significantly higher rotarod scores than UT^{Cln6nclf} mice, regardless of gender, by 12 months (male UT^{Cln6nclf} mean rotarod score = 61.14 seconds; male Gemfib^{AAV9} mean rotarod score = 190.4 seconds; **** $p \leq .0005$; male CBD^{AAV9} mean rotarod score = 193.6 seconds; **** $p \leq .0001$; male Combo^{AAV9} mean rotarod score = 170.7 seconds; *** p = .0001, **Appendix B.108**; female UT^{Cln6nclf} mean rotarod score = 71.25 seconds; female Gemfib^{AAV9} mean rotarod score = 230.4 seconds; **** $p \leq .0001$; female CBD^{AAV9} mean rotarod score = 209.2 seconds; **** $p \leq .0001$; female Combo^{AAV9} mean rotarod score = 251.4 seconds; **** $p \leq .0001$, **Appendix B.109**). n(per group) = 6-12.

3.4.2 Functional improvements in combination therapy mice: ***ataxia***

In order to characterise the effects combined gene and small molecule therapy might have on the Cln6^{nclf} ataxic behavioural phenotype, ten different experimental groups were assessed for signs of cerebellar ataxia at 6 and 9 months of age. Ataxia phenotyping scores for the combination therapy Cln6^{nclf} experimental groups were found to have normal (Gaussian) distributions using D'Agostino & Pearson normality tests, so all subsequent statistical analyses were conducted using parametric testing (**Appendix B.102**).

3.4.2.a Composite ataxia phenotype scores

Composite ataxia scores (0-9) for each mouse were calculated by adding together it's mean ledge, hindlimb clasping and gait ataxia phenotyping scores (0-3). Individual mouse composite ataxia scores were then averaged for each experimental group and presented as mean score (0-9) ± SEM. Comparisons between mean composite scores of age- and sex-matched Gemfib^{AAV9}, CBD^{AAV9}, Combo^{AAV9} treated and UT^{Cln6nclf} and WT mice were made using 1-way ANOVAs, with Tukey's post-hoc multiple comparisons tests conducted when significant differences were found to occur (**Appendices B.110-111**).

Male Combo^{AAV9} and CBD^{AAV9} treated mice demonstrated significantly improved (lower) composite ataxia scores than age- and sex-matched UT^{Cln6nclf} mice as early as 6 months of age (**Figure 3.27.Ai-ii**; . male 6 month UT^{Cln6nclf} mean score = 2.467; male 6 month CBD^{AAV9} mean score = 1.074; * p = .0431; **Appendix B.110**). The only female combination treatment group to demonstrate a significant difference in mean composite ataxia score at this time point was Combo^{AAV9}, which demonstrated a significantly lower score than UT^{Cln6nclf} mice (**Figure 3.27.Bi-ii**; female 6 month UT^{Cln6nclf} mean score= 3.00; female 6 month Gemfib^{PBS} mean score = 1.0; ** p = .0099; **Appendix B.111**).

By 12 months of age all combination treatments, male and female, demonstrated significantly lower (better) scores than age- and sex-matched UT^{Cln6nclf} mice, indicating that all three treatments (Gemfib^{AAV9}, Combo^{AAV9} and CBD^{AAV9}) could potentially confer some protection to Cln6^{nclf} mice from the diseased Cln6^{nclf} composite ataxia phenotype at this late stage in disease progression (**Figures 3.27.Ai-ii** and **3.27.Bi-ii**; male 12 month UT^{Cln6nclf} mean score = 4.833; male 12 month Gemfib^{AAV9} mean score = 2.433; **** p = .0008; male 12 month CBD^{AAV9} mean score = 2.708; ** p = .0059; male 12 month Combo^{AAV9} mean score = 2.667; ** p = .0027; **Appendix B.110**; female 12 month UT^{Cln6nclf} mean score = 5.0; female 12 month Gemfib^{AAV9} mean score = 2.250; **** $p \leq .0001$; female 12 month CBD^{AAV9} mean score = 2.0; ** **** $p \leq .0001$; female 12 month Combo^{AAV9} mean score = 1.963; **** $p \leq .0001$; **Appendix B.11**).

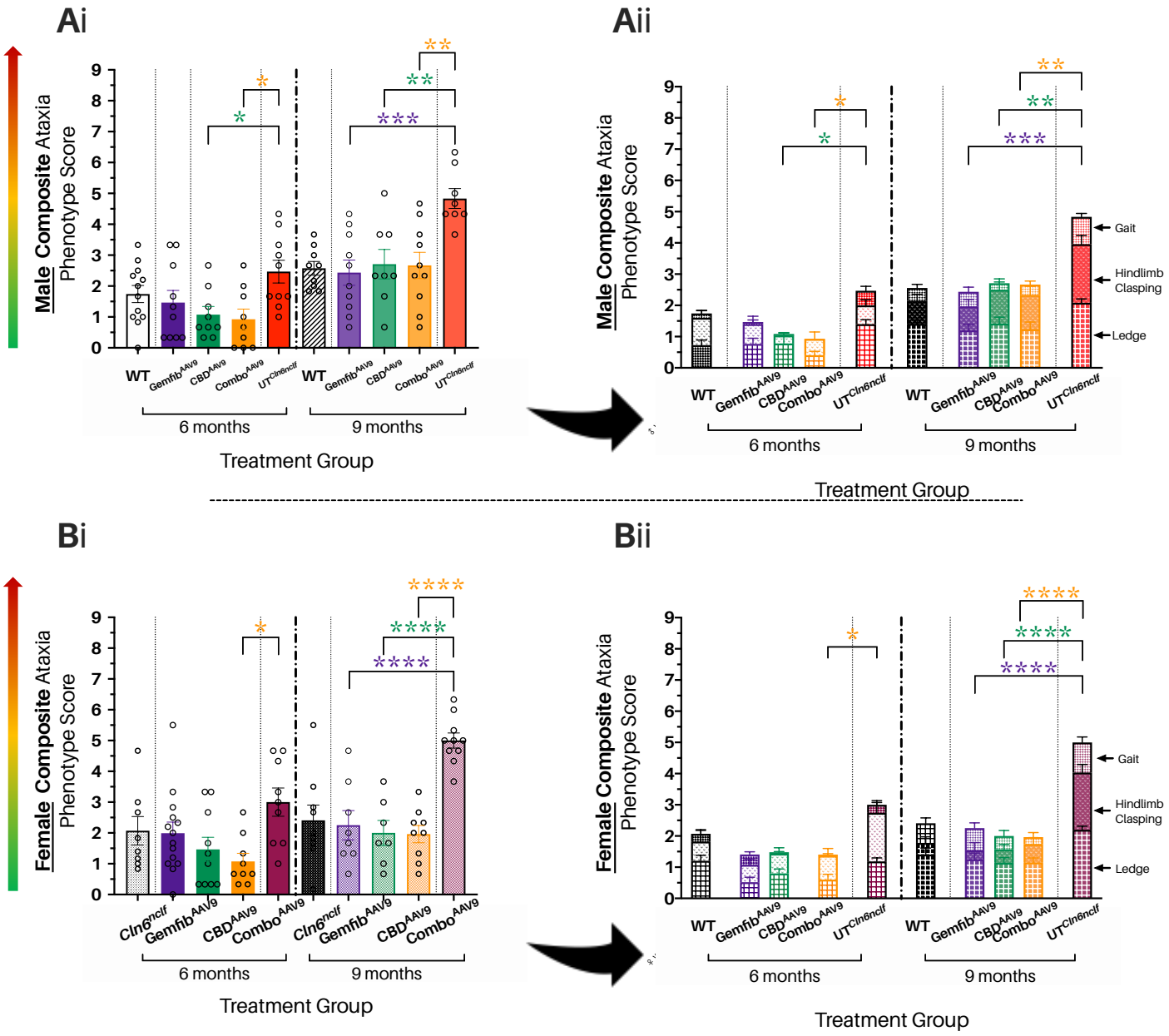
Ai
Male Composite Ataxia Phenotype Score
WT
GemfibAAV9
CBDAAV9
ComboAAV9
UTCln6ncl
6 months
9 months
Treatment Group
Aii
Gait
Hindlimb Clasping
Ledge
Bi
Female Composite Ataxia Phenotype Score
Cln6ncl
Bii

⇐ **Figure 3.27 | Functional improvements in combination therapy mice: composite ataxia scores (previous page).** *All three combinations of gene and small molecule therapy (Gemfib^{AAV9}, CBD^{AAV9} and Combo^{AAV9}) appear to protect both male and female Cln6^{nclf} mice from the diseased Cln6^{nclf} composite ataxia behavioural phenotype by 9 months of age.* Mean composite ataxia phenotype scores (0 to 9) were calculated using averaged ataxia test individual scores (ledge, hindlimb clasping and gait) for male (**Ai-ii**) and female (**Bi-ii**) *Cln6^{nclf}* mice treated with gene therapy and one of three drug regimens: gemfibrozil (Gemfib^{AAV9}), CBD (CBD^{AAV9}) or a combination of gemfibrozil and CBD (Combo^{AAV9}), and their untreated *Cln6^{nclf}* (UT^{Cln6nclf}) and wildtype (WT) C57Bl/6 counterparts across two different time points: 6 months (left) and 9 months (right). Different mice were tested at each time point (between-subjects study design). A low score (close to 0) indicates an absence of the ataxic phenotype as measured by the composite scoring system, while higher scores, closer to 9, indicate increasing levels of ataxic behaviour (coloured arrow on the left). The overall mean composite scores illustrated in **Ai** and **Bi** are further broken down into the average ledge (bottom segment), hindlimb clasping (middle segment) and gait (top segment) scores in segmented bar graphs (**Aii** and **Bii**). Individual, averaged composite scores are shown as clear circles in Ai and Bi, error bars = ± SEM. Analyses were conducted via 1-way ANOVAs and subsequent Tukey's multiple comparison post-hoc tests (**Appendices B.24-25**). n(per group per time point) = 7-14. **Ai-ii.** Histogram presenting the mean composite ataxia scores of male mice at 6 (left) and 9 (right) months of age. Male CBD^{AAV9} mice demonstrated a significantly better (lower) composite ataxia score than age- and sex-matched UT^{Cln6nclf} counterparts at 6 months of age (UT^{Cln6nclf} mean score = 2.467; CBD^{AAV9} mean score = 1.074; * p = .0431; **Appendix B.110**). Similarly, Combo^{AAV9} mice also performed significantly better than UT^{Cln6nclf} at 6 months (Combo^{AAV9} mean score = 0.9259; * p = 0.0196; **Appendix B.110**). At 9 months of age all three gene therapy and drug treated groups were performing significantly better than UT^{Cln6nclf} mice (UT^{Cln6nclf} mean score = 4.833; Gemfib^{AAV9} mean score = 2.433; **** p = .0008; CBD^{AAV9} mean score = 2.708; ** p = .0059; Combo^{AAV9} mean score = 2.667; ** p = .0027; **Appendix B.110**). n (per group, per time point) = 8-12 **Bi-ii.** Histogram presenting the mean composite ataxia scores of female mice at 6 (left) and 9 (right) months of age. Female Combo^{AAV9} Cln6^{nclf} mice performed better (significantly lower composite ataxia score) than UT^{Cln6nclf} at 6 months of age (UT^{Cln6nclf} mean score= 3.00; Gemfib^{PBS} mean score = 1.0; ** p = .0099; **Appendix B.111**). There was no significant difference in the composite scores of Gemfib^{AAV9} or CBD^{AAV9} female mice and their UT^{Cln6nclf} and WT counterpoints at 6 months. At 9 months (left), all three gene therapy and drug treatment groups (Gemfib^{AAV9}, CBD^{AAV9} and Combo^{AAV9}) were performing significantly better than UT^{Cln6nclf} mice (UT^{Cln6nclf} mean score = 5.0; Gemfib^{AAV9} mean score = 2.250; **** $p \leq .0001$; CBD^{AAV9} mean score = 2.0; ** **** $p \leq .0001$; Combo^{AAV9} mean score = 1.963; **** $p \leq .0001$; **Appendix B.111**). n (per group, per time point) = 7-14.

3.4.2.b Ledge test

Combo^{AAV9} treated male mice demonstrated a significantly lower (better) ledge score than age- and sex-matched UT^{Cln6nclf} counterparts as early as 6 months of age (**Figure 3.28.A**; male 6 month Combo^{AAV9} mean score = 0.4074; male 6 month UT^{Cln6nclf} mean score = 1.400; ** p = .0032; **Appendix B.112**). At 9 months, Combo^{AAV9} treated mice continue to maintain a significantly lower ledge score than UT^{Cln6nclf} (**Figure 3.28.A**; 9 month male UT^{Cln6nclf} mean score = 2.083; male 9 month Combo^{AAV9} mean ledge ataxia score = 1.233; * p = .0233; **Appendix B.112**). At this time point, male Gemfib^{AAV9} mice also begin to demonstrate a significantly

improved mean score when compared to UT^{Cln6nclf} (**Figure 3.28.A**; male 9 month Gemfib^{AAV9} mean score = 1.2; * *p* = .0161; **Appendix B.112**).

Gemfib^{AAV9} females peform well in the ledge ataxia task at 6 months of age, demonstrating a mean ledge score that was significantly lower (better) than both UT^{Cln6nclf} and WT controls (**Figure 3.28.B**; female 6 month Gemfib^{AAV9} mean score = 0.5185; female 6 month WT mean score = 1.204; * *p* = .0325; female 6 month UT^{Cln6nclf} mean score = 1.185; * *p* = .0320; **Appendix B.113**).

3.4.2.c Hindlimb clasping test

Mice treated with both gene therapy and either gemfibrozil, CBD or a combination of the two drugs, had their muscle function and control assessed via the hindlimb clasping test. Different mice were measured at each time point, making this assay between-subjets in design. Data are mean hindlimb clasping scores ± SEM.

In male mice (**Figure 3.28.C**), the first and only significant difference in mean hindlimb clasping score was observed at 9 months, with Gemfib^{AAV9} mice retracting their limbs to the abdomen more often and more consistently than age- and sex-matched UT^{Cln6nclf} counterparts (1-way ANOVA; male 12 month Gemfib^{AAV9} mean score = 0.7667;male 12 month UT^{Cln6nclf} mean score = 1.875; * *p* = .0258; **Appendix B.114**).

Female mice treated with a combination of gene and small molecule therapy (**Figure 3.28.D**) also failed to demonstrate a significant difference in mean hindlimb clasping score until 9 months of age. At 9 months, however, all three treatment groups performed significantly better (lower score) that age- and sex-matched UT^{Cln6nclf} mice (female 12 month UT^{Cln6nclf} mean score = 1.950; female 12 month Gemfib^{AAV9} mean score = 0.2917; **** *p* ≤

.0001; female 12 month CBD^{AAV9} mean score = 0.4286; *** p = .0003; female 12 month Combo^{AAV9} mean score = 0.5926; **** p = .0006; **Appendix B.115**).

3.4.2.d Gait test

Motor co-ordination and muscle function, as determined by a low score in the gait test, was assessed in Cln6^{nclf} mice treated with both gene therapy and either gemfibrozil, CBD or a combination of the two drugs, (**Figures 3.28.E** and **3.28.F**). Different mice were assessed at each time point (6 and 9 months), making the assay between subjects in design. Data are mean gait ataxia scores ± SEM.

All three male combination therapy groups (Gemfib^{AAV9}, CBD^{AAV9} and Combo^{AAV9}) performed significantly better at the gait ataxia test than age- and sex-matched UT^{Cln6nclf} controls at 6 months of age (**Figure 3.28.E**; male 6 month UT^{Cln6nclf} mean score = 0.4667; male 6 month Gemfib^{AAV9} mean score = 0.06667; * p = .0168; male 6 month CBD^{AAV9} mean score = 0.0370; * p = .0112; male 6 month Combo^{AAV9} mean score = 0.0; ** p = .0049 ; **Appendix B.116**). At 9 months, however, only Combo^{AAV9} and CBD^{AAV9} treated male animals continued to perform significantly better than UT^{Cln6nclf} mice (**Figure 3.28.E;** male 9 month UT^{Cln6nclf} mean score = 0.8750; male 9 month CBD^{AAV9} mean score = 0.2083; * p = .0105; male 9 month Combo^{AAV9} mean score = 0.3333; * p = 0.0380; **Appendix B.116**). For females, only Combo^{AAV9} mice at 9 months of age demonstrated an improved gait ataxic phenotype compared to UT^{Cln6nclf} counterparts (**Figure 3.28.F**; female 9 month Combo^{AAV9} mean score = 0.2222; female 9 month UT^{Cln6nclf} mean score = 0.9667; * p = .0189; **Appendix B.117**).

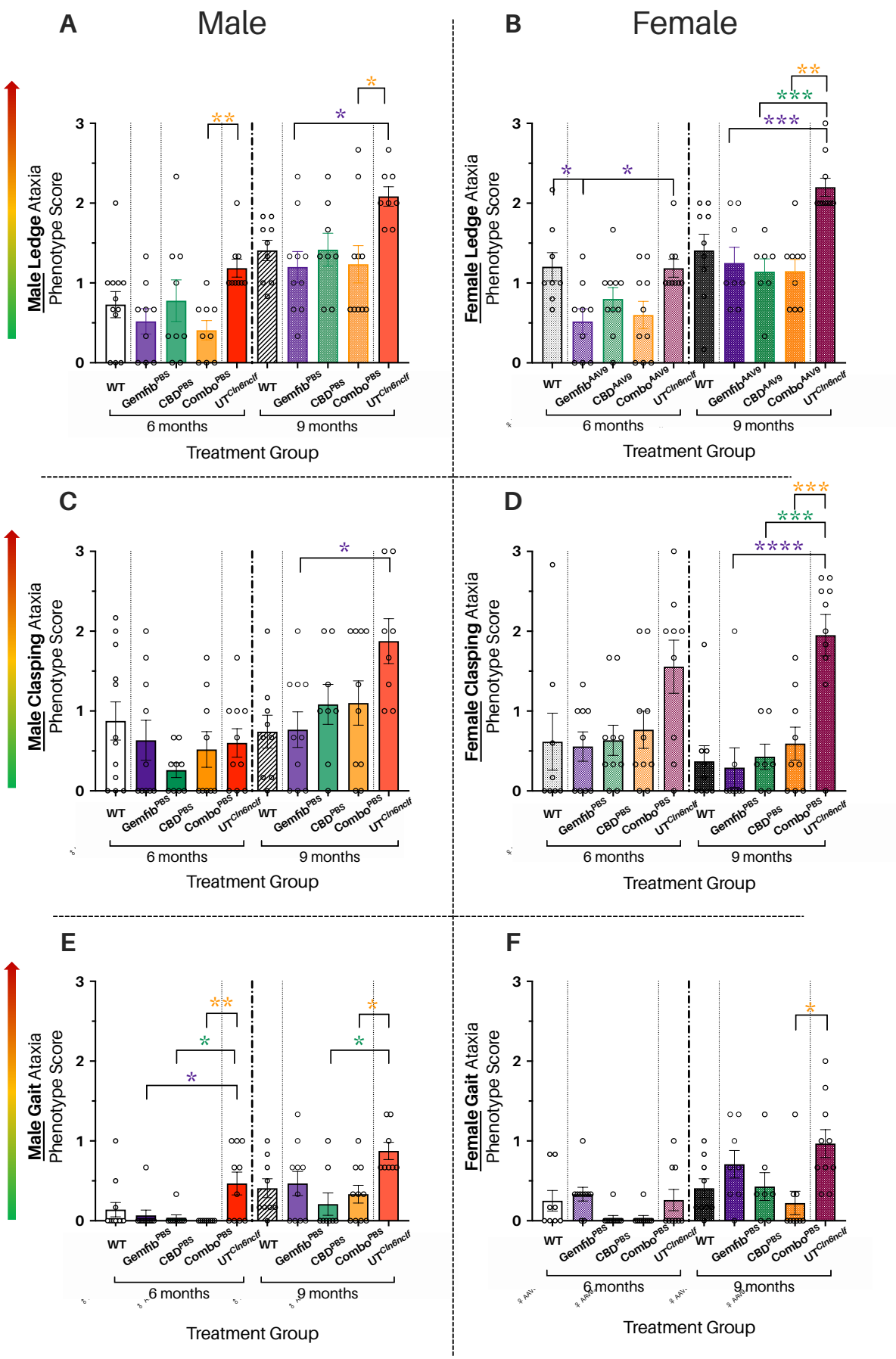
A
Male
B
Female
Male Ledge Ataxia Phenotype Score
Female Ledge Ataxia Phenotype Score
C
D
Male Clasping Ataxia Phenotype Score
Female Clasping Ataxia Phenotype Score
E
F
Male Gait Ataxia Phenotype Score
Female Gait Ataxia Phenotype Score
WT
GemfibPBS
CBDPBS
ComboPBS
UTCln6ncl/f
GemfibAAV9
CBDAAV9
ComboAAV9
6 months
9 months
Treatment Group

⇐ **Figure 3.28 | Functional improvements in combination therapy mice: ataxia phenotyping scores (previous page).** *Female Cln6^{nclf} mice treated with both gene therapy and combination small molecule therapy (Combo^{AAV9}) appear to be consistently protected from the diseased Cln6^{nclf} ataxia phenotype across all three ataxia assays (the ledge, hindlimb clasping and gait tests) by 9 months of age, while the other combined gene and small molecule therapy treatment groups (male Combo^{AAV9}, plus both male and female Gemfib^{AAV9} and CBD^{AAV9}) show varied differences in score from untreated Cln6^{nclf} (UT^{Cln6nclf}) mice across the different tests and time points (6 and 9 months).* Histograms presenting mean ataxia scores (0-3) for individual ataxia assays: ledge (**A**; males; **B**; females), hindlimb clasping (**C**; males; **D**; females), and gait (**E**; males; **F**; females). Scoring criteria and methodology can be found in **Chapter 2**, adapted from *Guyenet et al. 2010*. Different mice were assessed at each time point, making the experiment between-subjects in design. For each assay, a mouse could be assigned a score between 0 and 3, with 0 indicating a complete absence of the ataxic phenotype and 3 indicating a completely penetrant ataxic phenotype (coloured arrows on the left). Data are presented as mean scores, with error bars representing ± SEM. Individual (averaged) mouse scores are presented as clear circles. All analyses were conducted using 1-way ANOVAs (**Appendices B.112-117**), followed by Tukey's multiple comparisons post-hoc tests **A.** Histogram presenting mean male ledge scores for 6 months (left; darker coloured bars) and 9 months (right; lighter coloured bars) of age. No significant difference in ledge score was detected between male drug Gemfib^{AAV9} or CBD^{AAV9} mean ledge scores and their UT^{Cln6nclf} (red) and WT (C57Bl/6, white) counterparts at 6 months of age. Male Combo^{AAV9} treated mice, however, demonstrated a significantly better (lower) mean ledge ataxia score than UT^{Cln6nclf} mice at this time point (Combo^{AAV9} mean score = 0.4074; UT^{Cln6nclf} mean score = 1.400; ** p = .0032; **Appendix B.112**). At 9 months of age, CBD^{AAV9}'s mean ledge ataxia score remained statistically indistinguishable from both UT^{Cln6nclf} or WT mice. In comparison, male Gemfib^{AAV9} and Combo^{AAV9} treated mice demonstrate significantly better (lower) mean ledge scores at 9 months than UT^{Cln6nclf} mice (UT^{Cln6nclf} mean score = 2.083; Gemfib^{AAV9} mean score = 1.2; * p = .0161; Combo^{AAV9} mean score = 1.233; * p = .0233; **Appendix B.112**). n(per group per time point) = 8-12. **B.** Histogram presenting mean female ledge scores for 6 months (left; lighter coloured bars) and 9 months (right; darker coloured bars) of age. At 6 months the only significant difference in mean scores was between Gemfib^{AAV9} (mean score = 0.5185) and WT (WT mean score = 1.204); * p = .0325) and UT^{Cln6nclf} (UT^{Cln6nclf} mean score = 1.185; * p = .0320; **Appendix B.113**) scores. At 9 months, however, all three female gene therapy and drug-treated groups (Gemfib^{AAV9}, CBD^{AAV9} and Combo^{AAV9}) were performing significantly better than age- and sex-matched UT^{Cln6nclf} counterparts (UT^{Cln6nclf} mean score = 2.200; Gemfib^{AAV9} mean score = 1.250; ** p = .0018; CBD^{AAV9} mean score = 1.143; *** p = .0007; Combo^{AAV9} mean score = 1.148 *** p = .0003; **Appendix B.113**). n(per group per time point) = 7-10. **C.** Histogram presenting mean male hindlimb clasping ataxia scores for 6 (left; dark coloured bars) and 9 months of age (right; light coloured bars). No significant differences were found between any male experimental groups at 6 months of age (**Appendix B.114**). At 9 months, however, male Gemfib^{AAV9} treated mice were performing significantly better (lower score) than their age- and sex-matched UT^{Cln6nclf} counterparts (Gemfib^{AAV9} mean score = 0.7667; UT^{Cln6nclf} mean score = 1.875; * p = .0258; **Appendix B.114**). No other differences between gene therapy and drug treated groups and healthy or diseased controls was found at this time point. n(per group per time point) = 8-12. **D.** Histogram presenting mean female hindlimb clasping ataxia scores for 6 (left; dark coloured bars) and 9 (right; light coloured bars) of age. No significant differences in mean hindlimb clasping ataxia scores were detected between the mean scores of AAV and drug treated groups (Gemfib^{AAV9}, CBD^{AAV9} and Combo^{AAV9}) and age- and sex-matched WT or UT^{Cln6nclf} at 6 months of age (**Appendix B.115**). At 9 months, however, all three female AAV and drug treated groups were demonstrating significantly better (lower) hindlimb clasping scores than their age- and sex- matched UT^{Cln6nclf} counterparts (UT^{Cln6nclf} mean score = 1.950; Gemfib^{AAV9} mean score = 0.2917; **** $p \leq .0001$; CBD^{AAV9} mean score = 0.4286; *** p = .0003; Combo^{AAV9} mean score = 0.5926; **** p = .0006; **Appendix B.115**). n(per group per time point) = 7-10. **E.** Histogram presenting mean male gait ataxia scores at 6 (left; dark coloured bars) and 9 (right; light coloured bars) of age. All three male AAV and drug treated groups (Gemfib^{AAV9}, CBD^{AAV9} and Combo^{AAV9}) performed significantly better (lower scores) than UT^{Cln6nclf} counterparts at 6 months of age (UT^{Cln6nclf} mean score = 0.4667; Gemfib^{AAV9} mean score = 0.06667; * p = .0168; CBD^{AAV9} mean score = 0.0370; * p = .0112; Combo^{AAV9} mean score = 0.0; ** p = .0049 ; **Appendix B.116**). At 9 months, however, only male CBD^{AAV9} and Combo^{AAV9} groups presented significantly better (lower) scores than UT^{Cln6nclf} mice (UT^{Cln6nclf} mean score = 0.8750; CBD^{AAV9} mean score = 0.2083; * p = .0105; Combo^{AAV9} mean score = 0.3333; * p = 0.0380; **Appendix B.116**). n(per group per time point) = 8-12. **F.** Histogram presenting mean female gait ataxia scores at 6 (left; light coloured bars) and 9 months (right; dark coloured bars) of age. No significant differences in mean gait ataxia scores were detected between any female treatment groups at 6 months of age (**Appendix B.117**). At 9 months female Combo^{AAV9} treated mice performed significantly better than their age- and sex-matched UT^{Cln6nclf} counterparts (Combo^{AAV9} mean score = 0.2222; UT^{Cln6nclf} mean score = 0.9667; * p = .0189; **Appendix B.117**). No other significant differences were detected between treatment groups at this time point. n(per group per time point) = 7-10.

3.4.3 Functional improvements in combination therapy mice: ***survival and weight***

The survival curves (and median survival) of mice treated with gene therapy and either gemfibrozil, CBD and a combination of the two drugs were compared to WT and UT^{Cln6nclf} controls. Survival data are presented as percentage of the original cohort n, with curve comparisons between sex-matched Cln6^{nclf} and WT conducted via separate log-rank (Mantel-Cox) tests for each sex (**Appendices B.118-129**).

All male combination treated groups had significantly improved survival in comparison to UT^{Cln6nclf} mice (**Figure 3.29.A**) – with all three groups having 'undefined' median survivals at 14 months of age – meaning there had not been enough 'unplanned' deaths within the experimental group to determine a median survial by that time point (male UT^{Cln6nclf} median survival = 13.3 months; male Gemfib^{AAV9} median survival = undefined at 14 months; **** $p \leq .0001$; male CBD^{AAV9} median survival = undefined at 14 months; *** $p = .0013$; male Combo^{AAV9} median survival = undefined at 14 months; **** $p \leq .0001$; **Appendices B.118-123**).

Female survival demonstrated a similar trend (**Figure 3.29.B**). All combination treatment groups had significantly longer lifespans than UT^{Cln6nclf} mice (UT^{Cln6nclf} median survival = 12.5 months; Gemfib^{AAV9} median survival = undefined at 14 months; **** $p \leq .0001$; CBD^{AAV9} median survival = undefined at 14 months; ** $p = .0040$; Combo^{AAV9} median survival = undefined at 14 months; **** $p \leq .0001$; **Appendices B.124- 129**), indicating that all three combination treatments are potentially effective in protecting Cln6^{nclf} mice against the characteristically shortened Cln6^{nclf} lifespan phenotype.

Weights were also kept, as a measure of overall health, and body weight was recorded weekly (in grams). Average weights for each experimental group are presented here, however, monthly as it gives a clearer overview of weight progression throughout the lifespan. Simple

linear regression was conducted to determine the overall rate of weight change over the first 14 months of the trial. In males, Gemfib^{AAV9} and Combo^{AAV9} treated mice gained and lost weight in a fluctuating manner, resulting in significant differences in overall rate of weight gain and loss from both UT^{Cln6nclf} and WT mice (**Figure 3.30.A**; **Appendix B.130**). The only significant difference in mean male weights observed via 1-way ANOVA at 6, 9 or 12 months, however, was at 9 months, where CBD^{AAV9} and Combo^{AAV9} both demonstrated significantly lower weights, on average, than WT controls (**Figure 3.30.E**; male 9 month WT mean weight = 38.57 g; male 9 month CBD^{AAV9} mean weight = 36 g; * p = .0290; male 9 month Combo^{AAV9} mean weight = 34.53 g; *** p = .0001; **Appendix B.132**). At every other time point there were no significant differences detected between the mean weights of any of the male combined treatment groups and either WT or UT^{Cln6nclf} mice.

Females receiving Gemfib^{AAV9} or Combo^{AAV9} also appear to have gained and loss weight in a fluctuating manner, with their linear regression lines differing significantly from both UT^{Cln6nclf} mice and WT (**Figure 3.30.B**; **Appendix B.131**). All three female combination treatment groups demonstrated significantly lighter weights than age- and sex-matched WT controls at 6 months (**Figure 3.30.D**; **Appendix B.133**), but only Gemfib^{AAV9} and Combo^{AAV9} maintained significantly lighter mean weights by 9 months of age (**Figure 3.30.F**; female 9 month WT mean weight = 28.90 g; female 9 month Gemfib^{AAV9} mean weight = 26.05g; ** p = .0059; female 9 month Combo^{AAV9} mean weight = 26.32 g; * p = .0126; **Appendix B.133)**. There were no significant differences in mean weights for any treatment group by 12 months (**Figure 3.30.H**).

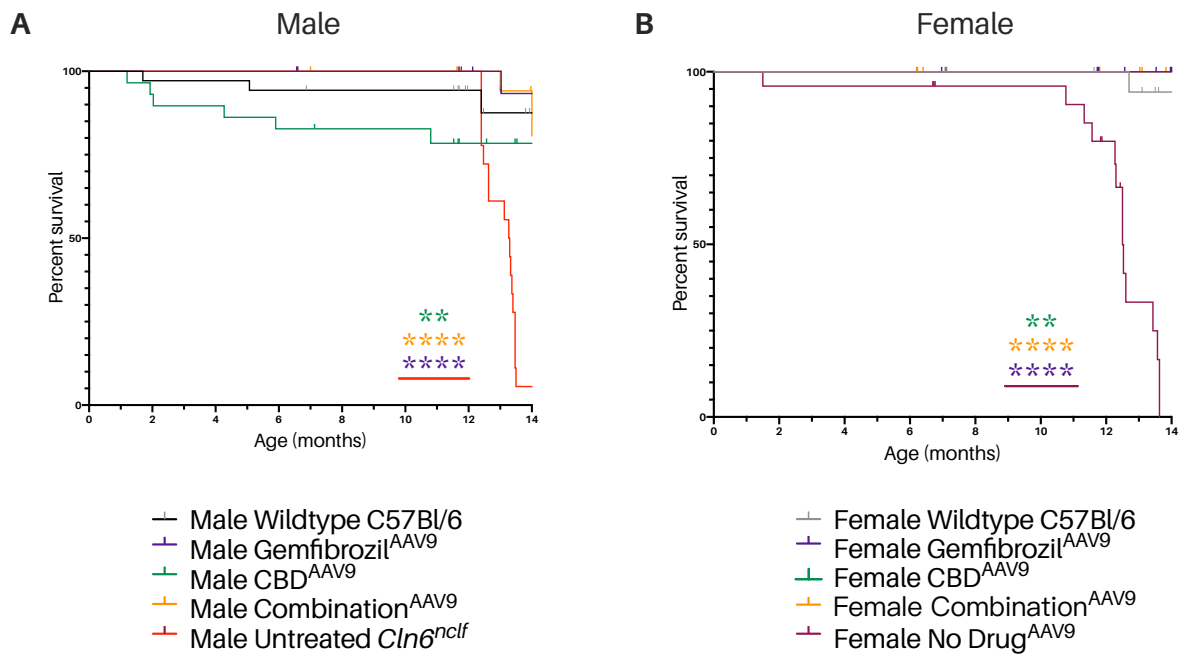

Figure 3.29 | Functional improvements in combination therapy mice: survival. *When given with scAAV9.CB.hCLN6 gene therapy, CBD (CBD^{AAV9}), gemfibrozil (Gemfib^{AAV9}), and combination (Combo^{AAV9}) small molecule therapies rescue Cln6^{nclf} mice from characteristically shortened lifespans.* Kaplan-Meier survival plots (%) comparing the survival curves of wildtype (WT; C57Bl/6; male = black lines; female = grey lines) and untreated *Cln6^{nclf}* mice (UT^{Cln6nclf} ; male = red lines; female = maroon lines) to *Cln6^{nclf}* mice treated with both gene therapy and one of three small molecule therapy regimens (Gemfib^{AAV9} = purple lines; CBD^{AAV9} = green lines; Combo^{AAV9} = orange lines). All survival curve comparisons were conducted using a log rank (Mantel-Cox) test in GraphPad Prism 8 (**Appendices B.118-129**). **A.** Male survival curves (%) from birth to 14 months of age. All three gene therapy and drug treatment groups (Gemfib^{AAV9}, CBD^{AAV9} and Combo^{AAV9}) demonstrated significantly improved survival compared to UT^{Cln6nclf} mice (UT^{Cln6nclf} median survival = 13.3 months; Gemfib^{AAV9} median survival = undefined at 14 months; **** $p \leq .0001$; CBD^{AAV9} median survival = undefined at 14 months; *** $p = .0013$; Combo^{AAV9} median survival = undefined at 14 months; **** $p \leq .0001$; **Appendices B.118-123**) Starting n = 27-35**. B.** Female survival curves (%) from birth to 14 months of age. All three gene therapy and drug treatment groups (Gemfib^{AAV9}, CBD^{AAV9} and Combo^{AAV9}) demonstrated significantly improved survival compared to UT^{Cln6nclf} mice (UT^{Cln6nclf} median survival = 12.5 months; Gemfib^{AAV9} median survival = undefined at 14 months; **** $p \leq .0001$; CBD^{AAV9} median survival = undefined at 14 months; ** $p = .0040$; Combo^{AAV9} median survival = undefined at 14 months; **** $p \leq .0001$; **Appendices B.124- 129**). Starting n = 22-28.

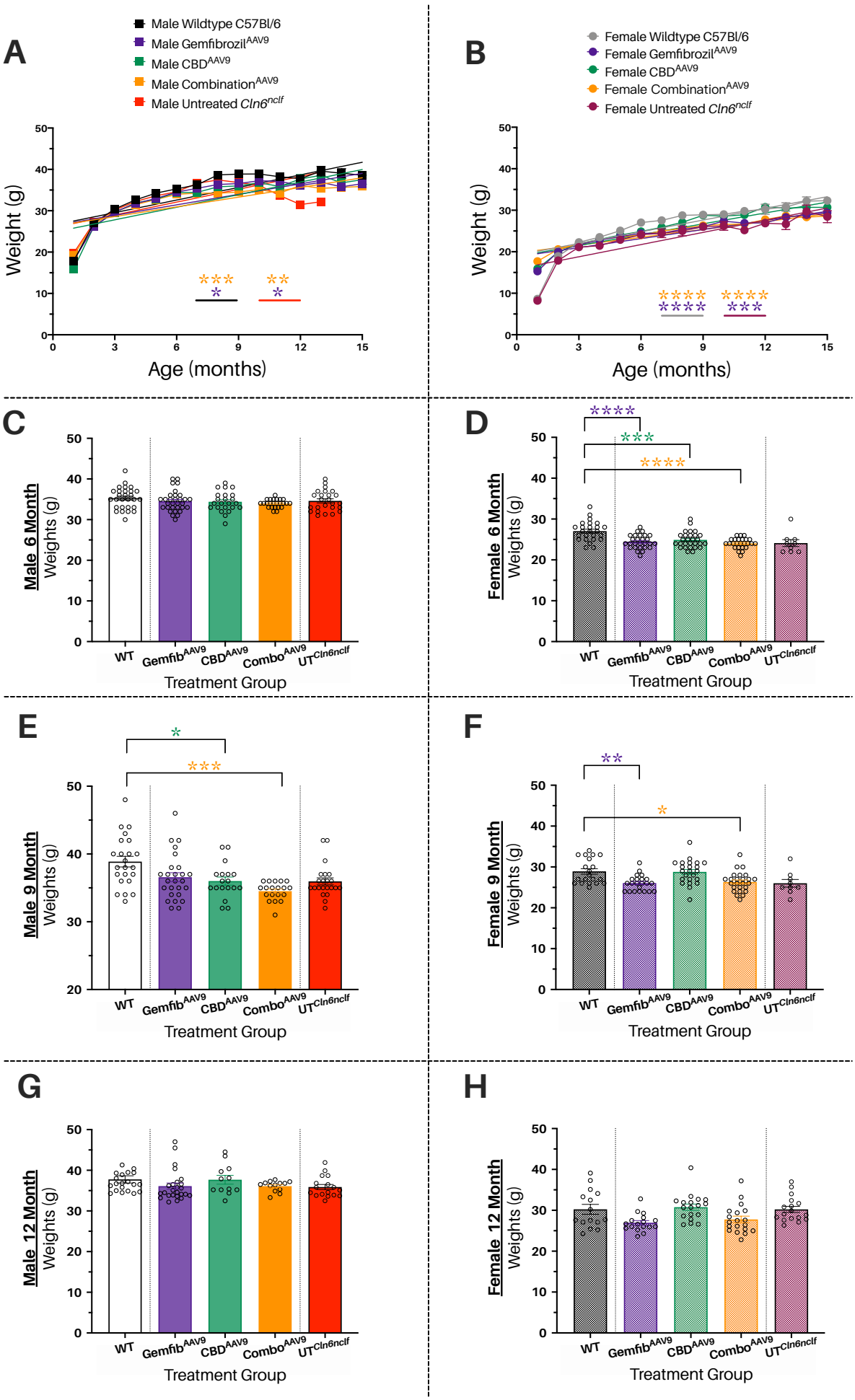
A
Male Wildtype C57Bl/6
Male Gemfibrozil AAV9
Male CBD AAV9
Male Combination AAV9
Male Untreated Cln6 nclf
Weight (g)
Age (months)
B
Female Wildtype C57Bl/6
Female Gemfibrozil AAV9
Female CBD AAV9
Female Combination AAV9
Female Untreated Cln6 nclf
Weight (g)
Age (months)
C
Male 6 Month Weights (g)
WT
Gemfib AAV9
CBD AAV9
Combo AAV9
UT Cln6nclf
Treatment Group
D
Female 6 Month Weights (g)
Treatment Group
E
Male 9 Month Weights (g)
Treatment Group
F
Female 9 Month Weights (g)
Treatment Group
G
Male 12 Month Weights (g)
Treatment Group
H
Female 12 Month Weights (g)
Treatment Group

⇐ **Figure 3.30 | Functional improvements in combination therapy mice: weights (opposite page)**. *Small molecule therapy, given in combination with sc.AAV9.CB.hCLN6 gene therapy, appears to have sexually dimorphic effects on the weights of Cln6^{nclf} mice during the first fourteen months of life.* Mice were weighed weekly from weaning (~28 days) to determine drug dosage and as a measure of general health. Weights are shown here from weaning to 15 months due to the time constraints of an MSc (weights continued to be tracked for the entire duration of the trial). Data are presented as average weights, error bars ± SEM. Analyses conducted via 1-way ANOVA with Tukey's multiple comparisons post-hoc tests where applicable. **A.** Average male weights, in grams, over 14 months (line graph). Linear regression lines are represented by solid coloured lines. Simple linear regression revealed that the overall rate of weight gain between WT mice and Gemfib^{AAV9} differed significantly during this 14 month period (* p = .0146; **Appendix B.130**), with male Gemfib^{AAV9} taking longer to gain weight than their WT counterparts and consistently weighing less at each time point measured. Similarly, the overall rate of weight gain in male Combo^{AAV9} mice was found to be less than that of WT via simple linear regression (*** p = .0007; **Appendix B.130**). Finally, both male Gemfib^{AAV9} and male Combo^{AAV9} mice gained weight significantly faster and maintained that weight longer than untreated Cln6^{nclf} (UT^{Cln6nclf}) mice (Gemfib^{AAV9} * p = .0340; Combo^{AAV9} ** p =.0018; **Appendix B.130**). Starting n for all groups = 25-31. **B.** Average female weights, in grams, over 14 months (line graph). Linear regression lines are represented by solid coloured lines. Simple linear regression revealed that the overall rate of weight gain between WT mice and Gemfib^{AAV9} differed significantly during this 14 month period (**** $p \leq .0001$; **Appendix B.131**), with female Gemfib^{AAV9} taking longer to gain weight than their WT counterparts and consistently weighing less at each time point measured. Similarly, the overall rate of weight gain in female Combo^{AAV9} mice was found to be less than that of WT via simple linear regression (**** $p \leq .0001$; **Appendix B.131**). Finally, both female Gemfib^{AAV9} and female Combo^{AAV9} mice gained weight significantly faster and maintained that weight longer than UT^{Cln6nclf} mice (Gemfib^{AAV9} *** p = .0003; Combo^{AAV9} **** $p \leq .0001$; **Appendix B.131**). Starting n for all groups = 25-33. **C.** Histogram of mean male weights (in grams) at 6 months of age. No significant differences were detected between the mean weights of the different treatment groups (**Appendix B. 132**). n(per group) = 24-31 **D.** Histogram of mean female weights (in grams) at 6 months of age. 1-way ANOVA analysis revealed that all three treatment groups (Gemfib^{AAV9}, CBD^{AAV9} and Combo^{AAV9}) weighed, on average, significantly less than age- and sex-matched WT controls at 6 months of age (WT mean weight = g; Gemfib^{AAV9} mean weight = g; **** p =; CBD^{AAV9} mean weight = g; *** p = ; Combo^{AAV9} mean weight = g; **** $p \leq .0001$; **Appendix B.133**). n (per group) = 25-28. **E.** Histogram of mean male weights (in grams) a 9 months of age. Both CBD^{AAV9} and Combo^{AAV9} mice demonstrated significantly lower weights than WT controls (WT mean weight = 38.57 g; CBD^{AAV9} mean weight = 36 g; * p = .0290; Combo^{AAV9} mean weight = 34.53 g; *** p = .0001; **Appendix B.132**). n (per group) = 18-26. **F.** Histogram of mean female weights (in grams) at 9 months of age. Both Gemfib^{AAV9} and Combo^{AAV9} mice demonstrated significantly lower weights than WT controls (WT mean weight = 28.90 g; Gemfib^{AAV9} mean weight = 26.05g; ** p = .0059; Combo^{AAV9} mean weight = 26.32 g; * p = .0126; **Appendix B.133**). n(per group) = 20-25. **G.** Histogram of mean male weights (in grams) at 12 months of age. No significant differences were detected between the mean weights of the different treatment groups (**Appendix B. 132**). n(per group) = 12-25. **H.** Histogram of mean female weights (in grams) at 12 months of age. No significant differences were detected between the mean weights of the different treatment groups (**Appendix B. 133**). n(per group) = 5-19.

*3.4.4 Functional improvements in combination therapy mice: **sex differences***

While the consideration of sex differences has been important throughout the practical component of this project, the investigation of sex-based differences in response to the three potential combination therapies (Gemfib^{AAV9}, CBD^{AAV9} and Combo^{AAV9}) is particularly pertinent in terms of informing potential complementary therapeutic strategies for CLN6 BD patients from the Gray Foundation's 2016 clinical trial. Patients involved in the trial were of both sexes, and may have sex-determined responses to the additional use of gemfibrozil, CBD or both

drugs in conjunction with the gene therapy they have already received. With this in mind, sex based differences in behavioural outcomes as experienced by Cln6^{nclf} mice are examined here – as a limited proxy for sex-based differences that may or may not be experienced by children from the trial.

3.4.4.a Rotarod sex differences

Male and female Gemfib^{AAV9} Cln6^{nclf} mice experienced statistically similar rates of decline in rotarod score over 6, 9 and 12 months of age (**Figure 3.31.A**; simple linear regression; **Appendix B.135**). They also demonstrate no significant differences in mean rotarod score at 6, 9 or 12 months of age, as determined by a series of unpaired student t-tests (**Figures 3.31.E-G**; **Appendix B.136**). Similarly, no significant differences in overall rate of decline (simple linear regression) and mean rotarod scores at 6, 9 and 12 months of age were detected between male and female CBD^{AAV9} treated mice (**Figures 3.31.B, E-G; Appendices B.135** and **B.137**). Combo^{AAV9} treated animals, however, demonstrated a significant difference in overall rate of rotarod score decline, with females experiencing a significantly slower decline in score compared to males (simple linear regression; **Figure 3.31.C; Appendix B.135**). Male and female Combo^{AAV9} mean rotarod scores are statistically indistinguishable until 12 months of age, at which point females perform significantly better than their age-matched male counterparts (**Figure 3.31.G**; male Combo^{AAV9} mean score = seconds; female Combo^{AAV9} mean score = seconds; *** p = .0001; **Appendix B.136-138**).

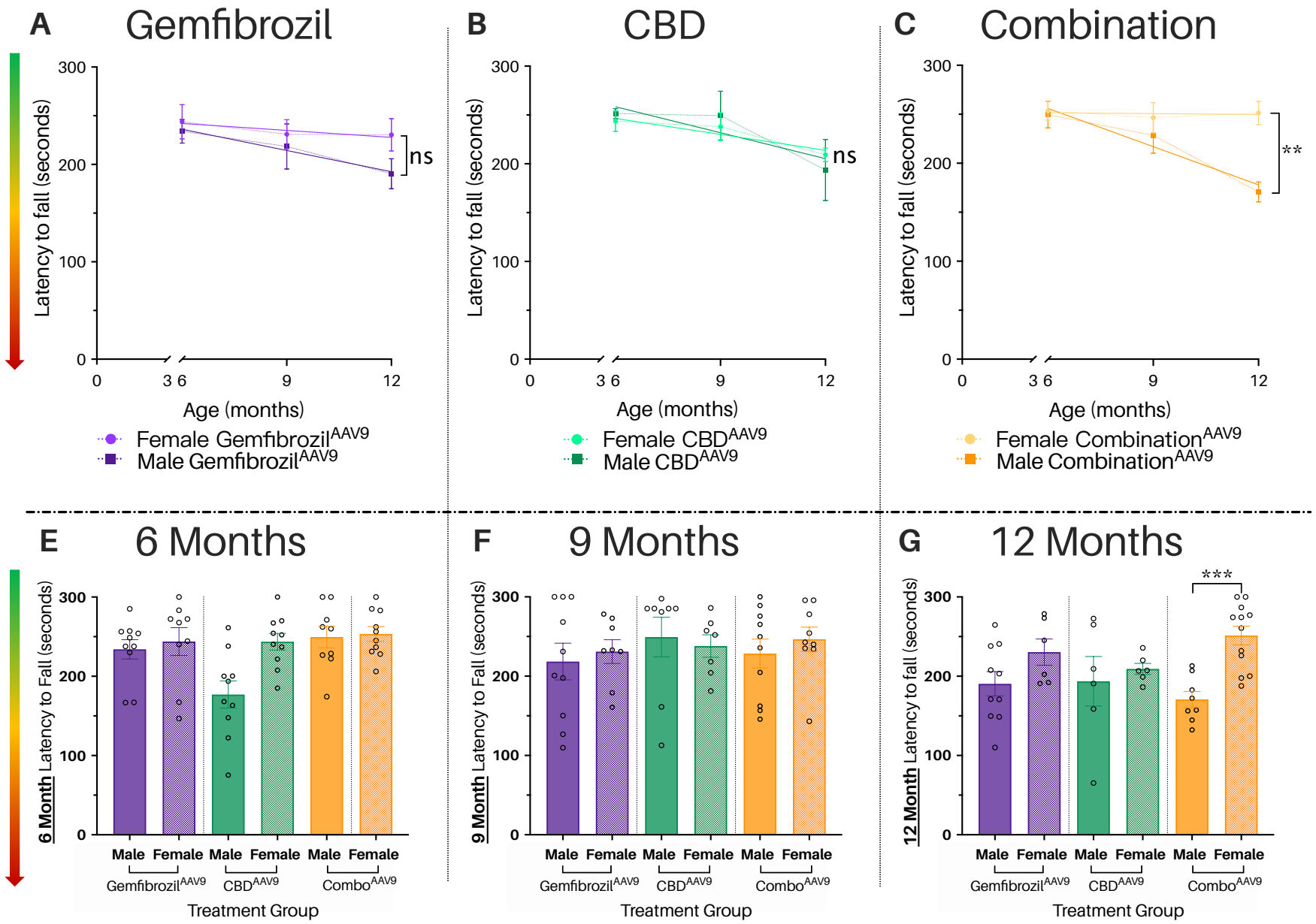
A
Gemfibrozil
B
CBD
C
Combination
Latency to fall (seconds)
300
200
100
0
0
3 6
9
12
Age (months)
ns
ns
**
Female Gemfibrozil AAV9
Male Gemfibrozil AAV9
Female CBD AAV9
Male CBD AAV9
Female Combination AAV9
Male Combination AAV9
E
6 Months
F
9 Months
G
12 Months
6 Month Latency to Fall (seconds)
9 Month Latency to Fall (seconds)
12 Month Latency to fall (seconds)
***
Male
Female
Gemfibrozil AAV9
CBD AAV9
Combo AAV9
Treatment Group

⇐ **Figure 3.31 | Functional improvements in combination therapy mice: sex differences in rotarod scores (previous page).** *No significant sex-based differences were detected in the rotarod scores and overall rate of decline of those scores for Cln6^{nclf} mice treated with a single dose of scAAV9.CB.hCLN6 at P0-2 in combination with either the gemfibrozil (Gemfib^{AAV9}) or CBD (CBD^{AAV9}) small molecule regimens.* Female Cln6^{nclf} mice, however, demonstrated significantly better (higher) rotarod scores than their male counterparts at 12 months of age when treated with both scAAV9.CB.*hCLN6* and combined small molecule therapy (Combo^{AAV9}). **A-C.** Line graphs presenting data as mean rotarod scores measured in latency to fall (seconds) for male (squares) and female (circle) Cln6^{nclf} mice, treated with gene therapy and either gemfibrozil (**A**; male = dark purple; female = light purple), CBD (**B**; male = dark green; female = light green) or a combination of the two (**C**; male = orange; female = yellow). Error bars represent ± SEM. Dotted lines indicate the expected trajectory of rotarod scores between measured time points (6, 9 and 12 months). Linear regression lines are represented by solid coloured lines (simple linear regression; **Appendices B.134** and **B.135**). **E-G**. Histograms presenting data as mean rotarod scores measured in latency to fall (seconds) for male (dark, solid coloured bars) and female (light, patterned bars) Cln6^{nclf} mice treated with gene therapy and either gemfibrozil (purple), CBD (green) or a combination of the two drugs (orange) at 6 (**E**), 9 (**F**) and 12 (**G**) months of age. Error bars represent ± SEM. Individual mouse scores are represented by clear circles. Analyses between male and female mean scores for each treatment group (Gemfib^{AAV9}, CBD^{AAV9} and Combo^{AAV9}) were conducted using unpaired student t-tests (**Appendices B.136-138**). **A.** Both male (dark purple squares and lines) and female (light purple lines and circles) Gemfib^{AAV9} treated Cln6^{nclf} mice demonstrated a decline in ability to stay on the rotarod from 6 to 12 months of age (negative slope gradients in line equations for both; **Appendix B.135**). Simple linear regression (solid lines) revealed that there was no significant difference between the overall rate of decline or elevation of decline in motor performance between Gemfib^{AAV9} treated males and females. n(per group, per time point) = 6-10. **B.** Both male (dark green lines and squares) and female (light green lines and circles) CBD^{AAV9} treated Cln6^{nclf} mice demonstrated a decline in ability to stay on the rotarod from 6 to 12 months of age (negative slope gradients in line equations for both; **Appendix B.135**). Simple linear regression (solid lines) revealed that there was no significant difference between the overall rate of decline or elevation of decline in motor performance between CBD^{AAV9} treated males and females, (**Appendix B.135**). n (per group, per time point) = 6-10. **C.** Both male (orange lines and squares) and female (yellow lines and circles) Combo^{AAV9} treated Cln6^{nclf} mice demonstrated a decline in ability to stay on the rotarod from 6 to 12 months of age (negative slope gradients in line equations for both; **Appendix B.135**). Simple linear regression (solid lines) revealed that there was a significant difference between the overall rate of decline in motor performance between CBD^{AAV9} treated males and females, with males declining at a greater rate than females (** p = .0067; **Appendix B.134**). n(per group, per time point) = 8-12. **D.** Histogram presenting average rotarod scores (latency to fall in seconds) of male (dark coloured bars) and female (light coloured bars) drug-only treated Cln6^{nclf} mice at 6 months of age. No significant difference was found between male and female scores for any drug treatment at 6 months (**Appendices B.136-138**). n(per group) = 9-10. **E.** Histogram presenting average rotarod scores (latency to fall in seconds) of male (dark coloured bars) and female (light coloured bars) drug-only treated Cln6^{nclf} mice at 9 months of age. No significant difference was found between male and female scores for any drug treatment at 9 months (**Appendices B.136-138**). n(per group) = 7-10. **F.** Histogram presenting average rotarod scores (latency to fall in seconds) of male (dark coloured bars) and female (light coloured bars) drug-only treated Cln6^{nclf} mice at 12 moths of age. No significant difference was found between male and female Gemfib^{AAV9} or male and female CBD^{AAV9} scores. There was, however, a significant difference between male and female scores for Combo^{AAV9} treated mice (male Combo^{AAV9} mean score = seconds; female Combo^{AAV9} mean score = seconds; *** p = .0001; **Appendix B.136-138**). n(per group) = 6-12.

3.4.4.b Composite ataxia sex differences

No significant differences in mean composite ataxia score were detected between male and female animals at either 6 or 9 months of age, regardless of treatment group (**Figure 3.32; Appendices B.139-141**).

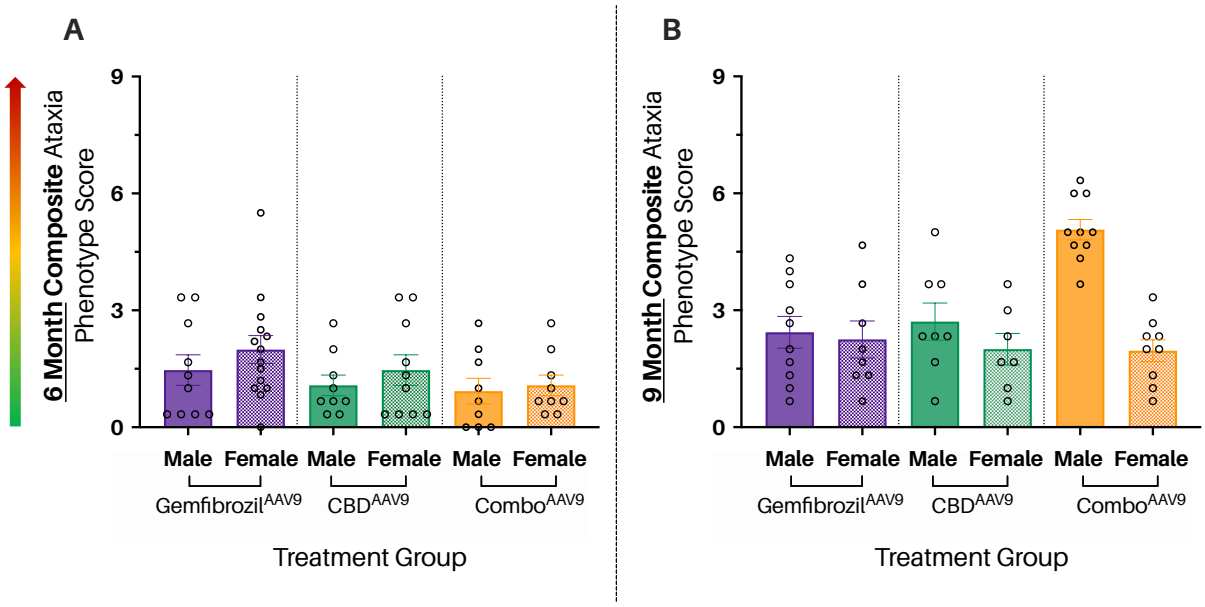

Figure 3.32 | Functional improvements in combination therapy mice: sex differences in composite ataxia scores. *Male and female Cln6^{nclf} mice treated with both scAAV9.CB.hCLN6 gene therapy and either gemfibrozil (Gemfib^{AAV9}), cannabidiol (CBD^{AAV9}), or a combination of the two small molecule therapies (Combo^{AAV9}), demonstrated statistically similar composite ataxia scores (0-9) at both 6 and 9 months of age.* Histograms demonstrating mean composite ataxia scores for male (dark coloured bars) and female (light, patterned bars) Cln6^{nclf} mice treated with gene therapy and either gemfibrozil (gemfibrozil^{AAV9}; purple), cannabidiol (CBD; CBD^{AAV9}; green) or a combination of gemfibrozil and CBD (Combo^{AAV9}), at 6 (**A**) and 9 (**B**) months of age. Different mice were tested at each time point (between-subjects study design). A low score (close to 0) indicates an absence of the ataxic phenotype as measured by the composite scoring system, while higher score (close to 9) indicate increasing levels of ataxic behaviour (arrow on the left). Individual mouse composite scores are shown as clear circles and error bars = ± SEM. Analyses between male and female mean scores for each treatment group at each time point were conducted via unpaired student t-tests (**Appendices B.139-141**). n(per group per time point) = 7-14. **A.** No significant differences were observed between mean male and female composite ataxia scores at 6 months, regardless of drug treatment regimen (unpaired student t-tests; **Appendices B.139-141**), though Gemfib^{AAV9} females appear to have (non-significantly) higher (worse) mean scores than age-matched Gemfib^{AAV9} males. **B.** No significant differences were observed between mean male and female composite ataxia scores at 9 months, regardless of drug treatment regimen (unpaired student t-tests; **Appendices B.139-141**), though Combo^{AAV9} males appear to have (non-significantly) higher (worse) mean score than age-matched Combo^{AAV9} females.

3.4.4.c Ledge ataxia sex differences

Male and female Cln6^{nclf} mice demonstrated no significant difference in mean ledge ataxia scores (**Figure 3.33.A** and **B**) at 6 or 9 months of age (unpaired t-tests; **Appendices B.142-144**), regardless of treatment group.

3.4.4.d Hindlimb clasping ataxia sex differences

Male and female Cln6^{nclf} mice demonstrated no significant difference in mean hindlimb clasping ataxia scores (**Figure 3.33.C** and **D**) at 6 or 9 months of age (unpaired t-tests; **Appendices B.145-147**), regardless of treatment group.

3.4.4.e Gait ataxia sex differences

Gemfib^{AAV9} female mice performed significantly worse (higher ataxia score) in the gait ataxia test than age-matched male counterparts at 6 months of age (Gemfib^{AAV9} female mean score = ; Gemfib^{AAV9} male mean score = ; * p = .0248 ; **Appendix B.148**), though this difference did not continue to 9 months, with no significant difference detected between male and female Gemfib^{AAV9} at this time point. In comparison, neither CBD^{PBS} or Combo^{PBS} treated Cln6^{nclf} demonstrated any sex differences in mean gait ataxia score at 6 or 9 months of age (**Appendix B.149** and **B.150**).

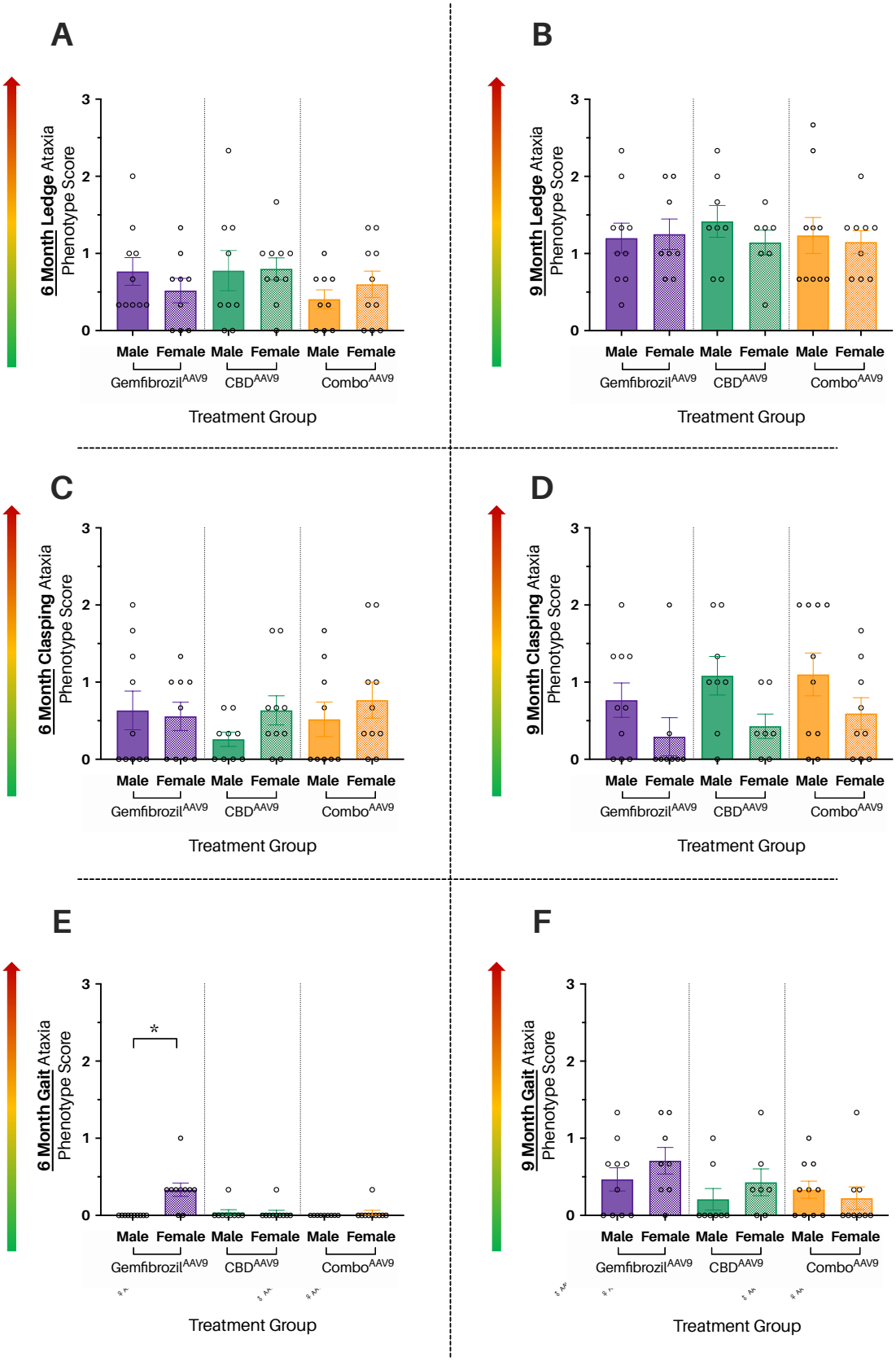
A
6 Month Ledge Ataxia Phenotype Score
B
9 Month Ledge Ataxia Phenotype Score
C
6 Month Clasping Ataxia Phenotype Score
D
9 Month Clasping Ataxia Phenotype Score
E
6 Month Gait Ataxia Phenotype Score
*
F
9 Month Gait Ataxia Phenotype Score
0
1
2
3
Male
Female
Gemfibrozil AAV9
CBD AAV9
Combo AAV9
Treatment Group

⇐ **Figure 3.33 | Functional improvements in combination therapy mice: sex differences in ataxia phenotyping scores (previous page).** *Male and female Cln6^{nclf} mice treated with both sc.AAV9.CB.hCLN6 gene therapy and either gemfibrozil (Gemfib^{AAV9}), CBD (CBD^{AAV9}), or a combination of gemfibrozil and cannabidiol (Combo^{AAV9}), demonstrated statistically similar ledge and hindlimb clasping ataxia scores at both 6 and 9 months of age, while Gemfib^{AAV9} females performed significantly worse than males in the gait ataxia assay at 6 months of age.* Mice underwent three trials of a sequence three different ataxia assays – the ledge test, the hindlimb clasping test and the gait test (adapted from *Guyenet et al., 2010*) – in order to determine the presence or absence of an ataxic phenotype at 6 and 9 months of age. Different mice were assessed at each time point, making the experiment between-subjects in design. For each assay, a mouse could be assigned a score between 0 and 3, with 0 indicating a complete absence of the ataxic phenotype and 3 indicating a completely penetrant ataxic phenotype (coloured arrows on the left). All data (**A-F**) are presented as the mean of averaged (3 trials; scored from 0-3) individual mouse scores, with clear circles representing the individual averaged scores. Error bars = ± SEM. All analyses between male and female mean ataxia scores were conducted using unpaired student t-tests (**Appendices B.142 -150**). **A and B.** Histograms of mean ledge test scores at 6 (**A**) and 9 (**B**) months of age for male (dark coloured bars) and female (light coloured, patterned bars) Cln6^{nclf} mice treated with gene therapy and either gemfibrozil (Gemfib^{AAV9}; purple), CBD (CBD^{AAV9}; green) or a combination of gemfibrozil and CBD (Combo^{AAV9}; orange) without. No significant differences were observed between the mean ledge scores of treatment- and age-matched male and female Cln6^{nclf} mice, regardless of drug treatment regimen. n(per group, per time point) = 7-10. **C** and **D.** Histograms of mean hindlimb clasping test scores at 6 (**C**) and 9 (**D**) months of age for male (dark coloured bars) and female (light coloured, patterned bars) Cln6^{nclf} mice treated with gene therapy and either gemfibrozil (Gemfib^{AAV9}; purple), CBD (CBD^{AAV9}; green) or a combination of gemfibrozil and CBD (Combo^{AAV9}; orange). No significant differences were observed between the mean hindlimb clasping scores of treatment- and age-matched male and female Cln6^{nclf} mice, regardless of drug treatment regimen. n(per group, per time point) = 7-10. **E.** Histogram of mean gait ataxia test scores at 6 months of age for male (dark coloured bars) and female (light coloured, patterned bars) Cln6^{nclf} mice treated with gene therapy and either gemfibrozil (Gemfib^{AAV9}; purple), CBD (CBD^{AAV9}; green) or a combination of gemfibrozil and CBD (Combo^{AAV9}; orange). Gemfib^{AAV9} treated female mice performed significantly worse than their age-matched male counterparts at 6 months (Gemfib^{AAV9} female mean score = ; Gemfib^{AAV9} male mean score = ; * p = .0248 ; **Appendix B.148**). n (per group) = 10. F. Histogram of mean gait ataxia scores at 9 months of age for male (dark coloured bars) and female (light coloured, patterned bars) Cln6^{nclf} mice treated with gene therapy and either gemfibrozil (Gemfib^{AAV9}; purple), CBD (CBD^{AAV9}; green) or a combination of gemfibrozil and CBD (Combo^{AAV9}; orange). No significant differences were observed between the mean gait ataxia scores of treatment- and age-matched male and female Cln6^{nclf} mice, regardless of drug treatment regimen. n (per group) = 7-10.

3.4.4.f Survival and weight sex differences

Male and female Cln6^{nclf} mice demonstrated no sex-based differences in survival, regardless of what composite therapy regimen they were on (**Figure 3.34**; **Appendices B.151-153**).

In terms of weight gain (**Figure 3.35**), however, male Cln6^{nclf} mice demonstrated significantly greater rates of weight change over 14 months compared to females for every combination treatment group (simple linear regression).

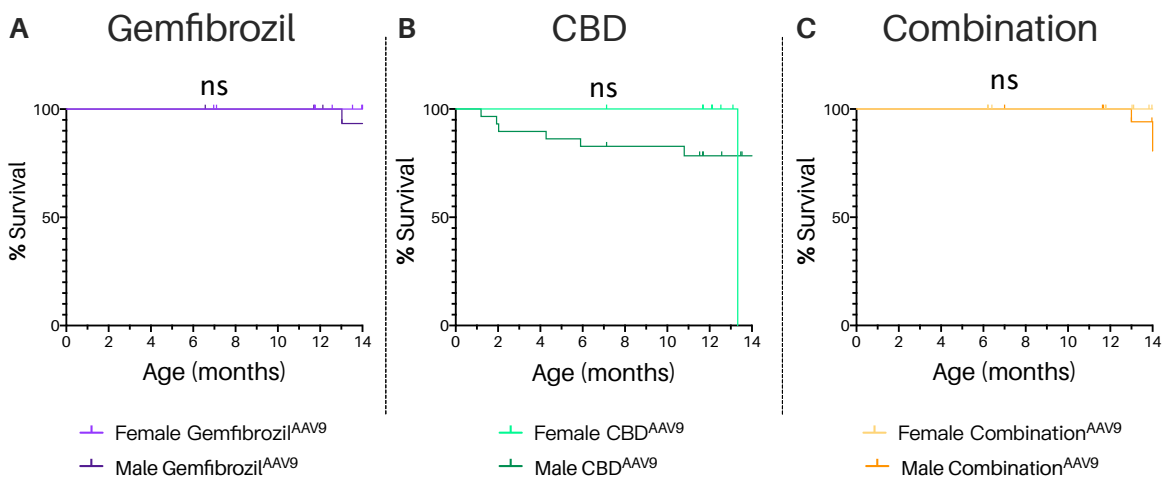

Figure 3.34 | Functional improvements in combination therapy mice: sex differences in survival. *Male and female Cln6^{nclf} mice treated with a combination of gene and small molecule therapy (Gemfib^{AAV9}, CBD^{AAV9} and Combo^{AAV9}) showed statistically similar survival curves, regardless of which small molecule therapy treatment they received.* Kaplan-Meier survival plots (%) comparing the survival curves of male and female Gemfib^{AAV9} treated Cln6^{nclf} mice (**A**), male and female CBD^{AAV9} treated Cln6^{nclf} mice (**B**), and male and female Combo^{AAV9} treated Cln6^{nclf} mice (**C**). All survival curve comparisons were conducted using log-rank (Mantel-Cox) tests in GraphPad Prism 8 (**Appendices B.151-153**). **A.** Male (dark purple) and female (light purple) Gemfib^{AAV9} treated Cln6^{nclf} survival curves from birth to 14 months of age. No significant difference was found between the median survival of male and female Gemfib^{aav9} treated mice (**Appendix B.151**). Starting n = 27-31. **B.** Male (dark green) and female (light green) CBD^{AAV9} treated Cln6^{nclf} survival curves from birth to 14 months of age. No significant difference was found between the median survival of male and female CBD^{AAV9} treated mice (**Appendix B.152**). Starting n = 28-29. **C.** Male (orange) and female (yellow) Combo^{AAV9} treated Cln6^{nclf} survival curves from birth to 14 months of age. No significant difference was found between the median survival of male and female Combo^{AAV9} treated mice (**Appendix B.153**). Starting n = 25-32.

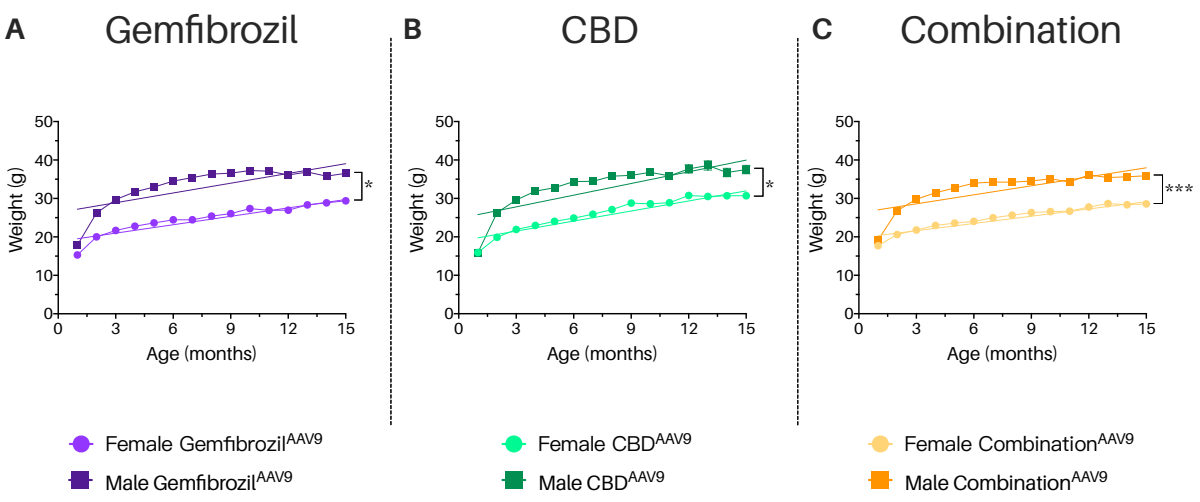

Figure 3.35 | Functional improvements in combination therapy mice: sex differences in weights. *Male and female Cln6^{nclf} mice treated with a combination of gene and small molecule therapy (Gemfib^{AAV9}, CBD^{AAV9} and Combo^{AAV9}) showed sex-based differences in their overall rate of weight gain over fourteen months – with males gaining more weight, more quickly, than females for all three combination therapy treatment groups.* Mice were weighed weekly from weaning (~28 days) to determine drug dosage and as a measure of general health. Weights are shown here from weaning to 15 months due to the time constraints of an MSc (weights continued to be tracked for the entire duration of the trial). Data are presented as average weights, error bars ± SEM. Comparisons between male and female weights were conducted via simple linear regression only, as there is always an expected dispairty between male and female mice. **A.** Average male (dark purple) and female (light purple) Gemfib^{AAV9} treated Cln6^{nclf} weights (in grams) plotted every month from weaning until 14 months of age (line graph). A significant difference in rate of weight gain was observed between male and female Gemfib^{AAV9} mice (simple linear regression; *p = .0397). Starting n = 27-31 **B.** Average male (dark green) and female (light green) CBD^{AAV9} treated Cln6^{nclf} weights (in grams) plotted every month from weaning until 14 months of age (line graph). A significant difference in rate of weight gain was observed between male and female CBD^{AAV9} mice (simple linear regression; *p = .0279). Starting n =28-29. **C.** Average male (orange) and female (yellow) Combo^{AAV9} treated Cln6^{nclf} weights (in grams) plotted every month from weaning until 14 months of age (line graph). A significant difference in rate of weight gain was observed between male and female Combo^{AAV9} mice (simple linear regression; *** p = .0008). Starting n = 25-32.

*3.4.5 Functional improvements in combination therapy mice: **summary***

Analysis of the behavioural, and survival data generated by male and female Cln6^{nclf} mice treated with a combination of gene therapy and either gemfibrozil (Gemfib^{AAV9}), CBD (CBD^{AAV9}) or both drugs (Combo^{AAV9}) indicates that all three combination therapies potentially offer protection against the several key deficits associated with the Cln6^{nclf} behavioural phenotype. Interestingly, however, no combination therapy was able to completely restore mean Cln6^{nclf} weights to those of healthy WT controls, with combination treatment mice showing no significant difference in mean weights from UT^{Cln6nclf} at every time point measured (6, 9 and 12 months) and often weighing significantly less than WT at one or more time points (**Figure 3.30**).

The median survival of male and female Gemfib^{AAV9}, CBD^{AAV9} and Combo^{AAV9} mice were all significantly increased compared to UT^{Cln6nclf} mice and statistically indistinguishable from the median survival of sex-matched WT groups by 15 months of age (**Figure 3.29**; **Tables 3.16** to **3.24**).

There were two isolated instances in which combination treatment mice achieved behavioural scores higher than those of age- and sex-matched WT controls: Gemfib^{AAV9} males performed significantly better than WT males on the rotarod at 12 months of age and Gemfib^{AAV9} females performed significantly better than WT females at the ledge ataxia test at 6 months of age (**Tables 3.16** and **3.17**).

Finally, there appeared to be no significant sex-based differences in behavioural scores or survival in response to any of the three combination therapies, with the exception of Combo^{AAV9} female mice outperforming males on the rotarod at 12 months of age (**Figure 3.31**).

Table 3.16 | Functional improvements in combination therapy mice: summary table of Gemfib^{AAV9} males.
Summary table of behavioural score (rotarod and ataxia), survival and weight comparisons carried out between male gene therapy and gemfibrozil (Gemfib^{AAV9}) treated Cln6^{nclf} mice and their age- and sex-matched WT and untreated Cln6^{nclf} (UT^{Cln6nclf}) counterparts at 6, 9 and 12 months of age. All behavioural score and weight comparisons were conducted using 1-way ANOVAs **(Appendices B.108, 110, 112, 114, 116** and **B.132**), with Tukey's post-hoc multiple comparisons tests where appropriate, while survival curves were compared using log rank (Mantel-Cox) tests (**Appendices B.118** and **B.121**). nsd = no significant difference; s = significant.

Gemfib^{AAV9} Cln6^{nclf} Males				
Behavioural Test	**Comparison Group**	**6 months**	**9 months**	**12 months**
Rotarod	UT^{Cln6nclf}	nsd	nsd	**Better (s)**
	WT	nsd	nsd	**Better (s)**
Composite	UT^{Cln6nclf}	nsd	**Better (s)**	-
	WT	nsd	nsd	-
Ledge	UT^{Cln6nclf}	nsd	**Better (s)**	-
	WT	nsd	nsd	-
Hindlimb Clasping	UT^{Cln6nclf}	nsd	**Better (s)**	-
	WT	nsd	nsd	-
Gait	UT^{Cln6nclf}	**Better (s)**	nsd	-
	WT	nsd	nsd	-
Survival	UT^{Cln6nclf}	**Increased survival (s)**		
	WT	nsd		
Weight	UT^{Cln6nclf}	nsd	nsd	nsd
	WT	nsd	nsd	nsd

Table 3.17 | Functional improvements in combination therapy mice: summary table of Gemfib^{AAV9} females. *Summary table of behavioural score (rotarod and ataxia), survival and weight comparisons carried out between female gene therapy and gemfibrozil (Gemfib^{AAV9}) treated Cln6^{nclf} mice and their age- and sex-matched WT and untreated Cln6^{nclf} (UT^{Cln6nclf}) counterparts at 6, 9 and 12 months of age.* All behavioural score and weight comparisons were conducted using 1-way ANOVAs (**Appendices B.109, 111, 113, 115, 117** and **B.133**), with Tukey's post-hoc multiple comparisons tests where appropriate, while survival curves were compared using log rank (Mantel-Cox) tests (**Appendices B.124** and **127**). nsd = no significant difference; s = significant.

Gemfib^{AAV9} Cln6^{nclf} Females				
Behavioural Test	**Comparison Group**	**6 months**	**9 months**	**12 months**
Rotarod	UT^{Cln6nclf}	nsd	nsd	Better (s)
	WT	nsd	nsd	nsd
Composite	UT^{Cln6nclf}	nsd	**Better (s)**	-
	WT	nsd	nsd	
Ledge	UT^{Cln6nclf}	**Better (s)**	**Better (s)**	-
	WT	**Better (s)**	nsd	
Hindlimb Clasping	UT^{Cln6nclf}	nsd	**Better (s)**	-
	WT	nsd	nsd	
Gait	UT^{Cln6nclf}	nsd	nsd	-
	WT	nsd	nsd	
Survival	UT^{Cln6nclf}	**Increased survival (s)**		
	WT	nsd		
Weight	UT^{Cln6nclf}	nsd	nsd	nsd
	WT	**Weigh less (s)**	**Weigh less (s)**	nsd

Table 3.18 | Functional improvements in combination therapy mice: summary table of Gemfib^{AAV9} males versus Gemfib^{AAV9} females. *Summary table of behavioural score (rotarod and ataxia), survival and weight comparisons carried out between male and female gene therapy and gemfibrozil (Gemfib^{AAV9}) treated Cln6^{nclf} mice at 6, 9 and 12 months of age.* All behavioural score and weight comparisons were conducted using unpaired student t-tests (**Appendices B.136, 139, 142, 145** and **B.148**), while survival curves were compared using log rank (Mantel-Cox) tests (**Appendix B.151**). nsd = no significant difference.

Gemfib^{AAV9} Cln6^{nclf} Males vs Females			
Behavioural test	**6 months**	**9 months**	**12 months**
Rotarod	nsd	nsd	nsd
Composite	nsd	nsd	-
Ledge	nsd	nsd	-
Hindlimb	nsd	nsd	-
Gait	nsd	nsd	-
Survival	nsd		

Table 3.19 | Functional improvements in combination therapy mice: summary table of CBD^{AAV9} males. *Summary table of behavioural score (rotarod and ataxia), survival and weight comparisons carried out between male gene therapy and cannabidiol (CBD^{AAV9}) treated $Cln6^{nclf}$ mice and their age- and sex-matched WT and untreated $Cln6^{nclf}$ ($UT^{Cln6nclf}$) counterparts at 6, 9 and 12 months of age.* All behavioural score and weight comparisons were conducted using 1-way ANOVAs (**Appendices B.108, 110, 112, 114, 116** and **133**), with Tukey's post-hoc multiple comparisons tests where appropriate, while survival curves were compared using log rank (Mantel-Cox) tests (**Appendices B.125** and **B.128**). nsd = no significant difference; s = significant.

CBD^{AAV9} $Cln6^{nclf}$ Males				
Behavioural Test	**Comparison Group**	**6 months**	**9 months**	**12 months**
Rotarod	$UT^{Cln6nclf}$	nsd	**Better (s)**	**Better (s)**
	WT	nsd	nsd	nsd
Composite	$UT^{Cln6nclf}$	**Better (s)**	**Better (s)**	-
	WT	nsd	nsd	-
Ledge	$UT^{Cln6nclf}$	nsd	**Better (s)**	-
	WT	nsd	nsd	-
Hindlimb Clasping	$UT^{Cln6nclf}$	nsd	nsd	-
	WT	nsd	nsd	-
Gait	$UT^{Cln6nclf}$	**Better (s)**	**Better (s)**	-
	WT	nsd	nsd	-
Survival	$UT^{Cln6nclf}$	**Increased survival (s)**		
	WT	nsd		
Weight	$UT^{Cln6nclf}$	nsd	nsd	nsd
	WT	nsd	**Weigh less (s)**	nsd

Table 3.20 | Functional improvements in combination therapy mice: summary table of CBD^{AAV9} females. *Summary table of behavioural score (rotarod and ataxia), survival and weight comparisons carried out between female gene therapy and cannabidiol (CBD^{AAV9}) treated Cln6^{nclf} mice and their age- and sex-matched WT and untreated Cln6^{nclf} (UT^{Cln6nclf}) counterparts at 6, 9 and 12 months of age.* All behavioural score and weight comparisons were conducted using 1-way ANOVAs (**Appendices B. 109, 111, 113, 115, 117** and **B.133**), with Tukey's post-hoc multiple comparisons tests where appropriate, while survival curves were compared using log rank (Mantel-Cox) tests (**Appendices B125** and **B.123**). nsd = no significant difference; s = significant.

CBD^{AAV9} Cln6^{nclf} Females

Behavioural Test	Comparison Group	6 months	9 months	12 months
Rotarod	UT^{Cln6nclf}	nsd	nsd	**Better (s)**
	WT	nsd	nsd	nsd
Composite	UT^{Cln6nclf}	nsd	**Better (s)**	-
	WT	nsd	nsd	
Ledge	UT^{Cln6nclf}	nsd	**Better (s)**	-
	WT	nsd	nsd	
Hindlimb Clasping	UT^{Cln6nclf}	nsd	**Better (s)**	-
	WT	nsd	nsd	
Gait	UT^{Cln6nclf}	nsd	nsd	-
	WT	nsd	nsd	
Survival	UT^{Cln6nclf}	**Increased survival (s)**		
	WT	nsd		
Weight	UT^{Cln6nclf}	nsd	nsd	nsd
	WT	**Weigh less (s)**	nsd	nsd

Table 3.21 | Functional improvements in combination therapy mice: summary table of CBD^{AAV9} males versus CBD^{AAV9} females. *Summary table of behavioural score (rotarod and ataxia), survival and weight comparisons carried out between male and female gene therapy and cannabidiol (CBD^{AAV9}) treated Cln6^{nclf} mice at 6, 9 and 12 months of age.* All behavioural score and weight comparisons were conducted using unpaired student t-tests (**Appendices B.137, 140, 143, 146** and **B.149**), while survival curves were compared using log rank (Mantel-Cox) tests (**Appendix B.152**). nsd = no significant difference.

CBD^{AAV9} Cln6^{nclf} Males vs Females

Behavioural test	6 months	9 months	12 months
Rotarod	nsd	nsd	nsd
Composite	nsd	nsd	-
Ledge	nsd	nsd	-
Hindlimb	nsd	nsd	-
Gait	nsd	nsd	-
Survival	nsd		

Table 3.22 | Functional improvements in combination therapy mice: summary table of Combo^{AAV9} males.
Summary table of behavioural score (rotarod and ataxia), survival and weight comparisons carried out between male gene therapy and combination small molecule therapy (Combo^{AAV9}) treated Cln6^{nclf} mice and their age- and sex-matched WT and untreated Cln6^{nclf} (UT^{Cln6nclf}) counterparts at 6, 9 and 12 months of age. All behavioural score and weight comparisons were conducted using 1-way ANOVAs (**Appendices B.108, 110, 112, 114, 116** and **B.132**), with Tukey's post-hoc multiple comparisons tests where appropriate, while survival curves were compared using log rank (Mantel-Cox) tests (**Appendices B.120** and **123**). nsd = no significant difference; s = significant.

Combo^{AAV9} Cln6^{nclf} Males				
Behavioural Test	**Comparison Group**	**6 months**	**9 months**	**12 months**
Rotarod	UT^{Cln6nclf}	nsd	**Better (s)**	**Better (s)**
	WT	nsd	nsd	nsd
Composite	UT^{Cln6nclf}	**Better (s)**	**Better (s)**	-
	WT	nsd	nsd	-
Ledge	UT^{Cln6nclf}	**Better (s)**	nsd	-
	WT	nsd	nsd	-
Hindlimb Clasping	UT^{Cln6nclf}	nsd	nsd	-
	WT	nsd	nsd	-
Gait	UT^{Cln6nclf}	**Better (s)**	**Better (s)**	-
	WT	nsd	nsd	-
Survival	UT^{Cln6nclf}	**Increased survival (s)**		
	WT	nsd		
Weight	UT^{Cln6nclf}	nsd	nsd	nsd
	WT	nsd	**Weigh less (s)**	nsd

Table 3.23 | Functional improvements in combination therapy mice: summary table of Combo^{AAV9} females. *Summary table of behavioural score (rotarod and ataxia), survival and weight comparisons carried out between female gene therapy and combination small molecule therarpy (Combo^{AAV9}) treated Cln6^{nclf} mice and their age- and sex-matched WT and UT^{Cln6nclf} Cln6^{nclf} (UT^{Cln6nclf}) counterparts at 6, 9 and 12 months of age*. All behavioural score and weight comparisons were conducted using 1-way ANOVAs (**Appendices B.109, 111, 113, 115, 117** and **113),** with Tukey's post-hoc multiple comparisons tests where appropriate, while survival curves were compared using log rank (Mantel-Cox) tests (**Appendices B.126** and **129**). nsd = no significant difference; s = significant.

Combo^{AAV9} Cln6^{nclf} Females				
Behavioural Test	**Comparison Group**	**6 months**	**9 months**	**12 months**
Rotarod	UT^{Cln6nclf}	nsd	**Better (s)**	**Better (s)**
	WT	nsd	nsd	nsd
Composite	UT^{Cln6nclf}	**Better (s)**	**Better (s)**	-
	WT	nsd	nsd	
Ledge	UT^{Cln6nclf}	nsd	**Better (s)**	-
	WT	nsd	nsd	
Hindlimb Clasping	UT^{Cln6nclf}	nsd	**Better (s)**	-
	WT	nsd	nsd	
Gait	UT^{Cln6nclf}	nsd	**Better (s)**	-
	WT	nsd	nsd	
Survival	UT^{Cln6nclf}	**Increased survival (s)**		
	WT	nsd		
Weight	UT^{Cln6nclf}	nsd	nsd	nsd
	WT	**Weigh less (s)**	**Weigh less (s)**	nsd

Table 3.24 | Functional improvements in combination therapy mice: summary table of Combo^{AAV9} males versus Combo^{AAV9} females. *Summary table of behavioural score (rotarod and ataxia), survival and weight comparisons carried out between male and female gene therapy and combination small molecule therapy (Combo^{AAV9}) treated Cln6^{nclf} mice at 6, 9 and 12 months of age.* All behavioural score and weight comparisons were conducted using unpaired student t-tests (**Appendices B.138, 141, 144, 147** and **B.150**), while survival curves were compared using log rank (Mantel-Cox) tests (**Appendix B.153**). nsd = no significant difference.

Combo^{AAV9} Cln6^{nclf} Males vs Females			
Behavioural test	**6 months**	**9 months**	**12 months**
Rotarod	nsd	nsd	**Females performed better (s)**
Composite	nsd	nsd	-
Ledge	nsd	nsd	-
Hindlimb	nsd	nsd	-
Gait	nsd	nsd	-
Survival	nsd		

3.5 Combination therapy offers no overt behavioural benefits to Cln6^{nclf} mice when compared to gene therapy alone

It is now apparent that AAV2/9-mediated gene therapy, alone or in combination with either gemfibrozil and/or CBD, may confer varying levels of protection to male and female Cln6^{nclf} mice against a range of CLN6 BD phenotypes. These results, in themselves, are optimistic – especially for parents of the participants of the Gray Foundation's 2016 gene therapy trial, as there are reports that several have been supplementing the gene therapy their children received with CBD based on anecdotal evidence (Wibbeler et al., 2019; Stephanie Hughes, personal communication).

Despite this, it is worth investigating whether any of the combination therapies (Gemfib^{AAV9}, CBD^{AAV9} or Combo^{AAV9}) result in significantly better or worse behavioural scores and survival than gene therapy on its own. This is for two main reasons: first, and perhaps most importantly, it is critical to ensure that efficacy of the gene therapy treatment is not being attenuated, even subtly, by the addition of small molecule therapy. There have been several instances recorded where the combination of two or more therapies has resulted in antagonism and a reduction in overall therapeutic efficacy, as was the case with attempts to combine ERT and AAV2/9-mediated gene therapy in *Ppt1*$^{-/-}$ mice (Pearse, 2015).

Secondly, because combination therapies, by their very nature, require additional resources to be administered, it is worth determining whether they are worth the investment of those additional resources. Regular dosing with small molecule therapy, for instance, will require an ongoing cost – either to the funding body or to the family of the patient – and in countries such as the United States of America, where there is no universal healthcare or pharmaceutical subsidies available without personal health insurance, this cost may end up being significant over the patient's lifetime. Additionally, regular dosing requires foresight and planning to ensure strict adherance to the dosing regimen, which can be taxing for the patient

and their family. In light of these practical considerations, it is important to determine whether the small molecule therapies investigated in this thesis are producing behavioural outcomes that outweigh the resources that will be required to use them in combination with gene therapy.

3.5.1 Combination therapy versus gene therapy alone: ***rotarod***

In an effort to elicit whether combination therapy offers any behavioural benefits over gene therapy alone, at least in terms of motor co-ordination or balance preservation as measured by the rotarod, eight different experimental groups were assessed with the rotarod at 6, 9 and 12 months of age. Six of these groups represented three unique combinations of gene and small molecule therapy: M/F Gemfib^{AAV9}, M/F CBD^{AAV9} and Combo^{AAV9} (treatment regimens as described in **section 3.4.1**), while the last two groups consisted of No Drug^{AAV9} mice (treatment regimen as described in **section 3.3.1**).

Linear regression was used to compare the overall rate of decline in mean rotarod scores over time and the associated elevation (range over which the decline occurred) of each combination therapy treated group versus sex-matched No Drug^{AAV9} mice (**Appendices B.154-156**). No significant differences were detected between any of the combination therapy groups and the groups treated with gene therapy alone, regardless of gender (**Figure 3.36**). This similarity was recapitulated by statistically indistinguishable mean rotarod scores at 6, 9 and 12 months of age (**Figure 3.37; Appendix B.154-156**).

⇒ **Figure 3.36 | Combination therapy versus gene therapy alone: rotarod scores (line graphs; opposite page)**. Cln6^{nclf} *mice treated with a combination of gene and small molecule therapy experience a decline in motor co-ordination, as measured by the rotarod, statistically similar to that experienced by sex-matched Cln6^{nclf} mice treated with gene therapy alone, regardless of sex or the type of small molecule therapy they were treated with.* Data are presented as a line graph of mean scores (latency to fall, in seconds), with error bars = ± SEM. Different mice were tested at different time points, making this experiment between-subjects in design. Dotted lines indicate the expected mean score trajectory for an experimental group between measured time points. Solid lines represent the regression lines of each experimental group, as calculated via simple linear regression (**Appendices B.154-156**). A high score (~300) indicates a high level of motor co-ordination as measured by the rotarod, while lower scores correlate to increasing levels of motor dysfunction (coloured arrow on the left). **A.-F.** No significant differences in overall rate of motor decline, as measured by the rotarod, can be detected between mice treated with gene therapy alone and those treated with gene and small molecule therapy, regardless of sex or which small molecule therapy treatment they receive. Starting n = 23-31.

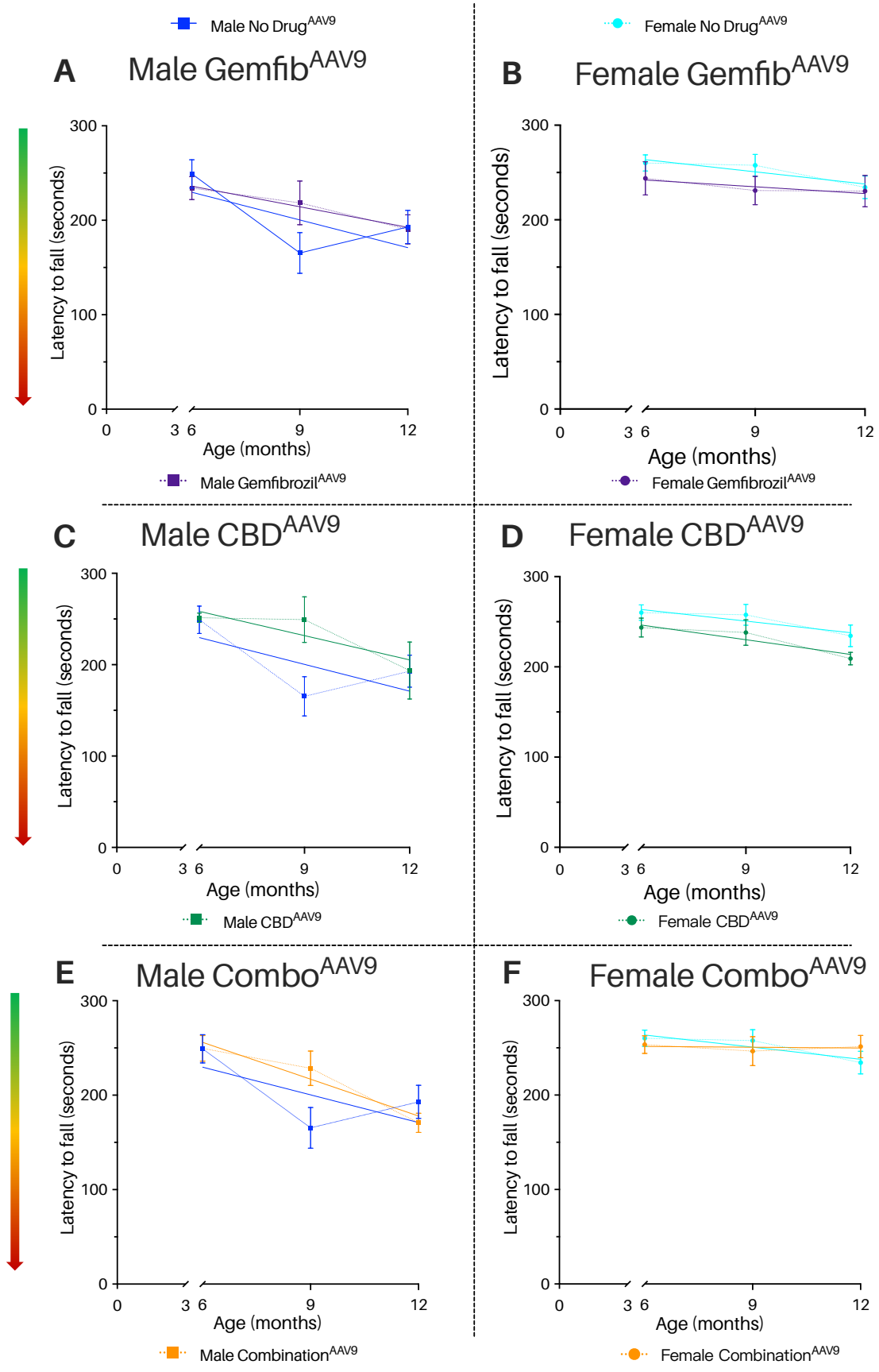
Male No Drug AAV9
A Male Gemfib AAV9
Latency to fall (seconds)
300
200
100
0
0 3 6 9 12
Age (months)
Male Gemfibrozil AAV9
Female No Drug AAV9
B Female Gemfib AAV9
Latency to fall (seconds)
300
200
100
0
0 3 6 9 12
Age (months)
Female Gemfibrozil AAV9
C Male CBD AAV9
Latency to fall (seconds)
300
200
100
0
0 3 6 9 12
Age (months)
Male CBD AAV9
D Female CBD AAV9
Latency to fall (seconds)
300
200
100
0
0 3 6 9 12
Age (months)
Female CBD AAV9
E Male Combo AAV9
Latency to fall (seconds)
300
200
100
0
0 3 6 9 12
Age (months)
Male Combination AAV9
F Female Combo AAV9
Latency to fall (seconds)
300
200
100
0
0 3 6 9 12
Age (months)
Female Combination AAV9

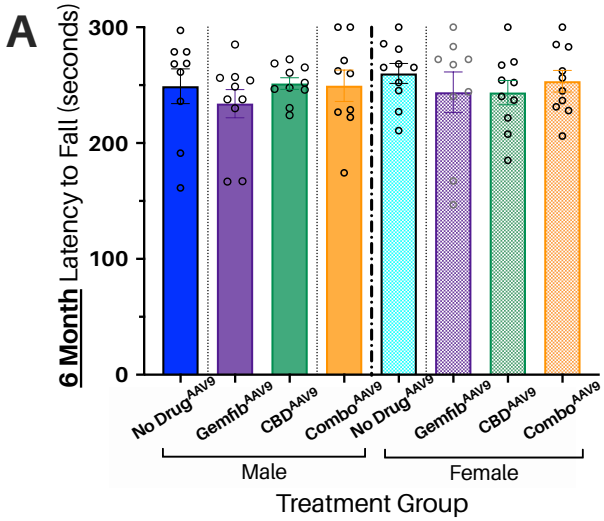
A
6 Month Latency to Fall (seconds)
300
200
100
0
No Drug AAV9
Gemfib AAV9
CBD AAV9
Combo AAV9
No Drug AAV9
Gemfib AAV9
CBD AAV9
Combo AAV9
Male
Female
Treatment Group

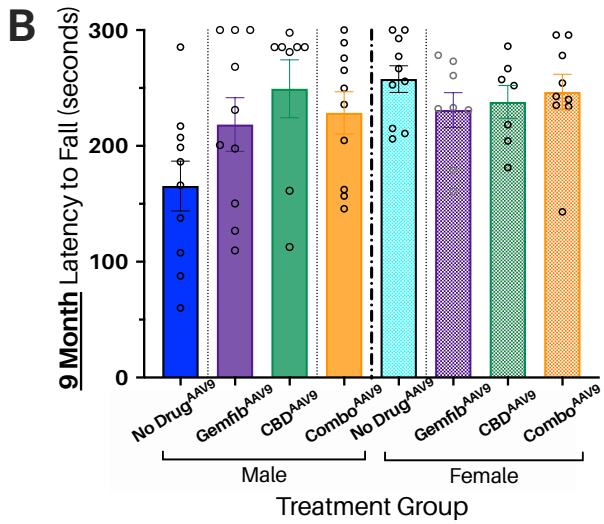
B
9 Month Latency to Fall (seconds)
300
200
100
0
No Drug AAV9
Gemfib AAV9
CBD AAV9
Combo AAV9
No Drug AAV9
Gemfib AAV9
CBD AAV9
Combo AAV9
Male
Female
Treatment Group

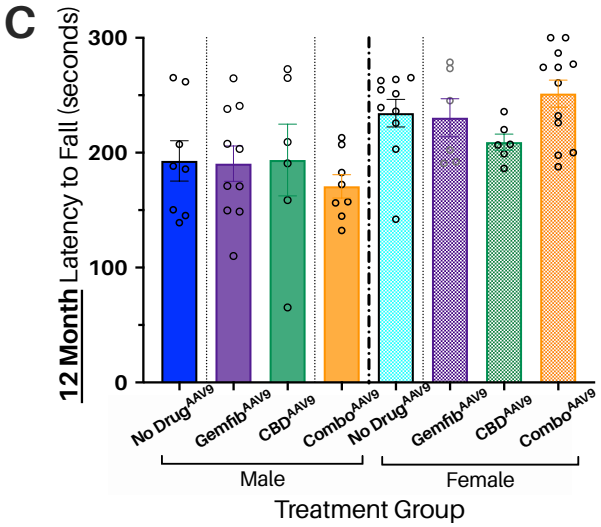
C
12 Month Latency to Fall (seconds)
300
200
100
0
No Drug AAV9
Gemfib AAV9
CBD AAV9
Combo AAV9
No Drug AAV9
Gemfib AAV9
CBD AAV9
Combo AAV9
Male
Female
Treatment Group

⇐ **Figure 3.37 | Combination therapy versus gene therapy alone: rotarod scores (histograms; opposite page)**. *No statistical differences were seen between mean rotarod scores at 6, 9 and 12 months for Cln6^{nclf} mice treated with gene therapy alone or in combination with one of three different small molecule therapies: gemfibrozil (Gemfib^{AAV9}), cannabidiol (CBD^{AAV9}) or both gemfibrozil and CBD (Combo^{AAV9}).* Histograms presenting mean rotarod scores (latency to fall in seconds) of male (left; plain coloured bars) and female (right; patterned bars) Cln6^{nclf} mice treated with gene therapy and either: vehicle (No Drug^{AAV9}), gemfibrozil (Gemfib^{AAV9}), CBD (CBD^{AAV9}), or a combination of the two (Combo^{AAV9}) and their age- and gender-matched untreated (UT^{Cln6nclf}) and WT (C57Bl/6) counterparts at 6 (**A**), 9 (**B**) and 12 (**C**) months of age. Data are presented as mean scores with error bars = ± SEM. Different mice were tested at each of the different time points, making the experiment between-subjects in design. All analyses were conducted using 1-way analysis of variances (ANOVAs) with Tukey's post-hoc comparisons used to elicit specific significant differences between experimental groups (**Appendix B.154-156**). Individual mean mouse rotarod scores indicated by clear circles. (**A-C).** No significant differences were seen in the mean scores of mice treated with gene therapy alone (No Drug^{AAV9}) and those of mice treated with gene therapy and small molecule therapy (Gemfib^{AAV9}, CBD^{AAV9} and Combo^{AAV9}), for either gender, at any time point. n(per group, per time point) = 6-12.

*3.5.2 Combination therapy versus gene therapy alone: **ataxia***

In order to determine wheether combined gene and small molecule therapy is more effective at protecting against the Cln6^{nclf} ataxic phenotype than gene therapy alone, eight different experimental groups were assessed for signs of cerebellar ataxia at 6 and 9 months of age. These included male and female (M/F) No Drug^{AAV9} , M/F Gemfib^{AAV9}, M/F CBD^{AAV9} and M/F Combo^{AAV9} mice. All mice received a dose of scAAV9.CB.*hCLN6* via i.c.v at P0-2. No Drug^{AAV9} mice received vehicle jelly after weaning, while the different combination therapy groups received their respective small molecule therapy (gemfibrozil, CBD or a combination of the two) in strawberry jelly after weaning.

3.5.2.a Composite ataxia phenotype scores

Composite ataxia scores (0-9) for each mouse were calculated by adding together mean ledge, hindlimb clasping and gait ataxia phenotyping scores (0-3). Scores were then averaged for each experimental group and presented as mean score (0-9) ± SEM. Comparisons between mean composite scores of age- and sex-matched No Drug^{AAV9} treated and combination therapy treated (Gemfib^{AAV9}, CBD^{AAV9} and Combo^{AAV9}) mice were made using 1-way ANOVAs, with Tukey's post-hoc multiple comparisons tests conducted when significant differences were found to occur (**Appendices B.159-160**).

No significant differences in mean composite ataxia scores were detected between the combination therapy groups (Gemfib^{AAV9}, CBD^{AAV9} and Combo^{AAV9}) and No Drug^{AAV9} mice at either 6 or 9 months of age, regardless of gender (**Figure 3.38**).

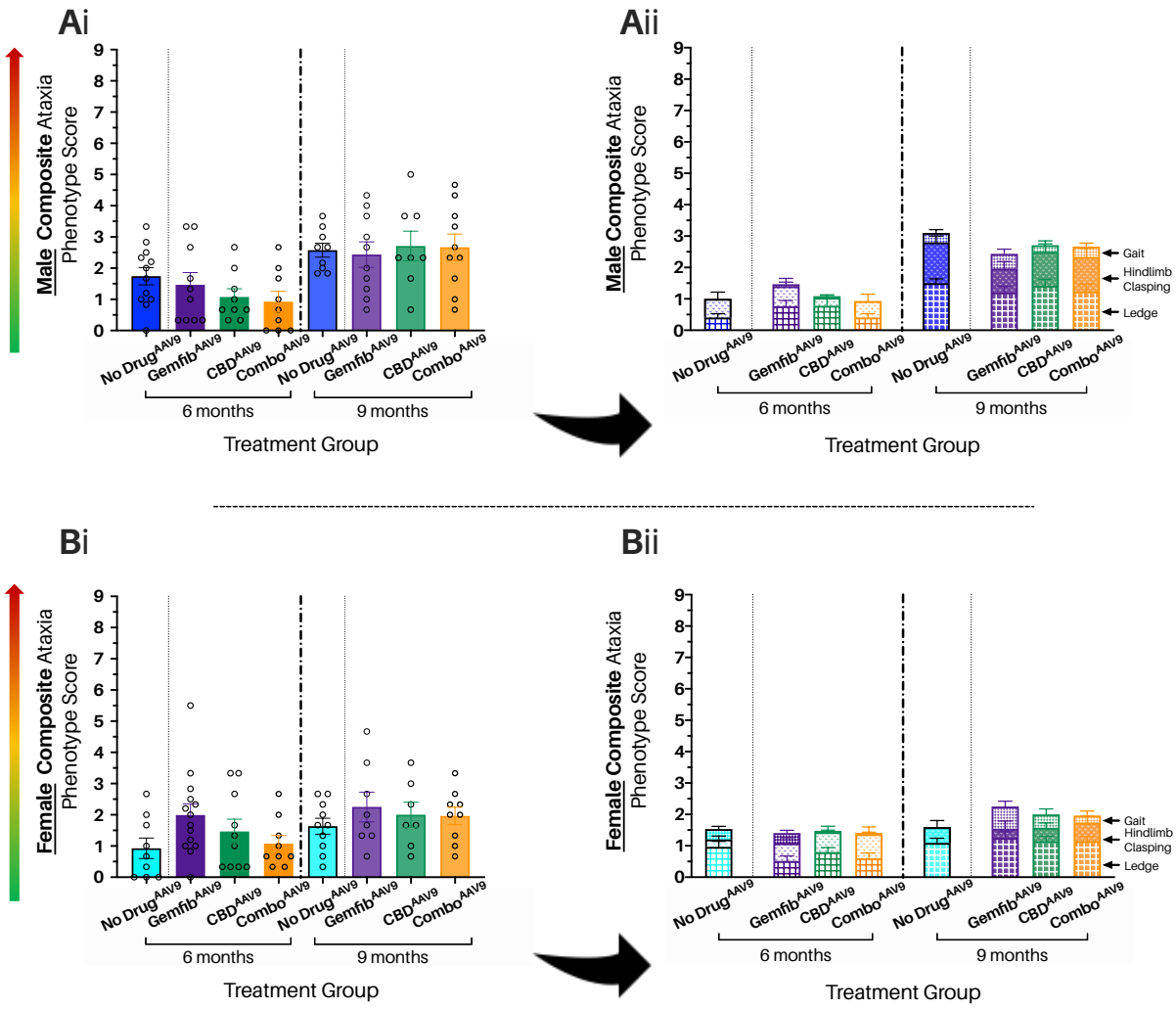

Figure 3.38 | Combination therapy versus gene therapy alone: composite ataxia scores. *No statistical differences were seen between mean composite ataxia scores at 6, 9 and 12 months for Cln6^{nclf} mice treated with gene therapy alone or in combination with one of three different small molecule therapies: gemfibrozil (Gemfib^{AAV9}), cannabidiol (CBD^{AAV9}) or both gemfibrozil and CBD (Combo^{AAV9}).* Mean composite ataxia phenotype scores (0 to 9) were calculated using averaged ataxia test individual scores (ledge, hindlimb clasping and gait) for male (**Ai-ii**) and female (**Bi-ii**) Cln6^{nclf} mice treated with gene therapy and one of three drug regimens: gemfibrozil (Gemfib^{AAV9}), CBD (CBD^{AAV9}) or a combination of gemfibrozil and CBD (Combo^{AAV9}), and Cln6^{nclf} mice treated with gene therapy alone (No Drug^{AAV9}). C57Bl/6 counterparts across two different time points: 6 months (left) and 9 months (right). Different mice were tested at each time point (between-subjects study design). A low score (close to 0) indicates an absence of the ataxic phenotype as measured by the composite scoring system, while higher scores, closer to 9, indicate increasing levels of ataxic behaviour (coloured arrow on the left). The overall mean composite scores illustrated in **Ai** and **Bi** are further broken down into the average ledge (bottom segment), hindlimb clasping (middle segment) and gait (top segment) scores in segmented bar graphs (**Aii** and **Bii**). Individual, averaged composite scores are shown as clear circles in Ai and Bi, error bars = ± SEM. Analyses were conducted via 1-way analysis of variances (ANOVAs) and subsequent Tukey's multiple comparison post-hoc tests (**Appendices B.159-160**). n(per group per time point) = 8-14. **Ai-ii** and **Bi-ii** No significant differences were found between any experimental groups mean composite ataxia scores at any time point, regardless of sex or treatment type.

3.5.2.b Ledge test

No significant differences were observed in mean ledge ataxia scores between combination treatment and gene therapy-only treated groups (**Figure 3.39.A** and **B**; **Appendices B.161** and **B.162**).

3.5.2.c Hindlimb clasping test

No significant differences were observed in mean hindlimb clasping ataxia scores between combination treatment and gene therapy-only treated groups (**Figure 3.39.C** and **D**; **Appendices B.163 and B.164**).

3.5.2.d Gait test

While no significant differences were observed in male mean gait test scores between combination treatment and gene therapy-only treated groups at 6 or 9 months (**Figure 3.39.E**; Appendix B.165), several significant differences were detected between female scores at both time points (**Figure 3.39.F**). Female CBD^{AAV9} and $Combo^{AAV9}$ performed significantly better at the gait test than age- and sex-matched No $Drug^{AAV9}$ counterparts at 6 months of age (No $Drug^{AAV9}$ mean score = 0.333; CBD^{AAV9} mean score = 0.0333; * p = .0128 ; $Combo^{AAV9}$ mean score = 0.0333; * p = .0128; **Appendix B.166**). At 9 months, however, these significant differences have disappeared and the only difference observed was between the mean score of $Gemfib^{AAV9}$ treated female mice and No $Drug^{AAV9}$ mice, with $Gemfib^{AAV9}$ performing significantly worse (higher score) at this time point (No $Drug^{AAV9}$ mean score = 0.0; ** p = .0029; **Appendix B.166**).

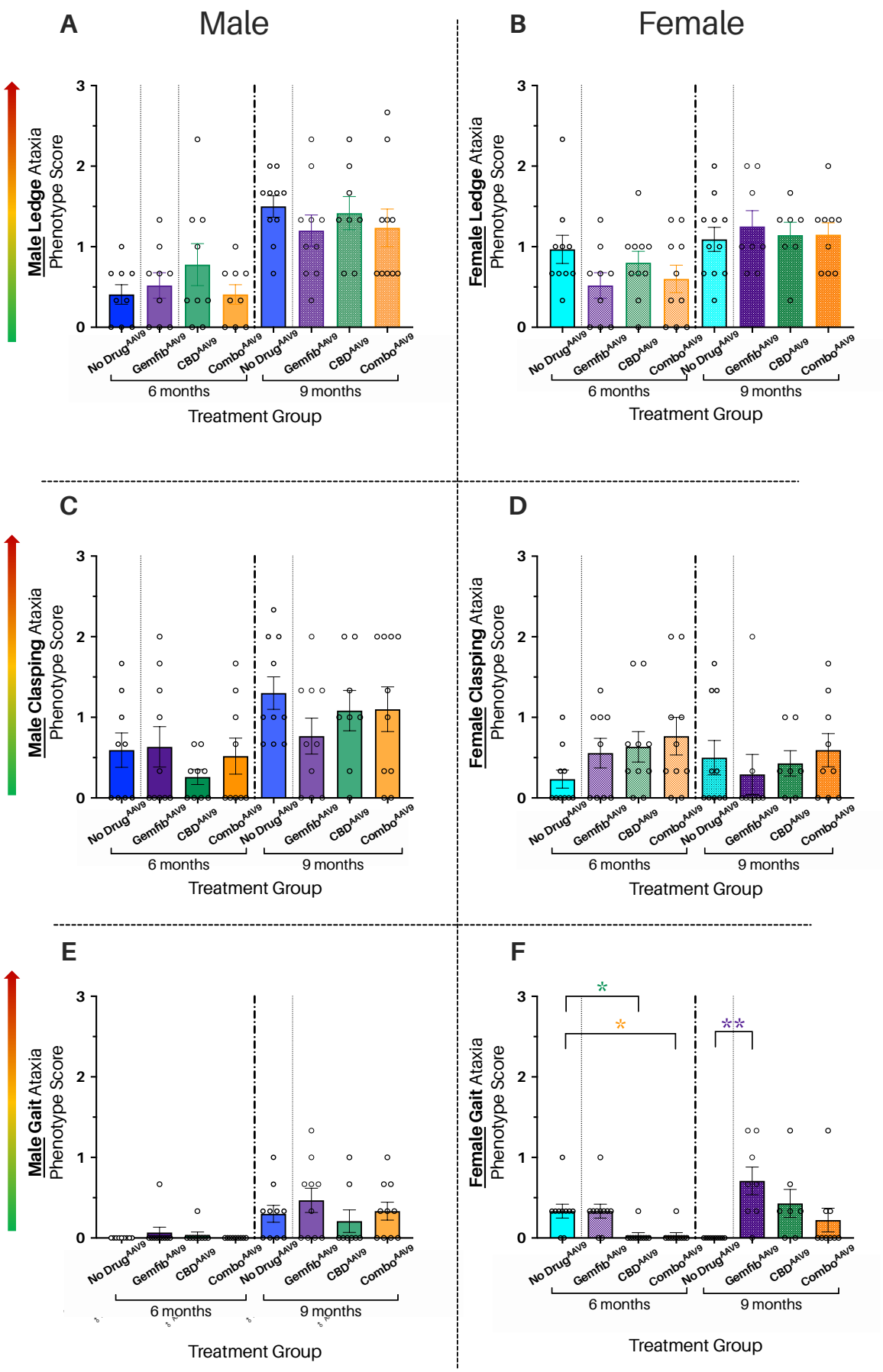
A
Male
B
Female
Male Ledge Ataxia Phenotype Score
Female Ledge Ataxia Phenotype Score
C
D
Male Clasping Ataxia Phenotype Score
Female Clasping Ataxia Phenotype Score
E
F
Male Gait Ataxia Phenotype Score
Female Gait Ataxia Phenotype Score
No Drug AAV9
Gemfib AAV9
CBD AAV9
Combo AAV9
6 months
9 months
Treatment Group
*
*
**

⇐ Figure 3.39 | Combination therapy versus gene therapy alone: ataxia phenotyping scores (previous page). *Only a few statistically significant differences were observed in mean ataxia assay scores between Cln6^{nclf} mice treated with a combination of gene and small molecule therapy (Gemfib^{AAV9}, CBD^{AAV9} and Combo^{AAV9}) and Cln6^{nclf} mice treated with gene therapy alone (No Drug^{AAV9})* Histograms presenting mean ataxia scores (0-3) for individual ataxia assays: ledge (**A**; males; **B**; females), hindlimb clasping (**C**; males; **D**; females), and gait (**E**; males; **F**; females). Scoring criteria and methodology can be found in **Chapter 2**, adapted from *Guyenet et al. 2010*. Different mice were assessed at each time point, making the experiment between-subjects in design. For each assay, a mouse could be assigned a score between 0 and 3, with 0 indicating a complete absence of the ataxic phenotype and 3 indicating a completely penetrant ataxic phenotype (coloured arrows on the left). Data are presented as mean scores, with error bars representing ± SEM. Individual (averaged) mouse scores are presented as clear circles. All analyses were conducted using 1-way ANOVAs (**Appendices B.161-166**), followed by Tukey's multiple comparisons post-hoc tests **A.** and **B.** Histograms presenting the mean ledge ataxia scores of male (**A**) and female (**B**) mice. No significant differences were detected between Gemfib^{AAV9} (purple), CBD^{AAV9} (green) and Combo^{AAV9} (orange) mean ledge ataxia scores and the mean scores of No Drug^{AAV9} mice at 6 (left hand side of histograms) or 9 months of age (right hand side of histograms) for either male (**A**) or female (**B**) mice (**Appendices B.161** and **B.162**). n(per group per time point) = 7-10 **C.** and **D.** Histograms presenting the mean hindlimb clasping ataxia scores of male (**C**) and female (**D**) mice. No significant differences were detected between Gemfib^{AAV9} (purple), CBD^{AAV9} (green) and Combo^{AAV9} (orange) mean hindlimb clasping ataxia scores and the mean scores of No Drug^{AAV9} mice at 6 (left hand side of histograms) or 9 months of age (right hand side of histograms) for either male (**C**) or female (**D**) mice (**Appendices B.163** and **B.164**). n(per group per time point) = 7-10 **E.** Histogram presenting mean gait ataxia scores for male mice at 6 (left; dark coloured bars) and 9 months of age (right; light coloured bars). No significant diffferences were detected between any of the experimental treatment groups at either time point (**Appendix B.165**). n(per group per time point) = 8-10. **F.** Histogram presenting mean gait ataxia scores for female mice at 6 (left; light coloured bars) and 9 months of age (right; dark coloured bars). At 6 months, female CBD^{AAV9} (green bars) and Combo^{AAV9} (orange bars) treatment groups demonstrated significantly lower (better) mean gait ataxia scores than age- and sex-matched No Drug^{AAV9} (light blue bars) mice (No Drug^{AAV9} mean score = 0.333; CBD^{AAV9} mean score = 0.0333; * p = .0128 ; Combo^{AAV9} mean score = 0.0333; * p = .0128; **Appendix B.166**). At 9 months, however, the only significant difference between mean scores is between the mean gait ataxia score of Gemfib^{AAV9} mice (0.7083) and that belonging to No Drug^{AAV9} mice (No Drug^{AAV9} mean score = 0.0; ** p = .0029; **Appendix B.166**). Gemfib^{AAV9} mice perform significantly worse (higher score) than No Drug^{AAV9} at 9 months of age. (per group per time point) = 7-10.

3.5.3 Combination therapy versus gene therapy alone: ***survival and weight***

The survival curves (and median survival) of Cln6^{nclf} mice treateed with both gene therapy and gemfibrozil, CBD and combination were compared to Cln6^{nclf} mice who received gene therapy alone. Survival data are presented as percentage of the original cohort n, with curve comparisons between sex-matched Cln6^{nclf} conducted via separate log-rank (Mantel-Cox) tests for each sex (**Appendices B.167-172**).

All experimental groups, for both male and female mice, had 'undefined' median survivals by 15 months – due to the fact that less than half of each group's cohort had passed away from unplanned deaths. Despite this, one significant difference in survival curve was detected for male mice, with CBD^{AAV9} mice having a significantly reduced survival curve compared to No Drug^{AAV9} mice (**Figure 3.40**; **Appendices B.170-172**).

Weights were also kept, as a measure of overall health, and body weight was recorded weekly (in grams). Average weights for each experimental group are presented here, however, monthly as it gives a clearer overview of weight progression throughout the lifespan. Simple linear regression was conducted to determine the overall rate of weight gain and/or loss over the first 14 months of the trial, but no differences were detected in the slopes of any experimental group. A series of 1-way ANOVA analyses were also used to compare the mean weights of combination therapy treated Cln6^{nclf} mice to age-matched No Drug^{AAV9} mice at 6, 9 and 12 months – which felt appropriate, as this is when behavioural assessments were carried out. Data are presented here as average weights, in grams ± SEM (**Figure 3.41**).

Male mean weights were found to be statistically indistinguishable at 6, 9 and 12 months of age (**Figure 3.41.A, C, E** and **G; Appendix B.173**). Females, however, did demonstrate so significant differences in mean weights at 6 and 12 months of age (**Figures**

3.41.B, D, and **H**). Gemfib^{AAV9} and Combo^{AAV9} treated female mice demonstrated significantly lower mean weights than No Drug^{AAV9} treated mice at 6 months of age (**Figures 3.41.D**; female 6 month No Drug^{AAV9} mean weight = 26.17 g; female 6 month Gemfib^{AAV9} mean weight = 24.44 g; * p = .0117; female 6 month Combo^{AAV9} mean weight = 24.04 g; ** p =.0014 ; **Appendix B.174**). Similarly, Gemfib^{AAV9} treated female mice were, on average, significantly lighter than No Drug^{AAV9} counterparts at 12 months of age (Gemfib^{AAV9} mean weight = 26.95 g; No Drug^{AAV9} mean weight = 30.22 g; * p = **Appendix B.174**).

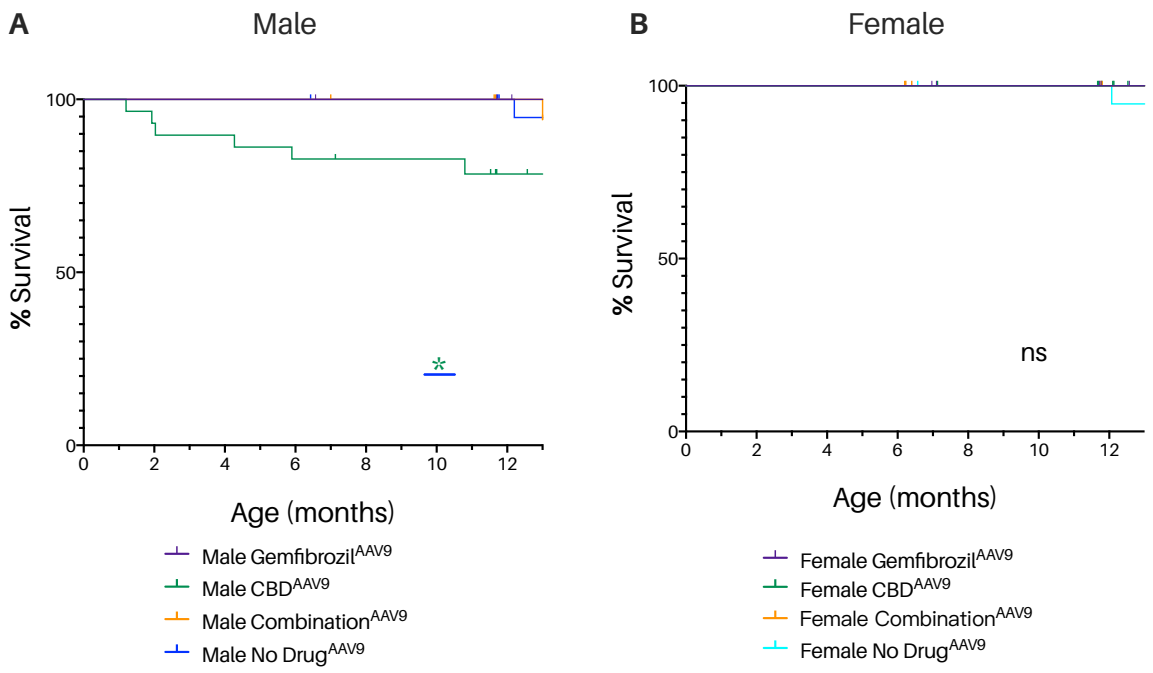

Figure 3.40 | Combination therapy versus gene therapy alone: survival. *While male Cln6^{nclf} mice that were treated with a combination of gene therapy and CBD small molecule therapy (CBD^{AAV9}) demonstrated reduced survival in comparison to sex-matched Cln6^{nclf} who received gene therapy alone (No Drug^{AAV9}), the rest of the Cln6^{nclf} mice, both male and female, who received both gene therapy and one of three small molecule therapy regimens demonstrated no significant difference in survival from that of No Drug^{AAV9}.* Kaplan-Meier survival plots (%) comparing the survival curves of No Drug^{AAV9} (male = blue lines; female = light blue lines)) to Cln6^{nclf} mice treated with one of three combination therapy regimens (gemfibrozil and gene therapy = purple lines; CBD and gene therapy = green lines; combination of gemfibrozil, CBD and gene therapy = orange lines). All survival curve comparisons were conducted using a log rank (Mantel-Cox) test in GraphPad Prism 8 (**Appendices B.167-172**). **A.** Male survival curves (%) from birth to 14 months of age. Only CBD^{AAV9} mice had a significantly shorter median survival rate than No Drug^{AAV9} (male No Drug^{AAV9} median survival aka 'ms' = undefined at 14 months; CBD^{AAV9} ms = undefined at 14 months; * p = .00373; **Appendix B.168**). While both experimental groups had not yet reached a median survival of 14 months, CBD^{AAV9}'s cohort had experienced several more unplanned deaths than No Drug^{AAV9}(6 deaths vs 1). Starting n(per group) = 27-31**. B.** No significant difference was detected between the survival curves of female No Drug^{AAV9}, Gemfib^{AAV9}, CBD^{AAV9} and Combo^{AAV9} mice (**Appendices B.170-172**). Starting n(per group) = 22-29.

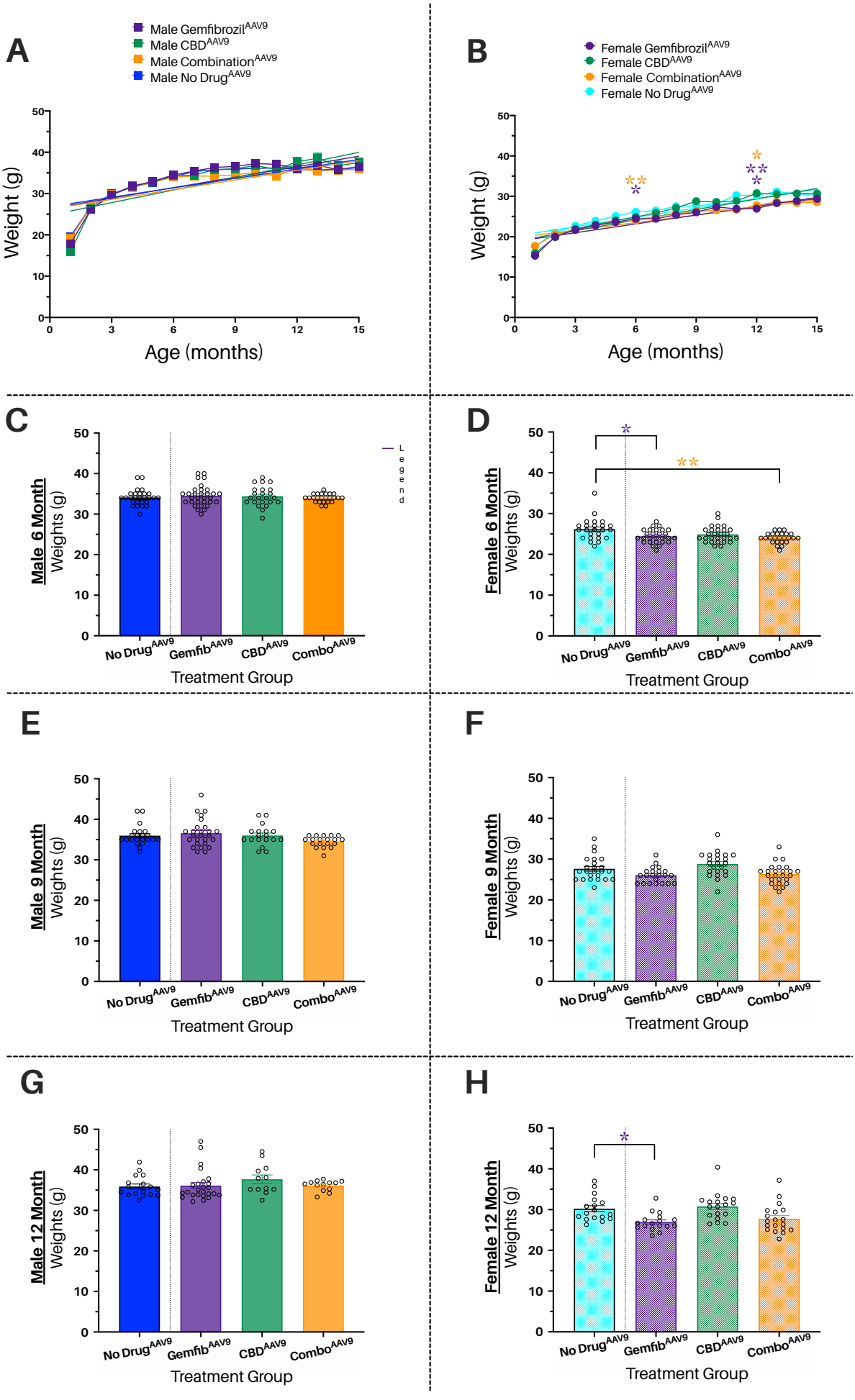
A
Male Gemfibrozil^AAV9
Male CBD^AAV9
Male Combination^AAV9
Male No Drug^AAV9
Weight (g)
Age (months)
B
Female Gemfibrozil^AAV9
Female CBD^AAV9
Female Combination^AAV9
Female No Drug^AAV9
Weight (g)
Age (months)
C
Male 6 Month
Weights (g)
Legend
No Drug^AAV9
Gemfib^AAV9
CBD^AAV9
Combo^AAV9
Treatment Group
D
Female 6 Month
Weights (g)
No Drug^AAV9
Gemfib^AAV9
CBD^AAV9
Combo^AAV9
Treatment Group
E
Male 9 Month
Weights (g)
No Drug^AAV9
Gemfib^AAV9
CBD^AAV9
Combo^AAV9
Treatment Group
F
Female 9 Month
Weights (g)
No Drug^AAV9
Gemfib^AAV9
CBD^AAV9
Combo^AAV9
Treatment Group
G
Male 12 Month
Weights (g)
No Drug^AAV9
Gemfib^AAV9
CBD^AAV9
Combo^AAV9
Treatment Group
H
Female 12 Month
Weights (g)
No Drug^AAV9
Gemfib^AAV9
CBD^AAV9
Combo^AAV9
Treatment Group

⇐ **Figure 3.41 | Combination therapy versus gene therapy alone: weights (opposite page)**. *Weights of male Cln6^{nclf} mice treated with combined gene and small molecule therapy do not differ significantly from those of male Cln6^{nclf} mice treated with gene therapy alone, while female Cln6^{nclf} who receive both gemfibrozil and gene therapy (Gemfib^{AAV9}) appear to have significantly lower weights than gene therapy only female Cln6^{nclf} mice by 12 months of age.* Mice were weighed weekly from weaning (~28 days) to determine drug dosage and as a measure of general health. Weights are shown here from weaning to 15 months due to the time constraints of an MSc (weights continued to be tracked for the entire duration of the trial). Data are presented as average weights, error bars ± SEM. Analyses conducted via 1-way ANOVA with Tukey's multiple comparisons post-hoc tests where applicable.**A.** Line graph of average male weights (in grams) over 14 months (from weaning to ~15 months). 1-way ANOVA analyses conducted between male No Drug^{AAV9} (blue squares and lines), Gemfib^{AAV9} (purple squares and lines) , CBD^{AAV9} (green squares and lines) and Combo^{AAV9} (orange squares and lines). Starting n(per group) = 23-31 **B.** Line graph of average female weights (in grams) over 14 months (from weaning to ~15 months). 1-way ANOVA analyses conducted between female No Drug^{AAV9} (light blue circles and lines), Gemfib^{AAV9} (purple circles and lines) , CBD^{AAV9} (green circles and lines) and Combo^{AAV9} (orange circles and lines). Starting n(per group) = 22-29. . **C.** Histogram of mean male No Drug^{AAV9} (blue bar) Gemfib^{AAV9} (purple bar), CBD^{AAV9} (green bar) and Combo^{AAV9} (orange bar) mice at 6 months of age. No significant differences in average weight were found between any of the experimental groups at this time point (1-way ANOVA; **Appendix B.173).** n (per group) = 23-31. **D.** Histogram of mean female No Drug^{AAV9} (light blue bar) Gemfib^{AAV9} (purple bar), CBD^{AAV9} (green bar) and Combo^{AAV9} (orange bar) mice at 6 months of age. Combo^{AAV9} and Gemfib^{AAV9} treated female mice weighed significantly less, on average, than No Drug^{AAV9} mice at this time point (female 6 month No Drug^{AAV9} mean weight = 26.17 g; female 6 month Gemfib^{AAV9} mean weight = 24.44 g; * p = .0117; female 6 month Combo^{AAV9} mean weight = 24.04 g; ** p =.0014 ; **Appendix B.174**). n (per group) = 24-28. **E.** Histogram of mean male No Drug^{AAV9}, Gemfib^{AAV9} CBD^{AAV9} and Combo^{AAV9} mice at 9 months of age. No significant differences in average weight were found between any of the experimental groups at this time point (1-way ANOVA; **Appendix B.173).** n(per group) = 19-26. **F.** Histogram presenting mean female No Drug^{AAV9}, Gemfib^{AAV9} CBD^{AAV9} and Combo^{AAV9} mice at 9 months of age. No significant differences in average weight were found between any of the experimental groups at this time point (1-way ANOVA; **Appendix B.174**). n(per group) = -25. **G.** Histogram of mean male No Drug^{AAV9}, Gemfib^{AAV9} CBD^{AAV9} and Combo^{AAV9} mice at 12 months of age. No significant differences in average weight were found between any of the experimental groups at this time point (1-way ANOVA; **Appendix B.173).** n(per group) = 12-25. **F.** Histogram presenting mean female No Drug^{AAV9}, Gemfib^{AAV9} CBD^{AAV9} and Combo^{AAV9} mice at 9 months of age. Female Gemfib^{AAV9} mice demonstrated a significantly lower mean weight (in grams) than their age- and sex-matched No Drug^{AAV9} counterparts (Gemfib^{AAV9} mean weight = 26.95 g; No Drug^{AAV9} mean weight = 30.22 g; * p = ; **Appendix B.174**). n(per group) = 17-19.

*3.5.4 Combination therapy versus gene therapy alone: **summary***

The behavioural scores, survival and weights of Cln6^{nclf} mice treated with gene therapy and one of three possible small molecule therapy regimens (gemfibrozil, CBD or a combination of both gemfibrozil and CBD) were directly compared to age- and sex- matched No Drug^{AAV9} Cln6^{nclf} counterparts, who had only received gene therapy and a vehicle instead of small molecule therapy. This was done to determine if the use of a combination treatment offered any additional therapeutic benefit against the Cln6^{nclf} compared to gene therapy alone, with the intention of informing potential future combined therapeutic strategies in CLN6 BD patients.

Overall, it appears that there were very few significant differences in behavioural, survival and weight outcomes between the different treatment groups – regardless of gender. There were only four instances in which a combination therapy group out performed No Drug^{AAV9} mice. Male CBD^{AAV9} and Combo^{AAV9} mice achieved a higher mean hindlimb clasping score than male No Drug^{AAV9} mice and female CBD^{AAV9} and Combo^{AAV9} mice achieved a higher gait ataxia score than female No Drug^{AAV9} mice, all differences occurring at 6 months of age.

Unfortunately there were also two instances in which a combination therapy treatment group performed significantly worse than No Drug^{AAV9} mice: CBD^{AAV9} male mice had a significantly reduced survival curve compared to male No Drug^{AAV9} mice and female Gemfib^{AAV9} mice performed significantly worse in the gait ataxia test than female No Drug^{AAV9} mice at 9 months.

This data, taken together, suggests that the overall effects of different combined therapeutic strategies on key Cln6^{nclf} phenotypes offer negligible benefit over the use of gene therapy alone, and in one or two cases even seem to antagonise the positive effects elicited by gene therapy.

Table 3.25 | Combination therapy versus gene therapy alone: summary table of male Gemfib^{AAV9} scores versus No Drug^{AAV9} scores. *Summary table of behavioural score (rotarod and ataxia), survival and weight comparisons carried out between male gene therapy and gemfibrozil (Gemfib^{AAV9}) treated Cln6^{nclf} mice and their age- and sex-matched gene therapy-only Cln6^{nclf} (No Drug^{AAV9}) counterparts at 6, 9 and 12 months of age.* All behavioural score and weight comparisons were conducted using 1-way ANOVAs **(Appendices B.157, 159, 161, 163** and **B.165**), with Tukey's post-hoc multiple comparisons tests where appropriate, while survival curves were compared using log rank (Mantel-Cox) tests (**Appendices B.167**). nsd = no significant difference; s = significant.

Gemfib^{AAV9} Cln6^{nclf} Males				
Behavioural Test	**Comparison Group**	**6 months**	**9 months**	**12 months**
Rotarod	No Drug^{AAV9}	nsd	nsd	nsd
Composite	No Drug^{AAV9}	nsd	nsd	-
Ledge	No Drug^{AAV9}	nsd	nsd	-
Hindlimb Clasping	No Drug^{AAV9}	nsd	nsd	-
Gait	No Drug^{AAV9}	nsd	nsd	-
Survival	No Drug^{AAV9}		nsd	
Weight	No Drug^{AAV9}	nsd	nsd	nsd

Table 3.26 | Combination therapy versus gene therapy alone: summary table of female Gemfib^{AAV9} scores versus No Drug^{AAV9} scores. *Summary table of behavioural score (rotarod and ataxia), survival and weight comparisons carried out between female gene therapy and gemfibrozil (Gemfib^{AAV9}) treated Cln6^{nclf} mice and their age- and sex-matched gene therapy-only Cln6^{nclf} (No Drug^{AAV9}) counterparts at 6, 9 and 12 months of age.* All behavioural score and weight comparisons were conducted using 1-way ANOVAs with Tukey's post-hoc multiple comparisons tests where appropriate, while survival curves were compared using log rank (Mantel-Cox) tests (**Appendices B.170**). nsd = no significant difference; s = significant.

Gemfib^{AAV9} Cln6^{nclf} Females				
Behavioural Test	**Comparison Group**	**6 months**	**9 months**	**12 months**
Rotarod	No Drug^{AAV9}	nsd	nsd	nsd
Composite	No Drug^{AAV9}	nsd	nsd	-
Ledge	No Drug^{AAV9}	nsd	nsd	-
Hindlimb Clasping	No Drug^{AAV9}	nsd	nsd	-
Gait	No Drug^{AAV9}	nsd	**Worse (s)**	-
Survival	No Drug^{AAV9}		nsd	
Weight	No Drug^{AAV9}	**Weigh Less (s)**	nsd	**Weigh less (s)**

Table 3.27 | Combination therapy versus gene therapy alone: summary table of male CBD^{AAV9} scores versus No Drug^{AAV9} scores. *Summary table of behavioural score (rotarod and ataxia), survival and weight comparisons carried out between male gene therapy and cannabidiol (CBD^{AAV9}) treated Cln6^{nclf} mice and their age- and sex-matched gene therapy-only Cln6^{nclf} (No Drug^{AAV9}) counterparts at 6, 9 and 12 months of age.* All behavioural score and weight comparisons were conducted using 1-way ANOVAs **(Appendices B.157, 159, 161, 163** and **B.165**), with Tukey's post-hoc multiple comparisons tests where appropriate, while survival curves were compared using log rank (Mantel-Cox) tests (**Appendices B.168**). nsd = no significant difference; s = significant.

CBD^{AAV9} Cln6^{nclf} Males				
Behavioural Test	**Comparison Group**	**6 months**	**9 months**	**12 months**
Rotarod	No Drug^{AAV9}	nsd	nsd	nsd
Composite	No Drug^{AAV9}	nsd	nsd	-
Ledge	No Drug^{AAV9}	nsd	nsd	-
Hindlimb Clasping	No Drug^{AAV9}	**Better (s)**	nsd	-
Gait	No Drug^{AAV9}	nsd	nsd	-
Survival	No Drug^{AAV9}	**Reduced survival (s)**		
Weight	No Drug^{AAV9}	nsd	nsd	nsd

Table 3.28 | Combination therapy versus gene therapy alone: summary table of female CBD^{AAV9} scores versus No Drug^{AAV9} scores. *Summary table of behavioural score (rotarod and ataxia), survival and weight comparisons carried out between female gene therapy and cannabidiol (CBD^{AAV9}) treated Cln6^{nclf} mice and their age- and sex-matched gene therapy-only Cln6^{nclf} (No Drug^{AAV9}) counterparts at 6, 9 and 12 months of age.* All behavioural score and weight comparisons were conducted using 1-way ANOVAs, with Tukey's post-hoc multiple comparisons tests where appropriate, while survival curves were compared using log rank (Mantel-Cox) tests (**Appendices B.171**). nsd = no significant difference; s = significant.

CBD^{AAV9} Cln6^{nclf} Females				
Behavioural Test	**Comparison Group**	**6 months**	**9 months**	**12 months**
Rotarod	No Drug^{AAV9}	nsd	nsd	nsd
Composite	No Drug^{AAV9}	nsd	nsd	-
Ledge	No Drug^{AAV9}	nsd	nsd	-
Hindlimb Clasping	No Drug^{AAV9}	nsd	nsd	-
Gait	No Drug^{AAV9}	**Better (s)**	nsd	-
Survival	No Drug^{AAV9}	nsd		
Weight	No Drug^{AAV9}	nsd	nsd	nsd

Table 3.29 | Combination therapy versus gene therapy alone: summary table of male Combo^{AAV9} scores versus No Drug^{AAV9} scores. *Summary table of behavioural score (rotarod and ataxia), survival and weight comparisons carried out between male gene therapy and combination small therapy (Combo^{AAV9}) treated Cln6^{nclf} mice and their age- and sex-matched gene therapy-only Cln6^{nclf} (No Drug^{AAV9}) counterparts at 6, 9 and 12 months of age.* All behavioural score and weight comparisons were conducted using 1-way analysis of variances (ANOVAs**; Appendices B.157, 159, 161, 163** and **B.165**), with Tukey's post-hoc multiple comparisons tests where appropriate, while survival curves were compared using log rank (Mantel-Cox) tests (**Appendices B.169**). nsd = no significant difference; s = significant.

Combo^{AAV9} Cln6^{nclf} Males				
Behavioural Test	Comparison Group	**6 months**	**9 months**	**12 months**
Rotarod	No Drug^{AAV9}	nsd	nsd	nsd
Composite	No Drug^{AAV9}	nsd	nsd	-
Ledge	No Drug^{AAV9}	nsd	nsd	-
Hindlimb Clasping	No Drug^{AAV9}	**Better (s)**	nsd	-
Gait	No Drug^{AAV9}	nsd	nsd	-
Survival	No Drug^{AAV9}	nsd		
Weight	No Drug^{AAV9}	nsd	nsd	nsd

Table 3.30 | Combination therapy versus gene therapy alone: summary table of female Combo^{AAV9} scores versus No Drug^{AAV9} scores. *Summary table of behavioural score (rotarod and ataxia), survival and weight comparisons carried out between male gene therapy and combination small therapy (Combo^{AAV9}) treated Cln6^{nclf} mice and their age- and sex-matched gene therapy-only Cln6^{nclf} (No Drug^{AAV9}) counterparts at 6, 9 and 12 months of age.* All behavioural score and weight comparisons were conducted using 1-way ANOVAs, with Tukey's post-hoc multiple comparisons tests where appropriate, while survival curves were compared using log rank (Mantel-Cox) tests (**Appendices B.172**). nsd = no significant difference; s = significant.

Combo^{AAV9} Cln6^{nclf} Females				
Behavioural Test	**Comparison Group**	**6 months**	**9 months**	**12 months**
Rotarod	No Drug^{AAV9}	nsd	nsd	nsd
Composite	No Drug^{AAV9}	nsd	nsd	-
Ledge	No Drug^{AAV9}	nsd	nsd	-
Hindlimb Clasping	No Drug^{AAV9}	nsd	nsd	-
Gait	No Drug^{AAV9}	**Better (s)**	nsd	-
Survival	No Drug^{AAV9}	nsd		
Weight	No Drug^{AAV9}	**Weigh less (s)**	nsd	nsd

Chapter 4: Discussion

4.1 Thesis summary and significance

The practical component of this thesis was designed to contribute to a larger pre-clinical trial, funded by the Gray Foundation and run by the Hughes Lab, to assess the efficacy of gene therapy when complemented by two different experimental small molecule therapeutics, alone and in combination, on the CLN6 BD phenotype. This thesis focuses solely on behavioural assessment, with plans being made by the Hughes Lab to conduct post-mortem biochemical analyses in the near future. Here, a naturally-occurring CLN6 BD animal model, the $Cln6^{nclf}$ mouse, was used to investigate whether the use of gemfibrozil, an FDA-approved fibrate, and/or cannabidiol (CBD), a cannabinoid with purported neuroprotective properties, would amplify or attenuate the efficacy of AAV2/9-mediated gene therapy in protecting against behavioural deficits typical of $UT^{Cln6nclf}$ mice. Sex differences in behavioural response to the different treatment regimens were also investigated, due to the mounting preclinical and clinical evidence that male and female experiences of the NCLs vary in terms of symptom onset and severity, as well as speed of progression (Cialone et al., 2012; Poppens et al., 2019).

In order to make meaningful observations regarding the efficacy of gemfibrozil and/or CBD as complementary therapies, it was first important to establish and characterise an $UT^{Cln6nclf}$ behavioural phenotype for each of the behavioural assays used, with which the behavioural scores of different treatment groups could later be compared. Here, the $UT^{Cln6nclf}$ mice were found to recapitulate previously described motor deficits in rotarod and ataxia tests. A significant ataxic phenotype could be detected as early as 6 months for males and 9 months for females, and all mice were performing significantly worse than WT on the rotarod by 12 months of age – indicating a reduction in motor co-ordination and balance.

Once healthy WT control and diseased Cln6^{nclf} behavioural baselines had been established, the effects of gemfibrozil and CBD, alone and in combination with each other, were investigated without gene therapy. These 'drug-only' Cln6^{nclf} experimental groups were included in the trial (and the practical component of this thesis) to better characterise any subtle therapeutic effects gemfibrozil and CBD might have on the Cln6^{nclf} behavioural phenotype. Little *in vivo* work has been conducted previously on the therapeutic efficacy of gemfibrozil and/or CBD in Cln6^{nclf} mice, and no published studies to date have specifically looked at their protective properties against the Cln6^{nclf} diseased behavioural phenotype. By investigating and characterising the effects of these two small molecule therapies on the behavioural phenotype of Cln6^{nclf} mice, this thesis represents the first publication to address this specific gap in the literature. At first glance, the data seemed to indicate that neither gemfibrozil nor CBD had any kind of effect on the Cln6^{nclf} behavioural phenotype – mice were still declining significantly by 9 months of age and had characteristically short lifespans. On closer examination, however, subtle effects became evident – with male mice who received any form of small molecule therapy appearing to have delayed disease onset in comparison to UT^{Cln6nclf} mice. Female mice also seemed to do a little better on gemfibrozil in the composite and gait ataxia assays, in comparison to UT^{Cln6nclf} counterparts, though this improvement was not present across all behavioural tests and would warrant further investigation.

While the primary aim of this work was to explore the possibility of combined gene and small molecule therapy, experimental groups of mice treated with gene therapy alone (No Drug^{AAV9}) were also assessed for behavioural performance in comparison to healthy WT controls and UT^{Cln6nclf} mice. This was done to validate and expand upon a series of published preclinical studies looking at AAV2/9-mediated gene transfer in the Cln6^{nclf} mouse and to recapitulate, to a certain extent, the therapeutic parameters of the 2016 Gray Foundation

CLN6 BD clinical trial (Cain et al., 2019; Trial No. NCT02725580, *Clinicaltrials.gov*). Here, it was found that a single neonatal i.c.v injection of scAAV9.CB.*hCLN6* appeared to protect Cln6^{nclf} mice, of both sexes, from a wide swathe of characteristic behavioural deficits. Compared to sex-matched UT^{Cln6nclf} counterparts, male and female No Drug^{AAV9} mice experienced significantly extended survival, significantly higher 12 month rotarod scores, as well as better 6 and 9 month composite and hindlimb clasping ataxia scores. Male No Drug^{AAV9} mice also performed significantly better than male UT^{Cln6nclf} mice at the ledge test at both 6 and 9 months, a significant improvement considering it was the 6 month ledge and composite ataxia tests where male UT^{Cln6nclf} mice first began to demonstrate deficits compared to WT controls (**section 3.1**). There were also several instances where No Drug^{AAV9} mice outperformed even the healthy WT controls, with both male and female No Drug^{AAV9} achieving significantly higher mean rotarod scores than WT at 12 months of age, and females outperforming WT in the gait ataxia test at 9 months of age. Females, overall, appear to have responded better to the gene therapy than males – with females producing significantly higher scores than males in four out of five behavioural assays. This data, taken together, confirms the efficacy of AAV2/9-mediated gene therapy as protection against the Cln6^{nclf} mouse and may even have produced a novel observation regarding a sex-based difference in response to CLN6 gene therapy.

Perhaps the most important aspect of this work was the investigation of the effects of combined gene and small molecule therapy on the Cln6^{nclf} behavioural phenotype. Here, Cln6^{nclf} treated with both AAV2/9-mediated gene therapy and either gemfibrozil, CBD or a combination of the two drugs were assessed in the hopes of finding a synergystic combination that could augment the protective qualities of gene therapy alone and potentially inform future therapeutic strategies for CLN6 BD children who have already received gene therapy. All three combination therapies (Gemfib^{AAV9}, CBD^{AAV9} and Combo^{AAV9}) showed promise by

protecting Cln6^{nclf} mice, of both genders, against the UT^{Cln6nclf} behavioural and survival phenotypes. Male Cln6^{nclf} mice treated with both gene therapy and gemfibrozil even outperformed healthy WT controls on the rotarod assay at 12 months, while female Gemfib^{AAV9} mice outperformed WT at 6 months in the ledge ataxia test – perhaps indicating a synergystic quality to the combination of gene therapy with gemfibrozil in this mouse model. Considering, again, however that these results were only for one assay out of five, further investigation into the effects of gemfibrozil in combination with gene therapy is warranted. It should also be noted that no combination of gene therapy and drug resulted in a rescue of mean weights to WT at 6, 9 or 12 months.

Finally, the behavioural, survival and weight data of combination therapy treated mice was compared to that of mice treated with gene therapy alone (No Drug^{AAV9}). This was to determine whether there is any added benefit to using combination therapy over gene therapy alone. The results were mixed, as is discussed below, and ultimately there were not enough significant improvements in behaviour produced by any combination therapy group to warrant concluding the superiority of their treatment regimen over gene therapy alone, especially in light of the risks, side-effects and additional costs associated with the combined use of a second therapeutic. Despite this, the work presented in this thesis represents a novel investigation into the treatment of CLN6 BD with combined therapeutic strategies and has produced several important and interesting observations that will require future research. This thesis also represents the first long term, in-depth investigation into the effects of CBD in an animal model of any NCL variant and builds on preliminary *in vivo* gemfibrozil studies for the NCLs by providing a detailed account of behavioural responses to long term treatment with this compound.

4.2 In mouse: the use of small molecule therapeutics for CLN6 BD (gemfibrozil)

Gemfibrozil is an FDA-approved, cholesterol-lowering drug and a member of a class of amphipathic carboxylic acids called 'fibrates'. Its potential as a complementary therapy to AAV2/9-mediated gene therapy in Cln6^{nclf} mice was investigated here because of its known ability to modulate autophagic and lysosomal processes via PPARα activation and subsequent TFEB upregulation. Gemfibrozil has also shown considerable promise in several *in vitro* and *in vivo* NCL models, including the a Cln2$^{-/-}$ mouse model (Ghosh et al., 2017) and a sheep CLN6 neural culture model (OCLN)(Best et al., 2017), and preliminary work conducted by other members of the Hughes lab has indicated both its safety and potential efficacy in Cln6^{nclf} mice (Best, 2017; Stephanie Mercer, Isaiah Cheong, Cliff Abrahams and Stephanie Hughes, unpublished work).

Here, the effects of gemfibrozil, alone and in combination with another small molecule therapy (cannabidiol; CBD), were examined – with and without gene therapy – on the Cln6^{nclf} behavioural phenotype. Ultimately, it was determined that the effects of gemfibrozil alone (**section 3.2**), in this study at least, were limited, with negligible protection conferred to either male or female Cln6^{nclf} mice who were dosed regularly with gemfibrozil alone from weaning and had received a neonatal 1x PBS i.c.v injection at P0-2. Despite this, subtle sex-based differences in response to gemfibrozil were observed – with female mice appearing to experience protection against the 6 month composite ataxia and 9 month gait ataxia Cln6^{nclf} phenotypes and having better behavioural scores than Cln6^{nclf} males overall. Interestingly, these sex-based differences appeared to be all but erased, even reversed, when gemfibrozil was used in conjunction with AAV2/9-mediated gene therapy (**section 3.4**). While one could attribute the majority of the behavioural improvements experienced by both sexes treated with this combination therapy to the gene therapy, rather than gemfibrozil, it is odd that the

difference in male and female Gemfib^{AAV9} behavioural scores becomes non-significant, across the battery of behavioural tests and tested time points, when females had been previously observed to have significantly improved scores compared to their male counterparts across many of the tested parameters, when treated with gemfibrozil and gene therapy separately. This discrepancy certainly warrants further investigation, as it could indicate a synergystic effect of gemfibrozil and gene therapy in male animals or alternatively an antagonistic effect in females.

It is possible that the dose used in this study (120 mg/kg) was not optimal for protecting against behavioural deficits in Cln6^{nclf} mice – though if the dose was to be increased there would have to be preliminary work conducted regarding tolerance and toxicity. It is also important that any behavioural data reported here is ultimately complemented by post mortem analyses, as the full therapeutic effect of gemfibrozil on Cln6^{nclf} pathology can't be understood without these. While, ultimately, it is the effect of therapeutic intervention on the disease state that is most important when treating patients, post mortem analysis might offer critical insights into the mode of action of gemfibrozil, *in vivo*, and even help answer basic biological questions regarding CLN6 BD pathology in general. At a minimum, post mortem analysis may help confirm whether gemfibrozil was managing to have any effect whatsoever on the nervous tissue of the tested mice – a critical question, as the bioavailability of any potential small molecule therapy, and its ability to cross the BBB, is paramount to treating any neurological disease like CLN6 BD.

Due to the voluntary nature of dosing (described in **section 2.5.2** and discussed in further detail below, in **section 4.7.4**), it is possible that the mice in this study were not receiving the full 120 mg/kg dose regularly – with many mice failing to eat all or some of their jelly tablets on occasion. It was observed, in fact, that the majority of mice who appeared to

develop taste aversion to the jelly tablets were being dosed with either gemfibrozil or a combination of gemfibrozil and CBD, so it is possible that the drug either had an unpalatable taste or smell, or resulted in unobserved side effects such as gastrointestinal irritation or nausea in the mice. While the cohort of mice who developed taste aversion was small, and most were reintroduced quite quickly to the correct dose via strategies described in **section 2.5.3**, the possibility that gemfibrozil dosed mice were not, in fact, receiving the full dose expected and the consequences this might have on behavioural outcomes needs to be considered. Detailed notes were taken of which animals developed taste aversion, so it would be worth cross-referencing the data collected and analysed here with these notes and perhaps eliminating or separating data produced by animals known to experience dosing difficulties. It may also be worth running a long-term *in vivo* trial in which $Cln6^{nclf}$ mice are dosed by oral gavage or intraperitoneal injection, two methods that have been commonly used to administer gemfibrozil in other trials, as this will ensure accurate dosing – though a smaller cohort would have to be used, due to the time consuming nature of these dosing strategies (Almad et al., 2011; Ghosh et al., 2012).

4.3 In mouse: the use of small molecule therapeutics for CLN6 BD (CBD)

Cannabidiol (CBD) is a non-psychoactive, natural compound produced by the *C. sativa* plant. It has been proven to possess a host of neuroprotective properties in both preclinical and clinical studies and its polymorphic modes of action have made it an appealing therapeutic candidate for a range of neurodegenerative disorders including Alzheimers, Parkinson's and Huntingtons. *In vivo* and *in vitro* preclinical studies specifically focusing on CBDs use in any variant of NCL, however, are limited. Despite this gap in the literature, the parents of many NCL patients have been reported as administering CBD to their children based on anecdotal evidence of its broad range of neuroprotective action (Wibbeler et al., 2019). For this reason, it is critical that more preclinical data is generated regarding its use in NCL variants. This thesis represents the first long-term, comprehensive study to examine the effects of CBD, alone and in combination with gemfibrozil and/or gene therapy, on the behavioural phenotype of an NCL animal model – the $Cln6^{nclf}$ mouse.

Overall, the oral administration of CBD on its own was determined to have no significant effect on the $UT^{Cln6nclf}$ behavioural phenotype and was unable to rescue $Cln6^{nclf}$ shortened lifespans (**section 3.2**). While this outcome is disappointing, it is encouraging to see that no CBD-treated mice performed significantly worse than $UT^{Cln6nclf}$ counterparts, indicating that while the treatment may not be protective, at least it doesn't appear to have a negative effect on behaviour.

An important observation made in this thesis, however, was the significantly reduced survival of male $Cln6^{nclf}$ mice treated with both CBD and AAV2/9-mediated gene therapy (CBD^{AAV9}), compared to the survival of No $Drug^{AAV9}$ counterparts (**section 3.4**). While this is, at first glance, an alarming result, several factors need to be taken into consideration: first, the

survival data generated for this thesis encompassed only the first 15 months of the trial being run by the Hughes Lab. This meant that the majority of all AAV2/9-treated mice, regardless of whether they were concommitantly receiving small molecule therapy, were still alive by the time the data was generated and analysed, giving an incomplete picture of the 'true' survival curves of these experimental groups. It is possible that after 15 months of age one or more groups suddenly experienced an increase in unplanned deaths, or that CBD^{AAV9} treated male mice maintained a steady survival rate that eventually became non-significant from that of the $No\ Drug^{AAV9}$ mice. More information and further analysis is required to confirm that male CBD^{AAV9} mice really do have a significantly decreased lifespan compared to $No\ Drug^{AAV9}$ mice. Secondly, the survival plots generated for this thesis included all unplanned deaths – this means that it included the deaths of animals who were euthanised for non-disease related welfare reasons. The nature of group housing rodents for long periods of time means that many animals can end up injuring each other, through fighting or simply through close proximity, and while every effort was made to identify and ameliorate these scenarios with the mice used in this study, several animals did have to be euthanised due to bite wounds or injuries that wouldn't respond to veterinary intervention. There was also a spate of hydrocephalus-related euthanisations that occurred early on in the trial, which are now believed to be the result of inaccurate or too deep needle placement during the neonatal i.c.v protocol. It is possible that, due to pure chance, a large number of these non-NCL-related deaths occurred within the male CBD^{AAV9} cohort. In order to determine whether or not this is the case, the data reported here would need to be cross-referenced with the meticulous notes kept regarding unplanned animal deaths.

Finally, while the results presented in this thesis indicate that CBD, on its own or in combination with gemfibrozil, does not protect against the rotarod performance deficits,

ataxic phenotype, shortened lifespan and reduced weights that are characteristic of UT^{Cln6nclf} mice, this does not exclude its usefulness as a therapeutic compound for other CLN6 BD symptoms. It would be useful to conduct an in-depth, long-term study of regular CBD dosing in Cln6^{nclf} mice which examines its analgesic effects, using a pain response assay, its antiepileptic effects, via measurement of seizure activity and hyperexcitability in the brain, its anxiolytic effects, via an anxiety assay such as marble burying, and/or its effect on disordered sleep and social activity. Anxiety, muscle pain, personality changes and mood and sleep disorders are all symptoms experiened by CLN6 BD patients, and a small molecule therapeutic, such as CBD, that could address one or more of these symptoms would be useful in elevating therapeutic outcomes – especially when used in conjunction with one or more other therapies that might be better suited for addressing underlying pathology and motor dysfunction, such as the AAV2/9-mediated gene therapy used here.

4.4 In (hu)man: the use of small molecule therapeutics for CLN6 BD

There are several potential advantages to the use of small molecule therapeutics, such as gemfibrozil and CBD, in children with lysosomal storage diseases like the NCLs, and in particular CLN6 BD. Both are oral medications that do not require invasive administration and have been previously proven to be well tolerated and have low toxicity in humans. Both medications have multiple modes of action, with many of CBDs properties still not fully understood or explored, and most of these mechanisms are known to promote neuronal health via autophagic upregulation, lysosomal clearance and reduction of inflammation.

Despite these advantages, however, the long term use of gemfibrozil and CBD as potential therapeutics for CLN6 BD would not be without risk. Chronic use of gemfibrozil has been known to cause deleterious side effects, including dizziness and nausea, as well as mood and gastrointestinal disturbances. There have even been some reported cases of patients developing rhabdomyolysis, which causes kidney dysfunction and muscle weakness (Roy & Pahan, 2009). While CBD appears to have less reported side effects than gemfibrozil, a recent publication implicated the role of 2-arachidonoylglycerol (2-AG), the most abundant endocannabinoid found in the brain, in promoting cerebellar inflammation (Martinez-Torres et al., 2019). While 2-AG is not CBD, and it's inflammatory action is purported to occur via CB_2 receptor signalling – while CBD's neuroprotective effects are believed to be conducted via a range of alternative signalling pathways - this paper highlights how much is still unknown regarding the use of cannabinoids as therapeutics, especially in the CNS, and the potential for a cannabinoid to exacerbate neuroinflammation should not be taken lightly.

In light of these risks and the inconclusive nature of the behavioural data reported here, as well as the limitations of this study (discussed below), the use of gemfibrozil and/or

CBD cannot yet be recommended with any certainty for use in human CLN6 BD patients. This is not to say that they won't be beneficial, but further investigation is critical in order to maximise therapeutic outcomes.

4.5 In mouse: the use of viral-mediated gene therapy to treat CLN6 BD

The survival, weight and behavioural data presented in this thesis demonstrates that a single neonatal i.c.v injection of scAAV9.CB.*hCLN6* offers significant protection against the diseased Cln6^{nclf} behavioural phenotype. Cln6^{nclf} mice treated with gene therapy alone demonstrated significantly increased lifespans, as well as improved rotarod and ataxia scores compared to UT^{Cln6nclf} counterparts. These results support a growing catalogue of preclinical literature that indicates gene therapy can ameliorate neurodegenerative processes in animal models of CLN6 BD. They also suggest that not only does neonatal gene transfer of the *CLN6* gene increase the lifespan of treated Cln6^{nclf} mice, but it is capable of increasing their quality of life – in so far as they retain functional mobility and motor skills over the first fourteen months of life. Mice from this study undertook a Morris Water Maze (MWM) test concurrently with the behavioural assays described in this thesis, though the MWM results were omitted due to time constraints. It would be valuable to include and compare the MWM results, once they have been analysed, with the rotarod and ataxia results described here, as MWM data will give an indication of cognitive and memory function in treated and UT^{Cln6nclf} mice. If CLN6 gene therapy is found to improve Cln6^{nclf} cognition, as it has been in previously published CLN6 BD gene therapy studies, then this will be further evidence of an improved 'quality of life' for these mice – a conclusion that is of great importance when considering transition from the lab to clinical application (Holthaus et al., 2019; Poppens et al., 2019; Weimer et al., 2019).

While the data from this thesis suggests that AAV2/9-mediated gene therapys is effective in treating some of the major features of CLN6 BD in mice, namely the deterioration of motor skills as the disease progresses, it has also produced some observations that merit further investigation. Primarily, the rotarod data collected for this thesis (**section 3.3.1**) indicates that gene therapy-treated Cln6^{nclf} mice, of both sexes, produce significantly higher

('better') rotarod scores than both UT^{Cln6nclf} *and* healthy WT controls at 9 (females only) and 12 months of age (males and females). This phenomenon of gene therapy-treated Cln6^{nclf} behavioural scores that supersedes even those of healthy controls has been observed and commented on elsewhere, for instance Holthaus et al (2019) noticed a similar trend in their open field test data. It has been suggested that this hyperactivity may be a previously uncharacterised cognitive phenotype belonging to the Cln6^{nclf} mouse, or CLN6 BD in general, that was uncovered by the preservation of mobility in Cln6^{nclf} animals at later stages of disease progression – or the result, perhaps, of overexpression of the human *CLN6* transcript in the brain (Holthaus et al., 2019).

The full effect of gene therapy treatment may have been obscured in the results published here, due to the fact that the UT^{Cln6nclf} experimental group's phenotype did not become fully evident until later time points in the behavioural assays used – with significant differences between healthy WT control scores and the UT^{Cln6nclf} cohort not becoming significant until 9 (for ataxia) and 12 months (for rotarod) of age. Certainly, previously published CLN6 gene therapy studies involving behavioural assays seem to produce more consistently significant differences in scores between gene therapy-treated and UT^{Cln6nclf} cohorts at earlier time points than are seen in the results published here. Without further post mortem analysis to confirm both the genotype of the UT^{Cln6nclf} animals and the presence of viral-mediated *CLN6* expression in the CNS of No Drug^{AAV9} animals, the reason(s) as to why the results published here differ from previously published studies involving AAV2/9-mediated gene therapy can only be hypothesised.

4.6 In (hu)man: the use of viral-mediated gene therapy to treat CLN6 BD

Interim clinical trial data, released in 2019 from Amicus Therapeutics, indicates that AAV2/9-mediated gene transfer of the *CLN6* gene via intrathecal injection was well tolerated in human CLN6 BD patients and has resulted in negligible side effects or toxicity (Amicus Therapeutics, 2019). This data also indicated that several younger patients, often siblings of patients who had already begun to show symptoms at the time of the trial, remain asymptomatic – despite reaching the ages that their older siblings were when they began to demonstrate disease onset (Amicus Therapeutics, 2019). This information is promising, but the trial is not yet considered complete and won't be until 2021. Additionally, these data were released by Amicus Therapeutics for an Amicus Therapeutics drug trial, which is an important consideration when drawing conclusions as the data could be subject to bias towads the interests of the company and its stakeholders. Previous, completed clinical trials involving AAV2/9-mediated gene therapy in a range of metabolic and genetic disorders, including another variant of NCL, suggest that while this trial may be successful in reducing or delaying symptoms, it is unlikely to be curative (Trial No. NCT00151216, *Clinicaltrials.gov;* Steinfeld et al., 2002; Worgall et al., 2008). In preparation for this outcome, ongoing research into the optimisation and/or augmentation of AAV2/9-mediated gene therapy for NCLs, and CLN6 BD in particular, is critical.

4.7 Combination therapy for CLN6 BD

While all three combined therapies (Gemfib^{AAV9}, CBD^{AAV9} and Combo^{AAV9}) tested in this trial demonstrated significant success in protecting against several Cln6^{nclf} behavioural phenotypes in both male and female mice (**section 3.4**), direct comparison of these results with those of mice treated with gene therapy alone (No Drug^{AAV9}) makes it difficult to justify the use of such combinations without further investigation.

Only a few positive significant differences were elicited between the behavioural scores, survival and weights of combination treated and gene therapy-only treated mice, with CBD^{AAV9} and Combo^{AAV9} male mice achieving better hindlimb clasping ataxia scores at 6 and 9 months of age, respectively, and female CBD^{AAV9} and Combo^{AAV9} mice achieving better gait scores at 6 months of age. Considering all four groups who demonstrated a significantly improved score received a regular dose of CBD, in some form, it is very possible that these improvements were due to one of CBD's many neurological effects, such as analgesia or muscle relaxation. Mice who experience less pain are more likely to walk comfortably, while mice with relaxed muscles are less likely to experience involuntary hindlimb contractions. At this stage, however, these hypotheses are untested and would require further investigation to determine what is causing these improved phenotypes and why gait is specifically improved in females while hindlimb clasping is specifically improved in males.

While promising, and the segregation of higher female scores to the gait assay and male scores to the hindlimb clasping assay is interesting in itself, these improvements represent only one significant improvement on gene therapy alone, per combination treatment group, out of five behavioural assays. It should also be taken into consideration that male CBD^{AAV9} treated mice experienced significantly reduced survival compared to No Drug^{AAV9} counterparts, and this could be a serious problem with the concomittant use of CBD

with gene therapy. Euthanasia records will need to be cross-referenced with the data presented here to determine whether the effect observed is the result of a response to the combined treatment, or simply coincidental loss of animals to a variety of non-disease related welfare end points.

4.8 Limitations

4.8.1 Use of the Cln6^{nclf} mouse model to study therapeutic efficacy

The use of animal models, large and small, to model and study disease has always been at the core of the biomedical sciences. They have offered and continue to offer researchers and clinicians insights into the anatomy, physiology, behaviour and biochemistry of health and disease that wouldn't be possible if they were limited to the use of cadavers or human patients. The use of the naturally occurring Cln6^{nclf} model as a proxy for CLN6 BD in children follows in this tradition and was a critical component of this thesis. The availability of such a model allowed for the cost-effective breeding of experimental cohorts (~30 mice per experimental group; 18 groups) that were large enough to provide significant statistical power to any results eludicated and the use of the Cln6^{nclf} mouse lent itself to rigorous, systematic assessment of diseased behaviour at different time points across the lifespan - all of which would not have been feasible with larger animal models or human patients.

Despite this, the use of such a model is not without it's limitations. The anatomy and physiology of mice, particularly their CNS, differs greatly from that of humans and this can often complicate the transition from preclinical animal studies to human trials. Recently, mouse models have been criticised for failing to predict the efficacy of clinical trials in several neurodegenerative diseases, including Alzheimer's disease (AD) and Amyotrophic Lateral Sclerosis (ALS)(Turner & Talbot, 2008; Zahs & Ashe, 2010), and so any study of neurodegenerative disease that depends on the interpretation of mouse behaviour needs to take into account the shortcomings and limitations of using such a model. These include the fact that rodents are lissencephalic, with small, smooth brains, compared to the large, gyrencephalic brains of the CLN6 BD patients they are being used to emulate. There are also significant differences between mouse and man in a variety of other body systems that would

play an important role in dictating the efficacy of a potential therapeutic, such as the immune and endocrine systems.

Aside from physiological disparities, using mouse behaviour as an absolute measure of therapeutic efficacy, as is done here, without accompanying post-mortem analyses, is risky as it involves several key assumptions, such as the assumption that gene therapy was correctly administered to the left ventricle at birth. A range of things may have gone wrong and resulted in an absence of viral-mediated CLN6 expression in the brains of animals tested here, compromising any results published. While the Hughes lab took every measure to ameliorate human error, and many of the observed behavioural effects are too large and too obvious to allow for ambiguity, this trial will only really be complete once post-mortem analysis has confirmed that the mice assessed under the assumption of having received gene therapy actually did receive that therapeutic intervention.

Finally, behavioural performance in rodents can be influenced by a wide range of genetic and environmental factors, some of which can't be controlled for, despite best efforts on behalf of the researcher. These include differences in behaviour based on whether they are group housed, the presence or absence of recreation, the proximity of other rodents of the opposite gender and the time of day when they are assessed for behaviour. Mice in this trial were assessed during the day, and were kept on a 12 hour light cycle that mirrored the one outside. Since rodents are nocturnal, mice were essentially being tested at a time of day when they would normally be asleep or less active – this may have had some impact on their behavioural performances. Unfortunately, due the sheer size of the study, this scheduling could not be avoided.

4.8.2 Voluntary oral dosing as a mode of therapeutic administration

Zhang's (2011) voluntary oral administration protocol was adapted to purpose for the practical component of this thesis and, overall, provided a convenient way of administering a variety of small molecule therapies (gemfibrozil, CBD and a combination of the two drugs) to a large number of animals on a regular basis (every second day for almost 2 years). Zhang's protocol offered an alternative to the more traditional form of oral administration – the intragastric gavage (oral gavage) technique. Oral gavage, while effective, would have been extremely time consuming to perform on ~500 animals and could have resulted in a significant number of injuries to both the researcher and animals due to need to handle and restrain individual animals in order to perform the technique correctly. Moreover, there is some evidence to suggest that regular restraint of research animals can induce short and long-term stress responses which may have ultimately influenced behavioural outcomes and compromised the study's results (Zhang et al., 2011; Balcombe et al., 2004).

Despite being safer, faster and less stressful than oral gavage, the use of voluntary oral dosing via fruit-flavoured gelatin (jelly) tablets in this study presented and created its own limitations. The sheer number of experimental animals involved in the study meant that, at its peak, the study required the production of ~1500x 1 mL gelatin tablets a week, divided into different drug types and concentrations. Administration and production of these could require upwards of 20 hours a week, *before* dosing even occurred. Dosing itself could take up to four hours a day, every day (the mice were split into two cohorts – with each dosed on alternating days). It is difficult to acertain whether this protocol could have been automated further, as many adaptations and alterations were made to the original to make the study do-able within these timeframes, but if it could have been, the skills required to do so would, no doubt, have lain outside a MSc Neuroscience student's skillset.

A second, significant jelly-related problem that developed during the study was the propensity of certain mice to develop taste aversion to the jelly tablets and refuse to eat parts, or even the entire tablet during the allocated dosing period (up to 2 hours). Previous studies, including several pilot studies conducted within the Hughes Lab, had indicated that this might be an issue and several tactics were enlisted to avoid, mitigate and correct such behaviour when it occurred. These included the introduction of 'drug-free' jelly to mice for approximately a week post-weaning and pre-dosing, to try and overcome the natural neophobia most mice exhibit towards new foods. Once mice were consistently eating the plain, drug-free jelly, they began their dosing regimen. Despite this, several mice still developed taste aversion. When this occurred, mice would be reintroduced to drug-free jelly for a short period of time. The concentration of the drug would then slowly be introduced and built up over time, until mice were once again receiving the full dose based on their weight. If they continued to show no interest in the jelly, the flavour would be switched – from strawberry to lime. Most animals would regain an interest in the jelly tablet once flavours had been switched, but some required multiple rounds of reducing the drug concentration and building it back before they began to consistently consume the correct dose of drug. Zhang et al. (2011) recommended 'fasting' animals who demonstrated an aversion to the tablets, but this technique was avoided in this study due to the fact that a starved state can induce autophagy in cells, and therefore has the potential to compromise any data collected from the study. Detailed notes were taken of the mice who experienced taste aversion, and it would be interesting to separate their behavioural data from the rest of their treatment group and compare them, to see if the difference in dosing had any meaningful impact on behavioural or post-mortem outcomes. Interestingly, it was observed that the vast majority of mice that did experience taste aversion were given jelly with gemfibrozil or a combination of gemfibrozil and CBD in it. Most vehicle or CBD treated mice ate t most or all of their jelly throughout the

duration of the study. This may be due to the flavour of the gemfibrozil, which is known to be strong and bitter, or perhaps due to some gemfibrozil-related side effect such as gastrointestinal disturbance or nausea. Further testing would need to be done to determine whether either of these scenarios are the case.

4.8.3 Disparities between this study and the Gray Foundation's clinical trial

In order to better inform possible complementary therapeutic strategies for CLN6 BD patients, this preclinical study was designed, in part, to recapitulate many of the parameters of the Gray Foundation's 2016 clinical phase I/II trial. The same viral vector, for instance, was used in both the clinical trial's CLN6 BD patients and the $Cln6^{nclf}$ mice treated for this study. Mice even received a human copy of *CLN6* via AAV2/9-mediate gene therapy, though this was not only to recapitulate the trial's vector but also because there are few readily available, effective mouse *Cln6* antibodies available and post-mortem analysis will require the use of antibodies to determine the level of *CLN6* expression in mouse tissues. Human *CLN6* will be easier to identify post-mortem (Stephanie Hughes, personal communication). Despite many similarities, however, there were several key differences, the most significant, perhaps, being the time of intervention.

It is now well-established in NCL literature that therapeutic efficacy is contingent on early intervention (Cabrera-Salazar et al., 2007). The efficacy of early treatment with viral-mediated gene therapy has been demonstrated in several animal models of lysosomal storage disorders, including a $Cln2^{-/-}$ mouse model, and the success of treating such diseases before symptom onset appears to be profound – even more so when performed during the neonatal period (Cabrera-Salazar et al., 2007; Consiglio et al., 2001; Sevin et al., 2007; Sevin et al., 2006; Waddington et al., 2004). This is problematic when considering the treatment of rare childhood disorders such as the NCLs for a variety of reasons, most significant being the fact

that most patients are identified via symptom onset. This was the case with the majority of patients involved in the 2016 Gray Foundation clinical trial, with only a few patients being presymptomatic due to their identification via genetic screening after having an older sibling diagnosed with the disease. This means that, by the time the majority of these patients received gene therapy intervention, they would have surpassed the optimal therapeutic window identified in preclinical studies. In fact, the neonatal murine brain represents a similar developmental stage to the human foetus, meaning an equivalent treatment period would require *in utero* administration of gene therapy in humans. In this study we elected to administer gene therapy at P0-2 (the neonatal period), despite it not accurately representing the developmental stage most of the patients in the 2016 clinical trial would have been at when receiving treatment. This was primarily due to the fact that administering gene therapy to mice at a later stage would have require stereotaxic surgery, a time consuming protocol with great risk to the mice, and would have made running a trial with over 500 mice impossible due to time constraints. It would be beneficial for future studies to look at the possibility of optimising gene therapy when administered at a later stage in disease progression, to better recapitulate the way in which gene therapy is currently administered to patients – post-symptom onset – and to produce results that may be a more relevant indication of potential success in children.

This disparity between the optimal therapeutic window for gene therapy and the way in which therapeutic need is currently identified in NCL patients, however, is an area of concern that will need to be addressed, especially if gene therapy becomes more commonplace. It also justifies the need for broader, more comprehensive prenatal and congenital genetic screening programs in humans, though these are associated with a variety of ethical considerations of their own.

4.8.4 Disparities between this study and the work of collaborators

The data in this thesis closely recapitulates Bronson et al's original findings which reported rear-limb paralysis starting at approximately 10 months of age, as male Cln6^{nclf} mice only demonstrated significantly reduced scores in two (ledge and composite ataxia) out of five (rotarod, as well as composite, ledge, hindlimb and gait ataxia) behavioural assessments conducted at 6 months (Bronson et al., 1999). At 9 months, however, males continued to demonstrate these significantly lower ledge and composite ataxia scores *and* females had significantly worse ataxia scores than age- and sex-matched WT controls in all four ataxia assays, suggesting the presence of stronger diseased phenotype across all Cln6^{nclf} mice at this later time point. Additionally, male and female Cln6^{nclf} rotarod scores collected for this thesis indicate that rotarod-specific motor deficits are not present until at least after 9 months of age, which also supports Bronson et al's behavioural observations (Bronson et al., 1999).

Morgan et al., however, were able to detect rotarod performance deficiencies as early as 3 months in their UT^{Cln6nclf} cohort (Morgan et al., 2013). It is difficult to determine what might cause this discrepancy between the data gathered here and their study, but there are several study design differences that need to be taken into account. Primarily, this thesis did not include behavioural testing at any age point before 6 months, nor did Morgan et al. choose to publish their day 270 (~9 months) rotarod results, so direct comparison of these results to those in Morgan et al.'s paper is impossible. We cannot, with the information given, eliminate the possibility that the Cln6^{nclf} mice in this study may have performed significantly worse than WT at 3 months of age, though when one considers the linear way in which neurodegenerative diseases progress this seems unlikely. One can also raise the question as to why Morgan et al didn't publish the 9 month rotarod data they collected, as it may have served to strengthen their characterisation of behavioural deficits in the Cln6^{nclf} mouse. However, it is possible that,

due to publication-related space and word limits, they simply chose to leave this information out as it was repeating findings already present at 3 months (Morgan et al., 2013).

4.9 Future directions

While the behavioural analyses outlined in this thesis represent a critical part of the larger Gray Foundation preclinical trial being conducted by the Hughes lab, a significant amount of work remains to be done before the trial can be considered complete. This will include post-mortem processing, imaging and analysis of the tissues removed from posthumously via transcardial perfusion, as well as the statistical analysis of over 300 hours of Morris Water Maze (MWM) behaviour recordings taken at 6, 9, 12 and 16 months. Some of the behavioural analyses reported here may also have to be reassessed in order to incorporate 12 and 16 month behavioural data that was, due to time restrictions, left out of this thesis.

Mice who reached one of the three humane endpoints outlined in **Chapter 2** were euthanised via transcardial perfusion and had their brains, spines, eyes, livers, kidneys, hearts and spleens removed, as well as a blood sample and tail tip taken. These materials are currently stored in a -80℃ freezer and will require a large amount of resources to process, image and analyse. Despite the amount of money and man-hours this will require, post-mortem analysis is well worth doing. First, post-mortem results will help better confirm the results produced for this thesis. Blood samples and tail tips can be used to genotype the mice that were assessed for behaviour and confirm that they were the correct genotype (either $Cln6^{nclf}$ or C57Bl/6) and that the $Cln6^{nclf}$ colony kept by the Hughes lab had not undergone genotypic drift over the years it has been maintained in Dunedin, New Zealand – a phenomenon that is not unheard of in mouse models of genetic disease (Benavides et al., 2019; Stevens et al., 2007; Zeldovich, 2017). This will validate any results and analyses reported in this thesis. Second, analysis of the brains of mice belonging to the AAV2/9-treated experimental groups (M/F No $Drug^{AAV9}$, M/F $Gemfib^{AAV9}$, M/F CBD^{AAV9} and M/F $Combo^{AAV9}$) will help confirm whether the AAV2/9-mediated gene therapy was administered correctly, via

direct injection into the left hemisphere cerebroventricular space. If *CLN6* expression is localised to the cerebral or meningeal layers surrounding the injection site, this will suggest that the needle was inserted incorrectly – either too shallowly, or too far to the left or right. Direct injection into the cerebroventricular space is critical for effective gene therapy, as this method takes advantage of the circulating cerebroventricular spinal fluid (CSF) and allows the vector to be carried throughout the central nervous system via this circulation. While AAV vectors demonstrate extremely effective local cellular transduction, a feature that made them attractive as a gene therapy vector in the first place, diseases that effect the entire nervous system – like CLN6 BD – require transduction throughout the brain and spinal cord.

Analysis of the spinal cord and visceral organs will also give a better understanding of how far the gene therapy spread *outside* the CNS, which may inform future decisions regarding vector choice. It is now becoming clear that, while the primary objective of NCL therapy development is to cease neurodegeneration, there may well be visceral pathologies that become problematic once the neurodegeneration has been dealt with. This could mean that efforts to develop a successful, CNS-restricted, gene therapy would only produce a short term solution, with patients dying at a later age from related pathologies in somatic tissues like the heart, liver or kidneys. An effective gene therapy would be one that focuses on the CNS, but also successfully transduces other critical tissues like cardiac muscle or hepatocytes.

Despite the fact that there is a large amount of work yet to be done in terms of MWM and post-mortem analysis, this project represents the first large-scale, longitudinal (>12 months) preclinical combination therapy trial of AAV2/9-mediated *hCLN6* gene therapy, gemfibrozil and cannabidiol (CBD) in the naturally-occurring $Cln6^{nclf}$ mouse model of CLN6 BD. It utilized and refined a series of novel techniques, including the use of cryotherapy and drawn glass needles to deliver gene therapy via i.c.v injection to newborn (P0-P2) mice and the

efficient mass production and delivery of small molecule jelly 'tablets', which allowed for ongoing voluntary oral dosing of around 500 mice for almost two years.

Furthermore, the project reinforced the findings of several other key preclinical CLN6 BD studies by documenting AAV2/9-mediated *hCLN6* gene therapy as successfully protecting Cln6^{nclf} mice, of both sexes, against several of the characteristic behavioural and motor deficits seen in untreated controls. Similarly, the project's findings reiterated the significant impact a single neonatal i.c.v injection of scAAV9.CB.*hCLN6* can have in terms of extending and restoring the lifespans of Cln6^{nclf} mice.

While neither gemfibrozil, CBD, or a combination of the two drugs appeared to make any consistently significant improvements to either untreated or gene-therapy treated Cln6^{nclf} mouse behavior, the project still represents the first attempt to characterize the impact of these particular small molecule therapies, alone and in combination, on the Cln6^{nclf} phenotype and raised some interesting questions regarding dosage, mode of therapeutic delivery and sex-based differences in response to each therapeutic modality that was trialed.

The work and results documented here do not, by any means, rule out the potential benefits of either gemfibrozil or CBD as complementary therapeutics for patients with CLN6 BD. Instead, they simply lay the foundation for further investigation and raise novel questions regarding other, still untested, benefits (such as analgesia or emotional modulation) that may be elicited from the use of either, or both, therapies, alone and in combination with AAV2/9-mediated *hCLN6* gene therapy.

References

Åberg, L., Talling, M., Härkönen, T., Lönnqvist, T., Knip, M., Alen, R., … Tyynelä, J. (2008). Intermittent Prednisolone and Autoantibodies to GAD65 in Juvenile Neuronal Ceroid Lipofuscinosis. *Neurology*, *70*(14), 1218–1220. https://doi.org/10.1212/01.wnl.0000307753.88839.29

Agarwal, S., Yadav, A., & Chaturvedi, R. K. (2017). Peroxisome Proliferator-Activated Receptors (PPARs) as Therapeutic target in neurodegenerative disorders. *Biochemical and Biophysical Research Communications*, Vol. 483, pp. 1166–1177. https://doi.org/10.1016/j.bbrc.2016.08.043

Agoston, D. V. (2017). How to Translate Time? The Temporal Aspect of Human and Rodent Biology. *Frontiers in Neurology*, Vol. 8, p. 92. https://doi.org/10.3389/fneur.2017.00092

Agurell, S., Carlsson, S., Lindgren, J. E., Ohlsson, A., Gillespie, H., & Hollister, L. (1981). Interactions of Δ11-Tetrahydrocannabinol with Cannabinol and Cannabidiol Following Oral Administration in Man. *Experientia*, *37*(10), 1090–1092. https://doi.org/10.1007/BF02085029

Ahtiainen, L., Van Diggelen, O. P., Jalanko, A., & Kopra, O. (2003). Palmitoyl Protein Thioesterase 1 is Targeted to the Axons in Neurons. *The Journal of Comparative Neurology*, *455*(3), 368–377. https://doi.org/10.1002/cne.10492

Almad, A., Lash, A. T., Wei, P., Lovett-Racke, A. E., & McTigue, D. M. (2011). The PPAR Alpha Agonist Gemfibrozil is an Ineffective Treatment for Spinal Cord Injured Mice. *Experimental Neurology*, *232*(2), 309–317. https://doi.org/10.1016/j.expneurol.2011.09.023

Alroy, J., Braulke, T., Cismondi, A., Cooper, J. D., Creegan, D., Elleder, M., … Shulz, A. (2011). CLN6. In S.E. Mole, R. E. Williams, & H. H. Goebel (Eds.), *The Neuronal Ceroid Lipofuscinoses (Batten Disease)* (pp. 159–175). Oxford: Oxford University Press.

Amicus Therapeutics. (2019). *Amicus Announces Positive Interim Clinical Data for AAV Gene Therapy in Children with CLN6 Batten Disease*.

Amur, S., Parekh, A., & Mummaneni, P. (2012). Sex Differences and Genomics in Autoimmune Diseases. *Journal of Autoimmunity*, *38*(2–3). https://doi.org/10.1016/j.jaut.2011.12.001

Anderson, G. D., & Chan, L. N. (2016). Pharmacokinetic Drug Interactions with Tobacco, Cannabinoids and Smoking Cessation Products. *Clinical Pharmacokinetics*, Vol. 55, pp. 1353–1368. https://doi.org/10.1007/s40262-016-0400-9

Andrews, K., & Fitzgerald, M. (1997). Barriers to Optimal Pain Management in Infants, Children, and Adolescents: Biological Barriers to Paediatric Pain Management. *Clinical Journal of Pain*, *13*(2), 138–143. https://doi.org/10.1097/00002508-199706000-00007

Angelini, C., & Semplicini, C. (2012). Enzyme Replacement Therapy for Pompe Disease. *Current Neurology and Neuroscience Reports*, *12*(1), 70–75. https://doi.org/10.1007/s11910-011-0236-5

Aoun, P., Simpkins, J. W., & Agarwal, N. (2003). Role of PPAR-γ Ligands in Neuroprotection Against Glutamate-Induced Cytotoxicity in Retinal Ganglion Cells. *Investigative Ophthalmology and Visual Science*, *44*(7), 2999–3004. https://doi.org/10.1167/iovs.02-1060

Appelmans, F., & De Duve, C. (1955). Tissue Fractionation Studies. 3. Further Observations on the Binding of Acid Phosphatase by Rat-Liver Particles. *The Biochemical Journal*, *59*(3), 426–433. Retrieved from http://www.ncbi.nlm.nih.gov/pubmed/14363112

Appelmans, F., Wattiaux, R., & De Duve, C. (1955). Tissue Fractionation Studies. 5. The Association of Acid Phosphatase with a Special Class of Cytoplasmic Granules in Rat Liver. *The Biochemical Journal*, *59*(3), 438–445. Retrieved from http://www.ncbi.nlm.nih.gov/pubmed/14363114

Aragão, R. E. M. de, Ramos, R. M. G., Pereira, F. B. A., Bezerra, A. F. R., & Fernandes, D. N. (2009). “Cherry Red Spot” in a Patient with Tay-Sachs Disease: Case Report. *Arquivos Brasileiros de Oftalmologia*, *72*(4), 537–539. https://doi.org/10.1590/s0004-27492009000400019

Augustine, E. F., Beck, C. A., Adams, H. R., Defendorf, S., Vierhile, A., Timm, D., … Marshall, F. J. (2019). Short-Term Administration of Mycophenolate is Well-Tolerated in CLN3 Disease (Juvenile Neuronal Ceroid Lipofuscinosis). In *JIMD Reports* (Vol. 43, pp. 117–124). https://doi.org/10.1007/8904_2018_113

Autti, T., Raininko, R., Launes, J., Nuutila, A., & Santavuori, P. (1992). Jansky-Bielschowsky Variant Disease: CT, MRI, and SPECT Findings. *Pediatric Neurology*, *8*(2), 121–126. https://doi.org/10.1016/0887-8994(92)90032-T

Awad, O., Sarkar, C., Panicker, L. M., Miller, D., Zeng, X., Sgambato, J. A., … Feldman, R. A. (2015). Altered TFEB-Mediated Lysosomal Biogenesis in Gaucher disease iPSC-Derived Neuronal Cells. *Human Molecular Genetics*, *24*(20), 5775–5788. https://doi.org/10.1093/hmg/ddv297

Awano, T., Katz, M. L., O'Brien, D. P., Taylor, J. F., Evans, J., Khan, S., … Johnson, G. S. (2006). A Mutation in the Cathepsin D gene (*CTSD*) in American Bulldogs with Neuronal Ceroid Lipofuscinosis. *Molecular Genetics and Metabolism*, *87*(4), 341–348. https://doi.org/10.1016/j.ymgme.2005.11.005

Baamonde, A., Lastra, A., Juarez, L., Hidalgo, A., & Menéndez, L. (2005). TRPV1 Desensitisation and Endogenous Vanilloid Involvement in the Enhanced Analgesia Induced by Capsaicin in Inflamed Tissues. *Brain Research Bulletin*, *67*(6), 476–481. https://doi.org/10.1016/j.brainresbull.2005.07.001

Bajaj, L., Ronza, A. di, Zheng, P., Eblimit, A., Pal, R., Sharma, J., … Sardiello, M. (2019). A CLN6-CLN8 Complex Recruits Lysosomal Enzymes at the ER for Golgi Transfer. *BioRxiv*, 773804. https://doi.org/10.1101/773804

Bakas, T., van Nieuwenhuijzen, P. S., Devenish, S. O., McGregor, I. S., Arnold, J. C., & Chebib, M. (2017). The Direct Actions of Cannabidiol and 2-Arachidonoyl Glycerol at GABAA Receptors. *Pharmacological Research*, *119*, 358–370. https://doi.org/10.1016/j.phrs.2017.02.022

Barney, C. C., Hoch, J., Byiers, B., Dimian, A., & Symons, F. J. (2015). A Case-Controlled Investigation of Pain Experience and Sensory Function in Neuronal Ceroid Lipofuscinosis. *Clinical Journal of Pain*, *31*(11), 998–1003. https://doi.org/10.1097/AJP.0000000000000192

Barreto, G., Huang, T. T., & Giffard, R. G. (2010). Age-Related Defects in Sensorimotor Activity, Spatial Learning, and Memory in C57Bl/6 mice. *Journal of Neurosurgical Anesthesiology*, *22*(3), 214–219. https://doi.org/10.1097/ANA.0b013e3181d56c98

Batten, F. (1902). Cerebral Degeneration with Symmetrical Changes in the Maculae in Two Members of a Family. *Transactions of the Opthalmolgocial Society of the United Kingdom*, *23*, 386–390.

Batten, F. E., & Mayou, M. S. (1915). Family Cerebral Degeneration with Macular Changes. *Proc R Soc Med*, *8*, 70–90. Retrieved from https://journals.sagepub.com/doi/pdf/10.1177/003591571500801624

Beery, A. K., & Zucker, I. (2011). Sex Bias in Neuroscience and Biomedical Research. *Neuroscience and Biobehavioral Reviews*, Vol. 35, pp. 565–572. https://doi.org/10.1016/j.neubiorev.2010.07.002

Benavides, F., Rülicke, T., Prins, J.-B., Bussell, J., Scavizzi, F., Cinelli, P., … Wedekind, D. (2019). Genetic Quality Assurance and Genetic Monitoring of Laboratory Mice and Rats: FELASA Working Group Report. *Laboratory Animals*, 002367721986771. https://doi.org/10.1177/0023677219867719

Bennett, M. J., & Hofmann, S. L. (1999). The Neuronal Ceroid-Lipofuscinsoses (Batten Disease): A New Class of Lysosomal Storage Diseases. *Journal of Inherited Metabolic Disease*, *22*(4), 535–544. https://doi.org/10.1023/A:1005564509027

Berger, J., & Moller, D. E. (2002). The Mechanisms of Action of PPARs. *Annual Review of Medicine*, *53*(1), 409–435. https://doi.org/10.1146/annurev.med.53.082901.104018

Bernardini, F., & Warburton, M. J. (2002). Lysosomal Degradation of Cholecystokinin-(29-33)-Amide in Mouse Brain is Dependent on Tripeptidyl Peptidase-I: Implications for the Degradation and Storage of Peptides in Classical Late-Infantile Neuronal Ceroid Lipofuscinosis. *Biochemical Journal*, *366*(2), 521–529. https://doi.org/10.1042/BJ20020467

Berthet, J., & de Duve, C. (1951). Tissue Fractionation Studies. I. The Existence of a Mitochondria-Linked, Enzymically Inactive Form of Acid Phosphatase in Rat-Liver Tissue. *The Biochemical Journal*, *50*(2), 174–181. Retrieved from http://www.ncbi.nlm.nih.gov/pubmed/14904389

Best, H. L. (2017). *Exploring CLN5 and CLN6 Batten Disease*. University of Otago.

Best, H. L., Neverman, N. J., Wicky, H. E., Mitchell, N. L., Leitch, B., & Hughes, S. M. (2017). Characterisation of Early Changes in Ovine CLN5 and CLN6 Batten Disease Neural Cultures for the Rapid Screening of Therapeutics. *Neurobiology of Disease*, *100*, 62–74. https://doi.org/10.1016/j.nbd.2017.01.001

Bethesda, M. (2009). Gemfibrozil. Retrieved April 3, 2021, from American Society of Health System Pharmacists website: https://www.ahfsdruginformation.com/

Bielschowsky, M. (1914). Über Spätinfantile Familiäre Amaurotische Idiotie Mit Kleinhirnsymptomen. *Deutsch. Ztschr. Nervenh.*, *50*, 7.

Boehme, D. H., Cottrell, J. C., Leonberg, S. C., & Zeman, W. (1971). A Dominant Form of Neuronal Ceroid Lipofuscinosis. *Brain*, *94*(4), 745–760. https://doi.org/10.1093/brain/94.4.745

Bond, M., Holthaus, S. M. kleine, Tammen, I., Tear, G., & Russell, C. (2013). Use of Model Organisms for the Study of Neuronal Ceroid Lipofuscinosis. *Biochimica et Biophysica Acta - Molecular Basis of Disease*, Vol. 1832, pp. 1842–1865. https://doi.org/10.1016/j.bbadis.2013.01.009

Bookout, A. L., Jeong, Y., Downes, M., Yu, R. T., Evans, R. M., & Mangelsdorf, D. J. (2006). Anatomical Profiling of Nuclear Receptor Expression Reveals a Hierarchical Transcriptional Network. *Cell*, *126*(4), 789–799. https://doi.org/10.1016/j.cell.2006.06.049

Bordet, R., Ouk, T., Petrault, O., Gelé, P., Gautier, S., Laprais, M., … Bastide, M. (2006). PPAR: A New Pharmacological Target for Neuroprotection in Stroke and Neurodegenerative Diseases. *Biochemical Society Transactions*, *34*(6), 1341–1346. https://doi.org/10.1042/BST0341341

Breasted, J. H. (1930). *The Edwin Smith Surgical Papyrus: Published in Facsimile and Hieroglyphic Transliteration with Translation and Commentary in Two Volumes* (Vol. 3). University of Chicago Press Chicago.

Breau, L., Camfield, C., & Camfield, P. (2010). The Pain Behaviour of Children with Neuronal Ceroid Lipofuscinosis: Variation Due to Child Factors and Pain History. *J Pain Manage*, *3*(3), 293–300.

Brett, E. M., & Lake, B. D. (1975). Reassessment of Rectal Approach to Neuropathology in Childhood: Review of 307 Biopsies over 11 Years. *Archives of Disease in Childhood*, *50*(10), 753–762. https://doi.org/10.1136/adc.50.10.753

Bronson, R., Donahue, L., Johnson, K., Tanner, A., Lane, P., & Faust, J. (1999). Neuronal Ceroid Lipofuscinosis (nclf), a New Disorder of The Mouse Linked to Chromosome 9. *American Journal of Medical Genetics*, *77*(4), 289–297.

Busse, K. H., Hadigan, C., Chairez, C., Alfaro, R. M., Formentini, E., Kovacs, J. A., & Penzak, S. R. (2009). Gemfibrozil Concentrations are Significantly Decreased in the Presence of Lopinavir-Ritonavir. *Journal of Acquired Immune Deficiency Syndromes*, *52*(2), 235–239. https://doi.org/10.1097/QAI.0b013e3181b0610e

Cabrera-Salazar, M., Roskelley, E., Bu, J., Hodges, B., Yew, N., Dodge, J., … Davidson, B. (2007). Timing of Therapeutic Intervention Determines Functional and Survival Outcomes in a Mouse Model of Late Infantile Batten Disease. *Molecular Therapy*, *15*(10), 1782–1788.

Cain, J. T., Likhite, S., White, K. A., Timm, D. J., Davis, S. S., Johnson, T. B., … Weimer, J. M. (2019). Gene Therapy Corrects Brain and Behavioral Pathologies in CLN6 Batten Disease. *Molecular Therapy*. https://doi.org/10.1016/J.YMTHE.2019.06.015

Calapai, F., Cardia, L., Sorbara, E. E., Navarra, M., Gangemi, S., Calapai, G., & Mannucci, C. (2020). Cannabinoids, Blood–Brain Barrier, and Brain Disposition. *Pharmaceutics*, Vol. 12. https://doi.org/10.3390/pharmaceutics12030265

Calcedo, R., & Wilson, J. M. (2013). Humoral Immune Response to AAV. *Frontiers in Immunology*, *4*. https://doi.org/10.3389/fimmu.2013.00341

Cannelli, N., Garavaglia, B., Simonati, A., Aiello, C., Barzaghi, C., Pezzini, F., … Santorelli, F. M. (2009). Variant Late Infantile Ceroid Lipofuscinoses Associated with Novel Mutations in CLN6. *Biochemical and Biophysical Research Communications*, *379*(4), 892–897. https://doi.org/10.1016/j.bbrc.2008.12.159

Carifio, J., & Perla, R. (2008). Resolving the 50-year Debate around Using and Misusing Likert Scales. *Medical Education*, *42*(12), 1150–1152. https://doi.org/10.1111/j.1365-2923.2008.03172.x

Carrier, E. J., Auchampach, J. A., & Hillard, C. J. (2006). Inhibition of an Equilibrative Nucleoside Transporter by Cannabidiol: A Mechanism of Cannabinoid Immunosuppression. *Proceedings of the National Academy of Sciences of the United States of America*, *103*(20), 7895–7900. https://doi.org/10.1073/pnas.0511232103

Casal, M., & Haskins, M. (2006). Large Animal Models and Gene Therapy. *European Journal of Human Genetics*, Vol. 14, pp. 266–272. https://doi.org/10.1038/sj.ejhg.5201535

Cave, A. J. E., & Demonstrator, A. (1939). The Evidence for the Incidence of Tuberculosis in Ancient Egypt. *British Journal of Tuberculosis*, *33*(3), 142–152. https://doi.org/10.1016/S0366-0850(39)80016-3

Chalkley, M. D., Armien, A. G., Gilliam, D. H., Johnson, G. S., Zeng, R., Wünschmann, A., … Katz, M. L. (2014). Characterization of Neuronal Ceroid Lipofuscinosis in 3 cats. *Veterinary Pathology*, *51*(4), 796–804. https://doi.org/10.1177/0300985813502818

Chang, J. T., Staffa, J. A., Parks, M., & Green, L. (2004). Rhabdomyolysis with HMG-CoA Reductase Inhibitors and Gemfibrozil Combination Therapy. *Pharmacoepidemiology and Drug Safety*, *13*(7), 417–426. https://doi.org/10.1002/pds.977

Chang, M., Cooper, J. D., Sleat, D. E., Cheng, S. H., Dodge, J. C., Passini, M. A., … Davidson, B. L. (2008). Intraventricular Enzyme Replacement Improves Disease Phenotypes in a Mouse Model of Late Infantile Neuronal Ceroid Lipofuscinosis. *Molecular Therapy*, *16*(4), 649–656. https://doi.org/10.1038/mt.2008.9

Chen, M., Dai, Y., Liu, S., Fan, Y., Ding, Z., & Li, D. (2021). TFEB Biology and Agonists at a Glance. *Cells*, *10*(2), 333. https://doi.org/10.3390/cells10020333

Chen, W. W., Zhang, X., & Huang, W. J. (2016). Role of Neuroinflammation in Neurodegenerative Diseases (Review). *Molecular Medicine Reports*, *13*(4), 3391–3396. https://doi.org/10.3892/mmr.2016.4948

Chicca, A., Raduner, S., Pellati, F., Strompen, T., Altmann, K.-H., Schoop, R., & Gertsch, J. (2009). Synergistic Immunomopharmacological Effects of N-alkylamides in E*chinacea purpurea* Herbal Extracts. *International Immunopharmacology*, *9*(7–8), 850–858. https://doi.org/10.1016/J.INTIMP.2009.03.006

Chini, M., & Hanganu-Opatz, I. L. (2021). Prefrontal Cortex Development in Health and Disease: Lessons from Rodents and Humans. *Trends in Neurosciences*, Vol. 44, pp. 227–240. https://doi.org/10.1016/j.tins.2020.10.017

Cialone, J., Adams, H., Augustine, E. F., Marshall, F. J., Kwon, J. M., Newhouse, N., … Mink, J. W. (2012). Females Experience a More Severe Disease Course in Batten Disease.[Erratum appears in J Inherit Metab Dis. 2012 May;35(3):559]. *Journal of Inherited Metabolic Disease*, *35*(3), 549–555. https://doi.org/http://dx.doi.org/10.1007/s10545-011-9421-6

Clancy, B., Finlay, B. L., Darlington, R. B., & Anand, K. J. S. (2007). Extrapolating Brain Development from Experimental Species to Humans. *NeuroToxicology*, *28*(5 SPEC. ISS.), 931–937. https://doi.org/10.1016/j.neuro.2007.01.014

Clinicaltrials.gov. (2016). *Patent No. NCT02725580*. Retrieved from https://clinicaltrials.gov/ct2/show/NCT02725580

Colacurcio, D. J., Pensalfini, A., Jiang, Y., & Nixon, R. A. (2018). Dysfunction of Autophagy and Endosomal-Lysosomal Pathways: Roles in Pathogenesis of Down Syndrome and Alzheimer's Disease. *Free Radical Biology and Medicine*, *114*, 40–51. https://doi.org/10.1016/J.FREERADBIOMED.2017.10.001

Consiglio, A., Quattrini, A., Martino, S., Bensadoun, J. C., Dolcetta, D., Trojani, A., … Naldini, L. (2001). *In vivo* Gene Therapy of Metachromatic Leukodystrophy by Lentiviral Vectors: Correction of Neuropathology and Protection Against Learning Impairments in Affected mice. *Nature Medicine*, *7*(3), 310–316. https://doi.org/10.1038/85454

Consroe, P., Kennedy, K., & Schram, K. (1991). Assay of Plasma Cannabidiol by Capillary Gas Chromatography/Ion Trap Mass Spectroscopy Following High-Dose Repeated Daily Oral Administration in Humans. *Pharmacology, Biochemistry and Behavior*, *40*(3), 517–522. https://doi.org/10.1016/0091-3057(91)90357-8

Cook, R., Jolly, R., Palmer, D., Tammen, I., Broom, M., & McKinnon, R. (2002). Neuronal Ceroid Lipofuscinosis in Merino Sheep. *Australian Veterinary Journal*, *80*(5), 292–297. https://doi.org/10.1111/j.1751-0813.2002.tb10847.x

Cooper, J., Tarczyluk, M., Najafi, A., Salzlechner, C., Lim, M., Pearce, D., … Williams, B. (2018). *57 Testing Combinatorial Therapies for Juvenile Batten Disease*. https://doi.org/10.1016/j.ymgme.2017.12.063

Cooper, J.D. (2003). Progress Towards Understanding the Neurobiology of Batten Disease: Current Opinion in Neurology. *Current Opinion in Neurology*, *16*(2), 121–128. Retrieved from https://journals.lww.com/co-neurology/Abstract/2003/04000/Progress_towards_understanding_the_neurobiology_of.1.aspx

Cooper, J. D., Tarczyluk, M. A., & Nelvagal, H. R. (2015). Towards a New Understanding of NCL Pathogenesis. *Biochimica et Biophysica Acta (BBA) - Molecular Basis of Disease*, *1852*(10), 2256–2261. https://doi.org/10.1016/J.BBADIS.2015.05.014

Costa, B. (2007). On the Pharmacological Properties of Δ9-Tetrahydrocannabinol (THC). *Chemistry & Biodiversity*, *4*(8), 1664–1677. https://doi.org/10.1002/cbdv.200790146

Cotman, S., Vrbanac, V., Lebel, L., Lee, R., Johnson, K., Donahue, L., … MacDonald, M. (2002). Cln3 Δex7/8 Knock-In Mice with the Common JNCL Mutation Exhibit Progressive Neurologic Disease that Begins Before Birth. *Human Molecular Genetics*, *11*(22), 2709–2721.

Coutinho, M., Santos, J., & Alves, S. (2016). Less Is More: Substrate Reduction Therapy for Lysosomal Storage Disorders. *International Journal of Molecular Sciences*, *17*(7), 1065. https://doi.org/10.3390/ijms17071065

da Fonseca, A. C. C., Matias, D., Garcia, C., Amaral, R., Geraldo, L. H., Freitas, C., & Lima, F. R. S. (2014). The Impact of Microglial Activation on Blood-Brain Barrier in Brain Diseases. *Frontiers in Cellular Neuroscience*, Vol. 8, pp. 1–13. https://doi.org/10.3389/fncel.2014.00362

Dane, A. P., Wowro, S. J., Cunningham, S. C., & Alexander, I. E. (2013). Comparison of Gene Transfer to the Murine Liver Following Intraperitoneal and Intraportal Delivery of Hepatotropic AAV Pseudo-Serotypes. *Gene Therapy*, *20*(4), 460–464. https://doi.org/10.1038/gt.2012.67

de Duve, C., Pressman, B. C., Gianetto, R., Wattiaux, R., & Appelmans, F. (1955). Tissue Fractionation Studies. 6. Intracellular Distribution Patterns of Enzymes in Rat-Liver Tissue. *The Biochemical Journal*, *60*(4), 604–617. Retrieved from http://www.ncbi.nlm.nih.gov/pubmed/13249955

de Duve, C. (1964). From Cytases to Lysosomes. *Federation Proceedings*, *23*, 1045.

Devane, W. A., Dysarz, F. A., Johnson, M. R., Melvin, L. S., & Howlett, A. C. (1988). Determination and Characterization of a Cannabinoid Receptor in Rat Brain. *Molecular Pharmacology*, *34*(5), 605–613.

Devinsky, O., Marsh, E., Friedman, D., Thiele, E., Laux, L., Sullivan, J., … Cilio, M. R. (2016). Cannabidiol in Patients with Treatment-Resistant Epilepsy: an Open-Label Interventional Trial. *The Lancet Neurology*, *15*(3), 270–278. https://doi.org/10.1016/S1474-4422(15)00379-8

DiCaglio, S. (2017). Staging Embryos. *Body & Society*, *23*(2), 3–24. https://doi.org/10.1177/1357034X17697801

Dinis-Oliveira, R. J. (2016). Metabolomics of δ9-tetrahydrocannabinol: Implications in Toxicity. *Drug Metabolism Reviews*, Vol. 48, pp. 80–87. https://doi.org/10.3109/03602532.2015.1137307

Dobbing, J, & Smart, J. L. (1974). Vulnerability of Developing Brain and Behaviour. *British Medical Bulletin*. Retrieved from https://psycnet.apa.org/record/1975-20435-001

Dobbing, J. (1970). Undernutrition and the Developing Brain: The Relevance of Animal Models to the Human Problem. *American Journal of Diseases of Children*, *120*(5), 411–415. https://doi.org/10.1001/archpedi.1970.02100100075005

Dobbing, J. (1974). The Later Growth of the Brain and its Vulnerability. *Pediatrics*, *53*(1).

Dobbing, J., & Sands, J. (1979). Comparative Aspects of the Brain Growth Spurt. *Early Human Development*, *3*(1), 79–83. https://doi.org/10.1016/0378-3782(79)90022-7

Dodge, J., Clarke, J., Passini, M., Song, A., O'Riordan, C., Cheng, S., & Stewart, G. (2005). *497. Sex and Estrous Cycle Stage Influence the Efficiency of AAV-Mediated Gene Transfer in the Rodent Brain*. Retrieved from https://search.proquest.com/docview/1793436808?pq-origsite=gscholar

Drew, P. D., Xu, J., Storer, P. D., Chavis, J. A., & Racke, M. K. (2006). Peroxisome Proliferator-Activated Receptor Agonist regulation of glial activation: Relevance to CNS inflammatory disorders. *Neurochemistry International*, *49*(2), 183–189. https://doi.org/10.1016/j.neuint.2006.04.003

Duffy, M. R., Parker, A. L., Bradshaw, A. C., & Baker, A. H. (2012). Manipulation of Adenovirus Interactions with Host Factors for Gene Therapy Applications. *Nanomedicine*, Vol. 7, pp. 271–278. https://doi.org/10.2217/nnm.11.186

Dutta, S., & Sengupta, P. (2016). Men and Mice: Relating Their Ages. *Life Sciences*, Vol. 152, pp. 244–248. https://doi.org/10.1016/j.lfs.2015.10.025

Duvanel, C. B., Honegger, P., Pershadsingh, H., Feinstein, D., & Matthieu, J.-M. (2003). Inhibition of Glial Cell Proinflammatory Activities by Peroxisome Proliferator-Activated Receptor Gamma Agonist Confers Partial Protection During Antimyelin Oligodendrocyte Glycoprotein Demyelination *in vitro*. *Journal of Neuroscience Research*, *71*(2), 246–255. https://doi.org/10.1002/jnr.10471

Eichler, M., Spinedi, L., Unfer-Grauwiler, S., Bodmer, M., Surber, C., Luedi, M., & Drewe, J. (2012). Heat Exposure of *Cannabis sativa* Extracts Affects the Pharmacokinetic and Metabolic Profile in Healthy Male Subjects. *Planta Med*, *78*, 686–691. Retrieved from https://pdfs.semanticscholar.org/9cc5/4fb63cdc746a2fbebc88652b1bc0a3e2c3ea.pdf

Eliason, S. L., Stein, C. S., Mao, Q., Tecedor, L., Ding, S. L., Gaines, D. M., & Davidson, B. L. (2007). A Knock-In Reporter Model of Batten Disease. *Journal of Neuroscience*, *27*(37), 9826–9834. https://doi.org/10.1523/JNEUROSCI.1710-07.2007

Elleder, M., Franc, J., Kraus, J., Nevsimalova, S., Sxtova, K., & Zeman, J. (1997). Neuronal Ceroid Lipofuscinosis in the Czech Republic: Analysis of 57 cases. Report of the “Prague NCL group”. *European Journal of Paediatric Neurology*, *1*, 109–114.

Endicott, K. M., & Lillie, R. D. (1944). Ceroid, the Pigment of Dietary Cirrhosis of Rats: Its Characteristics and Its Differentiation from Hemofuscin. *The American Journal of Pathology*, *20*(1), 149–153. Retrieved from http://www.ncbi.nlm.nih.gov/pubmed/19970741

Esmaeili, M. A., Yadav, S., Gupta, R. K., Waggoner, G. R., Deloach, A., Calingasan, N. Y., … Kiaei, M. (2016). Preferential PPAR-α Activation Reduces Neuroinflammation, and Blocks nNurodegeneration *in vivo*. *Human Molecular Genetics*, *25*(2), 317–327. https://doi.org/10.1093/hmg/ddv477

Esposito, G, Scuderi, C., Savani, C., Steardo, L., Filippis, D., Cottone, P., … Steardo, L. (2009). Cannabidiol *in vivo* Blunts β-amyloid Induced Neuroinflammation by Suppressing IL-1β and iNOS Expression. *British Journal of Pharmacology*, *151*(8), 1272–1279. https://doi.org/10.1038/sj.bjp.0707337

Esposito, Giuseppe, Scuderi, C., Valenza, M., Togna, G. I., Latina, V., de Filippis, D., … Steardo, L. (2011). Cannabidiol Reduces Aβ-Induced Neuroinflammation and Promotes Hippocampal Neurogenesis Through PPARγ Involvement. *PLoS ONE*, *6*(12). https://doi.org/10.1371/journal.pone.0028668

Fazio, S., & Linton, M. F. (2004). The Role of Fibrates in Managing Hyperlipidemia: Mechanisms of Action and Clinical Efficacy. *Current Atherosclerosis Reports*, Vol. 6, pp. 148–157. https://doi.org/10.1007/s11883-004-0104-8

FDA.gov. (2021). *LOPID* .

Fearnley, I. M., Walker, J. E., Martinus, R. D., Jolly, R. D., Kirkland, K. B., Shaw, G. J., & Palmer, D. N. (1990). The Sequence of the Major Protein Stored in Ovine Ceroid Lipofuscinosis is Identical with that of the Dicyclohexylcarbodi-Imide-Reactive Proteolipid of Mitochondrial ATP Synthase. *Biochemical Journal*, *268*(3), 751–758. https://doi.org/10.1042/bj2680751

Fereshetian, A. G., Davidson, M., Haber, H., & Black, D. M. (1998). Gemfibrozil Treatment in Patients with Elevated Lipoprotein A. A Pilot Study. *Clinical Drug Investigation*, *16*(1), 1–7. https://doi.org/10.2165/00044011-199816010-00001

Ferrari, F. K., Samulski, T., Shenk, T., & Samulski, R. J. (1996). Second-Strand Synthesis is a Rate-Limiting Step for Efficient Transduction by Recombinant Adeno-Associated Virus Vectors. *Journal of Virology*, *70*(5), 3227–3234. Retrieved from http://www.ncbi.nlm.nih.gov/pubmed/8627803

Fiske, R., & Storts, R. (1988). Neuronal Ceroid Lipofuscinosis in Nubian Goats. *Vet. Pathol*, *25*, 171–173.

Flurkey, K., Currer, J. M., & Harrison, D. E. (2007). Mouse Models in Aging Research. In *The Mouse in Biomedical Research* (Vol. 3, pp. 637–672). https://doi.org/10.1016/B978-012369454-6/50074-1

Formukong, E. A., Evans, A. T., & Evans, F. J. (1988). Analgesic and Antiinflammatory Activity of Constituents of *Cannabis sativa*. *Inflammation*, *12*(4), 361–371. https://doi.org/10.1007/BF00915771

Fox, J., Barthold, S., Davisson, M., Newcomer, C., Quimby, F., & A, S. (2006). *The Mouse in Biomedical Research: Normative Biology, Husbandry and Models*. Elsevier.

Frick, M. H., Elo, O., Haapa, K., Heinonen, O. P., Heinsalmi, P., Helo, P., … Nikkilä, E. A. (1987). Helsinki Heart Study: Primary-Prevention Trial with Gemfibrozil in Middle-Aged Men with Dyslipidemia. *New England Journal of Medicine*, *317*(20), 1237–1245. https://doi.org/10.1056/NEJM198711123172001

Gao, H., Boustany, R.-M. N., Espinola, J. A., Cotman, S. L., Srinidhi, L., Antonellis, K. A., … MacDonald, M. E. (2002). Mutations in a Novel CLN6-Encoded Transmembrane Protein Cause Variant Neuronal Ceroid Lipofuscinosis in Man and Mouse. *The American Journal of Human Genetics*, *70*(2), 324–335. https://doi.org/10.1086/338190

Gaoni, Y., Mechoulam, R. (1964). Isolation, Structure and Partial Synthesis of an Active Constituent of Hashish. *Journal of the American Chemical Society*, *86*(8), 1646–1647. Retrieved from https://pubs.acs.org/sharingguidelines

Gaston, T. E., & Friedman, D. (2017). Pharmacology of Cannabinoids in the Treatment of Epilepsy. *Epilepsy and Behavior*, Vol. 70, pp. 313–318. https://doi.org/10.1016/j.yebeh.2016.11.016

Gavin, M., Wen, G. Y., Messing, J., Adelman, S., Logush, A., Jenkins, E. C., … Velinov, M. (2013). Substrate Reduction Therapy in Four Patients with Milder CLN1 Mutations and Juvenile-Onset Batten Disease Using Cysteamine Bitartrate. In *JIMD Reports* (Vol. 11, pp. 87–92). https://doi.org/10.1007/8904_2013_226

Geraets, R. D., Koh, S. yon, Hastings, M. L., Kielian, T., Pearce, D. A., & Weimer, J. M. (2016). Moving Towards Effective Therapeutic Strategies for Neuronal Ceroid Lipofuscinosis. *Orphanet Journal of Rare Diseases*, *11*(1), 40. https://doi.org/10.1186/s13023-016-0414-2

Ghosh, A., Corbett, G. T., Gonzalez, F. J., & Pahan, K. (2012). Gemfibrozil and fenofibrate, food and drug administration-approved lipid-lowering drugs, up-regulate tripeptidyl-peptidase 1 in brain cells via peroxisome proliferator-activated receptor α: Implications for late infantile batten disease therapy. *Journal of Biological Chemistry*, *287*(46), 38922–38935. https://doi.org/10.1074/jbc.M112.365148

Gianetto, R., & de Duve, C. (1955). Tissue Fractionation Studies. 4. Comparative Study of the Binding of Acid Phosphatase, Beta-Glucuronidase and Cathepsin by Rat-Liver Particles. *The Biochemical Journal*, *59*(3), 433–438. Retrieved from http://www.ncbi.nlm.nih.gov/pubmed/14363113

Glascock, J. J., Osman, E. Y., Coady, T. H., Rose, F. F., Shababi, M., & Lorson, C. L. (2011). Delivery of Therapeutic Agents Through Intracerebroventricular (i.c.v) and Intravenous (i.v) Injection in Mice. *Journal of Visualized Experiments : JoVE*, (56). https://doi.org/10.3791/2968

The Goods Administration (2013). *Australian Public Assessment Report for Nabiximols About the Therapeutic Goods Administration (TGA)*. Retrieved from http://www.tga.gov.au

Green, P. D., & Little, P. B. (1974). Neuronal Ceroid Lipofuscin Storage in Siamese cats. *Canadian Journal of Comparative Medicine : Revue Canadienne de Medecine Comparee*, *38*(2), 207–212. Retrieved from http://www.ncbi.nlm.nih.gov/pubmed/4132965

Griffey, M. A., Wozniak, D., Wong, M., Bible, E., Johnson, K., Rothman, S. M., … Sands, M. S. (2006). CNS-Directed AAV2-Mediated Gene Therapy Ameliorates Functional Deficits in a Murine Model of Infantile Neuronal Ceroid Lipofuscinosis. *Molecular Therapy*, *13*(3), 538–547. https://doi.org/10.1016/j.ymthe.2005.11.008

Griffey, M., Bible, E., Vogler, C., Levy, B., Gupta, P., Cooper, J., & Sands, M. S. (2004). Adeno-Associated Virus 2-Mediated Gene Therapy Decreases Autofluorescent Storage Material and Increases Brain Mass in a Murine Model of Infantile Neuronal Ceroid Lipofuscinosis. *Neurobiology of Disease*, *16*(2), 360–369. https://doi.org/10.1016/j.nbd.2004.03.005

Griffey, M., Macauley, S. L., Ogilvie, J. M., & Sands, M. S. (2005). AAV2-Mediated Ocular Gene Therapy for Infantile Neuronal Ceroid Lipofuscinosis. *Molecular Therapy*, *12*(3), 413–421. https://doi.org/10.1016/j.ymthe.2005.04.018

Groh, J., Berve, K., & Martini, R. (2017). Fingolimod and Teriflunomide Attenuate Neurodegeneration in Mouse Models of Neuronal Ceroid Lipofuscinosis. *Molecular Therapy*, *25*, 1889–1899. https://doi.org/10.1016/j.ymthe.2017.04.021

Grotenhermen, F. (2003). Pharmacokinetics and Pharmacodynamics of Cannabinoids. *Clinical Pharmacokinetics*, Vol. 42, pp. 327–360. https://doi.org/10.2165/00003088-200342040-00003

Gupta, P., Soyombo, A. A., Atashband, A., Wisniewski, K. E., Shelton, J. M., Richardson, J. A., … Goldstein, J. L. (2001). Disruption of PPT1 or PPT2 Causes Neuronal Ceroid Lipofuscinosis in Knockout Mice. *Proceedings of the National Academy of Sciences*, 13566–13571. Retrieved from www.pnas.orgcgidoi10.1073pnas.251485198

Guyenet, S. J., Furrer, S. A., Damian, V. M., Baughan, T. D., la Spada, A. R., & Garden, G. A. (2010). A Simple Composite Phenotype Scoring System for Evaluating Mouse Models of Cerebellar Ataxia. *Journal of Visualized Experiments*, (39). https://doi.org/10.3791/1787

Haltia, M, Rapola, J., & Santavuori, P. (1973). Infantile Type of So-Called Neuronal Ceroid Lipofuscinosis. Histological and Electron Microscopic Studies. *Acta Neuropathologica*, *26*, 157–170.

Haltia, M, Rapola, J., Santavuori, P., & Keranen, A. (1973). Infantile Type of So-Called Neuronal Ceroid Lipofuscinosis. 2. Morphological and Biochemical Studies. *J Neurol Sci*, *18*, 269–285.

Haltia, M. (2003). The Neuronal Ceroid Lipofuscinoses. *Journal of Neuropathology & Experimental Neurology*, *62*(1), 1–13. https://doi.org/10.1093/jnen/62.1.1

Haltia, M. (2006). The Neuronal Ceroid Lipofuscinoses: From Past to Present. *Biochimica et Biophysica Acta (BBA) - Molecular Basis of Disease*, *1762*(10), 850–856. https://doi.org/10.1016/J.BBADIS.2006.06.010

Hanuš, L. O., Meyer, S. M., Muñoz, E., Taglialatela-Scafati, O., & Appendino, G. (2016). Phytocannabinoids: a Unified Critical Inventory. *Natural Product Reports*, *33*(12), 1357–1392. https://doi.org/10.1039/C6NP00074F

Heine, C., Heine, C., Quitsch, A., Storch, S., Martin, Y., Lonka, L., … Braulke, T. (2007). Topology and Endoplasmic Reticulum Retention Signals of the Lysosomal Storage Disease-Related Membrane Protein CLN6. *Molecular Membrane Biology*, *24*(1), 74–87. https://doi.org/10.1080/09687860600967317

Heinonen, O., Kyttälä, A., Lehmus, E., Paunio, T., Peltonen, L., & Jalanko, A. (2000). Expression of Palmitoyl Protein Thioesterase in Neurons. *Molecular Genetics and Metabolism*, *69*(2), 123–129. https://doi.org/10.1006/mgme.2000.2961

Heneka, M. T., Carson, M. J., Khoury, J. El, Landreth, G. E., Brosseron, F., Feinstein, D. L., … Kummer, M. P. (2015). Neuroinflammation in Alzheimer's disease. *The Lancet Neurology*, Vol. 14, pp. 388–405. https://doi.org/10.1016/S1474-4422(15)70016-5

Hers, H. G. (1965). Inborn Lysosomal Diseases. *Gastroenterology*, *48*(5), 625–633. https://doi.org/10.1016/S0016-5085(65)80041-5

Heuberger, J. A. A. C., Guan, Z., Oyetayo, O. O., Klumpers, L., Morrison, P. D., Beumer, T. L., … Freijer, J. (2015). Population Pharmacokinetic Model of THC Integrates Oral, Intravenous, and Pulmonary Dosing and Characterizes Short- and Long-Term Pharmacokinetics. *Clinical Pharmacokinetics*, *54*(2), 209–219. https://doi.org/10.1007/s40262-014-0195-5

Hirsch, E. C., Vyas, S., & Hunot, S. (2012). Neuroinflammation in Parkinson's disease. *Parkinsonism and Related Disorders*, *18*(SUPPL. 1). https://doi.org/10.1016/s1353-8020(11)70065-7

Hitoshi, N., Ken-ichi, Y., & Jun-ichi, M. (1991). Efficient selection for high-expression transfectants with a novel eukaryotic vector. *Gene*, *108*(2), 193–199. https://doi.org/10.1016/0378-1119(91)90434-D

Holthaus, S.-M. kleine, Martin-Herranz, S., Massaro, G., Aristorena, M., Hoke, J., Hughes, M. P., … Ali, R. R. (2019). Neonatal Brain-Directed Gene Therapy Rescues a Mouse Model of Neurodegenerative CLN6 Batten Disease. *BioRxiv*, 673848. https://doi.org/10.1101/673848

Hong, M., Song, K. D., Lee, H. K., Yi, S. S., Lee, Y. S., Heo, T. H., … Kim, S. J. (2016). Fibrates Inhibit the Apoptosis of Batten Disease Lymphoblast Cells via Autophagy Recovery and Regulation of Mitochondrial Membrane Potential. *In Vitro Cellular and Developmental Biology - Animal*, *52*(3), 349–355. https://doi.org/10.1007/s11626-015-9979-7

Houweling, P. J., Cavanagh, J. A. L., Palmer, D. N., Frugier, T., Mitchell, N. L., Windsor, P. A., … Tammen, I. (2006). Neuronal Ceroid Lipofuscinosis in Devon Cattle is Caused by a Single Base Duplication (c.662dupG) in the Bovine CLN5 Gene. *Biochimica et Biophysica Acta - Molecular Basis of Disease*, *1762*(10), 890–897. https://doi.org/10.1016/j.bbadis.2006.07.008

Howlett, A. C., Barth, F., Bonner, T. I., Cabral, G., Casellas, P., Devane, W. A., … Pertwee, R. G. (2002). International Union of Pharmacology. XXVII. Classification of cannabinoid receptors. *Pharmacological Reviews*, Vol. 54, pp. 161–202. https://doi.org/10.1124/pr.54.2.161

Hu, J., Lu, J. Y., Wong, A. M. S., Hynan, L. S., Birnbaum, S. G., Yilmaz, D. S., … Hofmann, S. L. (2012). Intravenous High-Dose Enzyme Replacement Therapy with Recombinant Palmitoyl-Protein Thioesterase Reduces Visceral Lysosomal Storage and Modestly Prolongs Survival in a Preclinical Mouse Model of Infantile Neuronal Ceroid Lipofuscinosis. *Molecular Genetics and Metabolism*, *107*(1–2), 213–221. https://doi.org/10.1016/j.ymgme.2012.05.009

Huber, R. J., Hughes, S. M., Liu, W., Morgan, A., Tuxworth, R. I., & Russell, C. (2020). The Contribution of Multicellular Model Organisms to Neuronal Ceroid Lipofuscinosis Research. *Biochimica et Biophysica Acta - Molecular Basis of Disease*, *1866*(9), 165614. https://doi.org/10.1016/j.bbadis.2019.165614

Hueck, W. (1912). Pigmentstudien. *Beitr. Path. Anat.*, *54*, 68.

Iannotti, F. A., Hill, C. L., Leo, A., Alhusaini, A., Soubrane, C., Mazzarella, E., … Stephens, G. J. (2014). Nonpsychotropic Plant Cannabinoids, Cannabidivarin (CBDV) and Cannabidiol (CBD), Activate and Desensitize Transient Receptor Potential Vanilloid 1 (TRPV1) Channels *in vitro*: Potential for the Treatment of Neuronal Hyperexcitability. *ACS Chemical Neuroscience*, *5*(11), 1131–1141. https://doi.org/10.1021/cn5000524

Jadav, R. H., Sinha, S., Yasha, T. C., Aravinda, H., Gayathri, N., Rao, S., … Satishchandra, P. (2014). Clinical, Electrophysiological, Imaging, and Ultrastructural Description in 68 Patients with Neuronal Ceroid Lipofuscinoses and Its Subtypes. *Pediatric Neurology*, *50*(1), 85–95. https://doi.org/10.1016/j.pediatrneurol.2013.08.008

Jalanko, A., Vesa, J., Manninen, T., Von Schantz, C., Minye, H., Fabritius, A. L., … Peltonen, L. (2005). Mice with Ppt1 Δex4 Mutation Replicate the INCL Phenotype and Show an Inflammation-Associated Loss of Interneurons. *Neurobiology of Disease*, *18*(1), 226–241. https://doi.org/10.1016/j.nbd.2004.08.013

Jankowiak, W., Kruszewski, K., Flachsbarth, K., Skevas, C., Richard, G., Rüther, K., … Bartsch, U. (2015). Sustained Neural Stem Cell-Based Intraocular Delivery of CNTF Attenuates Photoreceptor Loss in the nclf Mouse Model of Neuronal Ceroid Lipofuscinosis. *PLOS ONE*, *10*(5), e0127204. https://doi.org/10.1371/journal.pone.0127204

Jansky, J. (1909). Über Einen Noch Nicht Beschriebenen Fall der Familiären Amaurotischen Idiotie Mit Hypoplasie des Kleinhirns. *Ztschr. f.d. Erforsch. Und Behandl. Jugendl. Schwachsinns*, 86.

Jazin, E., & Cahill, L. (2010). Sex Differences in Molecular Neuroscience: From Fruit Flies to Humans. *Nature Reviews Neuroscience*, Vol. 11, pp. 9–17. https://doi.org/10.1038/nrn2754

Jennekens, F. G. I. (2014). A Short History of the Notion of Neurodegenerative Disease. *Journal of the History of the Neurosciences*, *23*(1), 85–94. https://doi.org/10.1080/0964704X.2013.809297

Johnson, J. R., ChB, M., Burnell-Nugent, M., BChir, M., Lossignol, D., Doina Ganae-Motan, E., … Luke, S. (2010). Multicenter, Double-Blind, Randomized, Placebo-Controlled, Parallel-Group Study of the Efficacy, Safety, and Tolerability of THC:CBD Extract and THC Extract in Patients with Intractable Cancer-Related Pain. *Journal of Pain and Symptom Management*, *39*(2). https://doi.org/10.1016/j.jpainsymman.2009.06.008

Johnson, T. B., Cain, J. T., White, K. A., Ramirez-Montealegre, D., Pearce, D. A., & Weimer, J. M. (2019). Therapeutic Landscape for Batten Disease: Current Treatments and Future Prospects. *Nature Reviews Neurology*, *15*(3), 161–178. https://doi.org/10.1038/s41582-019-0138-8

Johnson, T. B., Sturdevant, D. A., White, K. A., Drack, A. V., Bhattarai, S., Rogers, C., … Weimer, J. M. (2019). Characterization of a Novel Porcine Model of CLN3-Batten Disease. *Molecular Genetics and Metabolism*, *126*(2), S81. https://doi.org/10.1016/J.YMGME.2018.12.198

Jolly, R. D., & West, D. M. (1976). Letters to the Editor: Blindness in South Hampshire Sheep: A Neuronal Ceroid Lipofuscinosis. *New Zealand Veterinary Journal*, Vol. 24, p. 123. https://doi.org/10.1080/00480169.1976.34298

Jun-ichi, M., Satoshi, T., Kimi, A., Fumi, T., Akira, T., Kiyoshi, T., & Ken-ichi, Y. (1989). Expression Vector System Based on the Chicken β-Actin Promoter Directs Efficient Production of Interleukin-5. *Gene*, *79*(2), 269–277. https://doi.org/10.1016/0378-1119(89)90209-6

Kalueff, A. V., Stewart, A. M., & Gerlai, R. (2014). Zebrafish as an Emerging Model for Studying Complex Brain Disorders. *Trends in Pharmacological Sciences*, Vol. 35, pp. 63–75. https://doi.org/10.1016/j.tips.2013.12.002

Kanner, L. (1962). Emotionally Disturbed Children: A Historical Review. *Child Development*, *33*(1), 97. https://doi.org/10.2307/1126636

Kanninen, K. M., Grubman, A., Caragounis, A., Duncan, C., Parker, S. J., Lidgerwood, G. E., … White, A. R. (2013). Altered Biometal Homeostasis is Associated with CLN6 mRNA Loss in Mouse Neuronal Ceroid Lipofuscinosis. *Biology Open*, *2*(6), 635–646. https://doi.org/10.1242/bio.20134804

Kaplan, J. S., Stella, N., Catterall, W. A., & Westenbroek, R. E. (2017). Cannabidiol Attenuates Seizures and Social Deficits in a Mouse Model of Dravet Syndrome. *Proceedings of the National Academy of Sciences of the United States of America*, *114*(42), 11229–11234. https://doi.org/10.1073/pnas.1711351114

Katz, M. L., Khan, S., Awano, T., Shahid, S. A., Siakotos, A. N., & Johnson, G. S. (2005). A Mutation in the CLN8 Gene in English Setter Dogs with Neuronal Ceroid Lipofuscinosis. *Biochemical and Biophysical Research Communications*, *327*(2), 541–547. https://doi.org/10.1016/j.bbrc.2004.12.038

Katz, M. L., Shibuya, H., Liu, P.-C., Kaur, S., Gao, C.-L., & Johnson, G. S. (1999). A Mouse Gene Knockout Model for Juvenile Ceroid-Lipofuscinosis (Batten Disease). *Journal of Neuroscience Research*, *57*(4), 551–556. https://doi.org/10.1002/(SICI)1097-4547(19990815)57:4<551::AID-JNR15>3.0.CO;2-R

Kauffman, J. M. (1976). Nineteenth Century Views of Children's Behavior Disorders: Historical Contributions and Continuing Issues. *The Journal of Special Education*, *10*(4), 335–349. https://doi.org/10.1177/002246697601000402

Kay, C. (2011). Same Gene, Surprising Difference: Adult Neuronal Ceroid Lipofuscinosis Linked to CLN6, Mutated in Variant Late Infantile Form. *Clinical Genetics*, *80*(6), 505–506. https://doi.org/10.1111/j.1399-0004.2011.01761.

Kersten, S. (2008). Peroxisome Proliferator Activated Receptors and Lipoprotein Metabolism. *PPAR Research*. https://doi.org/10.1155/2008/132960

Kielar, C., Maddox, L., Bible, E., Pontikis, C. C., Macauley, S. L., Griffey, M. A., … Cooper, J. D. (2007). Successive Neuron Loss in the Thalamus and Cortex in a Mouse Model of Infantile Neuronal Ceroid Lipofuscinosis. *Neurobiology of Disease*, *25*(1), 150–162. https://doi.org/10.1016/j.nbd.2006.09.001

Kim, J.-Y., Grunke, S. D., Levites, Y., Golde, T. E., & Jankowsky, J. L. (2014). Intracerebroventricular Viral Injection of the Neonatal Mouse Brain for Persistent and Widespread Neuronal Transduction. *Journal of Visualized Experiments*, (91), e51863–e51863. https://doi.org/10.3791/51863

Koppang, N. (1992). English Setter Model and Juvenile Ceroid Lipofuscinosis in Man. *American Journal of Medical Genetics*, *42*(4), 599–604. https://doi.org/10.1002/ajmg.1320420434

Koppang, Nils. (1969). Neuronal Ceroid Lipofuscinosis in English Setters. Juvenile Amaurotic Familiar Idiocy (AFI) in English Setters. *Journal of Small Animal Practice*, *10*(11), 639–644. https://doi.org/10.1111/j.1748-5827.1969.tb04003.x

Kopra, O., Vesa, J., von Schantz, C., Manninen, T., Minye, H., Fabritius, A., … Peltonen, L. (2004). A Mouse Model for Finnish Variant Late Infantile Neuronal Ceroid Lipofuscinosis, CLN5, Reveals Neuropathology Associated with Early Aging. *Human Molecular Genetics*, *13*(23), 2893–2906.

Kufs, H. (1925). Über eine Spätform der Amaurotischen Idiotie und Ihre Heredofamiliären Grundlagen. *Zeitschrift Für Die Gesamte Neurologie Und Psychiatrie*, *95*(1), 169–188.

Kumar, A., Premoli, M., Aria, F., Bonini, S. A., Maccarinelli, G., Gianoncelli, A., … Mastinu, A. (2019). Cannabimimetic Plants: Are They New Cannabinoidergic Modulators? *Planta*, *249*(6), 1681–1694. https://doi.org/10.1007/s00425-019-03138-x

Kuronen, M. (2012). *Studies on the Molecular Pathogenesis of Neuronal Ceroid Lipofuscinoses in the Animal Models of CLN8 and CLN10*.

La Spada, A. R. (2012). PPARGC1A/PGC-1α, TFEB and Enhanced Proteostasis in Huntington Disease. *Autophagy*, *8*(12), 1845–1847. https://doi.org/10.4161/auto.21862

Lacoursiere, R. B., & Swatek, R. (1983). Adverse Interaction Between Disulfiram and Marijuana: A Case Report. *American Journal of Psychiatry*, *140*(2), 243–244. https://doi.org/10.1176/ajp.140.2.243

Lake, B. D., & Cavanagh, N. P. C. (1978). Early-Juvenile Batten's Disease — A Recognisable Sub-Group Distinct from Other Forms of Batten's Disease: Analysis of 5 Patients. *Journal of the Neurological Sciences*, *36*(2), 265–271. https://doi.org/10.1016/0022-510X(78)90087-4

Lalonde, R., & Strazielle, C. (2011). Brain Regions and Genes Affecting Limb-Clasping Responses. *Brain Research Reviews*, Vol. 67, pp. 252–259. https://doi.org/10.1016/j.brainresrev.2011.02.005

Laprairie, R. B., Bagher, A. M., Kelly, M. E. M., & Denovan-Wright, E. M. (2015). Cannabidiol is a Negative Allosteric Modulator of the Cannabinoid CB1 Receptor. *British Journal of Pharmacology*, *172*(20), 4790–4805. https://doi.org/10.1111/bph.13250

Lehtovirta, M. (2001). Palmitoyl Protein Thioesterase (PPT) Localizes into Synaptosomes and Synaptic Vesicles in Neurons: Implications for Infantile Neuronal Ceroid Lipofuscinosis (INCL). *Human Molecular Genetics*, *10*(1), 69–75. https://doi.org/10.1093/hmg/10.1.69

Levin, S. W., Baker, E. H., Zein, W. M., Zhang, Z., Quezado, Z. M. N., Miao, N., … Mukherjee, A. B. (2014). Oral Cysteamine Bitartrate and N-Acetylcysteine for Patients with Infantile Neuronal Ceroid Lipofuscinosis: A Pilot Study. *The Lancet Neurology*, *13*(8), 777–787. https://doi.org/10.1016/S1474-4422(14)70142-5

Lilja, J. J., Backman, J. T., & Neuvonen, P. J. (2005). Effect of Gemfibrozil on the Pharmacokinetics and Pharmacodynamics of Racemic Warfarin in Healthy Subjects. *British Journal of Clinical Pharmacology*, *59*(4), 433–439. https://doi.org/10.1111/j.1365-2125.2004.02323.x

Lillie, R. D., Daft, F. S., & Sebrell, W. H. (1941). Cirrhosis of the Liver in Rats on a Deficient Diet and the Effect of Alcohol. *Public Health Reports (1896-1970)*, *56*(23), 1255–1258. Retrieved from https://www.jstor.org/stable/pdf/4583764.pdf

Linterman, K. S., Palmer, D. N., Kay, G. W., Barry, L. A., Mitchell, N. L., McFarlane, R. G., … Hughes, S. M. (2011). Lentiviral-Mediated Gene Transfer to the Sheep Brain: Implications for Gene Therapy in Batten Disease. *Human Gene Therapy*, *22*(8), 1011–1020. https://doi.org/10.1089/hum.2011.026

Lorenz, R. (2005). A Causistic Rationale for the Treatment of Spastic and Myocloni in a Childhood Neurodegenerative Disease: Neuronal Ceroid Lipofuscinosis of the Type Jansky-Bielschowsky. *Neuroendocrinology Letters Nos*, *5623*. Retrieved from http://www.nel.edu/pdf_/NEL235602C01_Lorenz_.pdf

Loría, F., Petrosino, S., Hernangómez, M., Mestre, L., Spagnolo, A., Correa, F., … Guaza, C. (2010). An endocannabinoid tone limits excitotoxicity in vitro and in a model of multiple sclerosis. *Neurobiology of Disease*, *37*(1), 166–176. https://doi.org/10.1016/j.nbd.2009.09.020

Lu, J. Y., Hu, J., & Hofmann, S. L. (2010). Human Recombinant Palmitoyl-Protein Thioesterase-1 (PPT1) for Preclinical Evaluation of Enzyme Replacement Therapy for Infantile Neuronal Ceroid Lipofuscinosis. *Molecular Genetics and Metabolism*, *99*(4), 374–378. https://doi.org/10.1016/j.ymgme.2009.12.002

Lu, J. Y., Nelvagal, H. R., Wang, L., Birnbaum, S. G., Cooper, J. D., & Hofmann, S. L. (2015). Intrathecal Enzyme Replacement Therapy Improves Motor Function and Survival in a Preclinical Mouse Model of Infantile Neuronal Ceroid Lipofuscinosis. *Molecular Genetics and Metabolism*, *116*(1–2), 98–105. https://doi.org/10.1016/j.ymgme.2015.05.005

Lucas, C. J., Galettis, P., & Schneider, J. (2018). The Pharmacokinetics and the Pharmacodynamics of Cannabinoids. *British Journal of Clinical Pharmacology*, Vol. 84, pp. 2477–2482. https://doi.org/10.1111/bcp.13710

Luiro, K. (2001). CLN3 Protein is Targeted to Neuronal Synapses but Excluded From Synaptic Vesicles: New Clues to Batten Disease. *Human Molecular Genetics*, *10*(19), 2123–2131. https://doi.org/10.1093/hmg/10.19.2123

Lyly, A., von Schantz, C., Salonen, T., Kopra, O., Saarela, J., Jauhiainen, M., … Jalanko, A. (2007). Glycosylation, Transport, and Complex Formation of Palmitoyl Protein Thioesterase 1 (PPT1) - Distinct Characteristics in Neurons. *BMC Cell Biology*, *8*. https://doi.org/10.1186/1471-2121-8-22

Macauley, S. L., Roberts, M. S., Wong, A. M., McSloy, F., Reddy, A. S., Cooper, J. D., & Sands, M. S. (2012). Synergistic Effects of Central Nervous System-Directed Gene Therapy and Bone Marrow Transplantation in the Murine Model of Infantile Neuronal Ceroid lipofuscinosis. *Annals of Neurology*, *71*(6), 797–804. https://doi.org/10.1002/ana.23545

Mackie, J., & Clark, D. (1994). Cannabis Toxic Psychosis While on Disulfiram. *British Journal of Psychiatry*, Vol. 164, p. 421. https://doi.org/10.1192/bjp.164.3.421a

Mannerkoski, M. K., Heiskala, H. J., Santavuori, P. R. A., & Pouttu, J. A. (2001). Transdermal Fentanyl Therapy for Pains in Children With Infantile Neuronal Ceroid Lipofuscinosis. *European Journal of Paediatric Neurology*, *5*, 175–177. https://doi.org/10.1053/ejpn.2000.0457

McCarberg, B. H., & Barkin, R. L. (2007). The Future of Cannabinoids as Analgesic Agents: A Pharmacologic, Pharmacokinetic, and Pharmacodynamic Overview. *American Journal of Therapeutics*, *14*(5), 475–483. https://doi.org/10.1097/MJT.0b013e3180a5e581

McCarty, D. M., Fu, H., Monahan, P. E., Toulson, C. E., Naik, P., & Samulski, R. J. (2003). Adeno-Associated Virus Terminal Repeat (TR) Mutant Generates Self-Complementary Vectors to Overcome the Rate-Limiting Step to Transduction *in vivo*. *Gene Therapy*, *10*(26), 2112–2118. https://doi.org/10.1038/sj.gt.3302134

McCarty, D. M. (2008). Self-Complementary AAV Vectors; Advances and Applications. *Molecular Therapy*, Vol. 16, pp. 1648–1656. https://doi.org/10.1038/mt.2008.171

Mechoulam, R., & Gaoni, Y. (1965). A Total Synthesis of dl-Δ1-Tetrahydrocannabinol, the Active Constituent of Hashish. *Journal of the American Chemical Society*, *87*(14), 3273–3275. Retrieved from https://pubs.acs.org/sharingguidelines

Melville, S. A., Wilson, C. L., Chiang, C. S., Studdert, V. P., Lingaas, F., & Wilton, A. N. (2005). A Mutation in Canine CLN5 Causes Neuronal Ceroid Lipofuscinosis in Border Collie Dogs. *Genomics*, *86*(3), 287–294. https://doi.org/10.1016/j.ygeno.2005.06.005

Messer, A., & Flaherty, L. (1986). Autosomal Dominance in a Late-Onset Motor Neuron Disease in the Mouse. *Journal of Neurogenetics*, *3*(6), 345–355.

Miller, D. B., & Spence, J. D. (1998). Clinical Pharmacokinetics of Fibric Acid Derivatives (Fibrates). *Clinical Pharmacokinetics*, *34*(2), 155–162. https://doi.org/10.2165/00003088-199834020-00003

Mitchison, H. M., Bernard, D. J., Greene, N. D. E., Cooper, J. D., Junaid, M. A., Pullarkat, R. K., … Nussbaum, R. L. (1999). Targeted Disruption of the CLN3 Gene Provides a Mouse Model for Batten Disease. *Neurobiology of Disease*, *6*(5), 321–334. https://doi.org/10.1006/nbdi.1999.0267

Mitchison, H. M., Lim, M. J., & Cooper, J. D. (2004). Selectivity and Types of Cell Death in the Neuronal Ceroid Lipofuscinoses (NCLs). *Brain Pathology*, *14*(1), 86–96. https://doi.org/10.1111/j.1750-3639.2004.tb00502.x

Mole, S. E., Cotman, S.L. (2015). Genetics of the neuronal ceroid lipofuscinoses (Batten disease). *Biochimica et Biophysica Acta (BBA) - Molecular Basis of Disease*, *1852*(10), 2237–2241. https://doi.org/10.1016/J.BBADIS.2015.05.011

Mole, S. E., & Cotman, S. L. (2015). Genetics of the Neuronal Ceroid Lipofuscinoses (Batten Disease). *Biochimica et Biophysica Acta - Molecular Basis of Disease*, *1852*(10), 2237–2241. https://doi.org/10.1016/j.bbadis.2015.05.011

Mole, S. E., & Haltia, M. (2014). The Neuronal Ceroid-Lipofuscinoses (Batten Disease). In *Rosenberg's Molecular and Genetic Basis of Neurological and Psychiatric Disease: Fifth Edition* (pp. 793–808). https://doi.org/10.1016/B978-0-12-410529-4.00070-X

Mole, S, Anderson, G., Band, H., Berkovic, S., Cooper, J., klein Holthaus, S., … Smith, A. (2019). *Clinical Challenges and Future Therapeutic Approaches for the Neuronal Ceroid Lipofuscinosis*. 107–116.

Mole, S, Williams, R., & Goebel, H. (Eds.). (2011). *The Neuronal Ceroid Lipofuscinoses (Batten Disease)*. Retrieved from https://books.google.co.nz/books?id=Dp7FAgAAQBAJ&pg=PA11&lpg=PA11&dq=haltia+1973+ncl&source=bl&ots=IxhfPxTeAA&sig=ACfU3U1Esy8UZKc0fxntyBwLBqxgM_bknQ&hl=en&sa=X&ved=2ahUKEwic1NvtssbmAhVt7HMBHQKVDRQQ6AEwCXoECAkQAQ#v=onepage&q=haltia 1973 ncl&f=false

Mole, S. (2018). NCL Animal Models Database.

Morgan, J. P., Magee, H., Wong, A., Nelson, T., Koch, B., Cooper, J. D., & Weimer, J. M. (2013). A Murine Model of Variant Late Infantile Ceroid Lipofuscinosis Recapitulates Behavioral and Pathological Phenotypes of Human Disease. *PLoS ONE*, *8*(11), e78694. https://doi.org/10.1371/journal.pone.0078694

Morse, D., Brothwell, D., & Ucko, P. (1964). *Tuberculosis in Ancient Egypt*. 524–541. https://doi.org/10.1164/ARRD.1964.90.ISSUE-4;PAGE:STRING:ARTICLE

Moutal, A., White, K. A., Chefdeville, A., Laufmann, R. N., Vitiello, P. F., Feinstein, D., … Khanna, R. (2019). Dysregulation of CRMP2 Post-Translational Modifications Drive Its Pathological Functions. *Molecular Neurobiology*, 1–20. https://doi.org/10.1007/s12035-019-1568-4

Munro, S., Thomas, K. L., & Abu-Shaar, M. (1993). Molecular Characterization of a Peripheral Receptor for Cannabinoids. *Nature*, *365*(6441), 61–65. https://doi.org/10.1038/365061a0

Napolitano, G., & Ballabio, A. (2016). TFEB at a Glance. *Journal of Cell Science*, *129*(13), 2475–2481. https://doi.org/10.1242/jcs.146365

Naso, M. F., Tomkowicz, B., Perry, W. L., & Strohl, W. R. (2017). Adeno-Associated Virus (AAV) as a Vector for Gene Therapy. *BioDrugs*, Vol. 31, pp. 317–334. https://doi.org/10.1007/s40259-017-0234-5

Nelvagal, H. R., Lange, J., Takahashi, K., Tarczyluk-Wells, M. A., & Cooper, J. D. (2019). Pathomechanisms in the Neuronal Ceroid Lipofuscinoses. *Biochimica et Biophysica Acta (BBA) - Molecular Basis of Disease*, 165570. https://doi.org/10.1016/j.bbadis.2019.165570

Neuwelt, E. A., Barranger, J. A., Brady, R. O., Pagel, M., Furbish, F. S., Quirk, J. M., … Frenkel, E. (1981). Delivery of Hexosaminidase A to the Cerebrum After Osmotic Modification of the Blood-Brain Barrier. *Proceedings of the National Academy of Sciences of the United States of America*, *78*(9 II), 5838–5841. https://doi.org/10.1073/pnas.78.9.5838

Neverman, N. J., Best, H. L., Hofmann, S. L., & Hughes, S. M. (2015). Experimental Therapies in the Neuronal Ceroid Lipofuscinoses. *Biochimica et Biophysica Acta (BBA) - Molecular Basis of Disease*, *1852*(10), 2292–2300. https://doi.org/10.1016/J.BBADIS.2015.04.026

Newmeyer, M. N., Swortwood, M. J., Barnes, A. J., Abulseoud, O. A., Scheidweiler, K. B., & Huestis, M. A. (2016). Free and Glucuronide Whole Blood Cannabinoids' Pharmacokinetics after Controlled Smoked, Vaporized, and Oral Cannabis Administration in Frequent and Occasional Cannabis Users: Identification of Recent Cannabis Intake. *Clinical Chemistry*, *62*(12), 1579–1592. https://doi.org/10.1373/clinchem.2016.263475

Nicolson, T. J., Mellor, H. R., & Roberts, R. R. A. (2010). Gender Differences in Drug Toxicity. *Trends in Pharmacological Sciences*, *31*(3), 108–114. https://doi.org/10.1016/j.tips.2009.12.001

Niino, M. (2007). Peroxisome Proliferator-Activated Receptor Agonists as Potential Therapeutic Agents in Multiple Sclerosis. *Mini-Reviews in Medicinal Chemistry*, *7*(11), 1129–1135. https://doi.org/10.2174/138955707782331687

Nijssen, P. C. G., Ceuterick, C., Diggelen, O. P., Elleder, M., Martin, J.-J., Teepen, J. L. J. M., … Roos, R. A. C. (2006). Autosomal Dominant Adult Neuronal Ceroid Lipofuscinosis: a Novel Form of NCL with Granular Osmiophilic Deposits without Palmitoyl Protein Thioesterase 1 Deficiency. *Brain Pathology*, *13*(4), 574–581. https://doi.org/10.1111/j.1750-3639.2003.tb00486.x

Nissen, A. J. (1954). Juvenile Amaurotic Idiocy in Norway. *Nordisk Medicin*, *52*(45), 1542.

Nita, D. A., Mole, S. E., & Minassian, B. A. (2016). Neuronal Ceroid Lipofuscinoses. *Epileptic Disorders*, *18*(S2), 73–88. https://doi.org/10.1684/epd.2016.0844

Norman, G. (2010). Likert Scales, Levels of Measurement and the “Laws” of Statistics. *Advances in Health Sciences Education*, *15*(5), 625–632. https://doi.org/10.1007/s10459-010-9222-y

Nosková, L., Stránecký, V., Hartmannová, H., Přistoupilová, A., Barešová, V., Ivánek, R., … Kmoch, S. (2011). Mutations in DNAJC5, Encoding Cysteine-String Protein Alpha, Cause Autosomal-Dominant Adult-Onset Neuronal Ceroid Lipofuscinosis. *American Journal of Human Genetics*, *89*(2), 241–252. https://doi.org/10.1016/j.ajhg.2011.07.003

O’Sullivan, S. E. (2007). Cannabinoids Go Nuclear: Evidence for Activation of Peroxisome Proliferator-Activated Receptors. *British Journal of Pharmacology*, Vol. 152, pp. 576–582. https://doi.org/10.1038/sj.bjp.0707423

Ohlsson, A., Lindgren, J.-E., Andersson, S., Agurell, S., Gillespie, H., & Hollister, L. E. (1986). Single-Dose Kinetics of Deuterium-Labelled Cannabidiol in Man After Smoking and Intravenous Administration. *Biological Mass Spectrometry*, *13*(2), 77–83. https://doi.org/10.1002/bms.1200130206

Oswald, M. J., Kay, G. W., & Palmer, D. N. (2001). Changes in GABAergic Neuron Distribution *in situ* and in Neuron Cultures in Ovine (OCL6) Batten Disease. *European Journal of Paediatric Neurology*, *5*(SUPPL. A), 135–142. https://doi.org/10.1053/ejpn.2000.0450

Oswald, M. J., Palmer, D. N., Kay, G. W., Barwell, K. J., & Cooper, J. D. (2008). Location and Connectivity Determine GABAergic Interneuron Survival in the Brains of South Hampshire Sheep with CLN6 Neuronal Ceroid Lipofuscinosis. *Neurobiology of Disease*, *32*(1), 50–65. https://doi.org/10.1016/j.nbd.2008.06.004

Oswald, M. J., Palmer, D. N., Kay, G. W., Shemilt, S. J. A., Rezaie, P., & Cooper, J. D. (2005). Glial Activation Spreads from Specific Cerebral Foci and Precedes Neurodegeneration in Presymptomatic Ovine Neuronal Ceroid Lipofuscinosis (CLN6). *Neurobiology of Disease*, *20*(1), 49–63. https://doi.org/10.1016/j.nbd.2005.01.025

Packard, K. A., Backes, J. M., Lenz, T. L., Wurdeman, R. L., Destache, C. J., & Hilleman, D. E. (2002). Comparison of Gemfibrozil and Fenofibrate in Patients with Dyslipidemic Coronary Heart Disease. *Pharmacotherapy*, *22*(12), 1527–1532. https://doi.org/10.1592/phco.22.17.1527.34128

Palmer, D. N., Martinus, R. D., Barns, G., Reeves, R. D., Jolly, R. D., Opitz, J. M., … Pullarkat, R. K. (1988). Ovine Ceroid-Lipofuscinosis I: Lipopigment Composition is Indicative of a Lysosomal Proteinosis. *American Journal of Medical Genetics*, *31*(S5), 141–158. https://doi.org/10.1002/ajmg.1320310618

Palmer, D. N., Tyynelä, J., Van Mil, H. C., Westlake, V. J., & Jolly, R. D. (1997). Accumulation of Sphingolipid Activator Proteins (SAPs) A and D in Granular Osmiophilic Deposits in Miniature Schnauzer Dogs with Ceroid Lipofuscinosis. *Journal of Inherited Metabolic Disease*, Vol. 20, pp. 74–84. https://doi.org/10.1023/A:1005365709340

Palmer, D.N., Martinus, R. ., Cooper, S. ., Midwinter, G. ., Reid, J. ., & Jolly, R. . (1989). Ovine Ceroid Lipofuscinosis. The Major Lipopigment Protein and the Lipid-Binding Subunit of Mitochondrial ATP Synthase have the Same NH2-Terminal Sequence. Retrieved December 24, 2019, from J Biol Chem website: http://www.jbc.org.ezproxy.otago.ac.nz/content/264/10/5736

Palmer, D. N., Barry, L. A., Tyynelä, J., & Cooper, J. D. (2013). NCL Disease Mechanisms. *Biochimica et Biophysica Acta (BBA) - Molecular Basis of Disease*, *1832*(11), 1882–1893. https://doi.org/10.1016/J.BBADIS.2013.05.014

Partanen, S., Haapanen, A., Kielar, C., Pontikis, C., Alexander, N., Inkinen, T., … Tyynelä, J. (2008). Synaptic Changes in the Thalamocortical System of Cathepsin D-Deficient Mice. *Journal of Neuropathology & Experimental Neurology*, *67*(1), 16–29. https://doi.org/10.1097/nen.0b013e31815f3899

Partridge, M. (2017). *Voluntary Oral Dosing of Cannabidiol for the Treatment of Batten Disease* (University of Otago). Retrieved from https://ourarchive.otago.ac.nz/handle/10523/7648

Pearse, Y. E. O. (2015). *Exploring The Potential For Gene Therapy In Multiple Forms Of Neuronal Ceroid Lipofuscinosis (Batten Disease)*. King's College London.

Pfizer. (2021). *LOPID*

Phillips, S., Muzaffar, N., Codlin, S., Korey, C., Tachner, P., de Voer, G., … Pearce, D. (2006). Characterizing Pathogenic Processes in Batten Disease: Use of Small Eukaryotic Model Systems. *Biochemica et Biophysica Acta*, *1762*(10), 906–919.

Pillay, S., Zou, W., Cheng, F., Puschnik, A. S., Meyer, N. L., Ganaie, S. S., … Carette, J. E. (2017). Adeno-Associated Virus (AAV) Serotypes Have Distinctive Interactions with Domains of the Cellular AAV Receptor. *Journal of Virology*, *91*(18). https://doi.org/10.1128/jvi.00391-17

Poppens, M. J., Cain, J. T., Johnson, T. B., White, K. A., Davis, S. S., Laufmann, R., … Weimer, J. M. (2019). Tracking Sex-Dependent Differences in a Mouse Model of CLN6 Batten Disease. *Orphanet Journal of Rare Diseases*, *14*(1), 19. https://doi.org/10.1186/s13023-019-0994-8

Prueksaritanont, T., Richards, K. M., Qiu, Y., Strong-Basalyga, K., Miller, A., Li, C., … Carlini, E. J. (2005). Comparative Effects of Fibrates on Drug Metabolizing Enzymes in Human Hepatocytes. *Pharmaceutical Research*, *22*(1), 71–78. https://doi.org/10.1007/s11095-004-9011-5

Raduner, S., Majewska, A., Chen, J.-Z., Xie, X.-Q., Hamon, J., Faller, B., … Gertsch, J. (2006). Alkylamides from *Echinacea* are a New Class of Cannabinomimetics. Cannabinoid Type 2 Receptor-Dependent and -Independent Immunomodulatory Effects. *The Journal of Biological Chemistry*, *281*(20), 14192–14206. https://doi.org/10.1074/jbc.M601074200

Ranta, S., Zhang, Y., Ross, B., L, L., Takkunen, E., Messer, A., … Liu, W. (1999). The Neuronal Ceroid Lipofuscinoses in Human EPMR and mnd Mutant Mice are Associated with Mutations in CLN8. *Nature Genetics*, *23*(2), 233.

Read, W. K., & Bridges, C. H. (1969). Neuronal Lipodystrophy Occurrence in an Inbred Strain of Cattle. In *Path. vet* (Vol. 6).

Rhee, J., Inoue, Y., Yoon, J. C., Puigserver, P., Fan, M., Gonzalez, F. J., & Spiegelman, B. M. (2003). Regulation of Hepatic Fasting Response by PPARγ Coactivator-1α (PGC-1): Requirement for Hepatocyte Nuclear Factor 4α in Gluconeogenesis. *Proceedings of the National Academy of Sciences of the United States of America*, *100*(7), 4012–4017. https://doi.org/10.1073/pnas.0730870100

Rhee, M.-H., Vogel, Z., Barg, J., Bayewitch, M., Levy, R., Hanuš, L., … Mechoulam, R. (1997). Cannabinol Derivatives: Binding to Cannabinoid Receptors and Inhibition of Adenylylcyclase. *Journal of Medicinal Chemistry*, *40*(20), 3228–3233. https://doi.org/10.1021/jm970126f

Rider, J. A., Rider, D. L., Opitz, J. M., Reynolds, J. F., & Pullarkat, R. K. (1988). Batten Disease: Past, Present, and Future. *American Journal of Medical Genetics*, *31*(S5), 21–26. https://doi.org/10.1002/ajmg.1320310606

Rietdorf, K., Coode, E. E., Schulz, A., Wibbeler, E., Bootman, M. D., & Ostergaard, J. R. (2019). Cardiac Pathology in Neuronal Ceroid Lipofuscinoses (NCL): More Than a Mere Co-Morbidity. *Biochimica et Biophysica Acta (BBA) - Molecular Basis of Disease*, 165643. https://doi.org/10.1016/j.bbadis.2019.165643

Rite, I., Machado, A., Cano, J., & Venero, J. L. (2007). Blood-Brain Barrier Disruption Induces *in vivo* Degeneration of Nigral Dopaminergic Neurons. *Journal of Neurochemistry*, *101*(6), 1567–1582. https://doi.org/10.1111/j.1471-4159.2007.04567.x

Russell, C., & Mahmood, F. (2011). Nonsense-Suppression Does Not Rescue the NCL-Like Phenotype of a Zebrafish Model of Late Infantile Neuronal Ceroid Lipofuscinosis. *13th International Conference on Neuronal Ceroid Lipofuscinosis*, e21908.

Russo, E. B., Guy, G. W., & Robson, P. J. (2007). Cannabis, Pain, and Sleep: Lessons from Therapeutic Clinical Trials of Sativex®, a Cannabis-Based Medicine. *Chemistry & Biodiversity*, *4*(8), 1729–1743. https://doi.org/10.1002/cbdv.200790150

RXlist.com (2021). Lopid (Gemfibrozil): Uses, Dosage, Side Effects, Interactions, Warning. (2021). Retrieved April 3, 2021, from RXList.com website: https://www.rxlist.com/lopid-drug.htm

Sachs, B. (1896). A Family Form of Idiocy, Generally Fatal, Associated with Early Blindness. (Amaurotic Family Idiocy). *Journal of Nervous and Mental Disease*, Vol. 21, pp. 475–479. https://doi.org/10.1097/00005053-189607000-00005

Sandifier, P. (1959). The Neurolipidoses. In J. N. Cumings & M. Kremer (Eds.), *Biochemical Aspects of Neurological Disorders* (pp. 191–198). Oxford: Blackwell Scientific Publications.

Santavuori, P., Haltia, M., Rapola, J., & Raitta, C. (1973). Infantile Type of So-Called Neuronal Ceroid Lipofuscinosis. 1. A Clinical Study of 15 Patients. *J Neurol Sci*, *18*, 257–267.

Santavuori, P., Rapola, J., Nuutila, A., Raininko, R., Lappi, M., Launes, J., … Sainio, K. (1991). The Spectrum of Janksy-Bielschowsky Disease. *Neuropediatrics*, *22*, 92–96.

Santavuori, P., Rapola, J., Sainio, K., & Raitta, C. (1982). A Variant of Jansky-Bielschowsky Disease. *Neuropediatrics*, *13*, 135–141.

Saraiva, C., Praça, C., Ferreira, R., Santos, T., Ferreira, L., & Bernardino, L. (2016). Nanoparticle-Mediated Brain Drug Delivery: Overcoming Blood-Brain Barrier to Treat Neurodegenerative Diseases. *Journal of Controlled Release*, Vol. 235, pp. 34–47. https://doi.org/10.1016/j.jconrel.2016.05.044

Schaefer, R. M., Tylki-Szymańska, A., & Hilz, M. J. (2009). Enzyme Replacement Therapy for Fabry Disease: A Systematic Review of Available Evidence. *Drugs*, Vol. 69, pp. 2179–2205. https://doi.org/10.2165/11318300-000000000-00000

Schelleman, H., Han, X., Brensinger, C. M., Quinney, S. K., Bilker, W. B., Flockhart, D. A., … Hennessy, S. (2014). Pharmacoepidemiologic and *in vitro* Evaluation of Potential Drug-Drug Interactions of Sulfonylureas with Fibrates and Statins. *British Journal of Clinical Pharmacology*, *78*(3), 639–648. https://doi.org/10.1111/bcp.12353

Schmid, B., & Haass, C. (2013). Genomic Editing Opens New Avenues for Zebrafish as a Model for Neurodegeneration. *Journal of Neurochemistry*, *127*(4), 461–470. https://doi.org/10.1111/jnc.12460

Schulz, A., Ajayi, T., Specchio, N., de Los Reyes, E., Gissen, P., Ballon, D., … Kohlscutter, J. (2018). *Study of Intraventricular Cerliponase Alfa for CLN2 Disease*. 1898–1907. https://doi.org/10.1056/NEJMoa1712649

Schulz, A., Dhar, S., Rylova, S., Dbaibo, G., Alroy, J., Hagel, C., … Boustany, R.-M. (2004). Impaired Cell Adhesion and Apoptosis in a Novel CLN9 Batten Disease Variant. *Annals of Neurology*, *56*(3), 342–350. https://doi.org/10.1002/ana.20187

Schulz, A., Kohlschütter, A., Mink, J., Simonati, A., & Williams, R. (2013). NCL Diseases - Clinical Perspectives. *Biochimica et Biophysica Acta - Molecular Basis of Disease*, *1832*(11), 1801–1806. https://doi.org/10.1016/j.bbadis.2013.04.008

Schulz, A., Specchio, N., Gissen, P., de los Reyes, E., Cahan, H., Slasor, P., … Jacoby, D. (2017). Long-Term Safety and Efficacy of Intracerebroventricular Enzyme Replacement Therapy with Cerliponase Alfa in Children with CLN2 Disease: Interim Results from an Ongoing Multicenter, Multinational Extension Study. *Molecular Genetics and Metabolism*, *120*(1–2), S120. https://doi.org/10.1016/j.ymgme.2016.11.311

Scuderi, C., Esposito, G., Blasio, A., Valenza, M., Arietti, P., Steardo Jr, L., … Steardo, L. (2011). Palmitoylethanolamide Counteracts Reactive Astrogliosis Induced by β-Amyloid Peptide. *Journal of Cellular and Molecular Medicine*, *15*(12), 2664–2674. https://doi.org/10.1111/j.1582-4934.2011.01267.x

Scuderi, C., Valenza, M., Stecca, C., Esposito, G., Carratù, M. R., & Steardo, L. (2012). Palmitoylethanolamide Exerts Neuroprotective Effects in Mixed Neuroglial Cultures and Organotypic Hippocampal Slices via Peroxisome Proliferator-Activated Receptor-α. *Journal of Neuroinflammation*, *9*. https://doi.org/10.1186/1742-2094-9-49

Seehafer, S. S., & Pearce, D. A. (2006). You Say Lipofuscin, We Say Ceroid: Defining Autofluorescent Storage Material. *Neurobiology of Aging*, *27*(4), 576–588. https://doi.org/10.1016/J.NEUROBIOLAGING.2005.12.006

Seehafer, S. S., Ramirez-Montealegre, D., Wong, A. M. S., Chan, C. H., Castaneda, J., Horak, M., … Pearce, D. A. (2011). Immunosuppression Alters Disease Severity in Juvenile Batten Disease Mice. *Journal of Neuroimmunology*, *230*(1–2), 169–172. https://doi.org/10.1016/j.jneuroim.2010.08.024

Selden, N., Al-Uzri, A., Huhn, S., Koch, T., Sikora, D., Nguyen-Driver, M., … Steiner, R. (2013). *Central Nervous System Stem Cell Transplantation for Children with Neuronal Ceroid Lipofuscinosis*.

Settembre, C., & Ballabio, A. (2011). TFEB Regulates Autophagy: An Integrated Coordination of Cellular Degradation and Recycling Processes. *Autophagy*, Vol. 7, pp. 1379–1381. https://doi.org/10.4161/auto.7.11.17166

Settembre, C., Di Malta, C., Polito, V. A., Arencibia, M. G., Vetrini, F., Erdin, S., … Ballabio, A. (2011). TFEB Links Autophagy to Lysosomal Biogenesis. *Science*, *332*(6036), 1429–1433. https://doi.org/10.1126/science.1204592

Sevin, C., Verot, L., Benraiss, A., Van Dam, D., Bonnin, D., Nagels, G., … Cartier, N. (2007). Partial Cure of Established Disease in an Animal Model of Metachromatic Leukodystrophy After Intracerebral Adeno-Associated Virus-Mediated Gene Transfer. *Gene Therapy*, *14*(5), 405–414. https://doi.org/10.1038/sj.gt.3302883

Sevin, C., Benraiss, A., Van Dam, D., Bonnin, D., Nagels, G., Verot, L., … Cartier, N. (2006). Intracerebral Adeno-Associated Virus-Mediated Gene Transfer in Rapidly Progressive Forms of Metachromatic Leukodystrophy. *Human Molecular Genetics*, *15*(1), 53–64. https://doi.org/10.1093/hmg/ddi425

Shoji, H., Takao, K., Hattori, S., & Miyakawa, T. (2016). Age-Related Changes in Behavior in C57BL/6J Mice from Young Adulthood to Middle Age. *Molecular Brain*, *9*(1). https://doi.org/10.1186/s13041-016-0191-9

Sjögren, T. (1931). Die Juvenile Amaurotischë Idiotie. Klinische und Erblichkeitsmedizinische Untersuchungen. *Hereditas*, *14*(3), 197–425. https://doi.org/10.1111/j.1601-5223.1931.tb02535.x

Sleat, D., Donnelly, R., Lackland, H., Liu, C., Sohar, I., Pullarkat, R., & Lobel, P. (1997). Association of Mutations in a Lysosomal Protein Classical Late-Infantile Neuronal Ceroid Lipofuscinosis. *Science*, *277*(5333), 1802–1805.

Sleat, D. E., Wiseman, J. A., El-Banna, M., Kim, K. H., Mao, Q., Price, S., … Lobel, P. (2004). A Mouse Model of Classical Late-Infantile Neuronal Ceroid Lipofuscinosis Based on Targeted Disruption of the CLN2 Gene Results in a Loss of Tripeptidyl-Peptidase I Activity and Progressive Neurodegeneration. *Journal of Neuroscience*, *24*(41), 9117–9126. https://doi.org/10.1523/JNEUROSCI.2729-04.2004

Smith-Kielland, A., Skuterud, B., & Mørland, J. (1999). Urinary Excretion of 11-Nor-9-Carboxy-Δ9-Tetrahydrocannabinol and Cannabinoids in Frequent and Infrequent Drug Users. *Journal of Analytical Toxicology*, *23*(5), 323–332. https://doi.org/10.1093/jat/23.5.323

Soldin, O. P., Chung, S. H., & Mattison, D. R. (2011). Sex Differences in Drug Disposition. *BioMed Research International*, *23*.

Sondhi, D., Peterson, D., Edelstein, A., del Fierro, K., Hackett, N., & Crystal, R. (2008). Survival Advantage of Neonatal CNS Gene Transfer for Late Infantile Ceroid Lipofuscinosis. *Experimental Neurology*, *213*, 18–27.

Sondhi, D., Hackett, N. R., Peterson, D. A., Stratton, J., Baad, M., Travis, K. M., … Crystal, R. G. (2007). Enhanced Survival of the LINCL Mouse Following CLN2 Gene Transfer Using the rh.10 Rhesus Macaque-Derived Adeno-Associated Virus Vector. *Molecular Therapy*, *15*(3), 481–491. https://doi.org/10.1038/sj.mt.6300049

Sondhi, D., Johnson, L., Purpura, K., Monette, S., Souweidane, M. M., Kaplitt, M. G., … Crystal, R. G. (2012). Long-Term Expression and Safety of Administration of AAVrh.10hCLN2 to the Brain of Rats and Nonhuman Primates for the Treatment of Late Infantile Neuronal Ceroid Lipofuscinosis. *Human Gene Therapy Methods*, *23*(5), 324–335. https://doi.org/10.1089/hgtb.2012.120

Song, W., Wang, F., Savini, M., Ake, A., di ronza, A., Sardiello, M., & Segatori, L. (2013). TFEB Regulates Lysosomal Proteostasis. *Human Molecular Genetics*, *22*(10), 1994–2009. https://doi.org/10.1093/hmg/ddt052

Spence, J. D. (1998). Metabolism of Fibric Acid Derivatives. *Clinical Pharmacokinetics*, *34*(5), 419–420. https://doi.org/10.2165/00003088-199834050-00006

Spielmeyer, W. (1905). Über Familiäre Amaurotische Idiotien. *Neurol. Centralbl.*, *24*, 620.

Staels, B., Dallongeville, J., Auwerx, J., Schoonjans, K., Leitersdorf, E., & Fruchart, J. C. (1998). Mechanism of Action of Fibrates on Lipid and Lipoprotein Metabolism. *Circulation*, *98*(19), 2088–2093. https://doi.org/10.1161/01.CIR.98.19.2088

Steinfeld, R., Heim, P., von Gregory, H., Meyer, K., Ullrich, K., Goebel, H. H., & Kohlschütter, A. (2002). Late Infantile Neuronal Ceroid Lipofuscinosis: Quantitative Description of the Clinical Course in Patients with CLN2 Mutations. *American Journal of Medical Genetics*, *112*(4), 347–354. https://doi.org/10.1002/ajmg.10660

Stengel, C. (1826). Account of a Singular Illness Among Four Siblings in the Vicinity of Roraas. *Eyr (Christiana) 1*, *1*, 347–352.

Stevens, J. C., Banks, G. T., Festing, M. F. W., & Fisher, E. M. C. (2007). Quiet Mutations in Inbred Strains of Mice. *Trends in Molecular Medicine*, Vol. 13, pp. 512–519. https://doi.org/10.1016/j.molmed.2007.10.001

Tamaki, S. J., Jacobs, Y., Dohse, M., Capela, A., Cooper, J. D., Reitsma, M., … Uchida, N. (2009). Neuroprotection of Host Cells by Human Central Nervous System Stem Cells in a Mouse Model of Infantile Neuronal Ceroid Lipofuscinosis. *Cell Stem Cell*, *5*(3), 310–319. https://doi.org/10.1016/j.stem.2009.05.022

Tay, W. (1884). Symmetrical Changes in the Region of the Yellow Spot in Each Eye of an Infant. *Transactions of the Opthalmolgocial Society of the United Kingdom*, *iv*. https://doi.org/10.1001/archneur.1969.00480070114014

Thelen, M., Damme, M., Schweizer, M., Hagel, C., Wong, A. M. S., Cooper, J. D., … Galliciotti, G. (2012). Correction: Disruption of the Autophagy-Lysosome Pathway Is Involved in Neuropathology of the nclf Mouse Model of Neuronal Ceroid Lipofuscinosis. *PLoS ONE*, *7*(5). https://doi.org/10.1371/annotation/a4b06d46-8eb9-4d15-a15a-41bf4b5ccb8b

Toennes, S. W., Ramaekers, J. G., Theunissen, E. L., Moeller, M. R., & Kauert, G. F. (2008). Comparison of Cannabinoid Pharmacokinetic Properties in Occasional and Heavy Users Smoking a Marijuana or Placebo Joint. *Journal of Analytical Toxicology*, *32*(7), 470–477. https://doi.org/10.1093/jat/32.7.470

Tooze, S. A., & Schiavo, G. (2008). Liaisons Dangereuses: Autophagy, Neuronal Survival and Neurodegeneration. *Current Opinion in Neurobiology*, Vol. 18, pp. 504–515. https://doi.org/10.1016/j.conb.2008.09.015

Tornio, A., Neuvonen, P. J., Niemi, M., & Backman, J. T. (2017). Role of Gemfibrozil as an Inhibitor of CYP2C8 and Membrane Transporters. *Expert Opinion on Drug Metabolism and Toxicology*, Vol. 13, pp. 83–95. https://doi.org/10.1080/17425255.2016.1227791

Toyota, M., Kinugawa, T., & Asakawa, Y. (1994). Bibenzyl Cannabinoid and Bisbibenzyl Derivative from the Liverwort *Radula perrottetii. Phytochemistry*, *37*(3), 859–862. https://doi.org/10.1016/S0031-9422(00)90371-6

Tseng, K. Y., Chambers, R. A., & Lipska, B. K. (2009). The Neonatal Ventral Hippocampal Lesion as a Heuristic Neurodevelopmental Model of Schizophrenia. *Behavioural Brain Research*, Vol. 204, pp. 295–305. https://doi.org/10.1016/j.bbr.2008.11.039

Tsunemi, T., Ashe, T. D., Morrison, B. E., Soriano, K. R., Au, J., Roque, R. A. V., … La Spada, A. R. (2012). PGC-1a Rescues Huntington's Disease Proteotoxicity by Preventing Oxidative Stress and Promoting TFEB Function. *Science Translational Medicine*, *4*(142), 142ra97-142ra97. https://doi.org/10.1126/scitranslmed.3003799

Turkanis, S. A., Cely, W., Olsen, D. M., & Karler, R. (1974). Anticonvulsant Properties of Cannabidiol. *RES.COMMUN.CHEM.PATH.PHARMACOL.*, *8*(2), 231–246.

Turner, B. J., & Talbot, K. (2008). Transgenics, Toxicity and Therapeutics in Rodent Models of Mutant SOD1-Mediated Familial ALS. *Progress in Neurobiology*, Vol. 85, pp. 94–134. https://doi.org/10.1016/j.pneurobio.2008.01.001

Tyynelä, J., Suopanki, J., Santavuori, P., Baumman, M., & Haltia, M. (1997). Variant Late Infantile Neuronal Ceroid Lipofuscinosis: pathology and biochemistry. *J Neuropathol Exp Neurol*, *56*, 369–375.

Tyynelä, J., Palmer, D. N., Baumann, M., & Haltia, M. (1993). Storage of Saposins A and D in Infantile Neuronal Ceroid Lipofuscinosis. *FEBS Letters*, *330*(1), 8–12. https://doi.org/10.1016/0014-5793(93)80908-D

Uryu, S., Harada, J., Hisamoto, M., & Oda, T. (2002). Troglitazone Inhibits Both Post-Glutamate Neurotoxicity and Low-Potassium-Induced Apoptosis in Cerebellar Granule Neurons. *Brain Research*, *924*(2), 229–236. https://doi.org/10.1016/S0006-8993(01)03242-5

Vantaggiato, C., Redaelli, F., Falcone, S., Perrotta, C., Tonelli, A., Bondioni, S., … Bassi, M. (2009). A Novel CLN8 Mutation in Late-Infantile-Onset Neuronal Ceroid Lipofuscinosis (LINCL) Reveals Aspects of CLN8 Neurobiological Function. *Human Mutation*, *30*(7), 1104–1116.

Vesa, J., Hellsten, E., Verkruyse, L. A., Camp, L. A., Rapola, J., Santavuori, P., … Peltonen, L. (1995). Mutations in the Palmitoyl Protein Thioesterase Gene Causing Infantile Neuronal Ceroid Lipofuscinosis. *Nature*, *376*(6541), 584–587. https://doi.org/10.1038/376584a0

Vogt, H. (1905). Über Familiäre Amaurotische Idiotie und Verwandte Krankheitsbilder. *Monatsschr. Psychiat. u. Neurol.*, *18*, 161.

von Schantz, C., Kielar, C., Hansen, S. N., Pontikis, C. C., Alexander, N. A., Kopra, O., … Cooper, J. D. (2009). Progressive Thalamocortical Neuron Loss in Cln5 Deficient Mice: Distinct Effects in Finnish Variant Late Infantile NCL. *Neurobiology of Disease*, *34*(2), 308–319. https://doi.org/10.1016/j.nbd.2009.02.001

Vuillemenot, B. R., Kennedy, D., Cooper, J. D., Wong, A. M. S., Sri, S., Doeleman, T., … O'Neill, C. A. (2015). Nonclinical Evaluation of CNS-Administered TPP1 Enzyme Replacement in Canine CLN2 Neuronal Ceroid Lipofuscinosis. *Molecular Genetics and Metabolism*, *114*(2), 281–293. https://doi.org/10.1016/j.ymgme.2014.09.004

Waddington, S. N., Kennea, N. L., Buckley, S. M. K., Gregory, L. G., Themis, M., & Coutelle, C. (2004). Fetal and Neonatal Gene Therapy: Benefits and Pitfalls. *Gene Therapy*, Vol. 11, pp. S92–S97. https://doi.org/10.1038/sj.gt.3302375

Walkley, S. (2007). Pathogenic Mechanisms in Lysosomal Disease: A Reappraisal of the Role of the Lysosome. *Acta Paediatrica*, *96*, 26–32.

Wang, W., Liu, X., Gelinas, D., Ciruna, B., & Sun, Y. (2007). A Fully Automated Robotic System for Microinjection of Zebrafish Embryos. *PLoS ONE*, *2*(9), e862. https://doi.org/10.1371/journal.pone.0000862

Watzl, B., Scuderi, P., & Watson, R. R. (1991). Marijuana Components Stimulate Human Peripheral Blood Mononuclear Cell Secretion of Interferon-Gamma and Suppress Interleukin-1 Alpha *in vitro*. *International Journal of Immunopharmacology*, *13*(8), 1091–1097. https://doi.org/10.1016/0192-0561(91)90160-9

Weimer, J., Cain, J., Johnson, T., White, K., Likhite, S., & Meyer, K. (2019). Promise of AAV9 Gene Therapy in the Treatment of Batten Disease: Systematic Approach in Therapy Design Reduces Pathological and Behavioral Deficits and Prolongs Survival in Mouse Models of CLN3-, CLN6-, and CLN8 Batten Disease. *Molecular Genetics and Metabolism*, *126*(2), S151. https://doi.org/10.1016/J.YMGME.2018.12.390

Weinreb, N. J., Charrow, J., Andersson, H. C., Kaplan, P., Kolodny, E. H., Mistry, P., … Zimran, A. (2002). Effectiveness of Enzyme Replacement Therapy in 1028 Patients with Type 1 Gaucher Disease after 2 to 5 Years of Treatment: A Report from the Gaucher Registry. *American Journal of Medicine*, *113*(2), 112–119. https://doi.org/10.1016/S0002-9343(02)01150-6

Wells, D. J., & Goldspink, G. (1992). Age and sex Influence Expression of Plasmid DNA Directly Injected Into Mouse Skeletal Muscle. *FEBS Letters*, *306*(2–3), 203–205. https://doi.org/10.1016/0014-5793(92)81000-C

Wen, R., Tao, W., Li, Y., & Sieving, P. A. (2012). CNTF and Retina. *Progress in Retinal and Eye Research*, Vol. 31, pp. 136–151. https://doi.org/10.1016/j.preteyeres.2011.11.005

Wheeler, R. B., Sharp, J. D., Schultz, R. A., Joslin, J. M., Williams, R. E., & Mole, S. E. (2002). The Gene Mutated in Variant Late-Infantile Neuronal Ceroid Lipofuscinosis (CLN6) and in nclf Mutant Mice Encodes a Novel Predicted Transmembrane Protein. *The American Journal of Human Genetics*, *70*(2), 537–542. https://doi.org/10.1086/338708

When are Mice Considered Old? (2020). Retrieved May 8, 2021, from https://www.jax.org/news-and-insights/jax-blog/2017/november/when-are-mice-considered-old#

White, K. A., Cain, J. T., Magee, H., Yeon, S. K., Park, K. D., Khanna, R., & Weimer, J. M. (2019). Modulation of CRMP2 via (S)-Lacosamide Shows Therapeutic Promise but is Ultimately Ineffective in a Mouse Model of CLN6 Batten Disease. *Neuronal Signaling*, *3*, 20190001. https://doi.org/10.1042/NS20190001

White, K. A., Nelvagal, H. R., Poole, T. A., Lu, B., Johnson, T. B., Davis, S., … Weimer, J. M. (2021). Intracranial Delivery of AAV9 Gene Therapy Partially Prevents Retinal Degeneration and Visual Deficits in CLN6 Batten Disease Mice. *Molecular Therapy - Methods and Clinical Development*, *20*, 497–507. https://doi.org/10.1016/j.omtm.2020.12.014

Wibbeler, E., Schulz, A., Nickel, M., & Schwering, C. (2019). *Experiences with Cannabidiol in Patients with NCL Disease*. https://doi.org/10.1055/s-0039-1698230

Williams, R. E., Topcu, M., Lake, B. D., Mitchell, W., & Mole, S. E. (1999). Turkish Variant Late Infantile NCL. In *The Neuronal Ceroid Lipofuscinoses (Batten Disease)* (pp. 114–116). Amsterdam: IOS Press.

Williams, R., E. (2011). Appendix 1: NCL Incidence and Prevalence Data. In Sara E. Mole, R. E. Williams, & H. H. Goebel (Eds.), *The Neuronal Ceroid Lipofuscinoses (Batten Disease)* (Second, pp. 361–365). Oxford: Oxford University Press.

Wlodawer, A., Durell, S., Li, M., Oyama, H., Oda, K., & Dunn, B. (2003). A Model of Tripeptidyl-Peptidase I (CLN2), a Ubiquitous and Highly Conserved Member of the Sedolisin Family of Serine-Carboxyl Peptidases. *BMC Structural Biology*, *3*(1), 8. https://doi.org/10.1186/1472-6807-3-8

Worgall, S., Sondhi, D., Hackett, N. R., Kosofsky, B., Kekatpure, M. V., Neyzi, N., … Crystal, R. G. (2008). Treatment of Late Infantile Neuronal Ceroid Lipofuscinosis by CNS Administration of a Serotype 2 Adeno-Associated Virus Expressing CLN2 cDNA. *Human Gene Therapy*, *19*(5), 463–474. https://doi.org/10.1089/hum.2008.022

Wyburn-Mason, R. (1943a). On Some Anomalous Forms of Amaurotic Idiocy and Their Bearing on the Relationship of the Various Types. *The British Journal of Ophthalmology*, *27*(4), 145–173. https://doi.org/10.1136/bjo.27.4.145

Wyburn-Mason, R. (1943b). The British-Journal of Opthalmology: May, 1943 Communications on Some Anomalous Forms of Amaurotic Idiocy and Their Bearing on the Relationship of the Various Types. Retrieved from http://bjo.bmj.com/

Xu, J., Storer, P. D., Chavis, J. A., Racke, M. K., & Drew, P. D. (2005). Agonists for the Peroxisome Proliferator-Activated Receptor-α and the Retinoid X Receptor Inhibit Inflammatory Responses of Microglia. *Journal of Neuroscience Research*, *81*(3), 403–411. https://doi.org/10.1002/jnr.20518

Yan, Z., Liu, X., Lei, C.-M., Luo, M., & Engelhardt, J. F. (2005). AAV Vectors: Vector Biology. Adeno-Associated Virus Type-1 Vectors Efficiently Transduce Human Polarized Airway Epithelia without Polarity Bias Species-Specific Differences in the Polarity of rAAV5 and rAAV2 Transduction of Mouse and Human Airway Epithelia. In *Molecular Therapy* (Vol. 11).

Young, P. P., Fantz, C. R., & Sands, M. S. (2004). VEGF Disrupts the Neonatal Blood-Brain Barrier and Increases Life Span After Non-Ablative BMT in a Murine Model of Congenital Neurodegeneration Caused by a Lysosomal Enzyme Deficiency. *Experimental Neurology*, *188*(1), 104–114. https://doi.org/10.1016/j.expneurol.2004.03.007

Zahs, K. R., & Ashe, K. H. (2010). “Too Much Good News” - are Alzheimer Mouse Models Trying to Tell Us How to Prevent, Not Cure, Alzheimer’s Disease? *Trends in Neurosciences*, Vol. 33, pp. 381–389. https://doi.org/10.1016/j.tins.2010.05.004

Zander, T., Kraus, J. A., Grommes, C., Schlegel, U., Feinstein, D., Klockgether, T., … Heneka, M. T. (2002). Induction of Apoptosis in Human and Rat Glioma by Agonists of the Nuclear Receptor PPARγ. *Journal of Neurochemistry*, *81*(5), 1052–1060. https://doi.org/10.1046/j.1471-4159.2002.00899.x

Zanelati, T., Biojone, C., Moreira, F., Guimarães, F., & Joca, S. (2010). Antidepressant-Like Effects of Cannabidiol in Mice: Possible Involvement of 5-HT1A Receptors. *British Journal of Pharmacology*, *159*(1), 122–128. https://doi.org/10.1111/j.1476-5381.2009.00521.x

Zeldovich, L. (2017). Genetic Drift: The Ghost in the Genome. *Lab Animal*, *46*(6), 255–257. https://doi.org/10.1038/laban.1275

Zeman, W. (1976). The Neuronal Ceroid Lipofuscinosis. *Progress in Neuropathology*, *3*, 203–223.

Zeman, W., & Dyken, P. (1969). Neuronal Ceroid Lipofuscinosis (Batten's Disease): Relationship to Amaurotic Family Idiocy? *Pediatrics*, *44*(4), 570–583. Retrieved from http://www.ncbi.nlm.nih.gov/pubmed/5346636

Zeman, W., & Hoffman, J. (1962). Juvenile and Late Forms of Amaurotic Idiocy in One Family. In *J. Neurol. Neurosurg. Psychiat* (Vol. 25). Retrieved from http://jnnp.bmj.com/

Zhang, L., & Zhang, L. (2011). Voluntary Oral Administration of Drugs in Mice. *Protocol Exchange*. https://doi.org/10.1038/protex.2011.236

Zhao, X., & Bhattacharyya, A. (2018). Human Models Are Needed for Studying Human Neurodevelopmental Disorders. *American Journal of Human Genetics*, Vol. 103, pp. 829–857. https://doi.org/10.1016/j.ajhg.2018.10.009

Zuardi, A. W. (2008). Cannabidiol: From an Inactive Cannabinoid to a Drug with Wide Spectrum of Action. *Revista Brasileira de Psiquiatria*, Vol. 30, pp. 271–280. https://doi.org/10.1590/S1516-44462008000300015

Appendix A: supplementary information for **Chapter 2**

Appendix. A.1 Reagents and chemicals

Listed in alphabetical order.

Acetic acid (solution; CH_3COOH; 96%)

Manufacturer: ExpertQ®

Ref: AC0353005P

Supplier: Scharlau

Adeno-associated virus (AAV) serotype 2/9 with human *CLN6* (*hCLN6*) DNA (solution)

Manufacturer: Nationwide Ohio Children's Hospital Viral Vector Core

Supplier: Nationwide Ohio Children's Hospital Viral Vector Core

Bulk ethanol (solution)

Manufacturer: Merck

Ref: 100983

Supplier: LabSupply

Cannabidiol oil (*Cannabis sativa*; solution; 5.25%; 6x 30 mL bottles)

Manufacturer: Medropharm Health Science

Supplier: Herba Healthcare Australia

(D^+) sucrose for molecular biology (powder; $C_{12}H_{22}O_{11}$)

Manufacturer: Neofroxx

Ref: 1104KG001

Supplier: Lab Supply Ltd.

Dimethyl sulfoxide (solution; DMSO; C_2H_6OS; ≥99.9%)

Manufacturer: Sigma-Aldrich (Merck)

Ref: D2650-100 mL

Supplier: Sigma-Aldrich New Zealand

Di-sodium hydrogen phosphate (powder; disodium phosphate; Na_2HPO_4)

Manufacturer: Emsure® (Merck)

Ref: F2026086838

Supplier: Sigma-Aldrich New Zealand

Emla® needle anaesthetic (cream; 5%; 30 mg/ml)

Manufacturer: Astra Zeneca

Ref: #TA6856

Supplier: University of Otago Animal Welfare Office (AWO)

Gemfibrozil (powder; $C_{15}H_{22}O_3$)

Manufacturer: Pfizer

Ref: G9518-25 G

Supplier: Sigma-Aldrich New Zealand

Hydrogen peroxide (solution; H_2O_2; 3%)

Manufacturer: PSM Healthcare Ltd trading as API

Ref: 11053253

Supplier: Central City Life Pharmacy NZ, Dunedin

Instant adhesive (gel)

Manufacturer: Selleys®

Ref: 371419

Supplier: Mitre10 New Zealand, South Dunedin

Isopropyl alcohol (solution; 2-propanol; $(CH_3)_2CHOH$; ≥99.7%)

Manufacturer: AnalaR NORMAPURE®

Ref: 20842.312

Supplier: VWR™ Chemicals international

Jelly (crystals; lime; 80 g)

Manufacturer: Value (Safeway Traders NZ)

Supplier: Centre City New World, Dunedin, NZ

Jelly (crystals; strawberry; 2.5 kg)

Manufacturer: Champion Professional

Ref: 4187991

Supplier: Trents Wholesale

Methylcellulose (powder; viscosity: 4,000 cP)

Manufacturer: Sigma-Aldrich (Merck)

Ref: M0512-100 G

Supplier: Sigma-Aldrich New Zealand

Paraformaldehyde (powder; $OH(CH_2O)_nH$ (n = 8-100))

Manufacturer: Sigma-Aldrich (Merck)

Ref: P6148

Supplier: Sigma-Aldrich New Zealand

Phosphate buffer saline (solution; 1x; pH 7.4)

Manufacturer: Gibco™

Ref: 1001000-49

Supplier: Life Technologies New Zealand Pty Ltd (ThermoFisher Scientific)

Sodium azide (solution; NaN_3; ≥99.5%)

Manufacturer: Fluka™ (Honeywell Research Chemicals)

Ref: 71289

Sodium chloride (powder; NaCl)

Manufacturer: Emsure® (Merck)

Ref: K49451104832

Supplier: Sigma-Aldrich New Zealand

Sodium pentobarbital (solution; $C_{11}H_{18}N_2O_3$; 30 mg/ml)

Diluted from 300 mg/ml by University of Otago's Drug Control Officer (DCO)

Manufacturer: Provet NZ Pty Ltd.

Supplier: University of Otago AWO

Sodium phosphate monobasic (powder; monosodium phosphate; NaH_2PO_4)

Manufacturer: Sigma-Aldrich (Merck)

Ref: SO751-500 G

Supplier: Sigma-Aldrich New Zealand

Splenda® sweetener (powder; 120 g)

Manufacturer: Splenda®

Ref: 3076946

Supplier: Trents Wholesale

TriGene (concentrate)

Manufacturer: TriGene Advance

Ref: EATTRIG36

Supplier: InVitro Technologies

Trypan blue (solution; 0.05%)

Diluted from 0.4% in lab

Manufacturer: Logos Biosystems

Ref: #T13001

Supplier: Logos Biosystems

Tween® 20 (solution; polysorbate 20; $C_{58}H_{114}O_{26}$; ≥40.0%)

Manufacturer: Sigma-Aldrich (Merck)

Ref: P2287-500 mL

Supplier: Sigma-Aldrich New Zealand

Unflavoured gelatin (crystals; 2.5 kg)

Manufacturer: Davis (Gelita)

Ref: 3055956

Supplier: Trents Wholesale

Appendix.A.2 Lab-made solutions and buffers

Listed in alphabetical order.

CBD stock solution (solution; dosage of 120 mg per kg)

1. Follow all steps outlined below in **Gemfibrozil stock solution** *except:*

   CBD used in this thesis had a stock solution concentration of 50 mg per mL, therefore use 50 mg per mL for C2 in C1V1 = C2V2.

   Despite the CBD already coming in a liquid form, the CBD jelly tablets must also have vehicle in them, to control for any possible side effects of Tween20 and DMSO. This ratio is 1:1. Therefore, if you put 100 uL of CBD oil in the jelly, then also put in 100 uL of vehicle (50 uL of Tween20 and 50 uL of DMSO).

CBD and gemfibrozil stock solution (solution; gemfibrozil dosage of 120 mg per kg + CBD dosage 120 mg per kg)

1. Follow all steps outlined below in **Gemfibrozil stock solution** *except:*

   You should calculate how much gemfibrozil and CBD to put into the jelly separately, even though they both end up in the same amount of jelly. You do not need to double the amount of jelly for two drugs. Also, because you are putting Tween20 and DMSO in the jelly as the vehicle for gemfibrozil, you do not need to put in extra vehicle for CBD. This would double the amount of vehicle each mouse gets compared to other mice in other treatment groups.

   Gemfibrozil stock solution (solution; dosage of 120 mg per kg)

1. Convert the gemfibrozil dosage (120 mg per kg) from mg per kg to mg per g by dividing by 1000: 120/1000 = 0.12 mg/g

2. Work out how much of gemfibrozil (in mg) you need per dose (per 1 mL of jelly) for each mouse within each weight 'range' (see **Table 2.2**). This will give you the concentration for all the jelly you need to make all the doses for the mice in that weight range overall.

   E.G. 0.12 mg/g + a 24 g mouse (treated as a 20 g mouse per **Table 2.2**) = 0.12 x 20 = 2.4 mg gemfibrozil required for that mouse's dose.

   If you have ten mice who all fall within the 20g – 24g weight range (**Table 2.2**), they will all receive 1 mL doses of jelly with a concentration of 2.4 mg/mL.

3. Now work out the total number of doses you need to make up for the week. This will give you the total volume of jelly you want to make up for all mice within a particular weight range that will receive 1 mL jelly tablets every second day with this particular gemfibrozil concentration.

# of doses = # of mice in weight range x # of days you want to dose those mice before making more jelly (approx 4 for one week).

E.G. 10 x 4 = 40 doses total, each dose is a 1 mL jelly tablet, therefore you want to make 40 mLs of jelly overall.

4. Jelly is difficult to manipulate because it is very viscous. Therefore, you want to make up more jelly than you actuall need – to leave room for measurement error. We used 20% error margin.

   E.G. Total volume of jelly needed (in mL) x 0.2 (20%) = Total volume of jelly to make, including error.

   E.G.2 40 mL x 0.2 = 48 mL

5. Now calculate how much gemfibrozil stock solution to add to your jelly (stock solution is always 1200 mg/mL). This means if you had one mL of solution (liquid – in this case, DMSO and Tween 20), you would have 1200 mg of powdered gemfibrozil dissolved in it.

6. You can either choose to make a 1 mL aliquot of stock solution, simply by adding 500 uL of Tween20, 500 uL of DMSO and 1200 mg of gemfibrozil, or you can calculate how much stock solution you are going to need for every weight range in gemfibrozil and then make up enough stock solution to supply all the different weight ranges (you might end up needing more or less than 1 mL of stock solution).

7. Use the following equation to calculate how much stock solution you need to dissolve in the liquid jelly given to a certain number of mice in a certain weight range:

   C1V1 = C2V2

   C1 (concentration 1 or initial concentration; concentration of gemfibrozil for each 1 mL jelly tablet made, as calculated in step 2) x V1 (volume 1 or initial volume; volume of jelly calculated in step 4) = C2 (concentration 2 or final concentration; concentration of gemfibrozil stock solution) x V2 (volume 2 or final volume; volume of gemfibrozil stock solution required to make C1 in V1)

   Rearrange this equation to get V2, the volume of stock solution required.

   E.G 2.4 mg/mL (concentration 1 – concentration of the jelly) x 48 mL (volume 1 - volume of jelly needed) / 1200 mg/mL (concentration 2 – concentration of stock solution) = 0.096 mL (volume 2 – the volume of stock solution required, in mLs).

   The answer is given in mL. To convert to µL (for pipetting), simply x 1000.

   E.G.2 0.096 mL x 1000 = 96 µL.

Modified Davidson's fixative (solution; makes 1 L)

200 mL formalin (37%)

300 mL bulk ethanol

100 mL acetic acid

300 mL dH_2O

TriGene (solution; 10%; makes 100 mL)

10 mL TriGene concentrate

90 mL dH_2O

Paraformaldehyde (PFA; solution; 4%; makes 1 L)

40 g paraformaldehyde (PFA)

500 mL 0.1 M phosphate buffer (PB) or 500 mL dH_2O

Heat to 60℃ with stirring until PFA has dissolved

Make up to 1 L with 0.1 M PB or dH_2O

Filter and pH to 7.4

Phosphate buffer (PB; solution; 0.1 M; makes 2 L)

Solution A: 27.6 g sodium phosphate monobasic ($NaH_2PO_4H_2O$)

Solution B: 53.6 g sodium phosphate dibasic ($Na_2HPO_47H_2O$)

Mix 280 mL of solution A with 720 mL solution B

Adjust pH to 7.2

Make to 2 L with ddH_2O

Phosphate buffer saline (PBS; solution; 10x; makes 1 L)

80 g NaCl

11.5 g Na_2HPO_4

2 g KH_2PO_4

2 g KCl

800 mL dH_2O

Stir to dissolve and make up to 1 L with ddH_2O

PBS (1x) (solution; makes 1 L)

100 mL 10x PBS

900 mL ddH_2O

PBS-sodium azide (solution; 0.02%; makes 500 mL)

50 L PBS (1x)

0.1 mg sodium azide powder (0.02% w/v)

Make up to 500 mL with dH_2O

Sucrose (solution; 30%)

30 g sucrose

Made to 100 mL with 0.1 M PB or dH_2O

Vehicle (solution; makes 10 mL)

5 mL dimethyl sulfoxide (DMSO)

5 mL Tween® 20

Appendix.A.3 Instruments and equipment

Listed in alphabetical order.

0.6 mL microcentrifuge tubes

Manufacturer : Corning® Axygen®

Ref: MCT-060-C-S

Supplier: Sigma-Aldrich New Zealand

1 mL disposable slip-lock syringes

Manufacturer: BD Luer-Lock™ (Becton, Dickinson and Company)

Ref: 309628

Supplier: Medshop NZ

1.5 mL microcentrifuge tubes

Manufacturer : Corning® Axygen®

Ref: MCT-150-C-S

Supplier: Sigma-Aldrich New Zealand

15 mL plastic centrifuge tubes

Manufacturer: Corning®

Ref: CLS430791-500

Supplier: Sigma-Aldrich New Zealand

160 grid mini silicon ice cube trays (12.1 cm x 23.8 cm; 1 cm x 1 cm wells)

Supplier: Hinxin on amazon.com

https://www.amazon.com/Hinxin3Pack160-Grid-Mini-Silicone-Cube/dp/B07RX1H394/ref=sr_1_1?keywords=Hinxin&qid=1573522320&sr=8-1

2 mL microcentrifuge tubes

Manufacturer: Corning ® Axygen®

Ref: MCT-200-C

Supplier: Sigma-Aldrich New Zealand

20 mL syringe with a slip lock

Manufacturer: Basik

Ref: 217418

Manufacturer: Shoof Vet

2-20 µL filter pipette tips

Manufacturer: Neptune

Ref: CPBT20

Supplier: MediRay

25 gauge (G) x 5/8" disposable needle (0.50 x 16 mm)

Manufacturer: Terumo Europe

Supplier: University of Otago's Department of Biochemistry

3-way stopcock

Manufacturer: Terumo Europe

Ref: 211 663

Supplier: Shoof Vet

5-Lane RotaRod for Mice

Manufacturer: Med Associates Inc

Ref: ENV-574M

Supplier: Med Associates Inc

50 mL plastic centrifuge tubes

Manufacturer: Corning®

Ref: CLS4558-300

Supplier: Sigma-Aldrich New Zealand

Brain Matrix

Manufacturer: Pelco®

Ref: 15001-15069

Supplier: Ted Pella Inc

Cotton-tipped, non-sterile applicators

Sterilised via autoclaving

Manufacturer: Nanjing Lustre Medical + Healthcare

Ref: 40059030063

Supplier: University of Otago's Department of Biochemistry

Electric kettle

Manufacturer: Breville

Ref: BKE270

Supplier: Briscoes NZ

Heating pads and re-chargable batteries

Supplier: University of Otago's Hercus-Taieri Resource Unit (HTRU)

Immersion blender

Manufacture: Bodum Bistro

Ref: ZIP473

Supplier: Briscoes NZ

Magnetic stirrer hotplate (500 V)

Manufacturer: Chiltern Scientific

Ref: C128

Supplier: Hughes Lab

Portable lab balance scales (0.001-60 g)

Manufacturer : Denvern Instrument (Sartorius)

Ref : S1-68

Supplier : Biostrategy Sales and Services Ltd

Portable scientific scales (0.01 g - 610 g)

Manufacturer: Denver Instrument (Sartorius)

Ref: MXX-612

Supplier: Biostrategy Sales and Services Ltd

Pulled glass needles (1 µm point)

Originally 6-inch Borosilicate Glass Capillaries with 1.0 mm outer diameter

Manufacturer: World Precision Instruments

Ref: 1B100-f6

Supplier: Fisher Scientific

Serrated hemostat kelly forceps

Manufacturer: Fisherbrand™

Ref: 08-907

Supplier: Hughes Lab

Silicon surgical tubing (1 mm inner-diameter)

Supplier: Weimer Lab, Sanford Research

Single-edge, blue carbon steel blades

Manufacturer: Pal®

Ref: 121-20

Supplier: Ted Pella Inc

Sharp-pointed dissection scissors (4.12”)

Manufacturer: Fisherbrand™

Ref: 08-935

Supplier: Hughes Lab

Spinbar® magnetic stirring fleas (assorted sizes)

Manufacturer: Spinbar®

Ref: Z283886-3EA

Supplier: Sigma-Aldrich New Zealand

Stainless steel, sterile surgical blades

Manufacturer: Swann-Morton ®

Ref: 0310

Supplier: University of Otago’s Department of Biochemistry

Standard dissection scissors (5.12”)

Manufacturer: Fisherbrand™

Ref: 08-951-25

Supplier: Hughes Lab

Sterile plastic cell-culture petri dish (various)

Manufacturer: Greiner

Supplier: Bio-one

Straight blunt/sharp dissection scissors (14 cm)

Manufacturer: Thermo Scientific™ Shandon™

Ref: 28252

Supplier: Hughes Lab

TC-treated multiple (24) well plates

Manufacturer: Corning® Costar®

Ref: CLS3527-100

Supplier: Sigma-Aldrich New Zealand

Universal, flat bottom container with screw cap (30 mL)

Ref: S8027SU

Supplier: MediRay

Waterbath (0-100℃; 3 L)

Manufacturer: Grant Instruments (Cambridge) Ltd

Ref: OE9528010 (Equivalent = T100)

Supplier: Biolab Scientific Ltd

Winged infusion set with protector

Manufacturer: Terumo Europe

Ref: SV*S21NL09

Supplier: Shoof Vet

Xtracare VSS fume cupboard

Manufacturer: Thermoplastic Engineering Ltd

Ref: 208B

Supplier: University of Otago's Department of Biochemistry

Appendix.A.4 Software

Listed in alphabetical order.

GraphPad Prism (version 8) for Mac

Manufacturer: GraphPad Software, San Diego, California, USA

Ref: Version 8

Supplier: University of Otago's Department of Biochemistry

IBM SPSS Statistics (version 25)

Manufacturer: IBM Corp, Armonk, NY, USA

Ref: 17918

Supplier: University of Otago's Student Information Technology Services

Microsoft® Excel for Mac (version 16.30)

Manufacturer: Microsoft Office

Ref: 19100300

Supplier: University of Otago's Student Information Technology Services

RotaRod 2

Manufacture: Med Associates Inc

Ref: SOF-571

Supplier: Med Associates Inc

Appendix B: supplementary information for **Chapter 3**

Statistical supplementary material available at:

https://drive.google.com/file/d/1StAQ4n41HjkFFCdC7bfHogfOLs67H4Zi/view?usp=sharing